UNIVERSITY OF SANTIAGO DE COMPOSTELA

SCHOOL OF ENGINEERING (E.T.S. E.)

Department of Chemical Engineering

DESULFURIZATION OF FUEL OILS BY SOLVENT EXTRACTION WITH IONIC LIQUIDS

A thesis submitted by MARIA FRANCISCO CASAL for the degree of Doctor in Chemical and Environmental Engineering to the University of Santiago de Compostela

Santiago de Compostela, February 2010

Autorization for submission by the thesis directors (in Spanish)

Alberto Arce Arce, Catedrático de Ingeniería Química, y **Ana M. Soto Campos**, Profesora titular de Ingeniería Química,

INFORMAN:

Que la presente memoria titulada *"Desulfurization of fuel oils by solvent extraction with ionic liquids",* que para optar al grado de Doctora en Ingeniería Química, Programa de Doctorado de Ingeniería Química y Ambiental, presenta **María Francisco Casal,** fue realizada bajo nuestra inmediata dirección en el Departamento de Ingeniería Química de la Universidad de Santiago de Compostela.

Considerando que constituye trabajo de Tesis, autorizan su presentación a la Comisión de Tercer Ciclo de la Universidad de Santiago de Compostela.

Y para que así conste, firman el presente informe en Santiago de Compostela a 1 de Febrero de 2010

Alberto Arce Arce Ana Soto Campos

To my parents and, to Alberto and Ana

ACKNOWLEDGEMENTS

Four years ago, I would have never dreamt about being at this point. Time has flown by, and now I feel like a cycle in life is closing. The present thesis comprises the work done for the last four years, and I would not forget about saying thanks to everybody who helped me and gave me the great opportunity of starting this wonderful adventure.

First of all, I would like to thank my thesis directors, Prof. Alberto Arce and Prof. Ana Soto, leaders of the Group of Phase Equilibria and Separation Processes at the Dpt. of Chemical Engineering of the University of Santiago de Compostela (Spain). They gave me the opportunity to join their group, and to develop this interesting researching work. They aroused my vocation for research. I am really indebted to them for such a superb guidance of my work and working environment. They put their trust in me, and now that this work is happily concluded I hope they will be proud of it.

I feel moved to extent my gratitude to all of the members of this mentioned Group who have been like a little family to me, wonderful friends and workmates. I will like to personally thank Alberto and Ana, who far away from being merely group leaders and bosses, they were sometimes guiding parents, adviser friends, and strong support in my life. I must say to them, "I already learned how important it is in life to be where and when I have to be".

I would like to thank Dr. Eva Rodil for all of those shared happy and bad moments, and for every minute I have enjoyed Sandra and Julio.

I would never forget this warm environment in this lab, thanks to everyone around: Dr. Alberto Arce Ceinos, Dr. Óscar Rodríguez, Dr. Luisa Alonso, Yamil Colon, but especially to Borja and Sara, who always drew a smile on my face and cheered me up in my worst moments. They made me realize how important it is sometimes not to grow up so quickly. A mention apart to Dr Héctor Rodríguez for all of his professional advices (I know you didn´t always tell me off, "it is just the way you express yourself") and for helping me to mature as workmate, friend and the best flatmate ever.

As part of this adventure, I´ve had the pleasure for two months, to work with the Group of the Laboratory of Thermodynamics and Phisicochemistry of Fluids. I would like to express my gratitude to Prof. Juán Ortega, leader of the mentioned Group and who I really professionally admire, for giving me the chance to join his hard working team and make me feel like at home in Las Palmas. I have had the great pleasure of knowing such great friends, Gisela and Ana, who I really love and miss.

As another fortunate stage of this journey, I had the good luck of spending a three months stay at the QUILL Centre (Queen's University Ionic Liquid Laboratories) world leader institution in ionic liquids research in Belfast (UK) as part of the Marie Curie Early Stage Trayning Site Fellowship, contract number MEST-CT-2004-505613 (European Union). I have had the satisfaction of working under the supervision of Prof. Robin D. Rogers, whose researching labour in ionic liquids field is widely known all over the world. I have learned so many things from his Group in such a short time! And as it can be imagine, having the chance of meeting so many people from all over the world, I left in Belfast a small piece of my heart. Thanks to everbody, and not forgetting anyone. I met in the "cloudiest city in the world", I can not carry on without mentioning Alberto and Gabi, who I really love and miss too.

As the last part of my acknowledgements, my warmest gratitude goes to my friends and family. "Thank you" Nico, María, Oliva, Susana, Patricia, Gus, Sandra and Juan for being part of my life and always there. To my parents, José Luis and Carmiña, for their unconditional support, Laura, Pablo and Lucas.

Closing these lines, I must thank the University of Santiago de Compostela, the European Union (Marie Curie Early Stage Training Site Fellowship) and the Ministry of Science and Innovation of Spain (Contract Reference 2004/PX130 and Research Personnel Training Grant with reference BES-2007-16693, under the project CTQ2006-07687) for the finantial support in the different stages of this work.

ABSTRACT

ABSTRACT

As one of the multiple applications of ionic liquids, extraction of sulfur- and nitrogen-containing compounds from fuels has been studied in this thesis.

Three imidazolium-based ionic liquids: 1-octyl-3-methylimidazolium tetrafluoborate ($[C_8mim][BF_4]$),1-octyl-3-ethylimidazolium bis{(trifluoromethylsulfonyl)imide}($[C_8mim][NTf_2]$) and 1-ethyl-3-methylimidazolium ethylsulfate($[C_2mim][EtSO_4]$) and a poly substituted pyridinium ionic liquid, 1-hexyl-3,5-dimethylpyridinium bis{(trifluoromethyl sulfonyl)imide} ($[C_6mmPy][NTf_2]$) were chosen as possible solvents .Thiophene and Pyridine were selected as representative sulfur- and nitrogen-containing compounds.

With this aim, liquid-liquid equilibrium data of ternary systems composed by {Ionic liquid (IL)+Thiophene/Pyridine+Fuel Representative Hydrocarbon } have been determined and discussed in terms of solute distribution ratio (β) and selectivity(S).

Three steps extraction experiments were carried out with two synthetic mixtures simulating gasoline and diesel and following raffinate composition after each one of the steps. Ability of the four ionic liquids to extract sulfur- and nitrogen-containing compounds has been demonstrated. The ionic liquid which gave the greatest extraction yield was $[C_6mmPy][NTf_2]$. Certain degree of dearomatization has been also observed.

Extraction performances using real samples from the refinery previous to desulfurization have been found to be in agreement with the model oil results.

CONTENTS

1. OBJECTIVE

1. OBJECTIVE

The principal objective of this thesis can be grouped under the more ambitious aim of studying the potential use of ionic liquids as solvents in petrochemical separations. This general idea was singled out in the study of the suitability of ionic liquids as solvents for the extraction of sulfur and nitrogen-containing compounds from fuels.

With this aim in mind, this project will be subdivided into several stages:

In the first place, the selection *a priori* of the most promising candidates from the huge family of ionic liquids.

For all chosen solvents, a second step will consist of the analysis of their suitability for our purposes according to thermodynamic criteria. For this reason, the study of liquid-liquid equilibrium of each one of the ternary systems composed by IL, a sulfur or nitrogen-containing compound and a fuel representative constituent is going to be carried out and experimental data are going to be correlated and analyzed.

All equilibria involving the use of each IL as a separating agent will be correlated together. The binary interaction parameters obtained are needed for the design of an extraction column for desulfurization of fuel-oils.

As a third step, two liquid mixtures simulating gasoline and gasoil respectively will undergo a three step extraction process employing the selected ionic liquids as entrainers. Composition of feed and raffinate after each one of the extraction steps will be analyzed with the aim of following not just the sulfur reduction, but also the evolution of fuel constituents along this extraction process.

Several samples of real diesel and gasoline previous to desulfurization process and provided directly by the refinery will be used to verify our conclusions. These samples will undergo the same three step extraction process, to confirm the appropriateness of using these ionic liquids as solvents in real industrial applications.

Based on these tests, the most suitable IL for desulfurization of gasoline and diesels will be selected. For this IL, the simulation of a counter-current continuous extraction column will be carried out, using the interaction parameters obtained in the correlation, to test the possible extent of the desulfurization process.

2. INTRODUCTION

2. INTRODUCTION

2.1 Environmental Background

Emissions of sulfur gases from both natural and anthropogenic sources strongly influence the atmosphere chemistry. When certain atmospheric pollutants (primarily carbon dioxide, sulfur dioxide, and nitrogen oxides) react in contact with water in the atmosphere or on the ground, they can be chemically converted to acidic substances. Sulfur and nitrogen oxides are transformed to strong acids (sulfuric and nitric acids) causing the undesirable acid rain [1].

Even though in 1852 Robert Angus Smith established for the first time the relationship between acid rain and atmospheric pollution in Manchester (England) it was not until the late 1960s when scientists began to seriously study this phenomenon. It was in fact in 1972 that the term "acid rain" was coined [2].

Since the industrial revolution, emissions of sulfur and nitrogen oxides have increased. Burning of fossil fuels caused the industrial growth and energy-generating facilities, are the main sources. These emissions, plus those from the transportation sector, are the major originators of increased nitrogen and sulphur oxides into the atmosphere. The gases may be carried hundreds of miles before they are converted to acids and deposited. The problem of acid rain not only has increased with population and industrial growth, it has become more widespread [3].

In order to endeavour this problem, The Protocol to the 1979 Convention on Long-Range Transboundary Air Pollution on Further Reduction of Sulphur Emissions is an agreement to provide for a further reduction in sulphur emissions or transboundary fluxes [4].

Over the last decade, environmental regulations focus attention on reduction of emissions from the transport sector with the purpose of improving air quality and welfare [5]. According to the Directive of the European Union, gasoline and diesel fuels in Europe should not exceed 10 ppm of total sulfur content starting from 2010 [6]. US regulations established a maximum of 15 ppm for diesel starting from 2006 and 30 ppm for gasoline starting from 2005 [7].

2.2 The problem of fuel desulfurization: an overview

2.2.1 Petroleum technology context

A modern refinery is a highly integrated industrial plant, the main task of which is to efficiently produce large yields of valuable products from a crude oil feed of variable composition.

Product improvement is the treatment of petroleum products to ensure that they meet utility and performance specifications. It usually involves changes in molecular shape (reforming and isomerisation) or in molecular size (alkylation and polymerization) and it can play a major role in product improvement.

A growing dependence on high-heteroatom heavy oils and residua has emerged as a result of continuing decreasing availability of conventional crude oil, owing to the depletion of reserves in various parts of the World. Thus, the ever-growing tendency to convert as much as possible of lower-grade feedstock to liquid products is causing an increase in the total sulphur content in refined products [8].

There are several valid reasons for removing heteroatoms from petroleum fractions. These reasons include:

- Reduction or elimination of corrosion during refining, handling or use of the various products
- Production of products having an acceptable degree of specifications
- Increasing the stability and performance of the transportation fuels
- Decreasing smoke formation in kerosene
- Reduction of heteroatom content in fuel oil to a level that improves burning characteristics and is environmentally acceptable.

As it is represented in Figure 1, products in the refining processes are hydrotreated and basically classified according to their boiling ranges. The primary objective of hydrotreating is to remove impurities, such as heteroatom- and metal-containing compounds from a feedstock or increase its hydrogen content and lower the molecular weight of the by-products without a substantial loss in liquid product yield. The specific impurities depend on the molecular weight of the feedstock to be processed. Lower molecular weight ones such as naphtha, gasoline, intermediate distillates, diesel fuels and home heating oil contain undesirable impurities such as sulphur-containing compounds, nitrogen-containing compounds, oxygen-containing compounds

and polynuclear aromatic compounds. The boiling range of the feedstock which is dictated by its molecular weight distribution and the product quality specifications are the major considerations to have into account when choosing a hydrotreating process.

Sulfur-, Nitrogen- and metal-containing compounds have different reactivities and chemistries depending on the boiling ranges of the fractions in which are found. Thus, specific processes have been developed for the removal of each one of these impurities and are classified as Hydrodesulfurization (HDS), Hydrodenitrogenation (HDN) and Hydrodemetallization (HDM) processes, respectively.

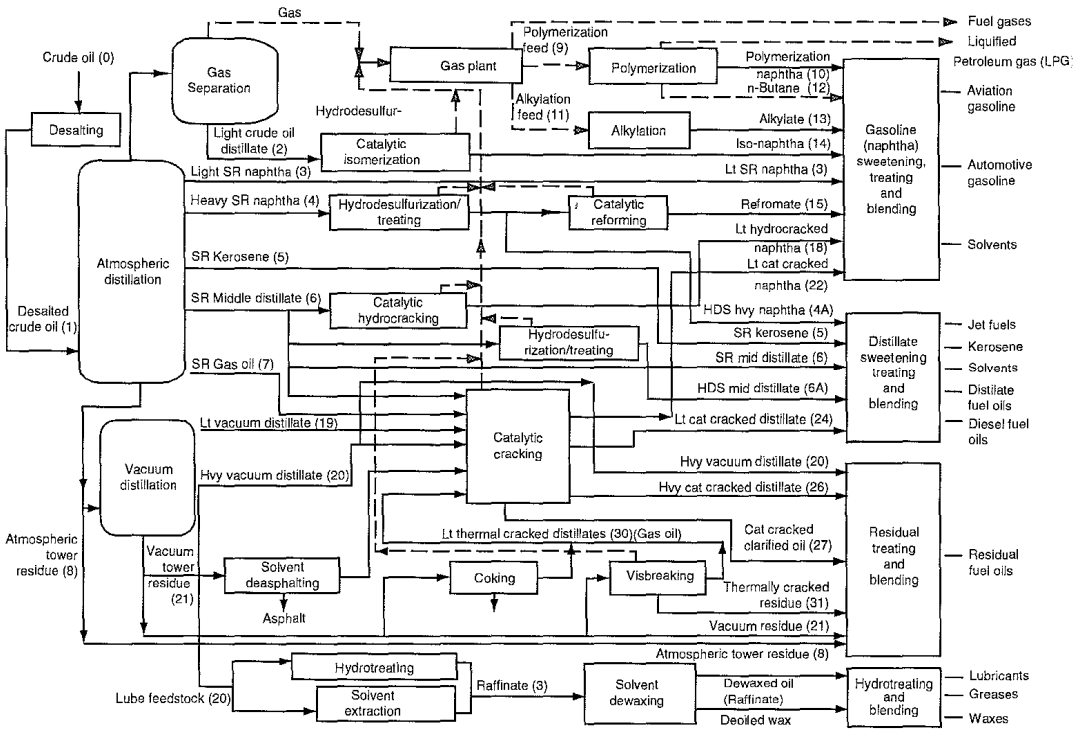

Figure 1. Representative scheme of refining process applied in petroleum industry.

In general, sulfur impurity is the major concern because S-compounds are often serious poisons and inhibitors for other secondary-process catalysts and their combustion products create serious environmental hazards. Thus, the main hydrotreating processes that have been developed for distillable feedstock are HDS processes. N-containing compounds are also removed during this process and also HDA reactions are occurred, even though quality requirements often require an HDA procedure after the initial HDS+HDN processes [9].

2.2.2 Current Process: Hydrodesulfurization (HDS)

Catalytic HDS of crude oil and refinery streams is carried out at elevated temperature and hydrogen partial pressure, converting organosulfur compounds to hydrogen sulfide (H_2S) and hydrocarbons.

The conventional HDS process is usually conducted over sulfided $CoMo/Al_2O_3$ and $NiMo/Al_2O_3$ catalysts [10]. Their performance in terms of desulfurization level, activity and selectivity depends on the properties of the specific catalyst used (active species concentration, support properties, synthesis route), the reaction conditions (sulfiding protocol, temperature, partial pressure of hydrogen and H_2S), nature and concentration of the sulfur compounds present in the feed stream, and reactor and process design.

This widely applied process easily allows the elimination of aliphatic and alicyclic sulfur compounds but removal of many thiophene and dibenzothiophene derivatives turns into a difficult task due to several catalyst surface interactions and stereo hindrance [11-15]. Due to these difficulties to remove some sulfur containing aromatic compounds highly resistant to hydrotreatment, several attempts to change operation conditions of HDS are under way [16].

Deep desulfurization of refinery streams becomes possible when the severity of the HDS process conditions is increased [17, 18]. Unfortunately, more severe conditions result not only in a higher level of desulfurization but also in undesired side reactions. When FCC gasoline is desulfurized at higher pressure, many olefins are saturated and the octane number decreases. Higher temperature processing leads to increased coke formation and subsequent catalyst deactivation.

It is also important to note that in practice the severity of the operating conditions is limited by the HDS unit design. In addition to applying more severe conditions, HDS catalysts with improved activity and selectivity must be used. New improvements related to new HDS-based techniques are being developed and already reviewed in literature [9, 15, 19]

In any case, to carry out the deep HDS processes, the energy and hydrogen consumption should be evidently increased and these severe operation conditions inevitably lead to high increase in capital expenditure.

Refineries with hydrotreaters are likely to achieve production of Ultra Low Sulfur products by modifying catalysts and operating conditions. Variations in feedstock sulfur content and the amount of cracked stock have a big influence in the process and operation conditions. Nonetheless, a two-stage deep desulfurization process will be required by most, if not all refiners,

to achieve legislative requirements. The second stage requires substantial modification of the desulfurization process, drastic higher pressure and increase of hydrogen rate, or retrofitted processes with new units [20]. That leads to an expensive process in terms of high operating cost and significant investment of capital.

2.2.3 Non HDS-based alternative technologies

The production of transportation fuels having very low content of sulfur became one of the priory actual challenges for oil refineries worldwide forced by new strict regulatory requirements. Under this context, many researchers have been developing methods to meet these sulfur regulations based on improving the current HDS process in refineries (highly active catalysts, reactor improvements, …) as it was previously mentioned. But it is also being stringently necessary to explore alternative desulfurization approaches as reactive distillation, several precipitation techniques, reactive alkylation, complexation, selective oxidation, adsorption, biodesulfurization, photochemical desulfurization, several utltrasonic extraction treatments, and their combinations already reviewed in literature [15, 19, 21-25]:

i. Reactive alkylation

When boiling point of organosulfur compounds is shifted to a higher value, they can be removed from light fractions by distillation and concentrated in the heavy boiling part of the refinery streams. Particularly, in the 1990s British Petroleum invented the Olefin Alkylation Thiophenic Sulfur (OATS) technology to be an alternative to HDS process [26]. The great advantages of the OATS process are the mild reaction conditions, and that other reactants but olefins and catalyst are needless. Moreover, OATS could alleviate the octane number loss of the treated gasoline. BP used this option for desulfurizing FCC gasoline streams [27, 28]. Therefore, OATS has the potential to be a complement of HDS process. Some works have appeared studying the OATS process in the model gasoline systems [29, 30]

ii. Precipitation techniques

Acheson and Harrison [31, 32] have reported that benzothiophenes (BTs) and dibenzothiophenes (DBTs) are successfully methylated by iodomethane in the presence of silver tetrafluoroborate to give rise at room temperature to crystalline powders of S-meghylated benzothiophenium and dibenzothiophenium tetrafluoroborates, respectively. These are highly polarized (soluble in water) and insoluble in non-polar hydrocarbon solvents. Thus, such a synthetic method, if applied to desulfurization of non-polar light oils, might be able to remove BT

and its derivates as precipitates under moderate conditions. This has been later demonstrated by Shiraishi et al. [33-36] and even applied for denitrogenation purposes.

Other desulfurizations by precipitation techniques are based on the formation and removal of insoluble Charge-Transfer Complexes (CTC). Moreover, there is a competition in complex formation between DBT compounds and other non-sulfur aromatics that results in low selectivity for DBT removal [37, 38].

iii. Selective oxidative desulfurization (ODS)

Generally this technique consists on the oxidation of sulfur compounds and subsequent separation of oxidized sulfur containing compounds from fuel streams by distillation, adsorption or thermal decomposition [39, 40]. The applicability of an oxidative desulfurization scheme depends on the kinetics and selectivity of the oxidation of the organic sulfur compounds to sulfones [41, 42]. To make this process efficient, an appropriate catalyst with high selectivity for oxidation should be identified.

In chemical synthesis the most common procedure to prepare sulfones is by oxidation reaction with a peroxycarboxylic acid generated in situ by hydrogen peroxide and the appropriate carboxylic acid [43]. Even sulfur compounds with low nucleophilicity such as DBT can be oxidized under mild conditions to sulfoxides or sulfones in large yields, extended reaction times and excessive decomposition of hydrogen peroxide was found in the reaction that made it impractical at industrial scale [42, 44].

iv. Adsorption techniques (ADS)

Desulfurization by adsorption is based on the ability of a solid sorbent to selectively adsorb organosulfur compounds from refinery streams [45-50].

Based on the mechanism of the sulfur compound interaction with the sorbent, ADS can be divided into different groups: “adsorptive desulfurization” (based on physical adsorption on the solid surface) and “reactive adsorption desuldurization” (chemisorptions, which means chemical interactions with the sorbent) and π-complexation adsorption. Physisorbed sulfur compounds can be easily removed from adsorbents (which are easy to regenerate). However the adsorptive selectivity and capability are not high. For chemisorption, adsorptive selectivity and capability are high but the adsorbents are hard to be regenerated. Interaction force of π-complexation is among that of physical adsorption and chemisorption.

v. Biodesulfurization

The concept of "biorefining" in petrochemistry is increasingly becoming a viable reality thanks to the low cost of biological technology. Biodesulfurization is a process that removes sulfur from fossil fuels using a series of enzyme-calalyzed reactions [51]. Certain microbial biocatalysts have been identified that can biotransform sulfur compounds found in fuels, including ones that selectively remove sulfur from dibenzothiophene heterocyclic compounds[52, 53]. Better understanding of the mechanism of biodesulfurization might be gained from some recent studies [54-58].These recent discoveries related to mechanisms, may lead to commercial applications of biodesulfurizaton. With bioprocess improvements that enhance biocatalyst stability, achieve faster kinetics, improve mass transfer limitations, temperature and solvent tolerance, as well as broaden substrate specificity to attack a greater range of heterocyclic compounds, biocatalysis may be a cost-effective approach to achieve the low sulfur fuels.

For a biodesulfurization process to be competitive with HDS, three main steps need to be followed: in first place, separation entailing some pretreatment of crude oil, in second place, conversion (biocatalytic process where the biocatalyst favours a selective desulfurization process without destroying useful products), and finally, it might be possible to separate crude oil from the biocatalyst and byproducts. Conversion and final separation are affected by biocatalyst specificity, stability, activity and bioreactor design [59].

Since 1935 [60, 61], when an early account of microbial desulfurization of curide oil was published, the ability of microorganisms to remove sulfur from hydrocarbons has been studied and reviewed in literature [62-69]. However, total desulfurization of fossil fuels by microbial approach is not expected to occur in early future and more research is needed to design a recombinant strain with a broader range of target sulfur compounds or to use successive desulfurizing microbial systems with high potency. Dealing with genuine fossil fuel has opened up new challenges to solve.

vi. Desulfurization via extraction

Extractive desulfurization is based on the fact that organosulfur compounds are more soluble than hydrocarbons in an appropriate solvent. The general process flow is showed in Figure 2. In a mixing tank, the sulfur compounds are transferred from the fuel oil into the solvent due to their higher solubility. The desulfurized hydrocarbon stream is used either as a component to be blended into the final product or as a feed for further transformations. The organosulfur compounds are separated by distillation and the solvent is recycled.

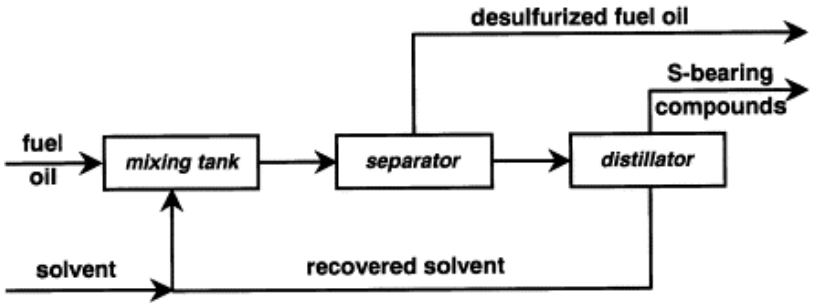

Figure 2. General view of an extractive desulfurization process [19].

The most attractive feature of the extractive desulfurization is the applicability at low temperature and low pressure. The mixing tank can even operate at ambient conditions. The process does not change the chemical structure of the fuel oil components. As the equipment used is rather conventional without special requirements, the process can be easily integrated into the refinery. To make the process efficient, the solvent must be carefully selected to satisfy a number of requirements. The organosulfur compounds must be highly soluble in the solvent. The solvent must have a boiling temperature different than that of the sulfur containing compounds, and it must be inexpensive to ensure economic feasibility of the process.

The efficiency of extractive desulfurization is mainly limited by the solubility of the organic sulfur compounds in the solvent. Solubility can be enhanced by choosing an appropriate solvent taking into account the nature of the sulfur compounds to be removed. A lot of organic solvents such as polyalkyleneglycol, polyalkyleneglycol ether, pyrrolidones, imidazolidinones, dimethyl sulfoxide and pyrimidinones were tried as extractants for the removal of sulfur compounds from fuel, but none of them obtaining satisfactory performances. This is usually achieved by using a ‘solvent cocktail’ such as acetone–ethanol [70] or a tetraethylene glycol–methoxytri glycol mixture [71]. Preparation of such a ‘solvent cocktail’ is rather difficult and intrinsically non-efficient since its composition depends strongly on the spectrum of the organosulfur compounds present in the feed stream.

vii. Combined extraction techniques

- *Extractive Distillation*

An extractive distillation process, GT-DeSulph™ has been reported by GTC company in 2002, which utilizes a proprietary aromatics selective solvent, effective in extracting thiophenic sulfur species and aromatics, and at a limited extent, mercaptans and sulphides as well. Combination of a solvent and a photosensitizer has to be optimized to increase the rate of the organosulfur compounds phototransformation [23].

- *Oxidation followed by solvent extraction*

After oxidation, the sulfur compounds are transformed to sulfones and sulfoxides. These compounds are considered to be easily removed from hydrocarbon mixtures by solvent extraction [78]. The oxidation method has capabilities, not only to decrease the sulfur content in light oil but also to recover the sulfur component as organic sulfur compound which can have a potential industrial use [79].

With respect to the commercial oxidation process development, Petrostar developed a desulfurization technology, which removes sulfur from diesel fuels using chemical oxidation [15]. Desulfurization of diesel fuel is accomplished by first forming a water emulsion with the diesel fuel. In the emulsion, the sulfur atom is oxidized to a sulfone using catalyzed peroxyacetic acid. With an oxygen atom attached to the sulfur one, the molecules become polar and hydrophilic and then move into the aqueous phase. The Environmental Protection Agency (EPA) has indicated that there is a similar process, except instead of keeping the sulfone intact; this process separates the oxidized sulfur atom from the hydrocarbon mixture immediately after the oxidation reaction.

2.3 Ionic Liquids

2.3.1. A little bit of history

Over the past years Ionic Liquids (ILs) became a promising family of substances that have been object of mushrooming research. From the beginning of this decade, they have been defined as salts with melting point below 100ºC [80-82]. This definition based on temperature does not imply much information about composition, properties...of those substances by itself, but the fact that they are completely ionic substances. This temperature does not have any chemical or physical significance and in fact, it is just now that it is being queried.

As John S. Wilkes said [83], *"The historical answer to the nature of the present ionic liquids is somewhat in the eye of the beholder. The very brief history presented here is just one of the many possible ones"*.

The ionic liquids researching field started in 1914 when Paul Walden (figure 3) described the physical properties of ethylammonium nitrate as a first example of an ionic liquid. This discovery did not attract too much attention at that time, despite the great open research opportunity which had been initiated.

Figure 3. Paul Walden, discoverer of the first ionic liquid

After more than 3 decades of silence, ionic liquids emerged after the Second World Ward in at least one patent in 1948 [84] and later on in open literature [86] when in 1951 Hurley and Wier developed low melting salts with chloroaluminate ions for low-temperature electroplanting

of aluminium which were known as "the first generation of ionic liquids". During the period covering the decades of 1970s and 1980s these liquids were studied mainly for electrochemical applications [86, 87]. This was an important discovery, but these solvents were chemically complicated and difficult to investigate, owing to rapid hydrolysis, which required inert atmosphere. In fact, this problem was not overcome since Osteryoung [88] (Figure 4) (Colorado State University) and Gilbert [89] (Figure 4) (University of Liege) studied the 1-butylpyridinium chloride and aluminium (III) chloride ionic liquids. They were liquid at room temperature, but only over a very narrow compositional range.

The compounds known as liquid clathrates are materials that now are recognized as ionic liquids. These materials were discovered in the 1970s by Prof. Jerry Atwood and his group in the University of Alabama. Liquid clathrates are composed by a salt combined with an aluminium alkyl, which forms a compound with one or more aromatic molecules [90]. They have and interesting but indirect connection with modern day ionic liquids. Some of the students of Prof. Atwood at this time were Robin Rogers, Richard Carlin, Michael Zaworotko and Joan Fuller, names that will intensively shine later in the research of ionic liquids.

One step further Osteryoung group, Wilkes (Figure 4) and Hussey [86] from the US Air Force Academy explored the 1,3-dialkylimidazolium chloroaluminate ionic liquids showing much wider liquid range. The motivation of their study was to develop an electrolyte with lower melting temperature for the thermal batteries. But a major drawback of all chloroaluminate (III) ionic liquids was their moisture sensitivity. J. S. Wilkes marks in his review of 2002 [81] "*the start of the modern era of ionic liquids as the simultaneous collaborative discovery of the 1-butylpyridinium chloride-aluminium chloride mixtrure (BPC-$AlCl_3$) by the groups of Colorado State University* (first published paper [89]) *and the Air Force Academy* (first granted patent [91])" showing how close the collaboration was.

Figure 4. Prof. Robert Osteryoung (left), Prof. Bernard Gilbert (center) and Prof. J. S. Wilkes(right)

In 1990s it became clear that many combinations of ions form air- and water-stable ionic liquids. In 1992, Wilkes and Zaworotko [92] reported the preparation and characterization of a new range of ionic liquids under the title "*Air and water stable 1-ethyl-3-methylimidazolium based ionic liquids",* and known as "the second generation of ionic liquids" Since then, ionic liquids have become increasingly popular in academia and industry. By the mid 1990s, the basic understanding of the ionic liquids concept was well known by a narrow scientific community, but this area of esoteric curiosity was of little interest, or too specialised, for synthetic industrial applications. However, there was a suggestion that ionic liquids could be used for green chemistry and industrial chemistry *"The reactions we have observed represent the tip of an iceberg-all the indications are that room temperature ionic liquids are the basis of a new industrial technology. They are truly designer solvents [...] for the first time, it is possible to design a solvent to optimise a reaction [...]. This, quite literally, revolutionises the methodology of synthetic organic chemistry: it will never be the same again!"*[93]

2.3.2. What can be called "ionic liquid"?

As T. Welton pointed in his first well- known review of 1999 [87] chemistry is dominated by the study of species in solution. When chemical engineers face with a unit operation which calls for a solvent, common ones all have a relatively narrow liquid region, so most processes have been developed under the constrains imposed by their relatively small range of temperatures. Ingenuity and tools of chemical engineering have been used to fight against these constrains, making products that have highly improved the quality of life on the Earth.

"A new class of compounds has emerged in the last ten years that may become a key ally in helping us meet the twin challenges of efficient and environmentally benign chemical processing. They have the potential to revolutionize the way we think of and use solvents."[80]

In simple words, ionic liquids are liquids that are comprised entirely by ions. In this sense, molten sodium chloride is an ionic liquid so, what constitutes an "ionic liquid" as different from a molten salt? It is generally accepted that ionic liquids have relatively low melting points, ideally below ambient temperature [93] (commonly known as "room temperature ionic liquids"). The distinction is arbitrarily based on the salt liquidity below a given temperature, often conveniently taken to be 100ºC.

Seddon also introduced in this context the term "neoteric solvents" well stablished in the English language. This term is used here to indicate a class of novel solvents that have remarkable

new properties, that "break new ground" and that offer a huge potential for industrial applications. It is applied not only to ionic liquids but also to supercritical fluids [94].

"*Ionic liquids have been showed many of the advantages of molten salts, and they avoid the worst disadvantages caused by high temperature*" [81]

Ionic liquids are organic salts, invariably possessing a high degree of asymmetry that frustrates packing and thus inhibits crystallization. The possible choices of cation and anion which results in the formation of ILs are numerous. There is virtually no limit in the number of salts with low melting points. In fact, Holbrey and Seddon have estimated this number to be of the order of 1 trillion [95]. "*It seems obvious to me and to most other chemists that the table of cations and anions that form ionic liquids can and will be extended to a nearly limitless number. The applications will be limited only by our imagination*" (Wilkes [92]). As there is no only one type of cation or anion, these solvents can be designed for a particular end use in mind or for a particular set of properties which has lead to the term "designer solvents" being applied to ionic liquids. [96] With the potential wide matrix of both cations and anions, it becomes clear that it will be impossible to screen any particular application using all ionic liquids, or even all within a subset containing only a single anion or cation. It was stated that selected properties, such as thermal stability and misciblility depend on the anion, while others, such as viscosity, surface tension or density depend on the length of the alkyl chain in the cation and/or shape or symmetry. Work is clearly needed to determine how properties of ionic liquids vary as functions of anion/cation/substitution patterns, etc. and to establish in any property changes in systematic ways [97].

In figure 5 we can see some of the usual combinations of cations and anions in current ionic liquids.

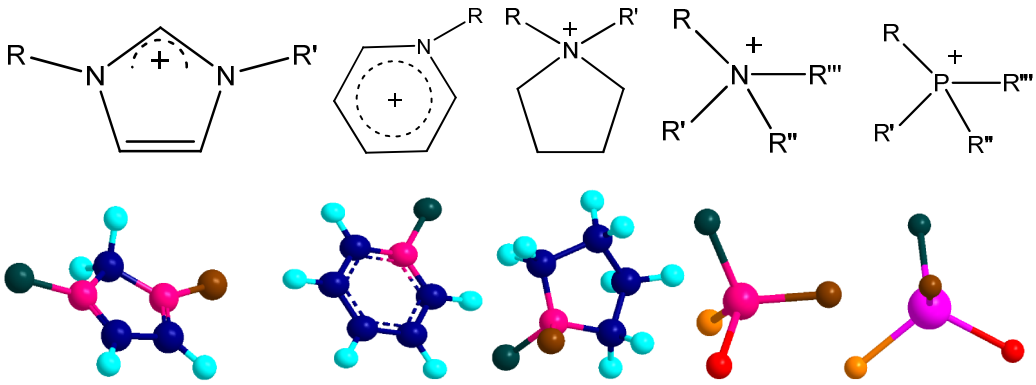

Figure 5a) Some of the common cations of current ionic liquids , figures in 2D(upper line) and in 3D(lower line) representing from left to right: 1,3-dialkylimidazolium, 1-alkylpyridinium, 1,1-dialkylpyrrolidinium, tetraalkylammonium and tetraalkylphosphonium

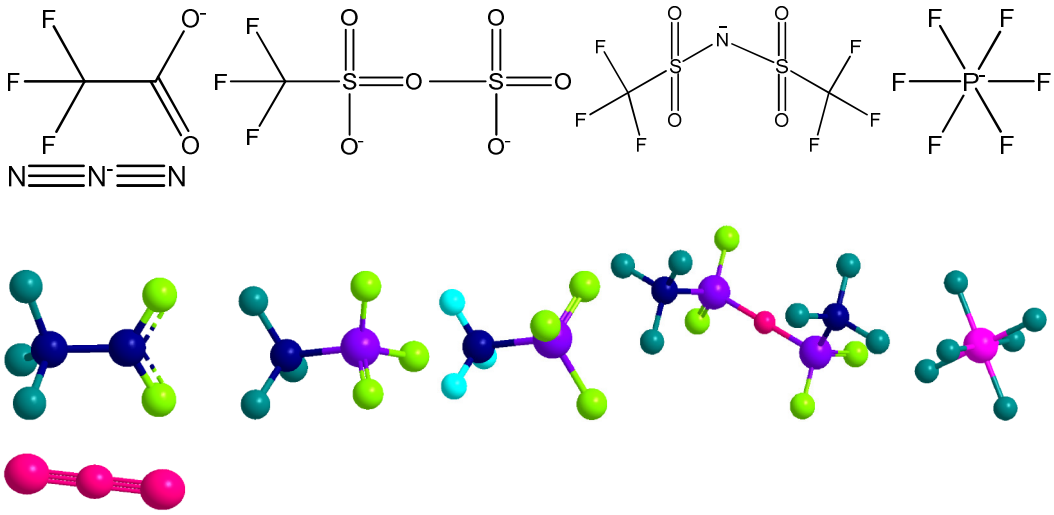

Figure 5. Some of the common anions of current ionic liquids , figures in 2D (upper line) and in 3D(lower line) representing from left to right: trifluoroacetate, trifluoromethanesulfonate or triflate, methanesulfonate or mesylate, bis{(trifluoromethyl)sulfonyl}amide, hexafluorophosphate and dicyanamide,.

2.3.3. Why to use ionic liquids?

Volatile organic solvents are the normal media for the industrial synthesis of organic chemicals (petrochemical and pharmaceutical). However, the environmental impact of these solvents is significant and the Montreal Protocol has resulted in a compelling need to revalue many chemical processes that have proved otherwise satisfactory for much of this century. Clean technology concerns the reduction of waste to a minimum, it requires the rethinking and redesign of many chemical processes.

Ionic liquids are organic salts that are liquid under ambient conditions, are being heralded as possible replacement solvents for volatile organics primarily because of the lack of any appreciable vapour pressures which in turn may greatly reduce emission and worker exposure hazards [98].

Ionic liquids have *inter alia*, the following desirable properties:

– The *liquid ranges* exhibited by ILs can be much greater than those found in common molecular solvents, allowing tremendous kinetic control: they are organic salts invariably having a high degree of asymmetry that frustrates packing, and thus, inhibits crystallization. This behaviour is consequence of a combination of dominant coulombic charge-charge attractions balanced against rotational and vibrational freedom of the ions. However, the absence of strong H-bonding is certainly a major contributor to low melting points, but this

effect was not observed when studying ILs (which can be seen as a contradiction comparing to other usual solvents), so this implies that Van der Waals interactions or methyl-π interactions...are more important than the H ones. In any case, it is important that the forces and interactions that govern the melting points of ILs cannot be considered in isolation. In fact, they also control the dissolution and solubility of different components in the ILs, etc [80, 94, 98-100].

- They are outstanding new solvents for a wide range of inorganic, organic and polymeric materials (high solubility implies small reactor volumes), being able to solvate large number of species including organometallic compounds [86, 101]. It must be highlighted that they can also provide a highly polar but at the same time non-coordinated medium [102, 103], so they can be immiscible with a number of organic solvents and/or water, being a promising choice for multiphase systems.
- They exhibit Brϕnsted, Lewis and Franklin acidity as well as superacidity [104-107]. Recently, interest in the development of protic ILs has considerably increased because of the great potential offered by these compounds for proton-transfer applications in advanced fuel-cell technologies [108].
- Their relative favourable viscosity and density characteristics [92]: the majority of ILs are denser than water, and most of them are viscous liquids, with viscosities comparable to oils being two or three times greater than those of conventional organic solvents [109]. Both properties can be easily tailored by simple changes to the structure of the ions.
- They have *no effective vapour pressure*: ionic liquids, consisting of totally ionized components and displaying relatively weak ion-ion pairing in comparison to molten salts, have little or no measurable vapour pressures. In fact, their lack of measurable vapour pressure facilitates their handle and forms one of the foundations of the "green" nature of ionic liquids [110]. In contrast to molecular solvents, the upper liquid limit for ionic liquids is usually that of the thermal decomposition rather than vaporization. They are most of them *highly thermally stable*. Eventually, at high temperatures the vapour pressure should become detectable, but in the high-temperature regime the thermal stability of ILs is of concern. Involatility had been assumed to be a property common to all ILs that do not undergo thermal decomposition. Earle and colleagues [111] changed that assumption, showing that certain ionic liquid structures known for their very high thermal stability can be evaporated and recondensed under relative mild conditions. Most interestingly, they also report the separation by distillation of two ionic liquids. Even if ILs have been used in extractive distillation processes and tested for their long-term stability showing no significant loss of ionic liquid (at high pressures or ultra-high vacuum) analysis did not detect any decomposing or evaporating. The finding of these authors means that non-volatility is not a property that can be assumed for all thermally stable ILs:

vapour pressure is just another physical-chemical property that depends on anion-cation combination, and will have to be checked experimentally for each new ionic liquid [112, 113].

- Their water sensitivity does not restrict their industrial applications, and there are nowadays many ionic liquids in use which are air- and water-stable [92, 114].
- In most of the cases, they show non flammability, high conductivity, and high hygroscopicity.
- They are *relatively cheap*, and easy to synthesize. There are a variety of challenges associated with turning ionic liquids from scientific curiosities into practical fluids for industrial use. It has to do with cost, lack of physical properties and corrosion data, and absence of toxicity data. Currently, ionic liquids are synthesized primarily in laboratory-scale quantities. To be competitive with conventional solvents, their price should be reduced by a factor of 100 or more. The major cost associated with adopting ILs in many of the industrial applications is the cost of the IL itself. It is entirely likely that they can be used with existing equipment in many of the suggested applications. Furthermore, ILs are a flexible technology. Their tunneability gives the engineers many more options in optimizing these materials for a given process [80].
- Ionic liquids are becoming established as potentially and environmentally viable as alternative to existing solvents. They present a greener alternative in many applications. As this maturation continues, green considerations for the evaluation of their development and use must also be continually raised. William L. Nelson give an initial rating of the ILs in the following table (Table1)

Table 1. Report Card [115]: G (good), P (poor), U (unknown)

Greening of ionic liquids	G	P	U
– Does the solvent use lead to less energy expenditure?		*	
– Does the solvated species react more efficanciously and selectively?	*		
– Does the solvent improve atom-economy?	*		
– What is solvent distribution into environment?			*
– Will the solvent be absorbed by organisms and how will it affect them?			*
– Is the solvent toxic? Can it be detoxified			*

2.3.4. Potential and current applications of ionic liquids: general notes

Since all the potential uses of ionic liquids have not yet been developed, they cannot be enumerated here. Nonetheless, some of the applications or fields for which unique properties of ionic liquids could be advantageous will be briefly commented:

As we pointed along the historical course of ionic liquids field, it seems as if everything was started with the right foot, when first finding these new substances to overcome molten salts limitations. Those first applications, which still growing in number and potentiality, were pointed to their use as electrolytes in batteries, lithium-ion batteries, electrochemical synthesis or electrodeposition of metals [81, 116].

Not so far away in time, several visionary authors, tried to take advantage of promising properties of ionic liquids as solvents and/or catalysts for multiple reactions already reviewed in the literature [80, 87, 114, 117] ILs have been used successfully for hydrogenations, hydroformilations, isomerizations, dimerizations, alkylations, Diels-Alder reactions, Heck and Suzuki coupling reactions...among others. In general, researchers have found that reaction rates and selectivities are as good or better in ILs as in conventional solvents. Recently, it has even show that they are excellent media for biocatalyzed reactions [118].

Since it was found that ILs tend to wet metal, polymeric and inorganic surfaces, and combined with their thermal stability and large liquid range, it makes them excellent candidates for lubricants in high temperature and/or low pressure applications. Very little research was found on this potential application.

Those same characteristics, allow them to have the potential to compete as heat-transfer fluids with even the most successful synthetic organic and silicone-based compounds in fluid market.

It was also studied the applicability of ionic liquids as versatile components in microemulsions and as solvents for the synthesis of nanomaterials [119].

Using imidazolium-based ILs as replacements for the traditional solvents to separate azeotropic mixtures as an alternative to extractive distillation has widely been investigated [120-124].

Based on the different in solubility of various gases and vapours, the potential use of ILs and actually trendy, is gas separations [125]. Some ionic liquids might even be considered “pump absorbents”, capable of absorbing large quantities of gases at low temperature and then, being

regenerated at high temperature or low pressure. ILs also would be ideally suited for gas separations using a supported liquid membrane. Some other innovative applications are studied as storage and delivery of hazardous gases absorbed in ILs [126].

Since the choice of cation-anion combinations provides a great opportunity to tailor the solubility of diverse compounds in the ILs, they should have many applications in selective separation of liquids. They may prove to be suitable replacements for the toxic, flammable and volatile organic compounds that are currently used in liquid-liquid separation processes. Prof. R. D. Rogers has demonstrated that partitioning of many organic solutes between an ionic liquid and water corresponds approximately to the distribution of the same compounds between organic solvents and water [103].Their properties led to their use as solvents or additives in solvent extraction processes, for instance, in aqueous biphasic systems [127]. The formation of biphasic, essentially non-volatile solvent system, with good thermal stability, simply upon mixing some ILs with some selected polymers with interesting credentials as process solvents has also been studied [128]. They can also be found as extremely useful GC stationary phases of original polarity [129, 130]. Additionally, it may be apparent that *"ionic liquids may in themselves be suitable, and indeed favourable, media for the design of novel liquid-liquid extraction systems"* [102, 130]. R. D. Rogers also said:*"We have shown that room-temperature ionic liquids can be viewed as classical solvents and that they are suitable for liquid-liquid extraction processes".* [132] Their potential use as solvents in liquid-liquid extraction applications has been demonstrated and extensively exposed in literature, highlighting the work done by our research group into the cited field [133-149].

2.3.5. Do we understand the recyclability of Ionic Liquids?

It is somewhat surprising that the easy recyclability, which is a key property of ILs responsible of their increasingly popularity has not been extensively studied. Owing to the lack of volatility, ILs do not contribute to the release of harmful vapours into the atmosphere. Moreover this property allows recovering them easily from mixtures with compounds which have low boiling points by simple distillation. However, direct vacuum distillation protocol is energy-consuming, particularly for non-volatile compound/IL systems. Moreover, if the IL has a tendency to undergo hydrolytic decomposition, direct heating should be avoided or at least, minimized.

Their release to aquatic environments can cause severe water contamination, because of their sometimes potential or inaccessible toxicity or biodegradability. Researches need to find

alternative ways to recycle them, as sometimes cleaning them up involves washing with water or volatile organic compounds which creates waste streams.

Many ILs can be recovered by using conventional organic solvents which in any case reduces the "green" aspect of their usage. Generally, hydrophobic ionic liquids can be extracted with water to separate water-soluble solutes from the IL into the aqueous phase. However, this method is not suitable for hydrophilic ionic liquids.

Supercritical Fluids (SFCs) may solve these problems [150]. The advantages of using them as extraction medium include nontoxic nature, recoverability and ease of separation from the products. Supercritical CO_2 is the most widely used [151-155].

Recently, Rogers and co-workers [156] demonstrated that the addition of a water-structuring salt to an aqueous solution of a hydrophilic ionic liquid produced an aqueous biphasic system (ABS), this salting-out effect provides hydrophilic ILs with the potential for recycling them from aqueous solutions.

Membrane separation technologies may be another alternative. A key among all performance advantages is that for removal of materials in the ionic size range, only distillation can provide a similar level of fluid purity. Therefore it is necessary to explore novel membrane treatment process for ILs recovery. Nanofiltration membranes were in fact employed by Livingston et al. [157].

Clearly, recycling is an important issue not only from the economical point of view, but for concerning about ionic liquids disposal, biodegradation and toxicity. We are only in the very beginning of the understanding of the recyclability of ILs. In few words, there is a long road ahead for large scale applications to be extended.

2.4 Ionic liquids as solvents in extractive desulfurization

ILs are promising replacements for conventional non desirable organic solvents [103, 129] to act as entrainers in liquid-liquid extraction. It has been explained that most of ionic liquids have many attractive properties such as chemical and thermal stability, nonflammability, high ionic conductivity, wide range of potential window and they possess a very low vapour pressure, which may be the single most attractive property for their use as solvents [93]. A key feature of ionic liquids is that their properties can be tailored by judicious selection of cation, anion and

substituents so they can be designed to perform selective liquid-liquid separations [93, 95, 110]. To improve the safety and environmental friendliness of this conventional separation technique, ionic liquids can be used as ideal substitutes of conventional solvents for the design of novel liquid-liquid extraction systems [103, 131].

The use of ionic liquids for the selective extraction of sulfur compounds from diesel fuel was described by Bössman et al. for the first time [158]. Keeping in mind that the most popular ionic liquids are undoubtedly the di-alkylimidazolium salts, due to their easy synthesis and attractive physical properties, and based on the initial idea of the extraction of sulfur compounds by chemical interaction, these authors investigated the extraction with Lewis- and Brønsted-acidic ionic liquids employing mixtures of n-butyl-3-methylimidazolium chloride and n-ethyl-3-methylimidazolium chloride with $AlCl_3$. Even though $AlCl_3$ and $AlCl_4$ based ionic liquids are effective for the removal of S-containing compounds[158], they often form dark precipitates and they are sensitive to water presence [159] generating HCl and making them unstable in air and of limited practical utility.

Ionic liquid extraction power for DBT has been proved to be not uniquely based on chemical interactions involving the acid proton, so different cation/anion combinations of neutral ILs were tested [158], showing that desulfurization is hardly affected by the chemical nature of the anion being the size of ions important for the extraction effect. A possible explanation for this behaviour may be that solubility of sulfur-containing compounds (DBT and derivates) is dependent on steric factors in the IL.

Several authors studied the use of PF_6- and BF_4- anions for imidazolium-based ionic liquids [161-163] significantly more stable to hydrolysis. Sulfur was preferentially removed from gasoline samples but also a change in the content of aromatics was observed, which can be problematic for maintaining octane number in gasoline. Several liquid-liquid equilibrium studies reinforce this conclusion [164-166] being part of this thesis work, and already published. Coulombian interactions between these ionic liquids and S-containing compounds were also studied [167]. Removal of sulfur-containing molecules with high density of aromatic π electrons is favoured due to stronger interactions with this kind of ILs. The extractive removal efficiency for aromatic nitrogen compounds is also high and extraction results indicated that these ILs are particulary selective for aromatic N-containing compounds from fuels. But the use of these PF_6 and BF_4 ILs as large scale extracting agents is not optimal because of the relative high price of starting material and additionally, the formation of hydrolysis products, especially HF- is observed at elevated temperatures in presence of water [168].

To avoid these stability and corrosion problems, the use of completely halogen-free ILs was suggested [169, 170]. N-alkyl-3-methylimidazolium alkylsulfates were tried as readily accessible from cheap starting materials.

Several studies of liquid-liquid equilibrium data of different fuel components and S-containing compounds were done strengthening conclusions of suitability of [EMIM][$EtSO_4$] as solvent extractant [171, 172] These investigations form part of this thesis work and are already published. It might look inconsistent to use S-containing ILs for desulfurization but leaching of IL into the oil phase is in any case unwanted. Nevertheless, certain degree of cross-solubility of hydrocarbons in the IL was observed. In the case of [BMIM][$OcSO_4$], distribution coefficients for S-compounds is two times higher than for [EMIM][$EtSO_4$] but the cross solubility is a factor four to sixteen times higher.

Also, N-alkyl-3-methylimidazolium bis(trifluoromethylsulfonyl)imide ionic liquids were studied and compared to tetrafluoborate or alkylsulfate ones [173-176], as an innovative part of this thesis work and already published not showing definitive conclusions about the better suitability of these ILs for this application. Searching in a different way, Huang et al. [177] proposed the use of CuCl-based ionic liquids, also moisture-insensitive and stable in air. These ILs showed remarkable desulfurization ability attributed to the π-complexation of Cu (I) with aromatic S-containing compounds.

As cheaper option for real industrial application, the use of imidazolium-based phosphoric ionic liquids was also analyzed [168, 178-180] with encouraging results. It was showed that desulfurization ability of the studied ILs varies following the order [BMIM][DBP]>[EMIM][DEP]>>[MMIM][DMP], however fuel solubility in ILs is noticeable following the same tendency. [EMIM][DEP] was the recommended IL. Later on the same authors suggest the use of [EEIM][DEP] [180]. Nie et al. [182] studied the effect of the length of the alkyl group of these cations for alkylphosphate ionic liquids, showing as expected that the longer the alkyl substitute of the anion or cation, the higher the partition coefficient value for the studied ionic liquid.

Among all cation-anion combination options which offer the huge family of ionic liquids, Holbrey et al. [183] investigated the DBT extraction power from dodecane for a range of ionic liquids varying cation and anion classes. Polyaromatic quinolinum-based ionic liquids were found to show the best extractive ability, nevertheless, these and other polyaromatic cations, such as 1,3-dibenzimidazolium are technically limited by their high melting points and only tend to form low-melting point ionic liquids when combined with highly flexible perfluorinated anions such as bis(trifluoromethylsulfonyl)amide. This studio ranks ionic liquids desulfurization ability by cation following the sequence methylpiridinium ≥ pyridinium ≈ imidazolium ≈ pyrrolidinium with much

less significant variation with anion type. Following this line, Gao et al. [184, 185] perform several extraction experiments with alkyl- and alkylmethyl-pyridinium-based ionic liquids, but best results were found for [alkyl-dmpy] + ionic liquids. With these cations, ethanoate and thiocyanate anions gave the best extraction performance (consistent with phase equilibrium studies from Domanska et al. [186]). In this way, these more benign and cheaper anions could be used as alternative to the perfluorinated and tetrafluoborate ones.

Continuum solvation models based on the COnductor like Screening MOdel (COSMO) along with its extension to Real Solvents (COSMO-RS) also reinforce the idea of suitability of methylpyridinium ionic liquids as solvents for desulfurization [187] and extracted conclusions were taken into account in the development of this researching work.

A more complex option is the use of Oxidative Desulfurization (ODS), which involves in a first step oxidizing sulfur compounds, such as DBT and its derivatives, to transform them into sulfones and sulfoxides [188]. In a second step these oxidized products are removed by selective extraction with polar solvents, such as dimethyl sulfoxide.

Taking a step forward, Lu et al. [189] described in their work a combination of ODS and extraction with BF_4 ILs. It was proved that desulfurization yield is increased by about one order of magnitude compared with merely extracting with ILs. Several authors had already tried this idea adding H_2O_2 as oxidant with several catalysts as acetic acid [190], phosphotungstenic acid [191], decatungstates [192], V_2O_5 [193], and several different ionic liquids (quaternary ammonium coordinated ionic liquids [194], n-methyl pyrrolidinium ionic liquids [195] or even task-specific ionic liquids [196]) as extractants. Zhu et al. [195] demonstrated using peroxotungsten and peroxomolybdenum complexes in ILs that when H_2O_2 and catalyst are introduced together, the removal of sulfur increased sharply. Zhao et al. [193, 196-198] studied ODS using [HNMP][BF_4] and [HNMP][H_2PO_4] which act also themselves as catalysts. However, imidazolium or pyrrolidinium-based ionic liquids are relatively expensive and impossible to use in ODS for industry. Lewis acidic ionic liquids containing metal halide anions such as $AlCl_4$ [162,200], $FeCl_4$ [201] and $CuCl_2$ [202a] or $ZnCl_2$ [202b] are being studied.

3. RESEARCH PROTOCOL

3. RESEARCH PROTOCOL

The development of this researching work is divided in three well differenced sections:

- In first place the studio of liquid-liquid equilibrium of the systems involved in the process, with the aim of evaluating the solvent ability for the extraction of sulfur and nitrogen compounds from transport fuels using thermodynamical criteria.

- In second place, to prove the efficiency of the process and the consistency with the previous stage exposed above, synthetic mixtures of both gasoline and diesel models which simulate the real ones will be prepared. A three step extraction experiment using the studied ionic liquids as solvents will be carried out, and the composition of each one of the compounds is going to be followed along each one of the extraction steps.

- Finally, this three steps extraction process is going to be repeated using real samples of gasoline and diesel previous to desulfurization process. Conclusions about the feasibility of the project are going to be exposed in base of the obtained results.

3.1. Selection of the ionic liquids

The first step in the work is the selection of the ionic liquids. The main concern about an "*a priori"* choice of a solvent for an extraction purpose is about solubilities. It is needed to search for a solvent which dissolve preferentially the organic sulfur-containing compounds and the nitrogen-containing compounds with the minimal or non appreciable solubility of the rest of the fuel constituents. Solubility tests with thiophene, pyridine and several different hydrocarbons have been carried out. Other relevant considerations are accessibility in terms of synthesis path and raw materials, manageability, toxicity, suitable physical properties, economy….

After this first screening, three imidazolium-based ionic liquids were chosen: 1-octyl-3-methylimidazolium tetrafluoborate ($[C_8mim][BF_4]$), 1-octyl-3-methylimidazolium bis{(trifluoromethyl sulfonyl)imide}($[C_8mim][NTf_2]$) and 1-ethyl-3-methylimidazolium ethylsulfate($[C_2mim][EtSO_4]$). Subsequently, a fourth poly substituted pyridinium ionic liquid, 1-hexyl-3,5-dimethylpyridinium bis(trifluoromethyl sulfonyl)imide ($[C_6mmPy][NTf_2]$) was selected basing this choice in recent literature data and COSMO-RS estimations.

3.2. Liquid-Liquid Equilibrium (LLE)

For the design of extraction processes with solvents, knowledge of liquid-liquid equilibrium is of vital importance. Given the complexity of the study of liquid-liquid equilibrium in multi-component systems of more than three components, from a practical point of view it is useful to study the involved ternary systems.

The studied ternary systems are the following:

Ternary systems with ionic liquid [C_8min][NTf_2.]:

- *[C_8mim][NTf_2.]+Thiophene+Hexane*
- *[C_8mim][NTf_2.]+Thiophene+Heptane*
- *[C_8mim][NTf_2.]+Thiophene+Dodecane*
- *[C_8mim][NTf_2.]+Thiophene+Hexadecane*
- *[C_8mim][NTf_2.]+Thiophene+i-Octane*
- *[C_8mim][NTf_2.]+Thiophene+Toluene*
- *[C_8mim][NTf_2.]+Pyridine+Hexane*

Ternary systems with ionic liquid [C_8min][BF_4]:

- *[C_8mim][BF_4.]+Thiophene+Hexane*
- *[C_8mim][BF_4.]+Thiophene+Heptane*
- *[C_8mim][BF_4.]+Thiophene+Dodecane*
- *[C_8mim][BF_4.]+Thiophene+Hexadecane*
- *[C_8mim][BF_4.]+Thiophene+i-Octane*
- *[C_8mim][BF_4.]+Thiophene+Toluene*
- *[C_8mim][BF_4.]+Pyridine+Hexane*

Ternary systems with ionic liquid [C_2min][$EtSO_4$.]:

- *[C_2mim][$EtSO_4$.]+Thiophene+Hexane*
- *[C_2mim][$EtSO_4$.]+Thiophene+Heptane*
- *[C_2mim][$EtSO_4$.]+Thiophene+Dodecane*
- *[C_2mim][$EtSO_4$.]+Thiophene+Hexadecane*
- *[C_2mim][$EtSO_4$.]+Thiophene+i-Octane*
- *[C_2mim][$EtSO_4$.]+Thiophene+Toluene*

- *[C_2mim][$EtSO_4$.]+Pyridine+Hexane*

Ternary systems with ionic liquid [C_6mmPy][NTf_2.]:

- *[C_6mmPy][NTf_2.]+Thiophene+Hexane*
- *[C_6mmPy][NTf_2.]+Thiophene+Heptane*
- *[C_6mmPy][NTf_2.]+Thiophene+Dodecane*
- *[C_6mmPy][NTf_2.]+Thiophene+Hexadecane*
- *[C_6mmPy][NTf_2.]+Thiophene+i-Octane*
- *[C_6mmPy][NTf_2.]+Thiophene+Toluene*
- *[C_6mmPy][NTf_2.]+Pyridine+Hexane*

3.2.1 Theoretical considerations on liquid-liquid equilibrium

Only generic considerations and fundamental thermodynamics are provided in this section. Very well known texts on LLE thermodynamics and fundamentals of solvent extraction are now reviewed. [203-205]

3.2.1.1.Thermodynamic considerations of liquid-liquid equilibrium

A system is defined as a part of the Universe isolated by certain boundaries which possesses determinate properties, and the surroundings as the part of the Universe which can interact with that system. A thermodynamic system is considered closed if there is no mass transfer with its surroundings. A phase is considered as a homogeneous region within the system. A system will be homogeneous or heterogeneous if it has one or more phases, respectively.

All systems can be described at a macroscopic level by their thermodynamic properties like volume (V), pressure (P), and temperature (T), and frequently, only two variables are required to define a simple system at equilibrium. The values of these variables determine the state of the system for which they receive the name of "state variables".

Similar to the thermodynamic variables, there are "thermodynamic functions". A very important type of these functions is "state functions". These only depend on the state of the system. In other words, the value of these functions depends on the initial and final state, not how they get there.

Classical thermodynamics studies systems at equilibrium. An isolated system is at equilibrium when its variables remain constant with time. An open system is at equilibrium when, in addition to the previously mentioned, there is no change in the properties when the system is no longer in contact with the surroundings.

Equilibrium represents the scenario in which there is no macroscopic variation in the properties with time. If a multi-component system composed of an arbitrary number of phases is considered to be at thermal and mechanical equilibrium with its surroundings, it can be shown that the change in Gibbs free energy is zero. Thermodynamics also provides the equations which relate this property with magnitudes which are easy to measure like composition, temperature, and pressure.

Starting from the laws of thermodynamics, functions like enthalpy *(H)*, Hemholtz free energy *(A),* and Gibbs free energy *(G)* can be defined. However, for this work, the following definitions are based exclusively on Gibbs free energy, since it is the function used for the calculations for equilibrium between phases.

Considering a system of volume *V,* internal energy *U,* and entropy *S*, the state functions of enthalpy and Gibbs free energy are defined as:

$$H = U + PV \qquad [3.1]$$

$$G = H - TS \qquad [3.2]$$

1) If the system is closed, and the process which takes place is reversible, from the first and second law of thermodynamics these equations are obtained:

$$dU = dQ + dW \qquad [3.3]$$

$$dQ = TdS \qquad [3.4]$$

$$dW = -PdV \qquad [3.5]$$

Combining all these equations, the following Gibbs free energy expression can be obtained:

$$dG = VdP - SdT \qquad [3.6]$$

which is known as the fundamental equation of Gibbs free energy, from which several relations follow:

$$G = f(T,P) \quad ; \quad V = \left(\frac{\partial G}{\partial P}\right)_T \quad ; \quad S = -\left(\frac{\partial G}{\partial T}\right)_P \qquad [3.7]$$

2) For the case of open systems (allows mass transfer), the function *G,* also depends on the number of moles:

$$G = G(T,P,n_1,n_2,\ldots,n_k) \qquad [3.8]$$

where *k*, is the number of components in the system. From this expression [3.8], following relation can be obtained for the differential change of *G*, due to the differential changes in *T*, *P,* and *n*:

$$dG = \left(\frac{\partial G}{\partial T}\right)_{P,n_i} dT + \left(\frac{\partial G}{\partial P}\right)_{T,n_i} dP + \sum \left(\frac{\partial G}{\partial n_i}\right)_{T,P,n_j} dn_i \qquad [3.9]$$

where i and j can be all values: 1,2,..., k , and $i \neq j$.

- ***Chemical potential***

Taking into consideration the values of the previous derivatives, according to equations [3.7] and [3.9]:

$$dG = -SdT + VdP + \sum \mu_i dn_i \qquad [3.10]$$

where μ_I, is defined as the chemical potential:

$$\mu_i = \left(\frac{\partial G}{\partial n_i}\right)_{T,P,n_j} = \left(\frac{\partial U}{\partial n_i}\right)_{V,S,n_j} = \left(\frac{\partial H}{\partial n_i}\right)_{S,P,n_j} = \left(\frac{\partial A}{\partial n_i}\right)_{V,T,n_j} \qquad [3.11]$$

The chemical potential, in terms of Gibbs free energy, represents the basic property for chemical and phase equilibrium calculations.

For a pure component, it can be written as:

$$\mu = \left(\frac{\partial G}{\partial n}\right)_{T,\ P} \qquad [3.12]$$

Hence, the following relation is obtained from equation [3.6]:

$$d\mu = -Sdt + VdP \qquad [3.13]$$

where S and V represent the molar entropy and volume respectively.

To calculate the chemical potential at a temperature (T) and pressure (P), the previous expression is integrated:

$$\mu(T,P) - \mu(T',P') = -\int_{T'}^{T} Sdt + \int_{P'}^{P} VdP \qquad [3.14]$$

where $\mu(T',P')$ is the chemical potential at a reference temperature T' and pressure P'.

- ***Fugacity and fugacity coefficient***

Related to chemical potential, G.N.Lewis introduced the concept of fugacity in 1901. If the change in chemical potential of a pure ideal gas is considered from pressure P_1 to P_2, at constant temperature, from equation [3.13], is obtained:

$$\mu_2 - \mu_1 = \mu(P_2,T) - \mu(P_1,T) = RT\ln(P_2 / P_1) \qquad [3.15]$$

This expression indicates that, for an ideal gas, the isothermal change of the chemical potential can be determined in function of the initial and final pressure. Applying this to real systems, Lewis introduced a new function: fugacity (f). This function represents the isothermal change in chemical potential of any component in a system which is written similarly to the previous one [3.15]:

$$\mu_2 - \mu_1 = \mu(P_2,T) - \mu(P_1,T) = RT\ln(f_2 / f_1) \qquad [3.16]$$

The fugacity coefficient is defined as the relation between the fugacity of a pure component at pressure P_1 and pressure P_2:

$$\phi = \frac{f}{P} \qquad [3.17]$$

Since ideal gas behavior is achieved as pressure approaches zero, it can be written that:

$$\lim_{P\to 0} \phi = \lim_{P\to 0} \frac{f}{P} = 1 \qquad [3.18]$$

Derivatives of equation [3.18], along with [3.16], lead to the following expression:

$$d\mu = RTd\ln f \qquad [3.19]$$

which is the relation between fugacity and the chemical potential of a pure component.

3.2.1.2 Properties of mixtures

Up until now, the deductions of chemical potential, fugacity, and fugacity coefficient, have been made under the assumption of only one pure component. But in reality, work will be done with mixtures of different components, for which it is necessary to make extensive definitions of multi-component mixtures and introduce new concepts in relation with the properties of these mixtures.

The nomenclature in this section will be the following:

M: molar property of a mixture (V, H, ...)

n: total number of moles in a mixture

nM: total property of a mixture (nV, nH, ...)

M_i : molar property of the pure component i (V_i, H_i, ...)

$\overline{M}_i$: partial molar property of component i of a mixture ($\overline{V}_i$, …)

M^E : excess property (G^E ,...)

ΔM : change in total property (ΔG, ΔH,...)

Considering that a mixture that contains n_1 moles of component 1, n_2 moles of component 2, ... y n_k moles of component k, where k is the number of components in the mixture for a total of n moles, the total quantity of the property of the mixture at a given temperature (T) and pressure (P) is:

$$nM = n_1 M_1 + n_2 M_2 + \ldots + n_k M_k = \sum n_i M_i \qquad [3.20]$$

with all M_i evaluated at the same T and P.

However, it has been documented that experimentally this expression is not correct and the real equations are:

$$nM = \sum n_i \overline{M}_i \qquad [3.21]$$

or dividing through by the total number of moles:

$$M = \sum x_i \overline{M}_i \qquad [3.22]$$

where $\overline{M}_i$ is defined as the partial molar property of component *i*.

A given property of a component *i*, has a different value when *i* is the component of a mixture compared to when *i* is in its pure state, both calculated at the same *T* and *P*. The differences in the values are a result of the intra and intermolecular forces and the molecular size and shape of the components in the mixture. If these differences are not present, then the mixture is called ideal.

- ***Partial molar magnitudes***

If an homogeneous mixture is considered to have $n_1, n_2, ..., n_k$ moles of the substances 1, 2, ..., *k* at constant temperature and pressure, to which a small amount of component *i* is added, dn_i, keeping *T*, *P* and the number of moles of the other n_j components constans; the partial molar property $\overline{M}_i$ is defined as the ratio of the change in total property *d(nM)* and the change in number of moles dn_i :

$$\overline{M}_i = \left(\frac{\partial (nM)}{\partial n_i} \right)_{T,P,n_j} \qquad [3.23]$$

$\overline{M}_i$ is the partial molar property of component *i* of the mixture at a determined *T*, *P* and composition, where the subindex *j* can be all values from 1 a *k*, except *i*. Hence, the partial molar properties are a function of temperature, pressure and composition:

$$\overline{M}_i = f(x_1, x_2, ..., T, P) \qquad [3.24]$$

- ***Mixture properties from partial molar properties***

The total property *nM* of an homogeneous mixture at a given *T* and *P*, will only be a function of the amount of its components:

$$nM = f(n_1, n_2, \ldots, n_k) \qquad [3.25]$$

Differentiation gives us:

$$d(nM) = \left(\frac{\partial (nM)}{\partial n_1}\right)_{T,P,n_j} dn_1 \; + \; \ldots \; + \left(\frac{\partial (nM)}{\partial n_k}\right)_{T,P,n_j} dn_k \qquad [3.26]$$

The values of the derivatives coincide with the definition of partial molar property of *nM*, as can be seen in equation [3.23], this way the previous expression [3.26], turns into:

$$d(nM) = \sum \overline{M}_i dn_i \qquad [3.27]$$

Integrating this expression from zero to the total number of moles at constant *T*, *P* and composition, it yields:

$$nM = \sum n_i \overline{M}_i \qquad [3.28]$$

or dividing by the total number of moles *n*:

$$M = \sum x_i \overline{M}_i \qquad [3.29]$$

which are the equations presented previously [3.21] and [3.22]. This way if the partial molar properties of a mixture at a given *T*, *P* and composition are known, then the corresponding properties of the mixture at those same conditions can be calculated.

- ***Partial molar properties from mixture properties***

Assuming an expression for *M* in terms of *T*, *P* and composition is given:

$$M = f(x_1, x_2, \ldots, x_k) \qquad [3.30]$$

and an expression will be developed for the calculation of the partial properties of the mixture.

From the definition of partial molar property [3.23]:

$$\overline{M}_i = \frac{\partial (nM)}{\partial n_i} = M + n\frac{\partial M}{\partial n_i} \qquad [3.31]$$

To evaluate the derivative $(\partial M/\partial n_i)$, given $\Sigma x_i = 1$ and using the properties of derivatives it can be written:

$$\overline{M}_i = M + n\sum\left(\frac{\partial M}{\partial x}_j \frac{\partial x_j}{\partial n_i}\right) = M + n\sum\left(\frac{\partial M}{\partial x_j}\frac{\partial (n_j / n)}{\partial n_i}\right) = M - \sum x_j \frac{\partial M}{\partial x_j}$$

[3.32]

This equation is more useful than [3.23], the definition of the partial molar magnitude, since in the most common case, an expression is given for M as a function of the composition rather than nM as a function of the number of moles of the components of the mixture.

- ***Gibbs-Duhem Equation***

In the most general case, the total property of the mixture nM is a function of the temperature (T) and pressure (P) in addition to the number of moles of its components, this way, equation [3.25] turns into:

$$nM = f(T, P, n_1, n_2, ..., n_k) \qquad [3.33]$$

Finding the derivative:

$$d(nM) = \left(\frac{\partial (nM)}{\partial T}\right)_{P,n_i} dT + \left(\frac{\partial (nM)}{\partial P}\right)_{T,n_i} dP + \sum\left(\frac{\partial (nM)}{\partial n_i}\right)_{t,P,n_j} dn_i =$$

$$= n\left(\frac{\partial M}{\partial T}\right)_{P,x_i} dT + n\left(\frac{\partial M}{\partial P}\right)_{T,n_i} dP + \sum \overline{M}_i dn_i \qquad [3.34]$$

and differentiating [32] and given that $nM = \sum n_i \overline{M}_i$, yields:

$$d(nM) = \sum n_i d\overline{M}_i + \sum \overline{M}_i dn_i \qquad [3.35]$$

Setting the expressions equal [3.34] and [3.35], and dividing by the number of moles n:

$$\sum x_i d\overline{M}_i - \left(\frac{\partial M}{\partial T}\right)_{P,x_i} dT - \left(\frac{\partial M}{\partial P}\right)_{T,x_i} dP = 0 \qquad [3.36]$$

which is the Gibbs-Duhem equation, which says that the intensive properties of a mixture: temperature (T), pressure (P) and partial molar properties ($\overline{M}_i$), cannot change independently. If T and P remain consant then:

$$\sum x_i d\overline{M}_i = 0 \qquad [3.37]$$

3.2.1.3 Calculations for mixture properties

It is noted that for the determination of the properties of a mixture, it is necessary to know the corresponding values of the partial molar properties, but to calculate the partial molar properties the corresponding mixture properties are needed. The mixture properties are obtained through experimental means, and if lacking, through estimations. Experimental data are available for many binary systems but for few multi-component systems, which represent the most common scenario in industrial settings. Hence it is necessary to study and determine phase equilibrium data for multi-component systems. The use of estimation techniques is the most used methodology for mixtures. The most popular techniques for the estimation of mixture properties are the Pitzer formulation of corresponding states and the equation of states, in particular the virial and cubics.

- ***Fugacity of mixtures***

The fugacity of the components of a mixture is very important in chemical engineering applications since they are the base for chemical and phase equilibrium calculations.

The fugacity $\hat{f}_i$ of a component i in a homogenous mixture is similar to that of the pure component:

$$d\mu_i = d\overline{G}_i = RTd\ln\hat{f}_i = \overline{V}_i dP \quad \text{at constant temperature} \qquad [3.38]$$

where:

$$\lim_{P\to 0}\frac{\hat{f}_i}{x_i P} = 1 \qquad [3.39]$$

The relation between f y $\hat{f}_i$, obtained from equations [3.19] and [3.38] and from integrating them from a pressure P* (at which the mixture would behave as an ideal gas), to a pressure P, at constant temperature and composition is the following:

$$\ln f = \sum x_i \ln\left(\frac{\hat{f}_i}{x_i}\right) \qquad [3.40]$$

both sides are divided by ln$P$:

$$\ln \phi = \sum x_i \ln \hat{\phi}_i \qquad [3.41]$$

These last two expressions indicate that $\ln(\hat{f}_i / x_i)$ and $\ln \hat{\phi}_i$ are partial molar properties, but not $\hat{f}_i$ nor $\hat{\phi}_i$. This explains why the symbol $(\hat{x})$ is used, and not $(\overline{x})$ to differentiate fugacity from the fugacity coefficient of a mixture of component i, from the corresponding pure state i .

- ***Activity and activity coefficient***

For polar systems, the intermolecular forces make it so the non ideal behavior of the mixture cannot be described with the available equation of states, specially for liquid phases. So a fugacity for component i in the liquid phase of a mixture with respect to its value at a reference state called standard state fugacity f_i^o :

$$\hat{f}_i = x_i \gamma_i f_i^o \qquad [3.42]$$

where γ_i is the activity coefficient.

Lewis, defined the activity a_i as the ratio:

$$a_i = \hat{f}_i / f_i^o \qquad [3.43]$$

The activity of a substance represents a measurement of the difference in chemical potential of the substance in a state of reference and the state of interest.

It can be shown that for a real liquid solution $a_i = x_i$. For any solution, the relationship between composition x_i and the activity a_i is given by the activity coefficient:

$$\gamma_i = \frac{a_i}{x_i} \qquad [3.44]$$

The fugacity of a component *i*, of a liquid mixture, can be evaluated by the following expression in which the concept of activity coefficient has been introduced:

$$\hat{f}_i = x_i \gamma_i P_i^S \phi_i^S \exp\left(\frac{V_i (P - P_i^S)}{RT}\right) \qquad [3.45]$$

where:

P_i^S : vapor pressure of the pure component *i* at temperature *T*

ϕ_i^S : fugacity coefficient of saturated vapor at temperature *T*

V_i : mean value of liquid molar volume at temperature *T* and in the range from P_i^S to *P*.

The exponential term in the previous equation is known as the Poynting factor and if the temperature of the system is close to the critical temperature of the pure component *i* , it should be replaced for this expression:

$$Pf = \exp \int_{P^S}^{P} \frac{V_l}{RT} dP \qquad \text{where } V_l \text{ is the liquid volume.} \qquad [3.46]$$

The phase equilibrium measurements, vapor-liquid or liquid-liquid, are the primary source for the determination of activity coefficients. Other methods of applications, although limited, that are useful in certain cases specially for non-volatile components are: osmotic pressure measurements, decrease in freezing point, increase in boiling point, decrease in vapor pressures, electrochemical cells…

3.2.1.4. Change in properties due to mixture effects

To define the properties of mixture changes, a mixture is considered of x_1 moles of component 1, x_2 moles of component 2 and x_k moles of component *k*, for a total mixture of 1 mol. The pure components and the mixture are at the same temperature (*T*) and pressure (*P*), so that the changes from the pure components to the mixture are only due to the mixture effects. The property of change due to the mixture or mixture property is defined as:

$$\Delta M = M - \sum x_i M_i \qquad [3.47]$$

where ΔM represents the property that has changed.

Replacing M in the previous equation and combining it with equation [3.29]:

$$\Delta M = \sum x_i (\overline{M}_i - M_i) = \sum x_i (\Delta \overline{M}_i) \qquad [3.48]$$

where $\Delta \overline{M}_i = \overline{M}_i - M_i$, represents the mixture effect of component i. [3.49]

Equation [3.45] can be written as

$$M = \sum x_i M_i + \Delta M \qquad [3.50]$$

which says that if ΔM is known, along with the properties of the pure components at the same T y P, the property M of the mixture can be determined.

If these equations are applied to an ideal solution, characterized because the forces between molecules are equal and because the size and shape of the molecules are the same, expressions for ΔM^{id}, can be developed, which in function of the Gibbs free energy, would yield the following equation:

$$\Delta G^{id} = G^{id} - \sum x_i G_i = \sum x_i \left[\overline{G}_i^{id} - G_i \right] \qquad [3.51]$$

Integrating expression [3.42] between the fugacity of the pure component i, f_i and that of the component i in the ideal solution at the same T and P, that by equation [3.52] is equal to $x_i f_i$, the expression obtained is:

$$\overline{G}_i^{id} - G_i = RT \ln \frac{x_i f_i}{f_i} = RT \ln x_i \qquad [3.52]$$

hence:

$$\Delta G^{id} = RT \sum x_i \ln x_i \qquad [3.53]$$

- ***Excess properties***

The difference between the value of a property M of a liquid mixture at a given T, P and composition and its value if the liquid mixture behaved as ideal M^{id} at the same conditions, represents the excess property M^E :

$$M^E = M - M^{id} \qquad [3.54]$$

and for a component i of the mixture:

$$\overline{M}_i^E = \overline{M}_i - \overline{M}_i^{id} \qquad [3.55]$$

It can be written as:

$$M^E = \sum x_i \overline{M}_i^E = \sum x_i \left[\overline{M}_i - \overline{M}_i^{id}\right] \qquad [3.56]$$

Excess properties provide a quantitative measure of the effect of the differences between the inter and intramolecular forces and the size and shape of the molecules. From a practical standpoint the most important excess property is the Gibbs free energy, because it relates the activity coefficients with the mixture components.

The following relation between fugacity and Gibbs free energy is obtained:

- $$d\overline{G}_i = RTd\ln\hat{f}_i \qquad [3.57]$$

If this expression is integrated from the ideal to the real state of the solution at a constant P, T and composition:

$$\overline{G}_i^E = \overline{G}_i - \overline{G}_i^{id} = RT\ln\left(\frac{x_i\gamma_i f_i^o}{x_i f_i^o}\right) = RT\ln\gamma_i \qquad [3.58]$$

and according to equation [3.54]:

$$G^E = \sum x_i \overline{G}_i^E = RT\sum x_i \ln\gamma_i \qquad [3.59]$$

which indicates $RT\sum\ln\gamma_i$ is a partial molar property of the Gibbs free energy, and then:

$$\ln\gamma_i = \left(\frac{\partial(nG^E/RT)}{\partial n_i}\right)_{T,P,n_j} \qquad [3.60]$$

In the previous equation, given that for an ideal mixture G^E = 0, all the activity coefficients would be equal to 1, if the mixture were ideal.

Equation [3.60] provides a basis for the development of analytic expressions of the activity coefficient. To achieve this goal, qualitative and quantitative arguments are used for the deviation of a real mixture compared to an ideal, to develop expressions for G^E as a function of temperature, pressure, and composition.

Differentiating these equations provides the analytic expression for the activity coefficient of each component of the solution. In the next chapter some of the equations (Wilson, TK-Wilson, NRTL and UNIQUAC) valid for the calculations of the activity coefficients, and consequently the correlation for experimental equilibrium data, will be studied.

In addition to the Gibbs free energy [3.58], the activity coefficients can be related with other excess functions, like the following: :

$$\left(\frac{\partial \ln \gamma_i}{\partial T}\right)_{P,x} = -\frac{\overline{H}^E}{RT^2} \quad ; \quad \left(\frac{\partial \ln \gamma_i}{\partial P}\right)_{T,x} = \frac{\overline{V}^E}{RT} \qquad [3.61]$$

3.2.1.5. Equilibrium criteria

The application of Thermodynamics to phase equilibrium permits establishing strict, necessary, and sufficient conditions for the equilibrium definition. This definition is important for the development of theoretical models of correlation and prediction of equilibrium.

Equilibrium conditions are deduced from first principles of Thermodynamics. Rigorously, a closed system, heterogeneous and multi-component is at equilibrium when at constant temperature (T) and pressure (P) the Gibbs free energy (G) is a minimum. Mathematically:

$$d(G)_{T,P} = 0 \qquad [3.62]$$

and this expression can be considered as a criteria or definition of equilibrium. Gibbs free energy is related to its independent variables temperature, pressure and number of (n), through the following expression:

$$dG = -S \cdot dT + V \cdot dP + \sum_i \mu_i \cdot dn_i \qquad [3.63]$$

where S and V are the entropy and volume of the system, respectively and μ_i is the chemical potential of component *i*. The concept of chemical equilibrium was introduced by J. W. Gibbs and it is essential for the application of Thermodynamics for phase equilibrium.

If a system, with various components and phases, is considered even if it is closed, every distinct phase is an open system which can transfer mass with the other phases. Equation [3.63] can be applied to each distinct phase, and the sum will be the Gibbs free energy combination of all the phases. If it is considered that temperature and pressure remain constant, it is obtained:

$$\begin{aligned}
(dG)^{(1)} &= -(S)^{(1)} \cdot dT + (V)^{(1)} \cdot dP + \sum_i (\mu_i \cdot dn_i)^{(1)} \\
(dG)^{(2)} &= -(S)^{(2)} \cdot dT + (V)^{(2)} \cdot dP + \sum_i (\mu_i \cdot dn_i)^{(2)} \\
&\vdots \\
(dG)^{(m)} &= -(S)^{(m)} \cdot dT + (V)^{(m)} \cdot dP + \sum_i (\mu_i \cdot dn_i)^{(m)} \\
\hline
(dG)_{P,T} &= \sum_i (\mu_i \cdot dn_i)^{(1)} + \sum_i (\mu_i \cdot dn_i)^{(2)} + \cdots + \sum_i (\mu_i \cdot dn_i)^{(m)} = 0
\end{aligned} \qquad [3.64]$$

where all the superscripts make reference to all the distinct phases (1, 2, … *m*).

If this equation is applied to a biphasic system, multi-component, at constant temperature and pressure, and that an infinitesimal amount of moles of component *i*, dn_i, pass from phase 1 to phase 2, it is obtained:

$$(\mu_i \cdot dn_i)^{(1)} = -(\mu_i \cdot dn_i)^{(2)} \Rightarrow (\mu_i^{(1)} - \mu_i^{(2)}) dn_i = 0 \Rightarrow \mu_i^{(1)} = \mu_i^{(2)} \qquad [3.65]$$

This equation constitutes the equilibrium criteria in function of the chemical potential of all the components in the mixture and can be extended to multi-phasic systems. In addition, to consider the system at equilibrium, thermal and mechanical equilibrium is also needed, hence, for a multi-phasic and multi-component system, the equilibrium conditions are:

$$T^{(1)} = T^{(2)} = \cdots = T^{(m)} \qquad [3.65a]$$

$$P^{(1)} = P^{(2)} = \cdots = P^{(m)} \qquad [3.65b]$$

$$\mu_i^{(1)} = \mu_i^{(2)} = \cdots = \mu_i^{(m)} \qquad [3.65c]$$

However, the chemical potential is an abstract concept which makes the previous criteria not very practical for experimentation. The chemical potential can be defined in function of thermodynamic potentials: internatl energy (*U*), enthalpy, (*H*), Helmholtz energy (*A*), and Gibbs free energy (*G*). The mathematical expressions are the following:

$$\mu_i = \left(\frac{\partial U}{\partial n_i}\right)_{S,V,n_j} = \left(\frac{\partial H}{\partial n_i}\right)_{S,P,n_j} = \left(\frac{\partial A}{\partial n_i}\right)_{V,T,n_j} = \left(\frac{\partial G}{\partial n_i}\right)_{P,T,n_j} \quad [3.66]$$

To be able to apply the equilibrium criteria to measurable magnitudes in the laboratory, the concept of fugacity is (*f*), defined by G. N. Lewis, and it satisfies the following equation:

$$\mu_i - \mu_{i,0} = R \cdot T \cdot \ln\left(\frac{f_i}{f_{i,0}}\right) \quad [3.67]$$

where the subindex 0 refers to a reference state. This reference state and its value of chemical ($\mu_{i,0}$) and fugacity ($f_{i,0}$) are arbitrary, although the values are not independent and by setting one, the other one is fixed by [3.67].

With equations [3.65c] and [3.67] the equilibrium criteria can be expressed in function of the fugacity resulting in:

$$f_i^{(1)} = f_i^{(2)} = \cdots = f_i^{(m)} \quad [3.68]$$

which is a more adequate expression from a practical point of view, and is valid as long as all the reference states for all the phases are a the same temperature.

G. N. Lewis defined the activity of a component *i* (a_i) as the ratio of its fugacity and the reference:

$$a_i = \frac{f_i}{f_{i,0}} \quad [3.69]$$

and when combined with equation [3.69] an equilibrium criteria in terms of activity is given:

$$a_i^{(1)} = a_i^{(2)} = \cdots = a_i^{(m)} \quad [3.70]$$

The activity is related to composition through the activity coefficient which is defined as the ratio of the two, hence the expression turns into:

$$(x_i \cdot \gamma_i)^{(1)} = (x_i \cdot \gamma_i)^{(2)} = \cdots = (x_i \cdot \gamma_i)^{(m)} \quad [3.71]$$

which is the criteria that will be used later in this work.

3.2.1.6. Particular aspects of liquid-liquid equilibria

The most important aspects of liquid-liquid equilibria according to Walas (1985)[227], are:

1) how to predict data from the properties of pure components or pairs of components

2) how to correlate available data to able them to be interpolated, extrapolated or combined to represent the behavior of multi-component systems.

3) how to obtain the data experimentally

There are three necessary conditions for equilibrium in liquid-liquid systems

1) mass conservation

2) the chemical potential of each component in the liquid phases must be equal

3) the Gibbs free energy must be a minimum at the *T* and *P* of the system.

3.2.1.7. Phase rule

In a system at equilibrium where the only significant intensive variables are the temperature, pressure, and chemical potential, the phase rule [228] allows the determination of the number of intensive variables that can be modified independently without changing the state of the system. This number of variables receives the name of "degrees of freedom" (*f*) and is related to the number of components (*c*) and the number of phases (ϕ), as shown below:

$$f = c + 2 - \phi \qquad [3.72]$$

It is a key in the study of equilibrium between phases and it is shown in the way the liquid-liquid equilibrium data are represented.

3.2.1.8. Liquid-Liquid Equilibrium diagrams

The graphic representation of phase equilibrium is useful for evaluating information that might lead to different applications like the selection of a solvent or the design of extraction equipment. The representation and interpretation of these diagrams are based on the phase rule.

- ***Binary systems***

For a liquid binary system, the most common representation for the liquid-liquid equilibrium is a temperature-composition diagram. In these kinds of representation, the pressure is taken to be constant (typically the case for liquid-liquid extractions), while temperature is the ordinate axis and composition, the abscissa as it is showed in Figure 3.1[230]

For this case, the degrees of freedom is f=2 while in homogenous conditions for the complete system, but will be f=1 if two immiscible phases are formed.

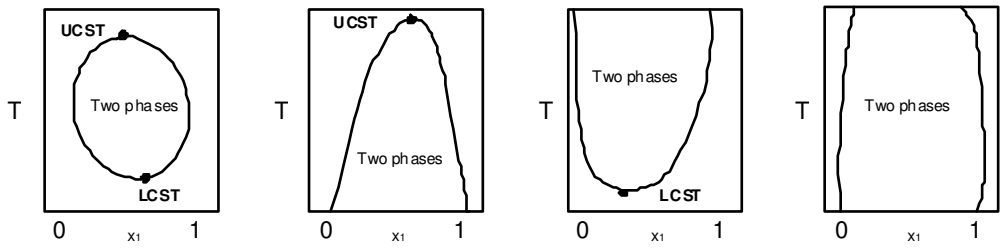

Figure 3.1 Types of binary liquid-liquid equilibria. From left to right, the first one showing lower and upper critical solution temperature (LCST, UCST), the second one showing UCST, the third one, LCST and the last one, two-phase region in the whole temperature range.

- ***Ternary systems***

Phase diagrams for ternary systems are typically represented as a equilateral triangular diagram, and pressure and temperature are taken to stay constant. Each corner of the triangle represents the pure components, the binary mixtures on the side, and any mixture that considers all three components is in the inside. The distance of a given point from the corners of the triangle depends on the composition. Furthermore, the addition or subtraction of a component of the represented mixture is reflected in a displacement of the point over the line that ties him with the corresponding pure component.

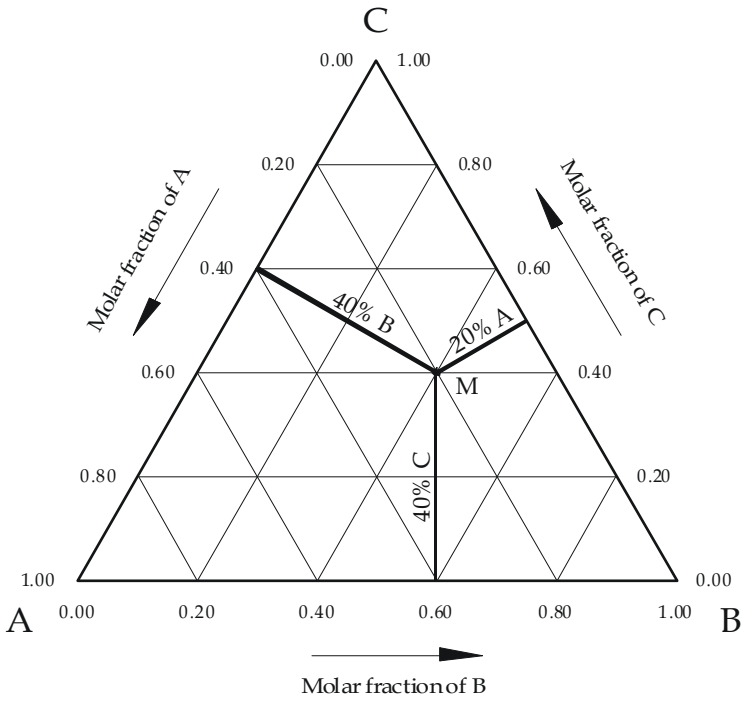

Figure 3.2. Equilateral triangular diagram, where vertices A, B and C represent the pure components of a ternary system. An example of how to determine the composition of a ternary mixture M, represented by an internal point of the triangle, is shown.

Under constant temperature and pressure conditions, for triangular diagrams, the phase rule is $f = 3 - \phi$, and the number of phases varies between 1 and 3. If for a given composition the ternary mixture presents a single homogeneous phase, there will be two degrees of freedom in the system. For a system with two liquid immiscible phases there will be one degree of freedom, hence, the composition of both phases will be determined, fixing the composition of one of the components in one of the two phases. For a ternary system with three phases in equilibrium, the system is completely determined.

When the composition of the ternary mixture is found in the biphasic region of the diagram, two phases are formed with compositions corresponding to the line which defines said region. If only one of the compositions is fixed, the other is automatically fixed in equilibrium. The straight lines which connect the two points are known as “tie-lines.”

The three phase regions in the triangular diagrams are generated by convergence of, typically, biphasic regions and their limits have triangular shape. Given that the system does not change, any mixture whose composition is found within the limits of the triangle, it will automatically separate in three phases whose compositions will be given by the vertices of said triangle.

It is possible to observe the temperature effect on the liquid-liquid equilibrium of ternary systems using a prismatic 3-D diagram.

Sometimes triangular rectangular diagrams are used for the representation of ternary systems, but in this work only equilateral triangular diagrams will be used.

- ***Ternary systems of interest in liquid-liquid equilibrium***

Treybal [228] makes a classification of the ternary systems which show partial miscibility with all components in a liquid state at the temperature of interest:

- Type I: With a pair of components partially soluble
- Type II: With two pairs of components partially soluble
- Type III: With three pairs of components partially soluble
- Type IV: With formation of solid phases

The majority of the systems which have been studied in liquid-liquid equilibrium are type I or type II. Figures 3.3 and 3.4 show several examples.

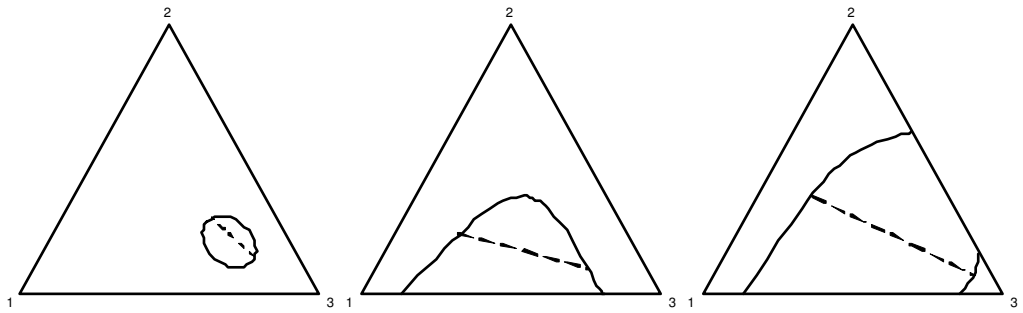

Figure 3.3 Triangular diagrams of ternary systems of liquid-liquid equilibrium: the first is type 0, the second is type I with two regions of immiscibility, and the third is type II with one immiscibility region.

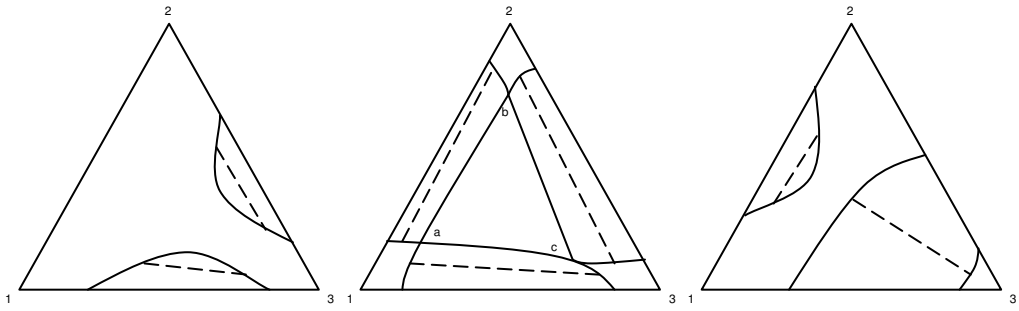

Figure 3.4 Triangular diagrams of ternary systems of liquid-liquid equilibrium: the first is type II a, with two regions of immiscibility, the middle one is type III and may have three coexisting liquid phases (point a, b, c) and the third one is type III a, with two immiscibility regions.

3.2.1.9 Experimental determination of liquid-liquid equilibrium

Different experimental techniques can be found in the bibliography for obtaining liquid-liquid equilibrium data: method of equilibrium cell, continuous measurements, and titration method [229, 230]

The equilibrium cell method is based on the direct analysis of the phases: a sample is prepared with a composition in the immiscibility region, it is introduced in a temperature controlled cell with vigorous stirring and equilibrium is allowed to be reached. Then, a sample is taken from each of the phases and their composition is determined with an adequate analytical method. The preferred methods involve chromatography.

Titration method requires the use of expensive analytical equipment and depends exclusively of titration and mass balances. It consists of two parts. In the first, the solubility curve is found using the cloud point [231] with one of the immiscible component or an homogeneous mixture of the components, the other immiscible component is added slowly until a 'cloud' is produced, reaching mutual insolubility. This procedure is repeated until the complete heterogeneous region is covered and the solubility curve is determined. Once it is known, only the analysis of one of the components is needed (acid-base or redox titration, physical properties…) in each of the equilibrium phases and the tie-lines are found.

Even though equilibrium data can be found in the bibliography using both methods, the titration method introduces a subjective element in the determination of the cloud point.

The method of continuous measurement is really a heat exchanger with a system of vigorous stirring and centrifugation for the separation of phases and allows the continuous measurements of both equilibrium phases.

3.2.1.10 Selection of the solvent: conclusions from equilibrium

The following properties of a potential solvent must be taken into account before its use in a liquid-liquid extraction [232]:

1. **Selectivity**: The relative or selective separation, *S,* of a solvent, as will be seen later, is the quotient of the ratio of the two components in the extraction solvent phase and the ratio of the same components in the feed solvent. The separation ability of a liquid-liquid system is regulated by the deviation of *S* with respect to unity. A relative separation with equal to unity does not separate the components in the liquid phase. In general, the dilute concentrations of solute provide the highest factors for relative separation.
2. **Recoverability**: In general, the extraction solvent should be recovered from the extract stream and the raffinate in an extraction process. Since distillation is often used, the relative volatility of the extract solvent with respect to the non-solvent components should be significantly greater or less than unity. For a volatile solvent a low latent heat of evaporation is desirable.
3. **Distribution coefficient**: The distribution coefficient of the solute, β, should be big, so a small quantity of solvent can be used with respect to the feed stream.
4. **Capacity**: This property refers to the amount of solute per extraction solvent that can be achieved in a single extraction layer, at the triple point of a type I system or at the solubility limit of a type II system.
5. **Solvent solubility**: A low solvent solubility of the extraction solvent in the raffinate usually results in a high relative volatility in the raffinate separation or a small loss of solvent if the raffinate does not dissolve. A low solubility of the feed solvent in the extract leads to a large relative separation and generally, small expenses in the solute recovery.
6. **Density**: The difference in density of the two liquid phases in equilibrium affects not only the streams of the fluids that in counter-current flow can be

reached in extraction equipment, but the coalescence velocity. The difference in density can reach zero at the triple point, but in some systems it can be equal to zero at an intermediate concentration of solute (isopycnic tie-line or double density) and can invert the phases to elevated concentrations.

7. **Interfacial tension**: An elevated superficial tension at the inter-phase promotes a fast coalescence, and in general, requires an elevated mechanical stirring to produce small drops. A small superficial tension at the inter-phase allows the breaking of the drop with low intensity stirring, but also leads to low coalescence speeds. The superficial tension at the inter-phase decreases, in general, when increasing solubility and solute concentration; it also tends towards zero at the triple point.
8. **Toxicity**: Due to the potential exposure to vapor inhalation or skin contact of the solvent, a low toxicity is required. Also, a low toxicity is desirable for aquatic life and bio-organisms when the extraction is used for waste water treatment. Often, the toxicity of the solvent will be small, if its water solubility is low.

Even though there are multiple qualities and properties which are desirable for a solvent like the ones mentioned, for an extraction solvent the most important parameters are a high capacity, distribution coefficient and selectivity.

The capacity of the solvent can be defined as the quantity extracted from the feed for a given quantity of solvent. This capacity is closely related to the concept of "distribution ratio" (β) [233], defined as:

$$\beta = \frac{x_s^{II}}{x_s^{I}} \qquad [3.73]$$

Where x represents the molar fraction of a component, the sub-indice s refer to the solute and the superscripts I and II represent the raffinate and extract phases respectively. For a high capacity, high values of β are needed as well as possible high values of x_s in the extract.

The selectivity (S) can be defined as the degree of extraction of solute by the solvent in the feed in presence of the inert. It represents a measurement of the feasibility of separation of the solute and the inert and is expressed mathematically by:

$$S = \frac{x_s^{II}}{x_s^{I}} \cdot \frac{x_i^{I}}{x_i^{II}} \qquad [3.74]$$

Where the sub indices i represent the inert, and the rest of the nomenclature remains the same as in equation [3.73].

It can be seen from comparison of the two previous equations that β has a direct effect on the selectivity, however, high values of β do not imply a high capacity and viceversa. A minimum solubility of the solvent in the inert is also important, given that it gives higher selectivity values and the recovery of the solvent is simplified.

Obviously, it is unusual to find a solvent that is ideal for a given application, but efforts must be made to find a suitable solvent.

3.2.1.11 Liquid-Liquid Equilibrium Correlations

The interpolation and extrapolation of liquid mixture data are necessary in chemical engineering for the design and optimisation of operations and processes. The ideal solution models are useful for a first approximation and for references, but the deviations from ideality are usually very high. These deviations are expressed in terms of the excess functions, like excess Gibbs free energy (G^E), which depend on the components of the mixture and the temperature. In this chapter, different models for the modeling of G^E will be studied.

The data correlation of liquid-liquid equilibrium (LLE) can take place using different methods [230] :

1) *models that empirically describe the distribution ratio (β_i) of a component in function of the composition.* Due to the empiric nature, these methods can only be used to store or interpolate data.

2) *semi empiric or theoretical models based on the phase equilibrium thermodynamics,* which describe the excess Gibss free energy (G^E) as a function of composition and temperature. The most important of these models will be studied later, since they are used for the experimental data.

3) *equations of state (EOS)*. EOS can be classified as analytic or non-analytic, and some of them include those stemming from the two-term Van der Waals equation and the virial expansions. Kolasinska (1986) [234] presents a review in the field of empirical equations for the

correlation and prediction of phase equilibrium. Regardless, the results from EOS are not acceptable for LLE behavior [235]. Some authors like Huang (1991) [236] or Verotti and Costa (1996) [237] have studied the possibility of combining both methods (those that describe G^E and EOS), with different results for binary systems.

From a theoretical development point of view, the excess Gibbs free energy leads to the activity coefficient, but in practice the process is inverted and (G^E) is determined from the activity coefficient. The basic relations, which have been developed in this theory section, are the following:

$$G^E / RT = \sum x_i \ln \gamma_i \qquad [3.75]$$

and

$$\ln \gamma_i = \frac{G^E}{RT} - \sum_{k \neq i} x_k \left(\frac{\partial (G^E / RT)}{\partial x_k} \right)_{T,P,x_j \neq ik} \qquad [3.76]$$

To correlate the experimental data, the following is needed:

- A GE model, or γi , as a function of composition and temperature
- A method for the calculation of the equilibrium compositions using the model defined previously.

To determine the most appropriate models for correlation of liquid-liquid equilibrium systems, different studies have been made, Sϕrensen et al. [230] stands out which employs the "*NonRandom, Two-Liquid*" (NRTL) and "*Universal QUAsi-Chemical*" (UNIQUAC) models for a great number of multi-component systems; Simonetty et al. (1982) [238], uses the NRTL, LEMF, and UNIQUAC equations for the prediction and correlation for LLE equilibrium data for 10 type I systems, obtaining good and similar results for all three equations; or García-Sánchez et al. (1996) [239], who make a description of the procedures of correlations and the methods of how to obtain the parameters for the NRTL, UNIQUAC, and extended UNIQUAC equations in multi-phasic and multi-component systems.

- ***Local composition concept***

For correlating the activity coefficients with composition, numerous (empirical and with a theoretical base) equations have been proposed to deal with the molecular interactions. However, as Mollerup studied (1981)[240], all models seem to have a common base of statistical mechanics.

Wilson (1964)[241] suggested that at a molecular level, a given solution, for instance, of two components, is composed of two types of clusters: one formed of molecules surrounded by

component 1 and the other of molecules surrounding that of component 2. Furthermore, due to the differences in intermolecular and intramolecular forces, the parameters of potential energy $\lambda_{12} = \lambda_{21}$, λ_{11} and λ_{22} are different, making the local compositions different from the global.

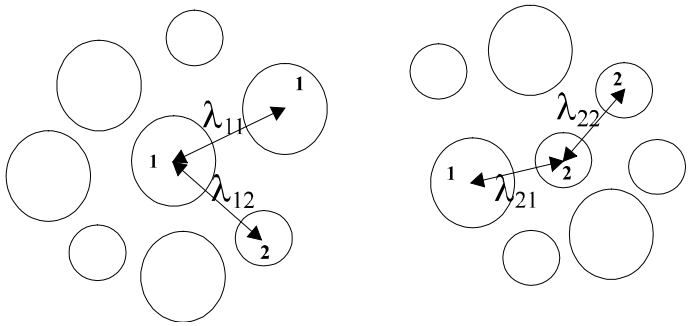

Figure 3.5 Representation of the local composition concept.

If for example, the 1-1 and 2-2 interactions are stronger than the 2-1, the molecules will surround themselves with molecules of the same kind. As a result, the molar fractions x_{ij} of a cluster, are referred to as local molar fractions with *i* representing the molecule at the center of the cluster, which are not the same in all clusters. In figure 3.5 the values would be $x_{12} = 3/7$; $x_{11} = 4/7$; $x_{21} = 3/7$; $x_{22} = 4/7$; although the global compositions would be $x_1 = x_2 = 0.5$.

The concept of local composition supposed a revolution in the development of expressions for the excess Gibbs free energy, and hence, the activity coefficient. Wilson used it in the equation that has his name, and Prausnitz and his collaborators used it in the development for their NRTL and UNIQUAC equations.

- ***NRTL Equation***

This equation was developed by Renon and Prausnitz (1968) [242] and presents a modification on the concept of local composition by introducing the parameter α_{ij}, which characterizes the trend of the j species and the i species to not assemble randomly, and allows for this equation to be applied to a variety of samples:

$$\frac{x_{ij}}{x_{ii}} = \frac{x_j}{x_i} \exp\left(\frac{-\alpha_{ij}(g_{ij} - g_{ii})}{RT}\right) \qquad [3.77]$$

where g_{ij} is the residual Gibbs free energy and $\alpha_{ij} = \alpha_{ji}$ which is the parameter that takes into account the non-randomness aleatory disposition of the molecules (when α_{ij} is equal to zero, the local molar fractions are equal to the molar fractions of the global solution). In a crude way, α_{ij} can be identified as the inverse of the number of nearest neighbours of a molecule in the mixture and would be expected to have a value in the range 0.1-0.3, approximately (Newsham, 1992)[229]. In principle, the non-randomness parameter can be specified according to a set of rules devised by the authors (Renon & Prausnitz, 1968) [242] that depend on the chemical nature of the components in the mixture, but it is usually given a fixed value in an empirical way, according to previous experiences in the reduction of experimental data of other systems.

Making use of this expression and Scott's two liquid theory (1956) [243], they developed an expression for excess Gibbs free energy from which the following equation for activity coefficients of component *i* in a multi-component mixture:

$$\ln \gamma_i = \frac{\sum x_j \tau_{ji} G_{ji}}{\sum x_k G_{ki}} + \sum \frac{x_j G_{ij}}{\sum x_k G_{kj}} \left(\tau_{ij} - \frac{\sum x_m G_{mj} \tau_{mj}}{\sum x_k G_{kj}} \right) \qquad [3.78]$$

where

$$\tau_{ij} = (g_{ij} - g_{jj}) / RT = \Delta g_{ij} / RT \quad \text{y} \quad G_{ij} = \exp(-\alpha_{ij} \tau_{ij}) \qquad [3.79]$$

The NRTL equation is applicable to multi-component systems with only binary parameters, which is an advantage for the use of this equation in the correlation of these types of systems. Furthermore, the parameter α_{ij} generally is independent of temperature and only depends on the molecular properties of the mixture components.

The α_{ij} value in the NRTL equation can be fixed according to the guidelines provided by Renon and Prausnitz (1968)[244], although they do not always apply. These authors suggest a range of 0.2-0.47, depending on the chemical nature of the constituents, given that they related the parameter α_{ij} with the inverse coordination number z, which represents the number of molecules per cluster that surrounds the reference molecule.

A later treatment of the NRTL equation was done by Renon and Cohen (1971) [245] where they include a computer program for the parameter determination. Marina and Tassios (1973) [246] showed that the value $\alpha_{ij} = -1$ gave good results for certain cases. This negative value was explained in the concept of local compositions in effective molar fractions (LEMF). Heidemann and Mandhane (1973)[247], in a study about different aspects of the NRTL equation, discovered that it can predict immiscibility of phases with values of $\alpha_{ij} > 0.426$, contrary to the previously

mentioned rules and there are groups of parameters that can adjust the solubility data with a fixed α_{ij}.

The values obtained by the experimental data correlation in the DECHEMA collection of vapor-liquid equilibrium data (1979), cover a range of positive values from $\alpha_{ij} = 0.1$ up to 100 or more, although these last values did not have a theoretical justification. Walas (1985)[227] compiles the optimal values according to the system components to study concluding that α_{ij} value should be on the order of 0.3 for non-aqueous mixtures and the order of 0.4 for aqueous organic mixtures. However, all the liquid-liquid equilibrium data of the DECHEMA are correlated with the parameter $\alpha_{ij} = 0.2$ and the majority of the publications fix α_{ij} at 0.1, 0.2 and 0.3. Van Zandijcke and Verhoeye (1974) [248], De Fre and Verhoeye (1976) [249], and Sugi and Katayama (1978) [250] have pointed out that the results obtained with α_{ij} as a fitting parameter does not show better results than being a fixed value.

Other studies and modifications of the NRTL equation can be found in works done by Cruz and Renon (1978) [251], Renon (1986) [252], Chen et al. (1986)[253], Gierycz et al. (1987)[254], Conneman et al. (1990)[255], Demirel (1993)[256] , Nagata and Nakajima (1991)[257], and more recently Wu et al. (1996)[258], using the modified NRTL equation for the calculation of phase equilibrium of electrolytes and polymer solutions.

- ***UNIQUAC 'UNIversal QUAsi-Chemical' equation***

In order to develop a truly two-parameter equation, Abrams and Prausnitz combined the theoretical concepts of the NRTL equation background with the quasi-chemical lattice model (Guggenheim, 1952)[259]. The resulting UNIQUAC equation for the excess Gibbs energy consists of two parts, the first is a combinatorial part that attempt to describe the dominant entropic contribution, and the second is a residual part that is primarily due to intermolecular forces that are responsible for the enthalpy of mixing:

$$\frac{G^E}{R \cdot T} = \left(\frac{G^E}{R \cdot T} \right)_C + \left(\frac{G^E}{R \cdot T} \right)_R \qquad [3.80]$$

with subscripts *C* and *R* denoting 'combinatorial' and 'residual', respectively. The combinatorial part is determined only by the composition and by the sizes and shapes of the molecules; it requires only pure-component data. The residual part, however, depends also on the intermolecular forces; the two adjustable parameters, therefore, appear only in the residual part [205].

For a multicomponent system, the UNIQUAC expressions for the terms in the right-hand side of Equation [3.90] are:

$$\left(\frac{G^E}{R\cdot T}\right)_C = \sum_{i=1}^{m} x_i \cdot \ln\frac{\phi_i}{x_i} + \frac{z}{2}\cdot\sum_{i=1}^{m} q_i \cdot x_i \cdot \ln\frac{\theta_i}{\phi_i} \qquad [3.81]$$

$$\left(\frac{G^E}{R\cdot T}\right)_R = -\sum_{i=1}^{m} q_i \cdot x_i \cdot \ln\left(\sum_{j=1}^{m}\theta_j \cdot \tau_{ji}\right) \qquad [3.82]$$

where z is the lattice coordination number, arbitrarily given a value of 10; and the segment fraction ϕ, the area fraction θ and the parameter τ are given by:

$$\phi_i = \frac{r_i \cdot x_i}{\sum_{j=1}^{m} r_j \cdot x_j} \qquad [3.83]$$

$$\theta_i = \frac{q_i \cdot x_i}{\sum_{j=1}^{m} q_j \cdot x_j} \qquad [3.84]$$

$$\tau_{ij} = \exp\left(-\frac{u_{ij} - u_{jj}}{R\cdot T}\right) \qquad [3.85]$$

where $(u_{ij} - u_{jj}) = \Delta u_{ij}$ are the adjusting parameters of the model and represent the description of the energy interaction between a molecule of i and a molecule of j; and the parameters r and q are pure-component molecular-structure constants depending on molecular size and external surface areas. These structural parameters can be obtained from crystallographic data, although it is also possible to estimate them through a group contribution method, using the Van der Waals volumes and areas of the functional groups [260, 261] and making them dimensionless by reference to the volume or area of a methylene element in an infinite hydrocarbon chain.

For any component i, the expression of the activity coefficient provided by the UNIQUAC model is:

$$\ln\gamma_i = \ln\frac{\phi_i}{x_i} + \frac{z}{2}\cdot q_i \cdot \ln\frac{\theta_i}{\phi_i} + l_i - \frac{\phi_i}{x_i}\cdot\sum_{j=1}^{m} x_j \cdot l_j -$$

$$- q_i \cdot \ln\left(\sum_{j=1}^{m}\theta_j \cdot \tau_{ji}\right) + + q_i - q_i \cdot \sum_{j=1}^{m}\left(\frac{\theta_j \cdot \tau_{ij}}{\sum_{k=1}^{m}\theta_k \cdot \tau_{kj}}\right) \qquad [3.86]$$

where:

$$l_j = \frac{z}{2}\cdot\left(r_j - q_j\right) - \left(r_j - 1\right) \qquad [3.87]$$

- ***The NRTL and UNIQUAC equations for the correlation of LLE data of systems involving ILs***

In spite of the adaptations to systems with electrolytes, the original NRTL equation has been satisfactorily tested for the correlation of the LLE data of most of the ternary systems involving ILs available in literature [163-165,171-174, 262-270]. Nevertheless, it seems that the fit is just appropriate, being hard to get valuable information from the binary interaction parameters in order to extrapolate their use to other systems. But, despite this limitation, the NRTL provides undoubtedly valuable correlations of the LLE data.

A way to remediate the problems in applying the UNIQUAC equation to LLE data of systems with imidazolium-based ILs was recently proposed [271]. It is based on quantum chemical calculation to estimate the molecular volumes and surface areas of ILs, being a rigorous method and not being limited to any class of compounds.

On the other hand, the absence of the volume and surface parameters poses a hindrance in calculation of the binary interaction parameters for the UNIQUAC model or its modified versions. Empirical equations have been used to compute the r and q values of the ILs, for example using the molar volume of the IL and estimating a bulk factor. But for many ILs, the molar volumes at standard temperature are not known and the general tendency to calculate the molar volume is by adding the volumes of the various groups in the molecule. In addition, the application of this alternative has been limited to the correlation of binary vapour-liquid equilibrium data [272, 273] or utilizing parameters derived from binary solid-liquid equilibrium data [274]. Several modified versions of this model can be found in literature specifically applied for ionic liquids [275].

3.2.2 Objective

In this part of the work the ability of several ionic liquids as extraction solvents in desulfurization will be evaluated from the thermodynamical point of view.

In the first place, the selection *a priori* of the most promising candidates from the huge family of ionic liquids was carried out. Basing our choice in experimental solubility tests, three imidazolium-based ionic liquids: 1-octyl-3-methylimidazolium tetrafluoborate ([C_8mim][BF_4]), 1-octyl-3-methylimidazolium bis{(trifluoromethyl sulfonyl)imide}([C_8mim][NTf_2]) and 1-ethyl-3-methylimidazolium ethylsulfate([C_2mim][$EtSO_4$]) and a poly substituted pyridinium ionic liquid, 1-hexyl-3,5-dimethylpyridinium bis(trifluoromethyl sulfonyl)imide ([C_6mmPy][NTf_2]) were chosen.

For all chosen solvents, a second step will consist on the analysis of their suitability for our purposes according to thermodynamic criteria. For this reason, the study of liquid-liquid equilibria of each one of the ternary systems composed by IL, a sulfur or nitrogen-containing compound and a fuel representative constituent is going to be carried out and experimental data are going to be correlated and analysed.

The determination of liquid-liquid equilibrium data of ternary mixtures composed by ionic liquid, thiophene and several hydrocarbons provides useful thermodynamic parameters, from the point of view of extraction, as the solution distribution ratio or the selectivity. Correlation of these data is needed to get useful parameters for the design of operation units.

3.2.3. Experimental

3.2.3.1 Chemicals

n-Hexane (Fluka, puriss. p.a. ACS ≥99.0 wt%), n-Heptane (Fluka, >99.5 wt%), n-dodecane and n-hexadecane (Aldrich, purum, >99.0 wt%), toluene (Sigma-Aldrich, purum, > 99.5 wt %), 2,2,4-trimethylpentane (i-octane) (Fluka, purum, > 99.5 wt %), thiophene (Aldrich, purum, >99.5 wt %), dibenzotiophene (Aldrich, 98 wt%) and pyridine (Riedel-de Häen, puriss. ≥99.5 wt%, GC) were used as received from supplier without further purification. Gas chromatography (GC) analysis did not detect any appreciable peak of impurities.

Synthesis of ionic liquids

The ionic liquids used in this work were synthesized in our laboratory following the reaction paths described in literature. Figure 3.6 show different experimental set up for synthesis and purification of ionic liquids

Preparation of [C_8mim][NTf_2]:

First, the salt [C_8mim][Cl] was prepared by direct alkylation of 1-methylimidazole with an excess of 1-chlorooctane, in a similar manner to that reported elsewhere [206]. This chloride ionic liquid was mixed with Li [NTf_2] salt in deionized water, thus obtaining the [C_8min][NTf_2] by ion methathesis which forms a dense nonaqueous phase [207, 208]. Dichloromethane was added to facilitate the separation of organic phase, with the desired ionic liquid, and the aqueous phase with the byproduct LiCl. The organic phase was washed several times with water, until there was no observance of a precipitate by adding silver (I) nitrate to the residual aqueous phase, thus indicating the absence of chloride in significant levels [209]. The dichloromethane was removed in a rotary evaporator, and the purification of the ionic liquid was completed by heating it under high vacuum for at least 48 h (1 mbar, 80 ºC). The final product was characterized by ^{1}H NMR and ^{13}C NMR spectroscopy (Figure A1 and Figure A2 in Apendix A) and its water content was verified by Karl Fischer titration.

Preparation of [C_8mim][BF_4]:

1-Methylimidazole was reacted with an excess of 1-bromooctane to produce 1-methyl-3-octylimidazolium bromide. The formed ionic liquid [C_8mim][Br] was mixed with Na[BF_4] salt, using deionized water as solvent, obtaining the [C_8min][NTf_2] by ion methathesis. The latter is

immiscible with water and thus, two phases appeared. The ionic liquid phase was decanted and dissolved in dichloromethane, and this mixture washed several times with water. A rotary evaporator was used first to remove the dichloromethane and water, and then purification was completed under high vacuum [210]. The final product was characterized by ^{1}H NMR and ^{13}C NMR (Figure A3 and Figure A4 in Apendix A) spectroscopy and its water content was verified by Karl Fischer titration.

Preparation of [C_2mim][$EtSO_4$.]:

The 1-ethyl-3-methylimidazolium ethylsulfate ionic liquid, [C_2mim][$EtSO_4$], was synthesized in our laboratory by direct reaction of equimolecular quantities of 1-methylimidazole (Aldrich, > 99 %, GC) and 1-ethoxysulfonyloxyethane (Aldrich, > 98 %, GC) in toluene [211]. The alkylation can be run under solvent-free conditions, however, the alkylation reactions are very exothermic, and the solvent acts as a diluent and heat sink to moderate and control the reactivity. A solution of 1-methylimidazole in toluene was prepared first and then diethyl sulfate was added drop-wise under helium atmosphere. Reaction was done on an ice bath to avoid rising of the temperature over 40 ºC. In addition, both reagents are soluble in toluene whereas the IL products form a biphase, thus facilitating simple isolation of pure products. As [C_2mim][$EtSO_4$] is non-soluble in toluene, it was separated from reagents and solvent and then washed several times with fresh toluene. Removal of residual volatile compounds in the ionic liquid was carried out first in a rotary evaporator (75 ºC,) and later under vacuum (1 mbar, 80 ºC) for 48 h. The purity of the IL was verified by 1H-NMR and 13C-NMR spectroscopy (Figure A5 and Figure A6 in Apendix A).

Preparation of [C_6mmPy][NTf_2.]

Synthesis path was based on previous general publications [212], 3,5-Lutidine (Aldrich, 98+%), was reacted in a first step with an excess of 1-bromohexane (Fluka, purum, > 98.0 wt %) at 70ºC under helium atmosphere until the reaction had come to completion to produce 1-hexyl-3,5-dimethylpyridinium bromide. In a second stage, synthesized [C_6mmpy]Br ionic liquid was mixed in aqueous solution with Li[NTf_2] salt obtaining the desired final product [C_6mmpy][NTf_2] by ion methatesis direct reaction. New formed ionic liquid remains in a dense nonaqueous phase while salt excess and byproduct LiBr are collected together in the aqueous layer. Bromide content in aqueous phase was tested adding silver (I) nitrate after washing several times with deionized water until no precipitate formation was detected. After extraction, ionic liquid water content was

removed by using a rotary evaporator and a further purification under high vacuum for 48h at 70ºC. The purity of the final product was adequately characterized by analyzing its ^{1}H NMR and ^{13}C NMR spectra (Figure A37 and Figure A8 in Apendix A).

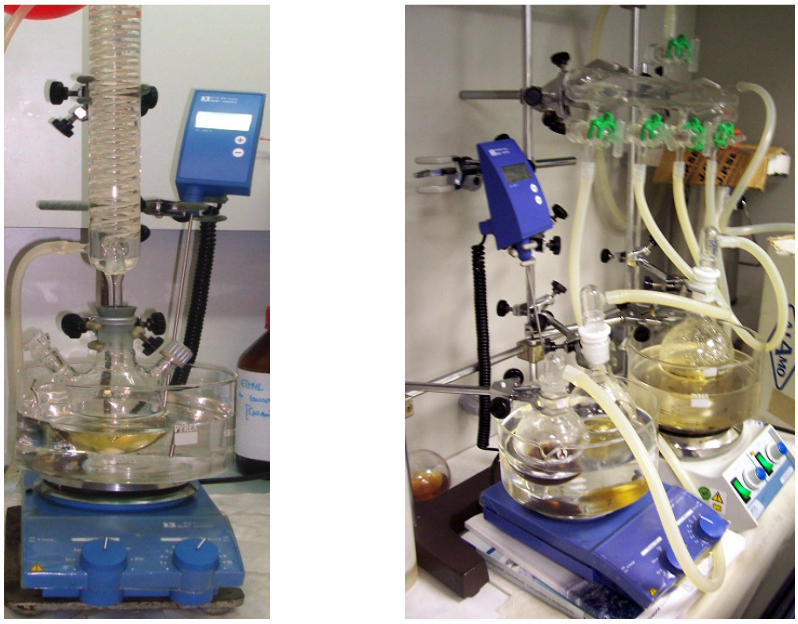

Figure 3.6 Experimental set up for synthesis and purification of ionic liquids.

In Table 3.1 water content of pure compounds is reported, and their experimental densities and refractive indices are compared with the available values published by other authors [213-215].

Table 3.1. CAS-register number, water mass fraction (ω_{H20}), and density (ρ) and refractive index (n_D) for the pure components at 298.15 K and atmospheric pressure.

Component	CAS	ω_{H20} (ppm)	ρ /g·cm^{-3}		n_D	
			exp.	lit.	exp.	lit.
n-Hexane	110-54-3	75	0.65506	0.65484[213]	1.37287	1.37226[213]
n-Dodecane	112-40-3	31	0.74532	0.74518 [213]	1.42011	1.41952[213]
n-Hexadecane	544-76-3	7.4	0.77115	0.77008[213]	1.43232	1.4329[213]
n-Heptane	142-82-5	4.8	0.67947	0.67946[213]	1.38517	1.38511[213]
2,2,4-Trimethylpentane	540-84-1	4.9	0.68784	0.68778[214]	1.38921	1.3895[214]
Toluene	108-88-3	174	0.86220	0.86219[214]	1.49393	1.49413[214]
Thiophene	110-02-1	314	1.05859	1.05887 [213]	1.52530	1.52572[213]
Pyridine	110-86-1	177	0.97802	0.97824[213]	1.50699	1.50745[213]
[C_6mmPy][NTf_2]	Not found	59.8	1.32814	1.33[215]	1.44978	Not found
[C_8mim][BF_4]	244193-52-0	51	1.10442	1.103506 [216]	1.43329	1.4322 [217]
[C_8mim][NTf_2]	178631-04-4	21	1.31978	1.31 [218]	1.43270	Not found
[C_2mim][$EtSO_4$]	342573-75-5	148	1.23817	1.23763 [219]	1.47903	1.47940 [219]

3.2.3.2. Experimental procedure

Physical Properties and Water content

Values for densities were obtained with viscosity correction in an Anton Paar DMA 5000 densimeter (Figure 3.7)with an uncertainty in the measurement of ±10-5 g·cm-3. Temperature of the densimeter, was measured with uncertainties of ± 0.01K.

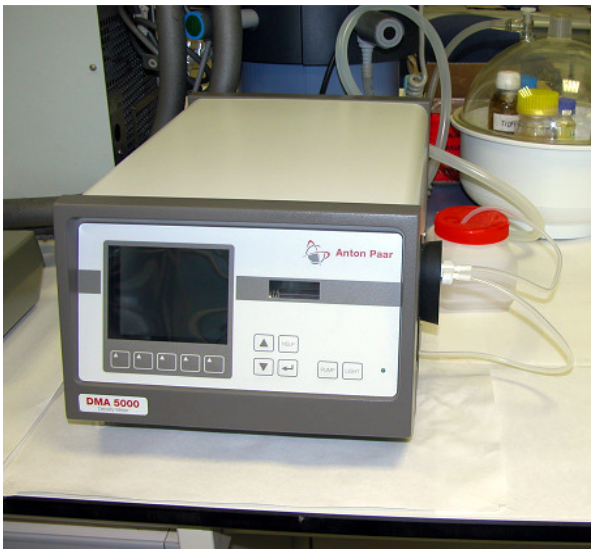

Figure 3.7 Densimeter Anton Paar DMA 5000

Refractive indices were measured in an ATAGO RX-5000 refractometer (Figure 3.8) connected to a Heto Therm thermostat to keep constant temperature with uncertainties of ± 0.02K.. The uncertainty in the refractive index measurement is ±4•10-5.

Figure 3.8 RX-5000 refractometer

Karl Fischer titration method using a Metrohm 737 KF coulometer (Figure 3.9) and Hydranal reagent (Riedel-de Haën) was employed for water contents measuring.

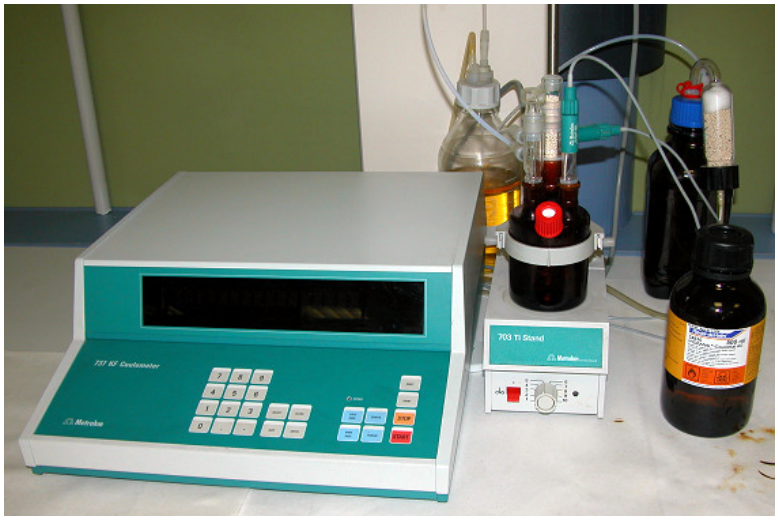

Figure 3.9 Metrohm 737 KF coulometer

All weighing was carried out in a Mettler Toledo AT 261 balance (Figure 3.10) with an accuracy of $\pm 10^{-4}$ g.

Figure 3.10 Mettler Toledo AT 261 balance

Experimental determination of LLE data

LLE data for ternary systems were experimentally determined by analysis of phases at equilibrium.

One pot extraction experiments were carried out for the determination of liquid-liquid equilibrium data. Mixtures of the three studied components lying into the immiscible region were introduced into a 30ml jacketed glass vessel containing a magnetic stirrer. These glass cells were fabricated in the glassblowing workshop of the U.S.C. The jackets were connected to a thermostatic bath (SELECTA 6000382) maintaining the temperature at 298.15 K with uncertainties of ± 0.03K. System must be properly sealed to avoid losses of volatile components by evaporation or moisture gain from atmosphere. Figures 3.11 a) and b) show the design characteristics and the set up of the employed equilibrium cells.

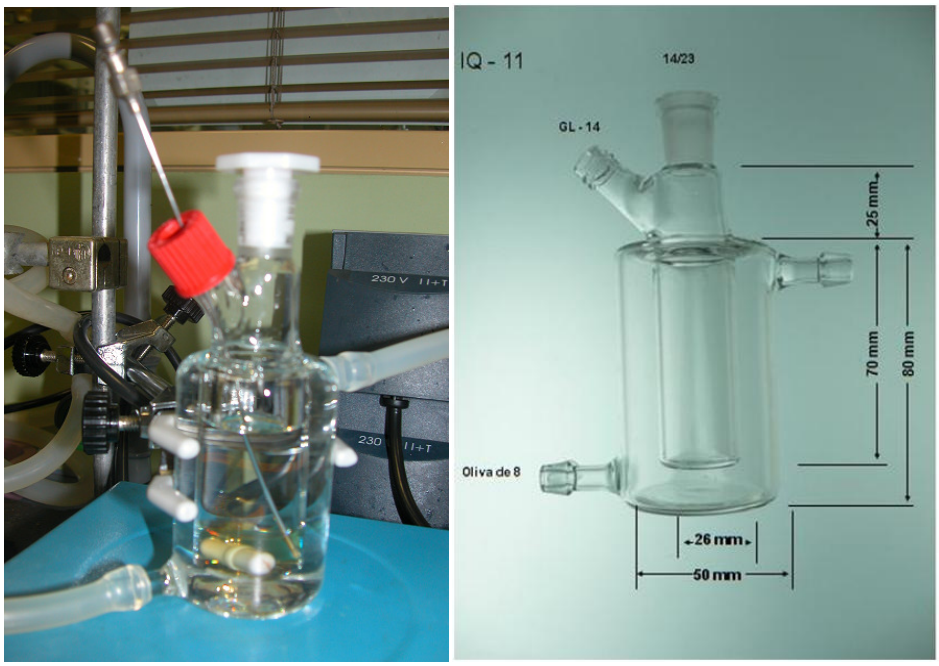

Figures 3.11 a) set up of the employed equilibrium cells and b) design characteristics of the employed equilibrium cells.

Several experiments were carried out with the aim of establishing required stirring times to reach equilibrium state. For the most difficult systems, after 16h of vigorous stirring to ensure good contact between phases, equilibrium was achieved and the system was settled down for 8h until phase separation is guaranteed.

Samples of both layers were withdrawn and analysed by gas chromatography to determine thiophene and hydrocarbon compositions using an internal standard method. ILs

compositions were determined by difference. Two HP 6890 Series gas chromatographs, both of them equipped with an Autosampler 7683 Series each, and two different detectors were used: a Flame Ionization Detector (FID) and a Thermal Conductivity Detector (TCD). A fused silica capillary column SPBTM-1 sulfur and an HP-FFAP Polyethylene Glycol TPA column were selected and protected with an empty pre-column to collect ionic liquid that could be not retained by the liner.The GC operating conditions are given in Table 3.2. All of the compositions for the ternary systems could be determined using both of GCs but the ones which contains toluene which drove to higher uncertainties in mole fraction when using the TCD.

All weighing to prepare samples for analysis calibration was carried out in a Mettler Toledo AT 261 balance with an accuracy of $\pm 10^{-4}$ g. A meticulous calibration during data acquisition provided estimated experimental uncertainties to be ±0.006 mole fraction in the hydrocarbon-rich phase and ±0.007 mole fraction in the ionic liquid-rich phase. All samples were injected five times, for improvement of the accuracy. To check the uncertainty in the determination of mole fraction compositions, eight samples were prepared by weight and compositions were calculated using the calibration curves and compared.

Figure 3.12. GC HP 6890 Series equipped with FID detector (above) and TCD detector (below)

Table 3.2. GC conditions employed for analysis of ternary systems composition. Injection 1μL, Split ratio 50:1

	IL + C_4H_4S + Hydrocarbon	IL + C_4H_4S + Hydrocarbon
Column	HP-FFAP Polyethylene Glycol TPA (25 m × 200 μm × 0.3 μm)	HP-5 5 % Phenyl Methyl Siloxane (30 m × 320 μm × 0.25μm)
Detector type	TCD	FID
Detector temperature	i-octane: 523.15 K	Toluene: 523.15 K
Injector temperature	523.15 K	583.15 K
Carrier gas	Helium	Helium
Flow rate	1 mL·min^{-1}	1 mL·min^{-1}
Toven	6.5 min at 353.15K $\xrightarrow{\text{ramp } 100K\cdot\text{min}^{-1}}$ 413.15 K isothermal for 6 min	3.5 min at 313.15K $\xrightarrow{\text{ramp } 8K\cdot\text{min}^{-1}}$ 333.15 K $\xrightarrow{\text{ramp } 50\,K\cdot\text{min}^{-1}}$ 433 K isothermal for 6 min

Column	HP-FFAP Polyethylene Glycol TPA (25m × 200μm × 0.3μm)
Detector type	TCD
Detector temperature	*n*-Hexane / *n*-Heptane: 250 ºC
	n-Dodecane / *n*-Hexadecane: 270 ºC
Carrier gas	Helium
Injector temperature	250 ºC
Flow rate	*n*-Hexane / *n*-Heptane: 0.9 mL·min^{-1}
	n-Dodecane / *n*-Hexadecane: 1.2 mL·min^{-1}
Column oven	*n*-Hexane / *n*-Heptane: 70 ºC (3 min) —› 100 ºC (100 ºC/min), 1min
	n-Dodecane: 90 ºC (2 min) —› 150 ºC (70 ºC/min), 1 min
	n-Hexadecane: 90 ºC (4 min) —› 180 ºC (50 ºC/min), 2 min

3.2.4. Results

The experimental LLE data for the ternary systems composed by IL+ thiophene + {n-hexane, n-heptane, n-dodecane, n-hexadecane, isooctane and toluene} and IL+ pyridine+n-hexane at 298.15 K and atmospheric pressure are reported in Tables 3.3 to 3.31. In these tables values for solute distribution ratio and selectivity are also shown. Equilateral triangular diagrams with the graphical representation of the experimental tie-lines are shown in Figures 3.7 to 3.35.

Solute distribution ratio (β) and selectivity (S) are defined by following equations:

$$\beta = \frac{x_2^{II}}{x_2^{I}} \qquad [3.88]$$

$$S = \frac{x_2^{II} \cdot x_1^{I}}{x_2^{I} \cdot x_1^{II}} \qquad [3.89]$$

where x represents mole fraction, subscripts 1 and 2 refer to inert (hydrocarbon) and solute (thiophene, pyridine) and superscripts I and II refer to inert-rich phase and IL-rich phase, respectively.

Table 3.3 Compositions of experimental tie-lines, solute distribution ratios (β) and selectivities (S) for {[C_8mim][NTf_2] (1) + Thiophene (2) + *n*-Hexane (3)} at 298.15 K and atmospheric pressure.

IL-rich phase			Hydrocarbon-rich phase			β	S
x^{II}_1	x^{II}_2	x^{II}_3	x^{I}_1	x^{I}_2	x^{I}_3		
0.711	0.000	0.289	0.000	0.000	1.000		
0.546	0.190	0.264	0.000	0.087	0.913	2.18	7.55
0.363	0.412	0.225	0.001	0.267	0.732	1.54	5.02
0.274	0.518	0.208	0.000	0.399	0.601	1.30	3.75
0.215	0.593	0.192	0.000	0.545	0.455	1.09	2.58
0.168	0.660	0.172	0.000	0.620	0.380	1.06	2.35
0.143	0.701	0.156	0.000	0.695	0.305	1.01	1.97
0.118	0.768	0.114	0.000	0.800	0.200	0.96	1.68
0.100	0.809	0.091	0.000	0.858	0.142	0.94	1.47
0.065	0.935	0.000	0.000	1.000	0.000	0.94	-

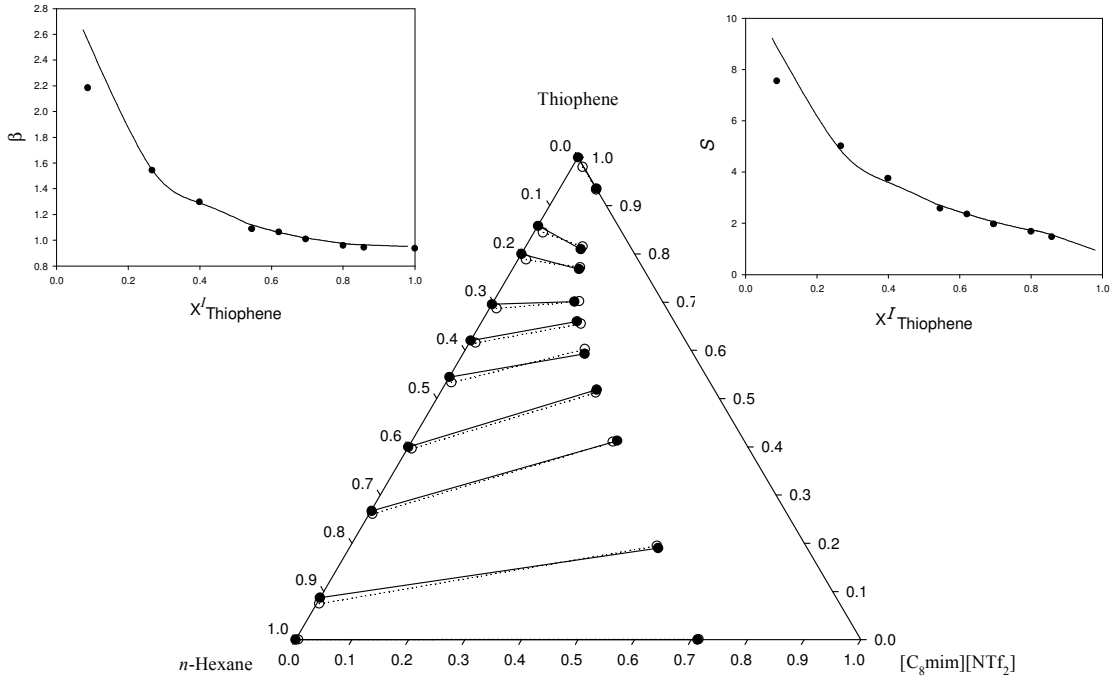

Figure 3.13. Experimental tie-lines (•, solid line), solute distribution ratio (β) and selectivites (S) for the LLE of the ternary system [C_8mim][NTf_2] (1) + Thiophene (2) + *n*-Hexane (3) at 298.15 K and atmospheric pressure. The corresponding tie-lines (o, dotted line), β and S correlated by means of the UNIQUAC equation, are also plotted.

Table 3.4 Compositions of experimental tie-lines, solute distribution ratios (β) and selectivities (S) for {[C_8mim][NTf_2] (1) + Thiophene (2) + *n*-Heptane (3)} at 298.15 K and atmospheric pressure.

IL-rich phase			Hydrocarbon-rich phase			β	S
x^{II}_1	x^{II}_2	x^{II}_3	x^{I}_1	x^{I}_2	x^{I}_3		
0.755	0.000	0.245	0.000	0.000	1.000		
0.560	0.225	0.215	0.001	0.098	0.901	2.30	9.62
0.399	0.409	0.192	0.001	0.232	0.767	1.76	7.04
0.273	0.552	0.175	0.000	0.405	0.595	1.36	4.63
0.181	0.665	0.154	0.000	0.634	0.366	1.05	2.49
0.140	0.731	0.129	0.000	0.782	0.218	0.94	1.58
0.117	0.788	0.095	0.000	0.872	0.128	0.90	1.22
0.088	0.862	0.050	0.000	0.950	0.050	0.91	0.91
0.065	0.935	0.000	0.000	1.000	0.000	0.94	

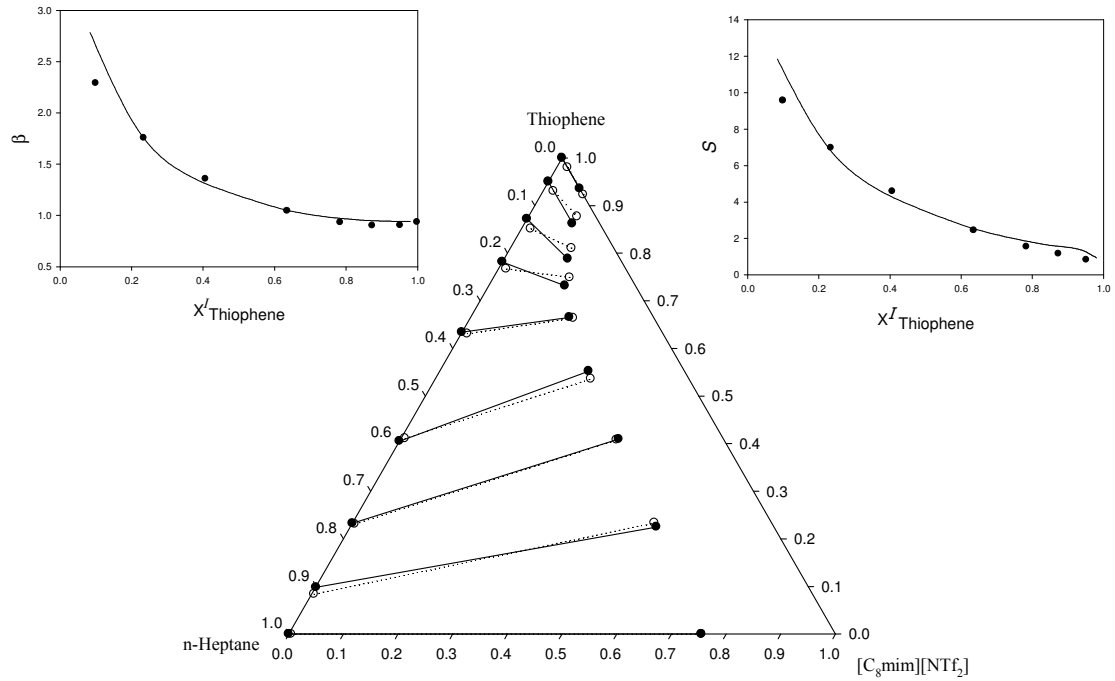

Figure 3.14. Experimental tie-lines (•, solid line), solute distribution ratio (β) and selectivites (S) for the LLE of the ternary system [C_8mim][NTf_2] (1) + Thiophene (2) + *n*-Heptane (3) at 298.15 K and atmospheric pressure. The corresponding tie-lines (o, dotted line), β and S correlated by means of the UNIQUAC equation, are also plotted.

Table 3.5 Compositions of experimental tie-lines, solute distribution ratios (β) and selectivities (S) for {[C_8mim][NTf_2] (1) + Thiophene (2) + n-Dodecane (3)} at 298.15 K and atmospheric pressure.

IL-rich phase			Hydrocarbon-rich phase			β	S
x^{II}_1	x^{II}_2	x^{II}_3	x^{I}_1	x^{I}_2	x^{I}_3		
0.911	0.000	0.089	0.000	0.000	1.000		
0.843	0.064	0.093	0.003	0.046	0.951	1.39	14.23
0.692	0.213	0.095	0.002	0.174	0.824	1.22	10.62
0.538	0.363	0.099	0.003	0.307	0.692	1.18	8.25
0.498	0.405	0.097	0.001	0.375	0.624	1.08	6.95
0.455	0.446	0.099	0.003	0.426	0.571	1.05	6.03
0.413	0.485	0.102	0.000	0.457	0.543	1.06	5.65
0.368	0.528	0.104	0.006	0.512	0.482	1.03	4.78
0.336	0.559	0.105	0.000	0.597	0.403	0.94	3.59
0.292	0.604	0.104	0.006	0.666	0.328	0.91	2.86
0.218	0.676	0.106	0.004	0.798	0.198	0.85	1.58
0.163	0.741	0.096	0.002	0.871	0.127	0.85	1.13
0.059	0.900	0.041	0.002	0.950	0.048	0.95	1.11
0.065	0.935	0.000	0.000	1.000	0.000	0.95	

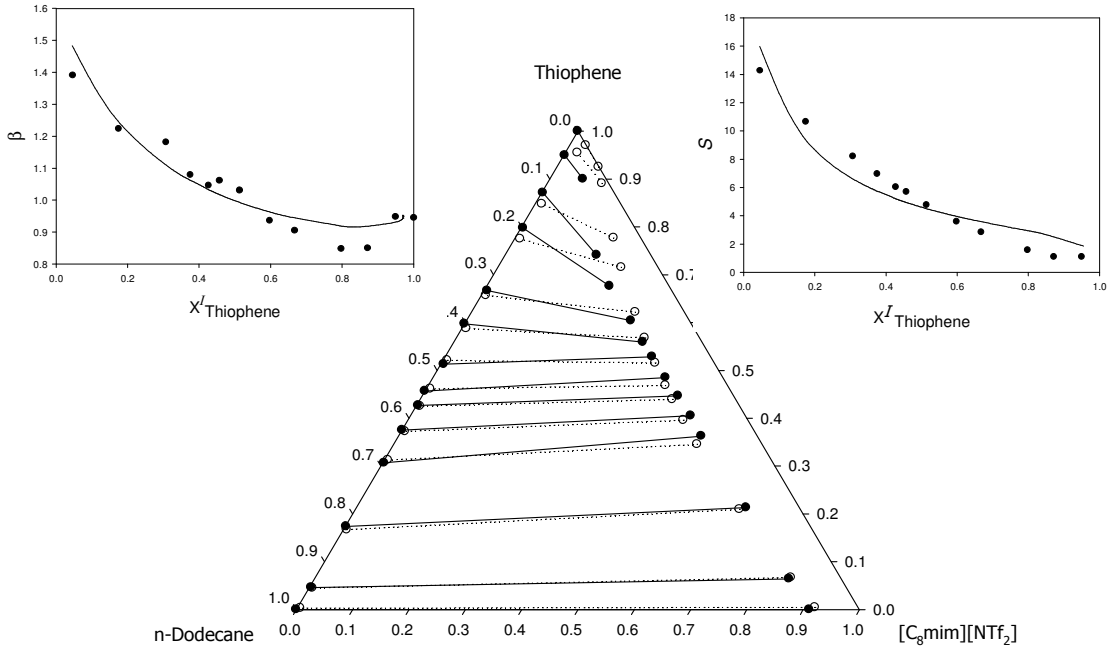

Figure 3.15. Experimental tie-lines (•, solid line), solute distribution ratio (β) and selectivites (S) for the LLE of the ternary system [C_8mim][NTf_2] (1) + Thiophene (2) + *n*-Dodecane (3) at 298.15 K and atmospheric pressure. The corresponding tie-lines (o, dotted line), β and S correlated by means of the NRTL equation, with α = 0.3 are also plotted.

Table 3.6 Compositions of experimental tie-lines, solute distribution ratios (β) and selectivities (S) for {[C_8mim][NTf_2] (1) + Thiophene (2) + *n*-Hexadecane (3)} at 298.15 K and atmospheric pressure.

IL-rich phase			Hydrocarbon-rich phase			β	S
x^{II}_1	x^{II}_2	x^{II}_3	x^{I}_1	x^{I}_2	x^{I}_3		
0.953	0.000	0.047	0.009	0.000	0.991		
0.845	0.106	0.049	0.004	0.143	0.853	0.74	12.89
0.696	0.242	0.062	0.007	0.297	0.696	0.81	9.15
0.592	0.343	0.065	0.008	0.469	0.523	0.73	5.88
0.471	0.450	0.079	0.001	0.634	0.365	0.72	3.28
0.407	0.515	0.078	0.009	0.741	0.250	0.69	2.22
0.313	0.599	0.088	0.005	0.880	0.115	0.68	0.89
0.226	0.702	0.072	0.007	0.952	0.041	0.74	0.42
0.065	0.935	0.000	0.000	1.000	0.000	0.94	

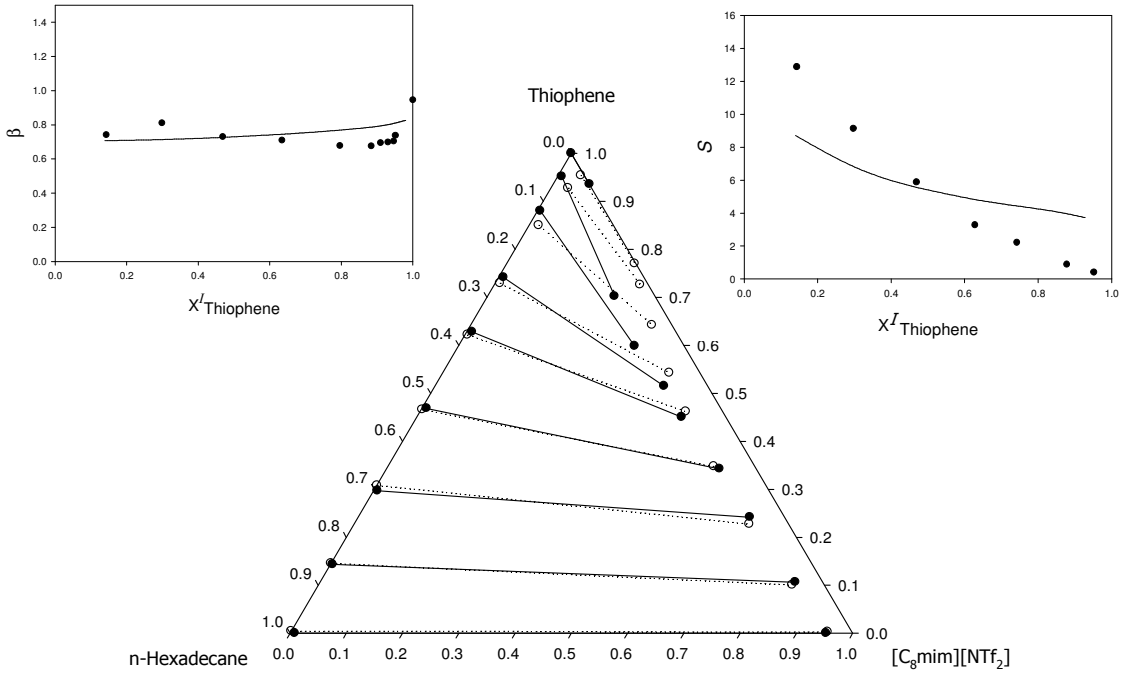

Figure 3.16. Experimental tie-lines (•, solid line), solute distribution ratio (β) and selectivites (S) for the LLE of the ternary system [C_8mim][NTf_2] (1) + Thiophene (2) + *n*-Hexadecane (3) at 298.15 K and atmospheric pressure. The corresponding tie-lines (o, dotted line), β and S correlated by means of the NRTL equation, with α = 0.3 are also plotted.

Table 3.7 Compositions of experimental tie-lines, solute distribution ratios (β) and selectivities (S) for {[C_8mim][NTf_2] (1) + Thiophene (2) + *i*-octane (3)} at 298.15 K and atmospheric pressure.

IL-rich phase			Hydrocarbon-rich phase			β	S
x^{II}_1	x^{II}_2	x^{II}_3	x^{I}_1	x^{I}_2	x^{I}_3		
0.774	0.000	0.226	0.001	0.000	0.999	-	-
0.660	0.135	0.205	0.003	0.044	0.953	3.04	14.17
0.572	0.237	0.191	0.002	0.089	0.909	2.67	12.71
0.441	0.393	0.166	0.006	0.193	0.801	2.04	9.82
0.317	0.525	0.158	0.000	0.328	0.672	1.60	6.79
0.220	0.640	0.140	0.001	0.482	0.517	1.33	4.89
0.163	0.716	0.121	0.002	0.639	0.359	1.12	3.32
0.135	0.758	0.107	0.000	0.740	0.260	1.02	2.49
0.106	0.804	0.090	0.000	0.835	0.165	0.96	1.78
0.074	0.890	0.036	0.000	0.957	0.043	0.93	1.12
0.065	0.935	0.000	0.000	1.000	0.000	0.94	-

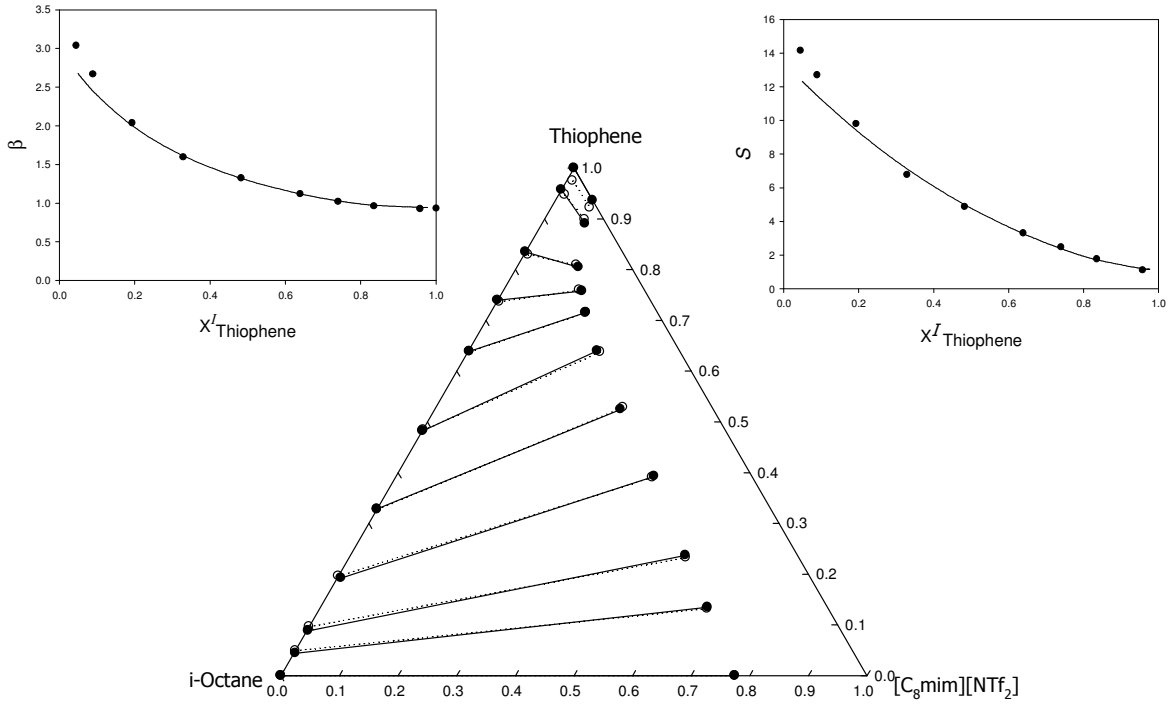

Figure 3.17. Experimental tie-lines (•, solid line), solute distribution ratio (β) and selectivites (S) for the LLE of the ternary system [C_8mim][NTf_2] (1) + Thiophene (2) + i-octane (3) at 298.15 K and atmospheric pressure. The corresponding tie-lines (o, dotted line), β and S correlated by means of the NRTL equation, with $\alpha = 0.3$, are also plotted.

Table 3.8 Compositions of experimental tie-lines, solute distribution ratios (β) and selectivities (S) for {[C_8mim][NTf_2] (1) + Thiophene (2) + Toluene (3)} at 298.15 K and atmospheric pressure.

IL-rich phase			Hydrocarbon-rich phase			β	S
x^{II}_1	x^{II}_2	x^{II}_3	x^{I}_1	x^{I}_2	x^{I}_3		
0.113	0.000	0.887	0.000	0.000	1.000	-	-
0.110	0.069	0.821	0.001	0.074	0.925	0.93	1.05
0.097	0.246	0.657	0.003	0.257	0.740	0.96	1.08
0.095	0.154	0.751	0.000	0.159	0.841	0.97	1.09
0.091	0.341	0.568	0.002	0.381	0.617	0.89	0.97
0.087	0.425	0.488	0.000	0.475	0.525	0.90	0.96
0.086	0.515	0.399	0.000	0.571	0.429	0.90	0.97
0.080	0.654	0.266	0.001	0.727	0.272	0.90	0.92
0.078	0.765	0.157	0.004	0.834	0.162	0.92	0.95
0.065	0.935	0.000	0.000	1.000	0.000	0.94	-

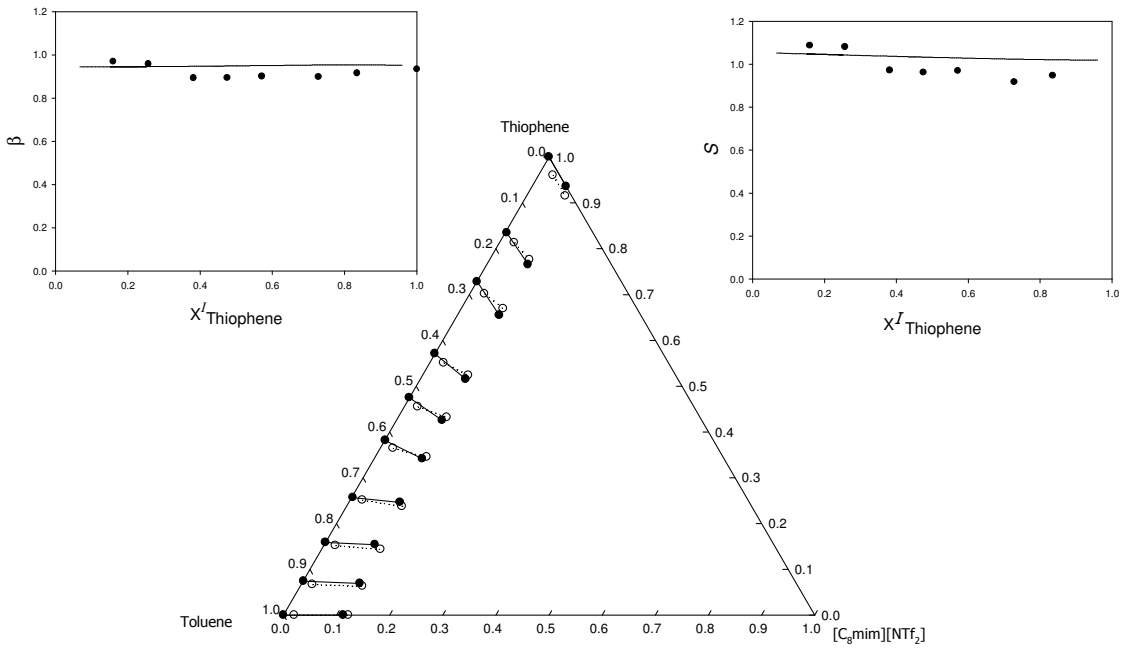

Figure 3.18. Experimental tie-lines (•, solid line), solute distribution ratio (β) and selectivites (S) for the LLE of the ternary system [C_8mim][NTf_2] (1) + Thiophene (2) + Toluene (3) at 298.15 K and atmospheric pressure. The corresponding tie-lines (o, dotted line), β and S correlated by means of the UNIQUAC equation, are also plotted.

Table 3.9 Compositions of experimental tie-lines, solute distribution ratios (β) and selectivities (S) for {[C_8mim][NTf_2] (1) + Pyridine (2) + n-Hexane(3)} at 298.15 K and atmospheric pressure.

IL-rich phase			Hydrocarbon-rich phase			β	S
x^{II}_1	x^{II}_2	x^{II}_3	x^{I}_1	x^{I}_2	x^{I}_3		
0.711	0.000	0.289	0.000	0.000	1.000		
0.597	0.160	0.243	0.006	0.018	0.976	9.14	36.77
0.499	0.276	0.225	0.000	0.047	0.953	5.89	24.96
0.408	0.381	0.211	0.004	0.061	0.935	6.23	27.53
0.353	0.442	0.205	0.006	0.080	0.914	5.51	24.53
0.278	0.519	0.203	0.005	0.119	0.876	4.37	18.88
0.213	0.584	0.203	0.003	0.149	0.848	3.92	16.41
0.126	0.635	0.239	0.004	0.297	0.699	2.14	6.26
0.066	0.642	0.292	0.001	0.425	0.574	1.51	2.97

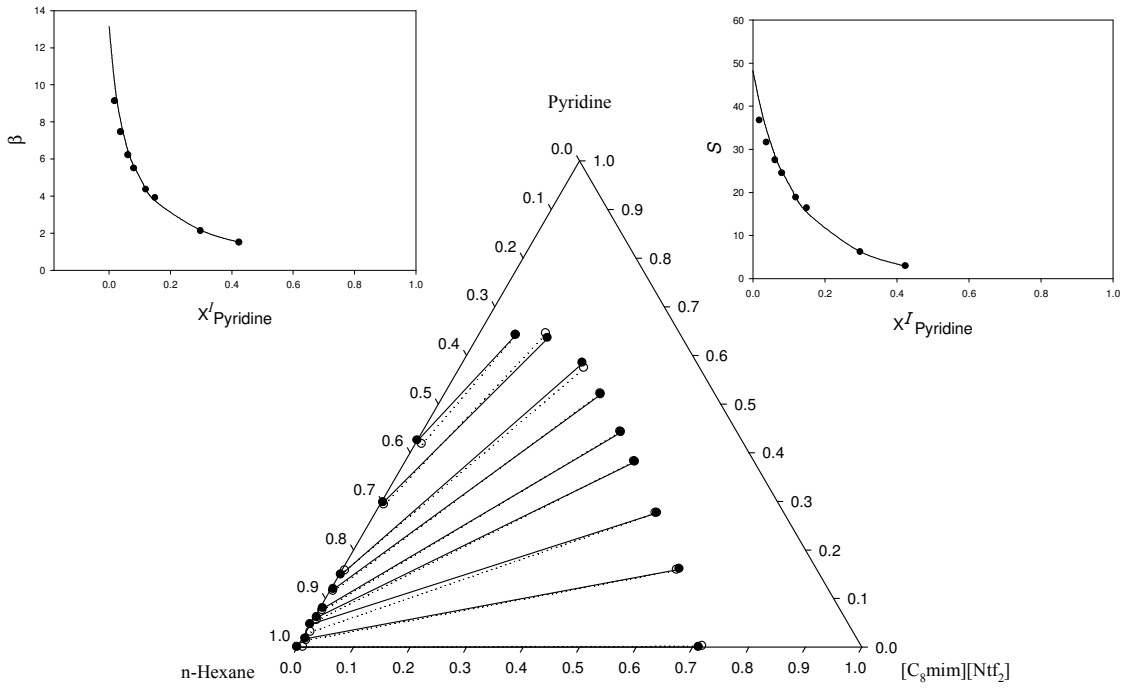

Figure 3.19. Experimental tie-lines (•, solid line), solute distribution ratio (β) and selectivites (S) for the LLE of the ternary system [C_8mim][NTf_2] (1) + Pyridine (2) + *n*-Hexane (3) at 298.15 K and atmospheric pressure. The corresponding tie-lines (o, dotted line), β and S correlated by means of the UNIQUAC equation, are also plotted.

Table 3.10 Compositions of experimental tie-lines, solute distribution ratios (β) and selectivities (S) for {[C_8mim][BF_4] (1) + Thiophene (2) + *n-H*exane (3)} at 298.15 K and atmospheric pressure.

IL-rich phase			Hydrocarbon-rich phase			β	S
x^{II}_1	x^{II}_2	x^{II}_3	x^{I}_1	x^{I}_2	x^{I}_3		
0.854	0.000	0.146	0.000	0.000	1.000	–	–
0.678	0.182	0.140	0.000	0.065	0.935	2.80	18.69
0.525	0.339	0.136	0.000	0.218	0.782	1.56	8.93
0.432	0.433	0.135	0.000	0.302	0.698	1.43	7.43
0.379	0.490	0.131	0.000	0.360	0.640	1.36	6.68
0.319	0.550	0.131	0.000	0.444	0.556	1.24	5.28
0.275	0.595	0.130	0.000	0.518	0.482	1.15	4.26
0.231	0.646	0.123	0.000	0.607	0.393	1.06	3.39
0.215	0.667	0.118	0.000	0.666	0.334	1.00	2.83
0.183	0.706	0.111	0.000	0.725	0.275	0.97	2.41
0.135	0.775	0.090	0.000	0.826	0.174	0.94	1.81
0.112	0.827	0.061	0.000	0.912	0.088	0.91	1.30
0.100	0.900	0.000	0.000	1.000	0.000	0.90	-

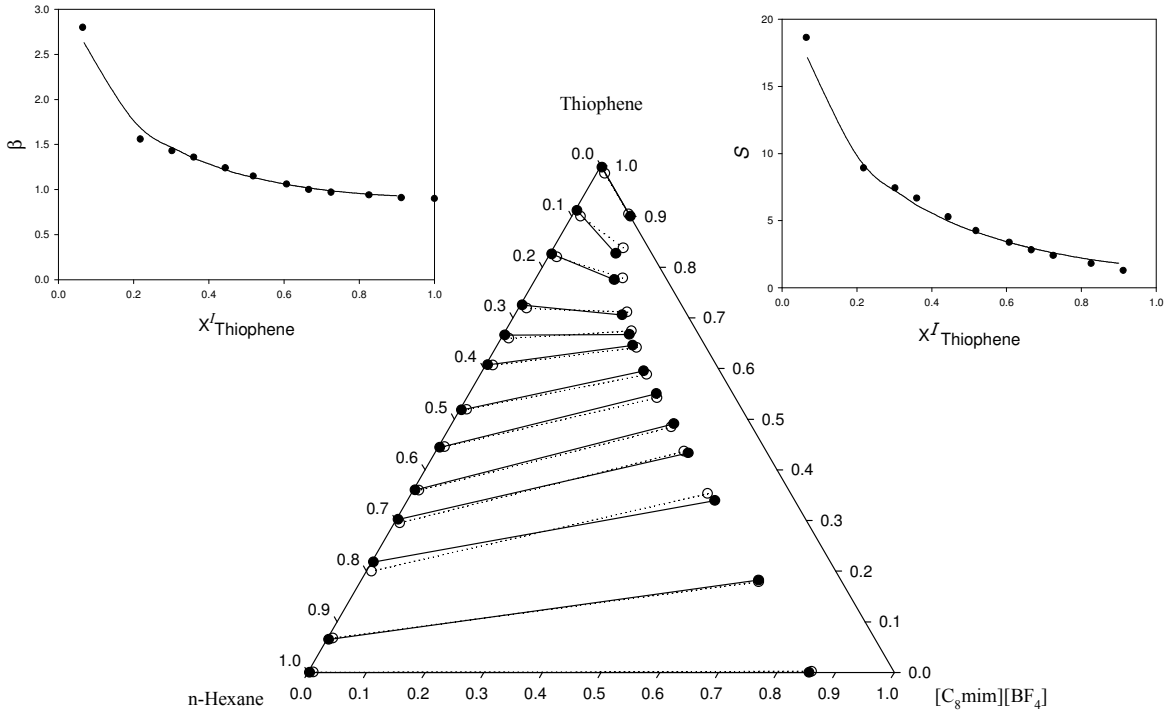

Figure 3.20. Experimental tie-lines (•, solid line), solute distribution ratio (β) and selectivites (S) for the LLE of the ternary system [C_8mim][BF_4] (1) + Thiophene (2) + *n*-Hexane (3) at 298.15 K and atmospheric pressure. The corresponding tie-lines (o, dotted line), β and S correlated by means of the NRTL equation, with $\alpha = 0.3$ are also plotted.

Table 3.11 Compositions of experimental tie-lines, solute distribution ratios (β) and selectivities (S) for {[C_8mim][BF_4] (1) + Thiophene (2) + *n*-Heptane (3)} at 298.15 K and atmospheric pressure.

IL-rich phase			Hydrocarbon-rich phase			β	S
x^{II}_1	x^{II}_2	x^{II}_3	x^{I}_1	x^{I}_2	x^{I}_3		
0.862	0.000	0.138	0.000	0.000	1.000		
0.709	0.152	0.139	0.004	0.094	0.902	1.61	10.48
0.557	0.306	0.137	0.004	0.226	0.770	1.35	7.63
0.444	0.422	0.134	0.004	0.370	0.626	1.14	5.34
0.362	0.508	0.130	0.003	0.510	0.487	1.00	3.72
0.312	0.562	0.126	0.000	0.651	0.349	0.86	2.40
0.260	0.627	0.113	0.000	0.771	0.229	0.81	1.65
0.224	0.679	0.097	0.000	0.846	0.154	0.80	1.27
0.122	0.836	0.042	0.000	0.954	0.046	0.88	0.95
0.100	0.900	0.000	0.000	1.000	0.000	0.90	

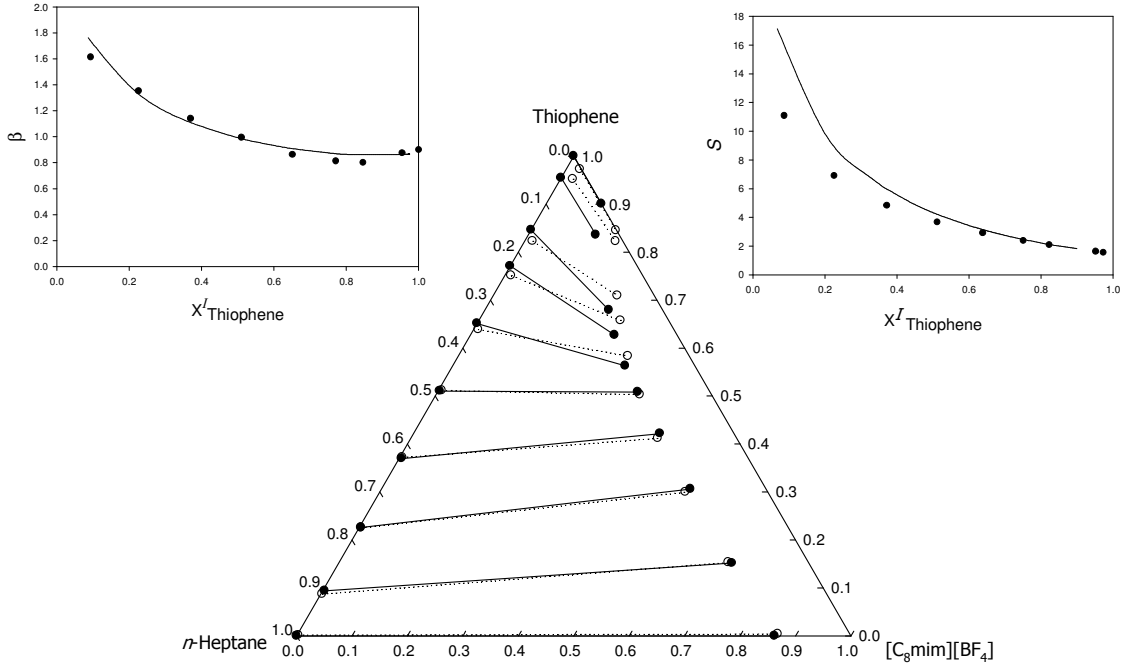

Figure 3.21. Experimental tie-lines (•, solid line), solute distribution ratio (β) and selectivites (S) for the LLE of the ternary system [C_8mim][BF_4] (1) + Thiophene (2) + *n*-Heptane (3) at 298.15 K and atmospheric pressure. The corresponding tie-lines (o, dotted line), β and S correlated by means of the UNIQUAC equation are also plotted.

Table 3.12 Compositions of experimental tie-lines, solute distribution ratios (β) and selectivities (S) for {[C_8mim][BF_4] (1) + Thiophene (2) + *n*-Dodecane (3)} at 298.15 K and atmospheric pressure.

IL-rich phase			Hydrocarbon-rich phase			β	S
x^{II}_1	x^{II}_2	x^{II}_3	x^{I}_1	x^{I}_2	x^{I}_3		
0.956	0.000	0.044	0.000	0.000	1.000		
0.834	0.116	0.050	0.000	0.117	0.883	1.00	17.62
0.691	0.254	0.055	0.000	0.273	0.727	0.93	12.29
0.550	0.389	0.061	0.000	0.452	0.548	0.86	7.76
0.437	0.494	0.069	0.005	0.631	0.364	0.78	4.10
0.417	0.512	0.071	0.002	0.659	0.339	0.78	3.72
0.344	0.580	0.076	0.005	0.769	0.226	0.75	2.23
0.299	0.621	0.080	0.006	0.856	0.138	0.73	1.25
0.255	0.675	0.070	0.000	0.902	0.098	0.75	1.05
0.207	0.730	0.063	0.000	0.933	0.067	0.78	0.83
0.152	0.811	0.037	0.000	0.963	0.037	0.84	0.84
0.100	0.900	0.000	0.000	1.000	0.000	0.90	

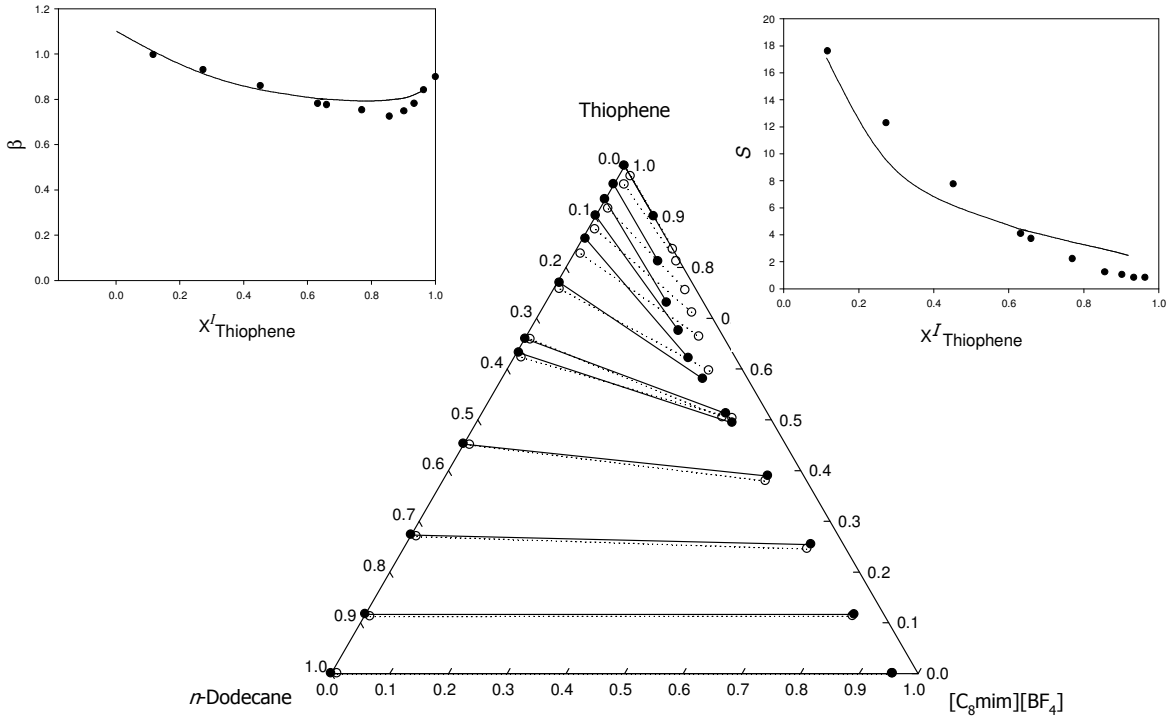

Figure 3.22. Experimental tie-lines (•, solid line), solute distribution ratio (β) and selectivites (S) for the LLE of the ternary system [C_8mim][BF_4] (1) + Thiophene (2) + *n*-Dodecane (3) at 298.15 K and atmospheric pressure. The corresponding tie-lines (o, dotted line), β and S correlated by means of the NRTL equation, with $\alpha = 0.3$ are also plotted.

Table 3.13 Compositions of experimental tie-lines, solute distribution ratios (β) and selectivities (S) for {[C_8mim][BF_4] (1) + Thiophene (2) + n-Hexadecane (3)} at 298.15 K at atmospheric pressure.

IL-rich phase			Hydrocarbon-rich phase			β	S
x^{II}_1	x^{II}_2	x^{II}_3	x^{I}_1	x^{I}_2	x^{I}_3		
0.979	0.000	0.021	0.000	0.000	1.000		
0.886	0.093	0.021	0.000	0.145	0.855	0.64	26.11
0.773	0.202	0.025	0.000	0.317	0.683	0.64	17.41
0.649	0.319	0.032	0.000	0.510	0.490	0.63	9.58
0.521	0.431	0.048	0.000	0.686	0.314	0.63	4.11
0.416	0.528	0.056	0.000	0.834	0.166	0.63	1.88
0.358	0.585	0.057	0.000	0.902	0.098	0.65	1.12
0.295	0.648	0.057	0.000	0.948	0.052	0.68	0.62
0.225	0.748	0.027	0.000	0.987	0.013	0.76	0.36
0.201	0.792	0.007	0.000	0.997	0.003	0.79	0.34
0.100	0.900	0.000	0.000	1.000	0.000	0.90	

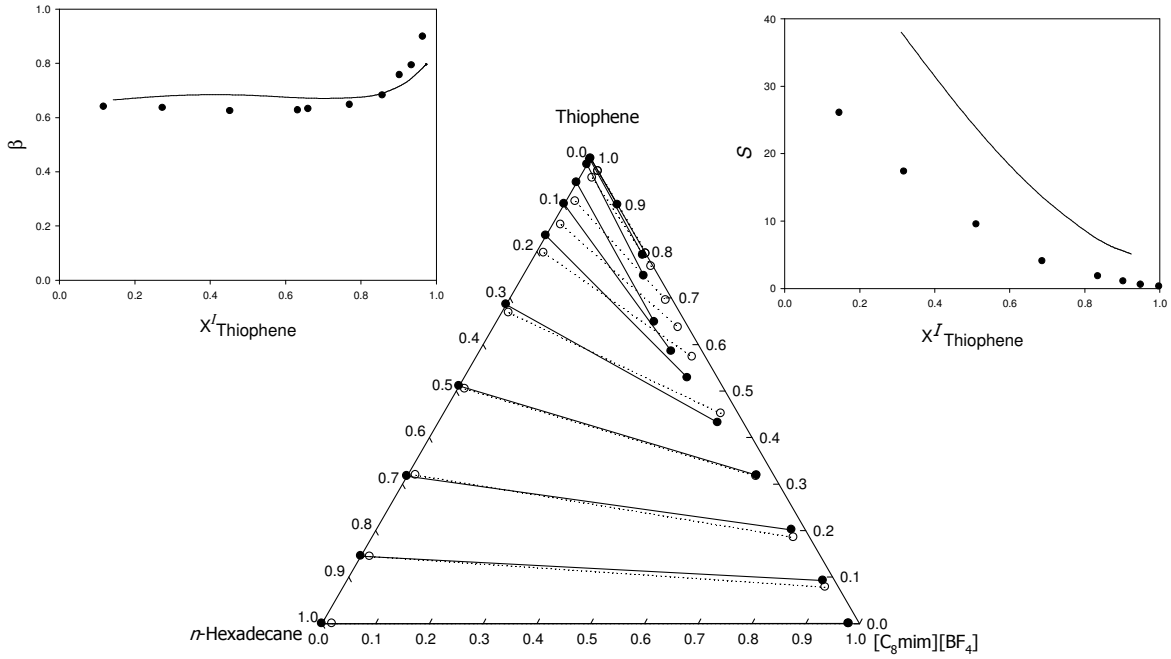

Figure 3.23. Experimental tie-lines (•, solid line), solute distribution ratio (β) and selectivites (S) for the LLE of the ternary system [C_8mim][BF_4] (1) + Thiophene (2) + n-Hexadecane (3) at 298.15 K and atmospheric pressure. The corresponding tie-lines (o, dotted line), β and S correlated by means of the UNIQUAC equation, are also plotted.

Table 3.14 Compositions of experimental tie-lines, solute distribution ratios (β) and selectivities (S) for {[C_8mim][BF_4] (1) + Thiophene (2) + i-octane (3)} at 298.15 K and atmospheric pressure.

IL-rich phase			Hydrocarbon-rich phase			β	S
x^{II}_1	x^{II}_2	x^{II}_3	x^{I}_1	x^{I}_2	x^{I}_3		
0.919	0.000	0.081	0.000	0.000	1.000	–	–
0.790	0.134	0.076	0.000	0.060	0.940	2.23	27.62
0.661	0.258	0.081	0.000	0.124	0.876	2.08	22.50
0.514	0.410	0.076	0.000	0.239	0.762	1.72	17.20
0.418	0.518	0.064	0.000	0.356	0.644	1.46	14.64
0.316	0.616	0.068	0.000	0.516	0.484	1.19	8.48
0.213	0.729	0.058	0.000	0.663	0.337	1.10	6.39
0.155	0.791	0.054	0.000	0.764	0.236	1.04	4.52
0.135	0.819	0.046	0.000	0.828	0.172	0.99	3.69
0.112	0.864	0.024	0.000	0.940	0.060	0.92	2.30
0.100	0.900	0.000	0.000	1.000	0.000	0.90	-

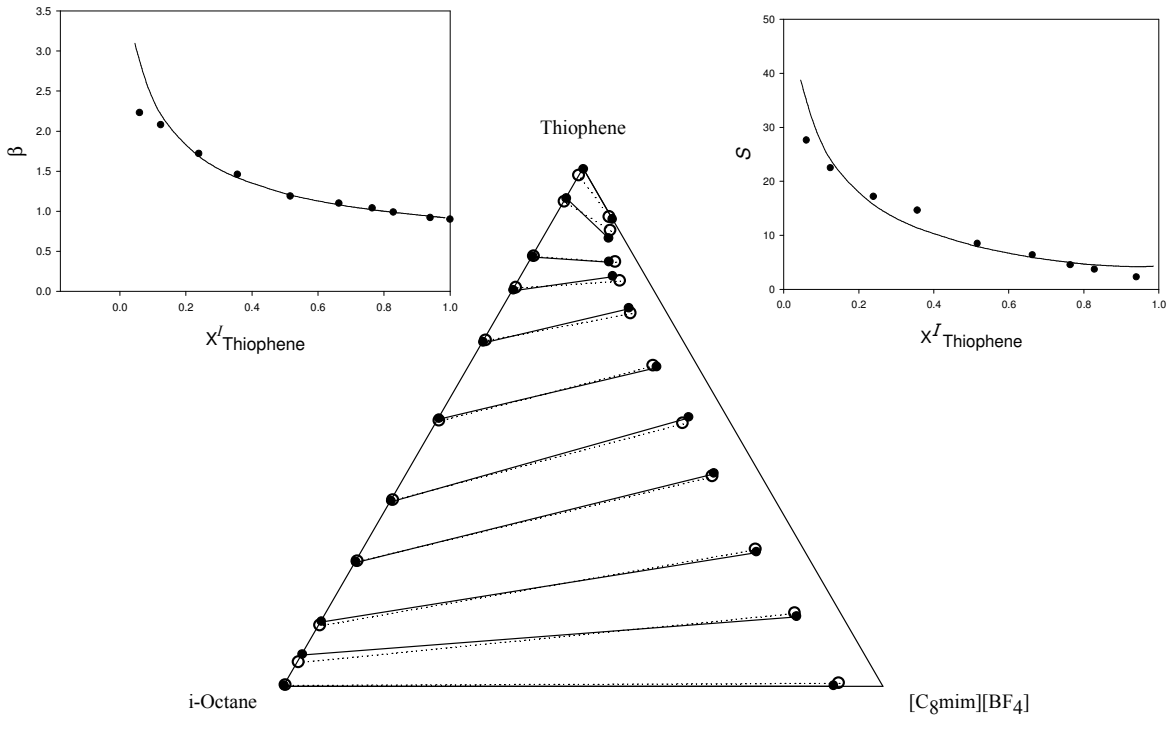

Figure 3.24. Experimental tie-lines (•, solid line), solute distribution ratio (β) and selectivites (S) for the LLE of the ternary system [C_8mim][BF_4] (1) + Thiophene (2) + i-octane (3) at 298.15 K and atmospheric pressure. The corresponding tie-lines (o, dotted line), β and S correlated by means of the UNIQUAC equation, are also plotted.

Table 3.15 Compositions of experimental tie-lines, solute distribution ratios (β) and selectivities (S) for {[C_8mim][BF_4] (1) + Thiophene (2) + Toluene (3)} at 298.15 K and atmospheric pressure.

IL-rich phase			Hydrocarbon-rich phase			β	S
x^{II}_1	x^{II}_2	x^{II}_3	x^{I}_1	x^{I}_2	x^{I}_3		
0.287	0.000	0.713	0.000	0.000	1.000	-	-
0.255	0.139	0.606	0.003	0.124	0.873	1.12	1.61
0.234	0.218	0.548	0.003	0.235	0.762	0.93	1.29
0.205	0.331	0.464	0.003	0.362	0.635	0.92	1.25
0.174	0.498	0.328	0.003	0.547	0.450	0.91	1.25
0.149	0.605	0.246	0.003	0.671	0.326	0.90	1.19
0.137	0.681	0.182	0.003	0.758	0.239	0.90	1.18
0.127	0.736	0.137	0.003	0.820	0.177	0.90	1.16
0.118	0.787	0.095	0.003	0.889	0.108	0.88	1.01
0.112	0.822	0.066	0.003	0.929	0.068	0.88	0.91
0.100	0.900	0.000	0.003	0.997	0.000	0.90	-

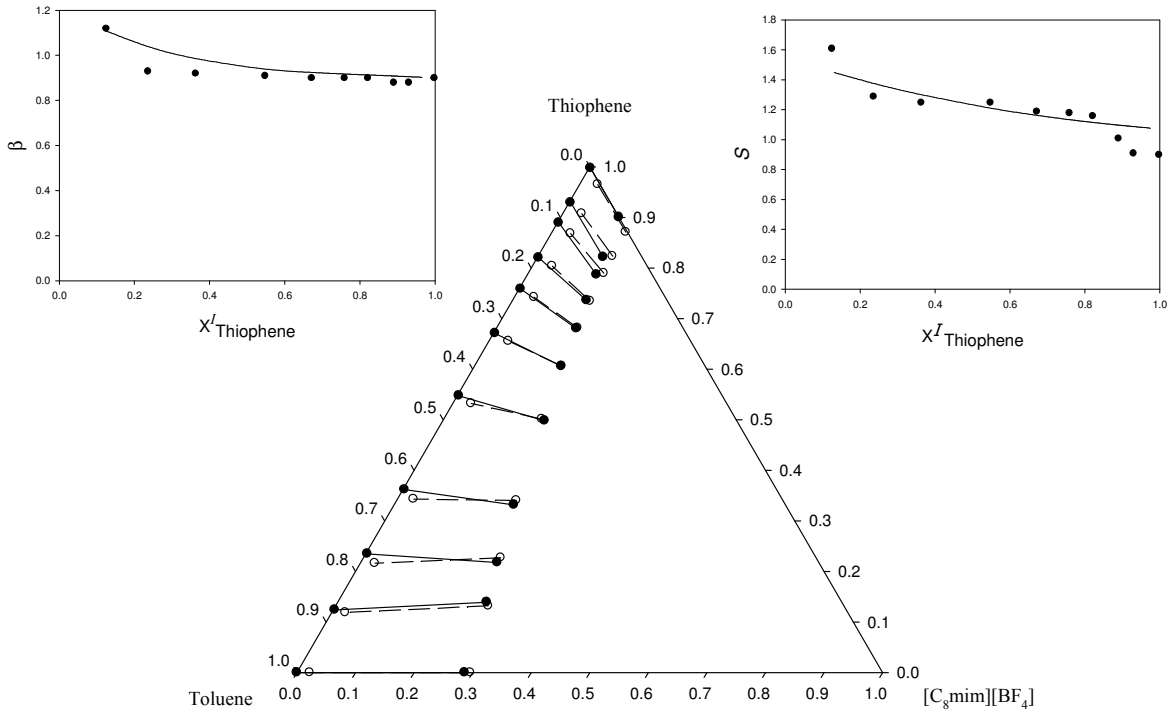

Figure 3.25. Experimental tie-lines (•, solid line), solute distribution ratio (β) and selectivites (S) for the LLE of the ternary system [C_8mim][BF_4] (1) + Thiophene (2) + Toluene (3) at 298.15 K and atmospheric pressure. The corresponding tie-lines (o, dotted line), β and S correlated by means of the UNIQUAC equation, are also plotted.

Table 3.16 Compositions of experimental tie-lines, solute distribution ratios (β) and selectivities (S) for {[C_8mim][BF_4] (1) + Pyridine (2) + *n*-Hexane (3)} at 298.15 K and atmospheric pressure.

IL-rich phase			Hydrocarbon-rich phase			β	S
x^{II}_1	x^{II}_2	x^{II}_3	x^{I}_1	x^{I}_2	x^{I}_3		
0.855	0.000	0.145	0.003	0.000	0.997	-	-
0.702	0.181	0.117	0.001	0.028	0.971	6.46	53.65
0.599	0.300	0.101	0.005	0.058	0.937	5.20	48.25
0.510	0.387	0.103	0.002	0.079	0.919	4.92	44.01
0.404	0.498	0.098	0.004	0.121	0.875	4.11	36.80
0.296	0.602	0.102	0.000	0.188	0.812	3.21	25.51
0.186	0.694	0.120	0.000	0.334	0.666	2.08	11.48
0.088	0.720	0.192	0.000	0.532	0.468	1.35	3.30

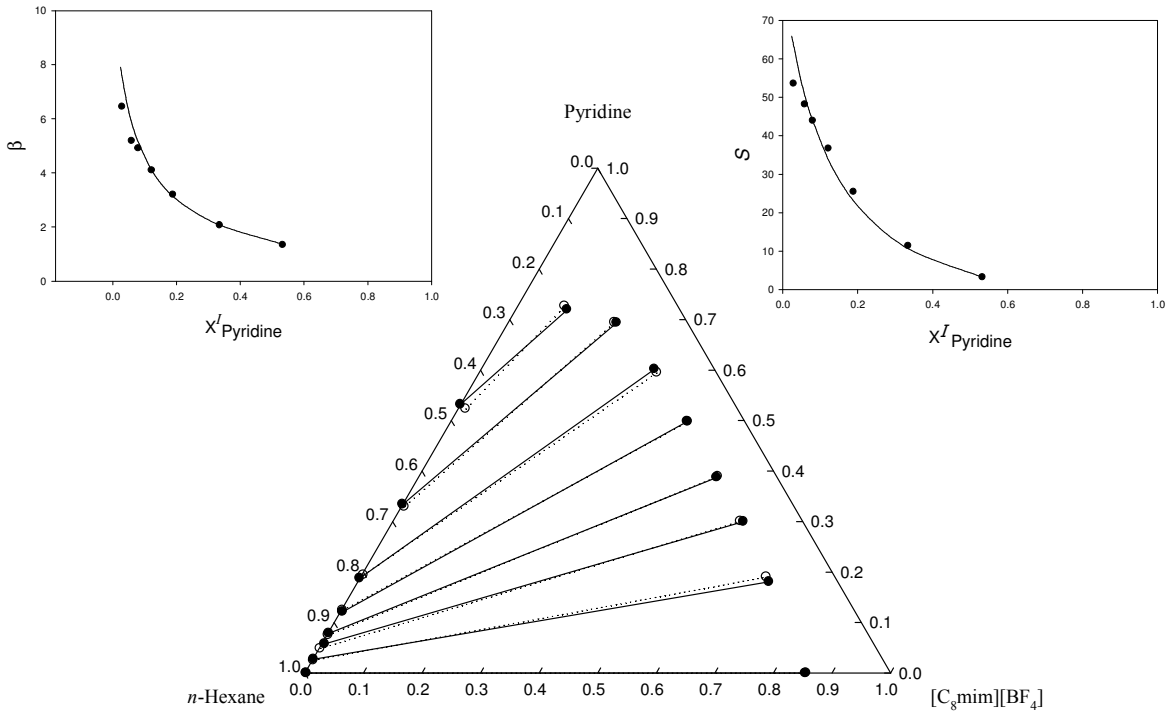

Figure 3.26. Experimental tie-lines (•, solid line), solute distribution ratio (β) and selectivites (S) for the LLE of the ternary system [C_8mim][BF_4] (1) + Pyridine (2) + *n*-Hexane (3) at 298.15 K and atmospheric pressure. The corresponding tie-lines (o, dotted line), β and S correlated by means of the NRTL equation, with $\alpha = 0.2$ equation, are also plotted.

Table 3.17 Compositions of experimental tie-lines, solute distribution ratios (β) and selectivities (S) for {[C_2mim][$EtSO_4$] (1) + Thiophene (2) + *n*-Hexane (3)} at 298.15 K and atmospheric pressure.

IL-rich phase			Hydrocarbon-rich phase			β	S
$x^{II}{}_1$	$x^{II}{}_2$	$x^{II}{}_3$	$x^{I}{}_1$	$x^{I}{}_2$	$x^{I}{}_3$		
0.993	0.000	0.007	0.000	0.000	1.000	-	-
0.860	0.131	0.009	0.000	0.082	0.918	1.59	162.18
0.733	0.257	0.010	0.000	0.188	0.812	1.37	111.24
0.649	0.343	0.008	0.010	0.381	0.609	0.90	68.51
0.488	0.503	0.009	0.014	0.641	0.345	0.78	29.90
0.465	0.524	0.011	0.005	0.732	0.263	0.72	17.21
0.448	0.543	0.009	0.005	0.807	0.188	0.67	14.00
0.352	0.641	0.007	0.004	0.901	0.095	0.71	9.64
0.293	0.703	0.004	0.000	0.953	0.047	0.74	8.69
0.288	0.712	0.000	0.000	1.000	0.000	0.71	-

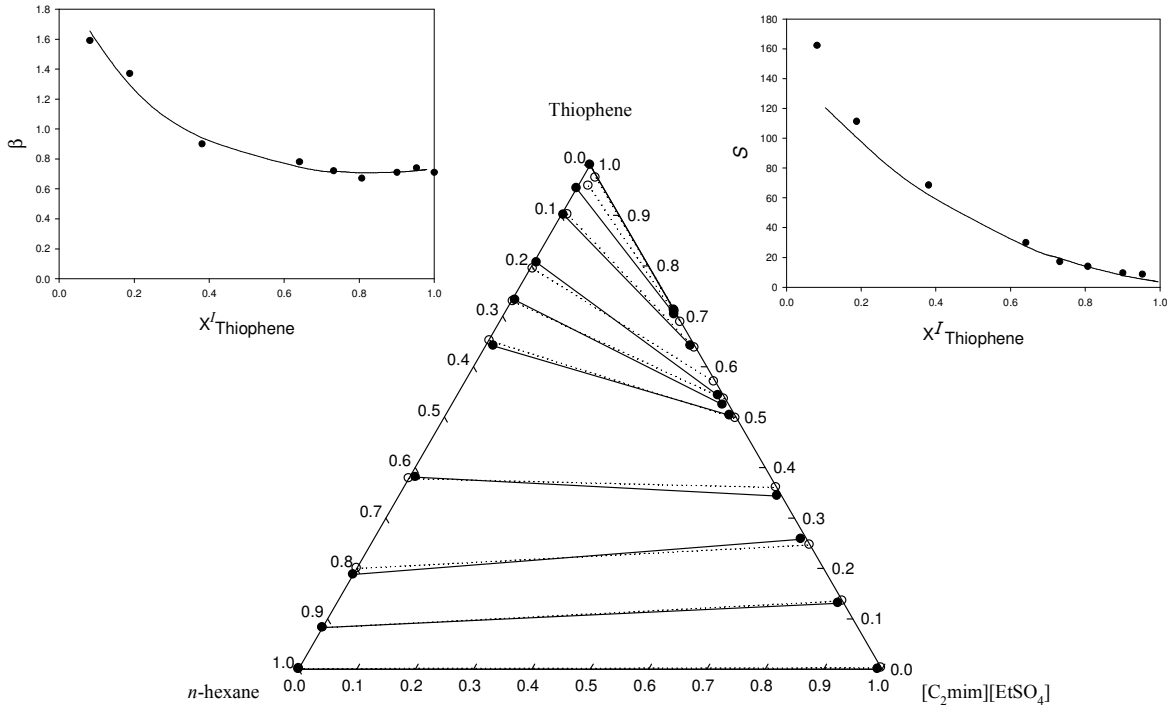

Figure 3.27. Experimental tie-lines (•, solid line), solute distribution ratio (β) and selectivites (S) for the LLE of the ternary system [C_2mim][$EtSO_4$] (1) + Thiophene (2) + *n*-Hexane (3) at 298.15 K and atmospheric pressure. The corresponding tie-lines (o, dotted line), β and S correlated by means of the UNIQUAC equation, are also plotted.

Table 3.18 Compositions of experimental tie-lines, solute distribution ratios (β) and selectivities (S) for {[C_2mim][$EtSO_4$] (1) + Thiophene (2) + *n*-Heptane (3)} at 298.15 K and atmospheric pressure.

IL-rich phase			Hydrocarbon-rich phase			β	S
x^{II}_1	x^{II}_2	x^{II}_3	x^{I}_1	x^{I}_2	x^{I}_3		
1.000	0.000	0.000	0.000	0.000	1.000	-	-
0.845	0.155	0.000	0.006	0.092	0.902	1.68	-
0.672	0.319	0.009	0.006	0.311	0.683	1.03	78.17
0.567	0.422	0.011	0.001	0.494	0.505	0.85	39.02
0.484	0.511	0.005	0.000	0.628	0.372	0.81	60.26
0.422	0.566	0.012	0.000	0.870	0.130	0.65	7.04
0.369	0.623	0.008	0.000	0.937	0.063	0.66	5.20
0.337	0.663	0.000	0.000	0.967	0.033	0.68	-
0.288	0.712	0.000	0.000	1.000	0.000	0.71	-

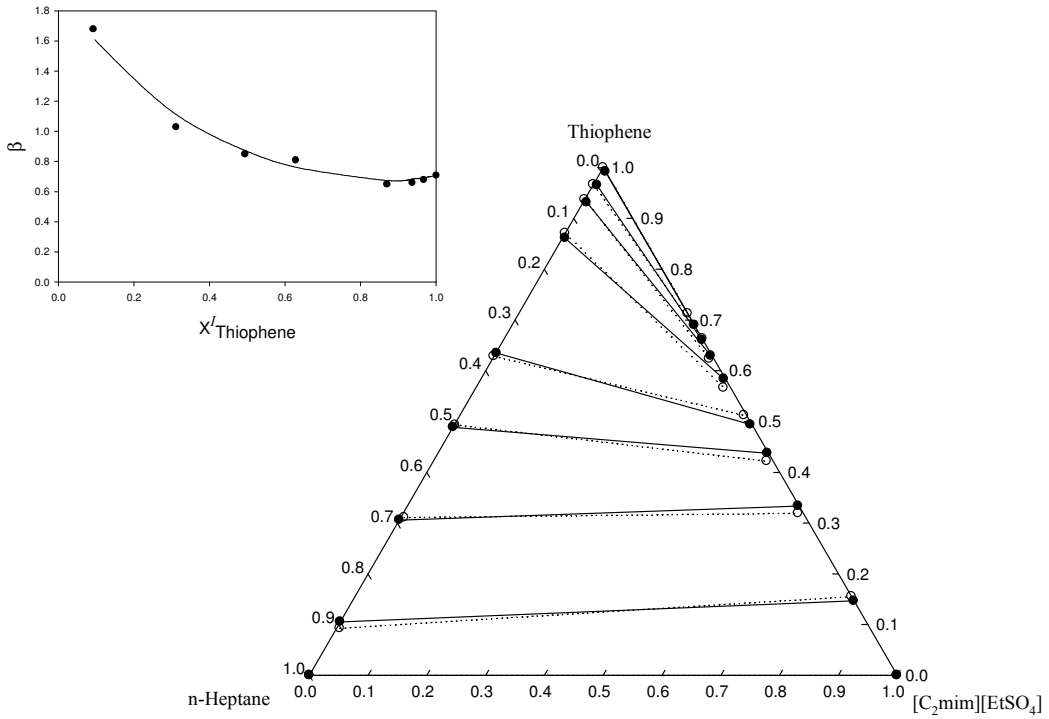

Figure 3.28. Experimental tie-lines (•, solid line), and solute distribution ratio (β) for the LLE of the ternary system [C_2mim][$EtSO_4$] (1) + Thiophene (2) + *n*-Heptane (3) at 298.15 K and atmospheric pressure. The corresponding tie-lines (o, dotted line) and β correlated by means of the NRTL equation, with $\alpha = 0.1$ equation, are also plotted.

Table 3.19 Compositions of experimental tie-lines, solute distribution ratios (β) and selectivities (S) for {[C_2mim][$EtSO_4$] (1) + Thiophene (2) + *n*-Dodecane (3)} at 298.15 K and atmospheric pressure.

IL-rich phase			Hydrocarbon-rich phase			β	S
x^{II}_1	x^{II}_2	x^{II}_3	x^{I}_1	x^{I}_2	x^{I}_3		
1.000	0.000	0.000	0.000	0.000	1.000	–	–
0.959	0.041	0.000	0.000	0.083	0.917	0.49	-
0.906	0.094	0.000	0.000	0.190	0.810	0.49	-
0.830	0.170	0.000	0.000	0.303	0.697	0.56	-
0.774	0.226	0.000	0.000	0.428	0.572	0.53	-
0.703	0.297	0.000	0.000	0.558	0.442	0.53	-
0.647	0.353	0.000	0.000	0.672	0.328	0.53	-
0.623	0.377	0.000	0.000	0.783	0.217	0.48	-
0.621	0.379	0.000	0.000	0.838	0.162	0.45	-
0.582	0.418	0.000	0.000	0.906	0.094	0.46	-
0.581	0.419	0.000	0.000	0.963	0.037	0.43	-
0.564	0.436	0.000	0.000	0.938	0.062	0.46	-
0.555	0.445	0.000	0.000	0.985	0.015	0.45	-
0.288	0.712	0.000	0.000	1.000	0.000	0.71	-

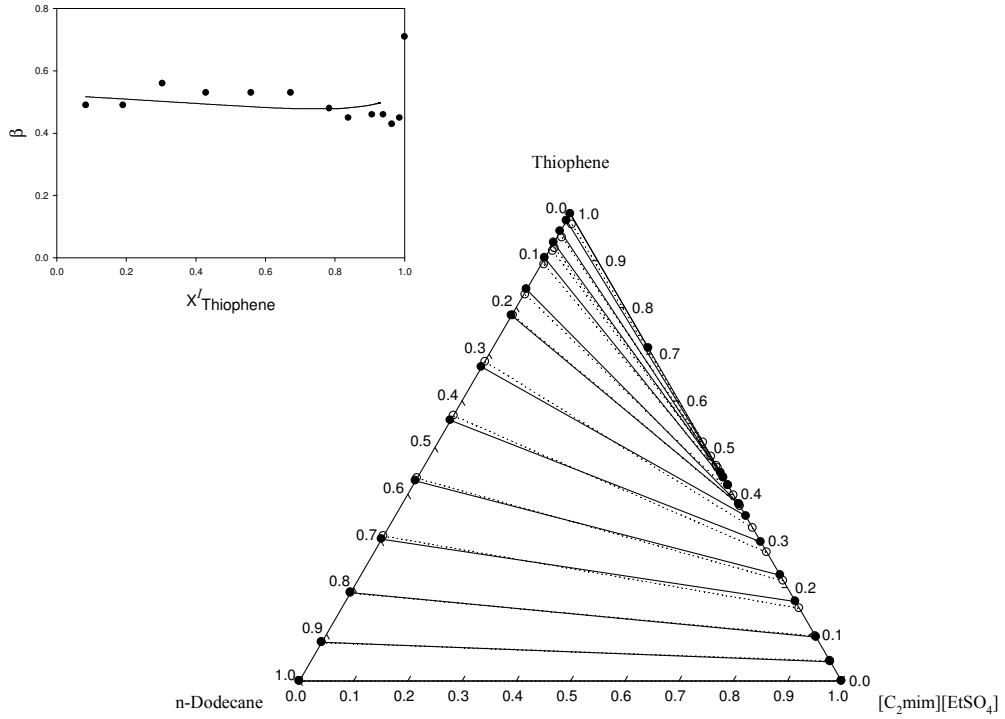

Figure 3.29. Experimental tie-lines (•, solid line) and solute distribution ratio (β) for the LLE of the ternary system [C_2mim][$EtSO_4$] (1) + Thiophene (2) + *n*-Dodecane (3) at 298.15 K and atmospheric pressure. The corresponding tie-lines (o, dotted line) and β correlated by means of the UNIQUAC equation, are also plotted.

Table 3.20 Compositions of experimental tie-lines, solute distribution ratios (β) and selectivities (S) for {[C_2mim][$EtSO_4$] (1) + Thiophene (2) + *n*-Hexadecane (3)} at 298.15 K and atmospheric pressure.

IL-rich phase			Hydrocarbon-rich phase			β	S
x^{II}_1	x^{II}_2	x^{II}_3	x^{I}_1	x^{I}_2	x^{I}_3		
1.000	0.000	0.000	0.000	0.000	1.000	–	–
0.912	0.088	0.000	0.000	0.130	0.870	0.68	-
0.880	0.120	0.000	0.000	0.290	0.710	0.41	-
0.837	0.163	0.000	0.000	0.436	0.564	0.37	-
0.810	0.190	0.000	0.000	0.576	0.424	0.33	-
0.738	0.262	0.000	0.000	0.665	0.335	0.39	-
0.727	0.273	0.000	0.000	0.716	0.284	0.38	-
0.612	0.388	0.000	0.000	0.879	0.121	0.44	-
0.579	0.421	0.000	0.000	0.977	0.023	0.43	-
0.545	0.455	0.000	0.000	0.919	0.081	0.50	-
0.436	0.564	0.000	0.000	0.955	0.045	0.59	-
0.288	0.712	0.000	0.000	1.000	0.000	0.71	-

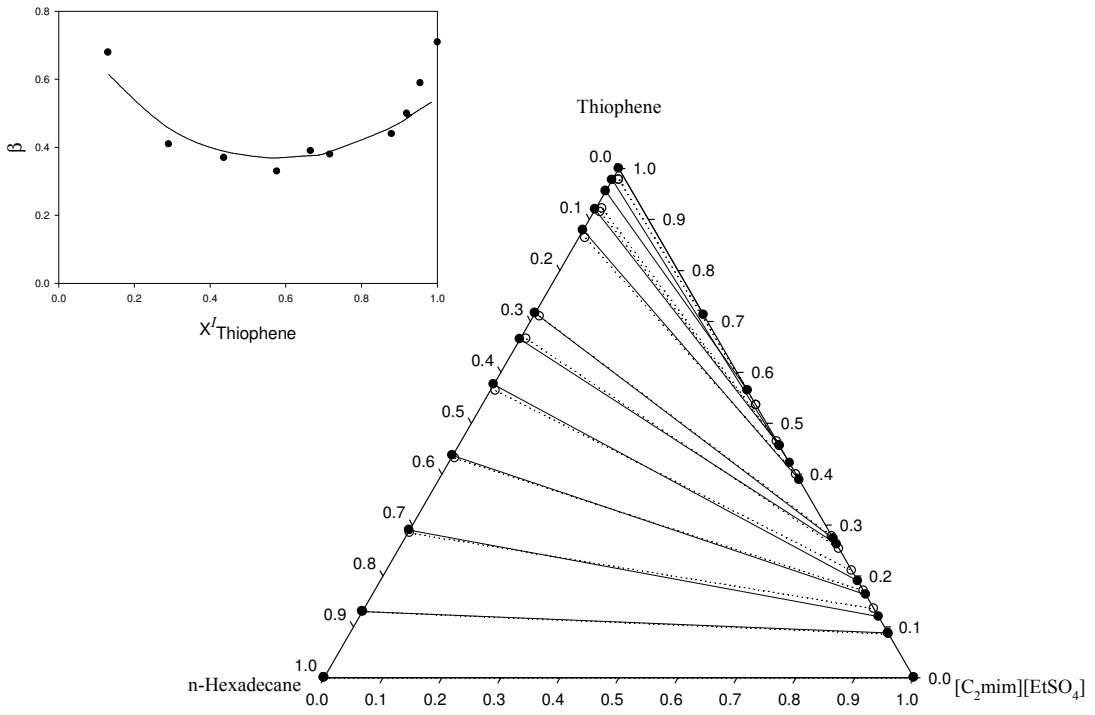

Figure 3.30. Experimental tie-lines (•, solid line) and solute distribution ratio (β) for the LLE of the ternary system [C_2mim][$EtSO_4$] (1) + Thiophene (2) + *n*-Hexadecane (3) at 298.15 K and atmospheric pressure. The corresponding tie-lines (o, dotted line) and β correlated by means of the UNIQUAC equation, are also plotted.

Table 3.21 Compositions of experimental tie-lines, solute distribution ratios (β) and selectivities (S) for {[C_2mim][$EtSO_4$] (1) + Thiophene (2) + *i*-octane (3)} at 298.15 K and atmospheric pressure.

IL-rich phase			Hydrocarbon-rich phase			β	S
x^{II}_1	x^{II}_2	x^{II}_3	x^{I}_1	x^{I}_2	x^{I}_3		
1.000	0.000	0.000	0.000	0.000	1.000		
0.907	0.093	0.000	0.000	0.097	0.903	0.96	-
0.788	0.212	0.000	0.003	0.213	0.784	1.00	-
0.683	0.317	0.000	0.004	0.424	0.572	0.75	-
0.615	0.385	0.000	0.009	0.550	0.441	0.70	-
0.569	0.431	0.000	0.000	0.659	0.341	0.65	-
0.555	0.445	0.000	0.000	0.853	0.147	0.52	-
0.501	0.499	0.000	0.000	0.903	0.097	0.55	-
0.443	0.557	0.000	0.000	0.943	0.057	0.59	-
0.288	0.712	0.000	0.000	1.000	0.000	0.71	

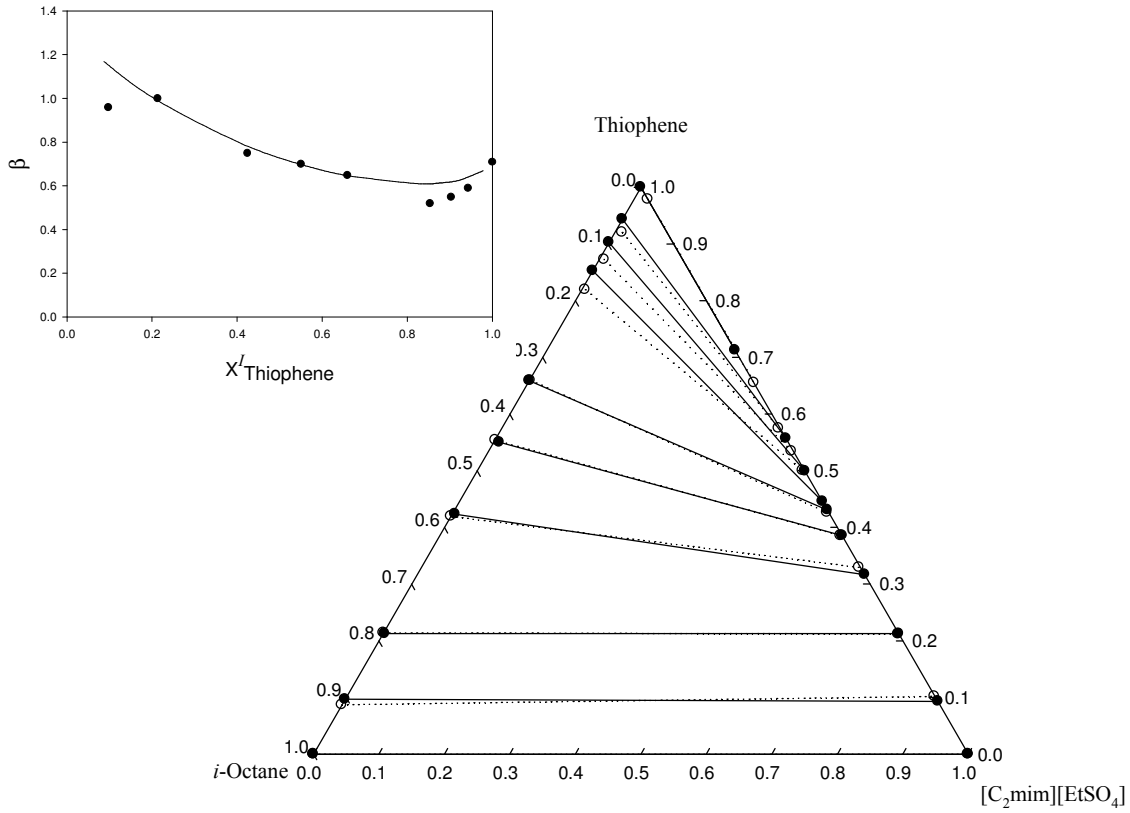

Figure 3.31. Experimental tie-lines (•, solid line) and solute distribution ratio (β) for the LLE of the ternary system [C_2mim][$EtSO_4$] (1) + Thiophene (2) + *i*-octane (3) at 298.15 K and atmospheric pressure. The corresponding tie-lines (o, dotted line) and β correlated by means of the NRTL equation, with $\alpha = 0.2$ equation, are also plotted.

Table 3.22 Compositions of experimental tie-lines, solute distribution ratios (β) and selectivities (S) for {[C_2mim][$EtSO_4$] (1) + Thiophene (2) + Toluene (3)} at 298.15 K and atmospheric pressure.

IL-rich phase			Hydrocarbon-rich phase			β	S
x^{II}_1	x^{II}_2	x^{II}_3	x^{I}_1	x^{I}_2	x^{I}_3		
0.732	0.000	0.268	0.000	0.000	1.000	–	–
0.695	0.047	0.258	0.000	0.064	0.936	0.73	2.65
0.650	0.106	0.244	0.000	0.137	0.863	0.77	2.74
0.601	0.174	0.225	0.000	0.248	0.752	0.70	2.34
0.552	0.254	0.194	0.000	0.354	0.646	0.72	2.40
0.503	0.328	0.169	0.000	0.467	0.533	0.70	2.22
0.466	0.383	0.151	0.000	0.542	0.458	0.71	2.14
0.442	0.428	0.130	0.000	0.618	0.382	0.69	2.04
0.413	0.472	0.115	0.000	0.669	0.331	0.71	2.02
0.370	0.552	0.078	0.000	0.788	0.212	0.70	1.92
0.341	0.602	0.057	0.000	0.865	0.135	0.70	1.67
0.327	0.637	0.036	0.000	0.915	0.085	0.70	1.65
0.288	0.712	0.000	0.000	1.000	0.000		

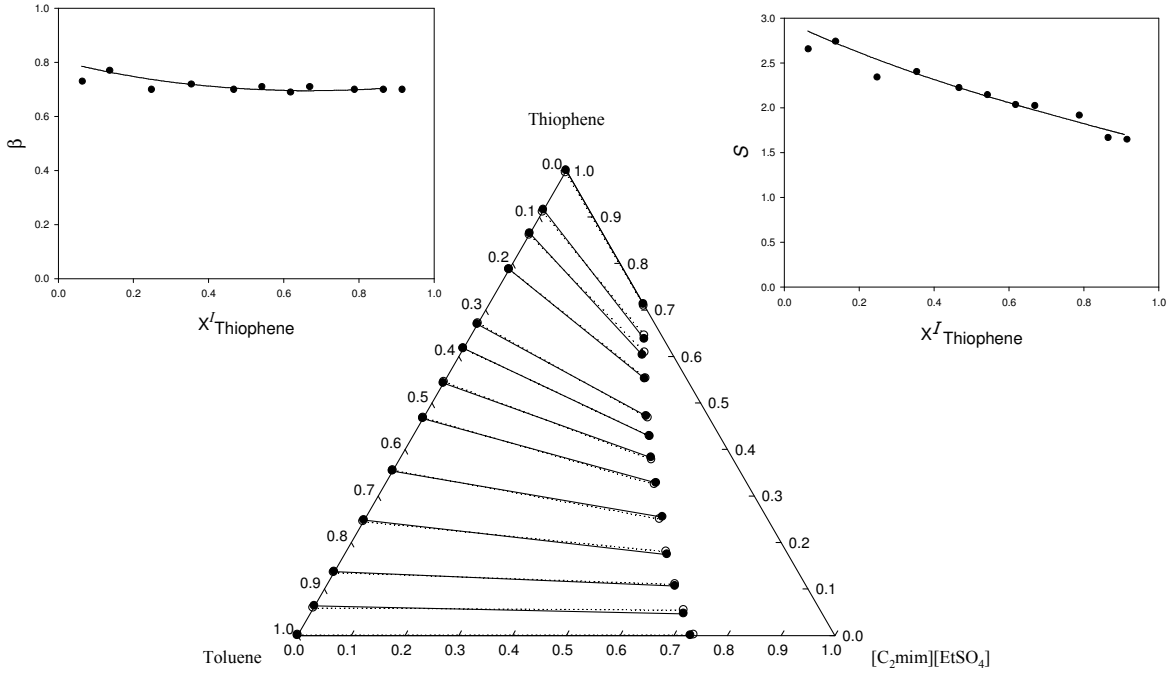

Figure 3.32. Experimental tie-lines (•, solid line), solute distribution ratio (β) and selectivites (S) for the LLE of the ternary system [C_2mim][$EtSO_4$] (1) + Thiophene (2) + Toluene (3) at 298.15 K and atmospheric pressure. The corresponding tie-lines (o, dotted line), β and S correlated by means of the UNIQUAC equation, are also plotted.

Table 3.23 Compositions of experimental tie-lines, solute distribution ratios (β) and selectivities (S) for {[C_2mim][$EtSO_4$] (1) + Pyridine (2) + n-Hexane (3)} at 298.15 K and atmospheric pressure.

IL-rich phase			Hydrocarbon-rich phase			β	S
x^{II}_1	x^{II}_2	x^{II}_3	x^{I}_1	x^{I}_2	x^{I}_3		
0.993	0.000	0.007	0.000	0.000	1.000		
0.869	0.123	0.008	0.002	0.048	0.951	2.58	316.25
0.705	0.286	0.009	0.000	0.094	0.906	3.02	293.96
0.540	0.447	0.013	0.000	0.206	0.794	2.17	130.66
0.395	0.586	0.019	0.000	0.341	0.659	1.72	58.86
0.320	0.657	0.023	0.000	0.515	0.485	1.28	27.02
0.248	0.724	0.028	0.000	0.625	0.375	1.16	15.81
0.168	0.787	0.045	0.000	0.771	0.229	1.02	5.17

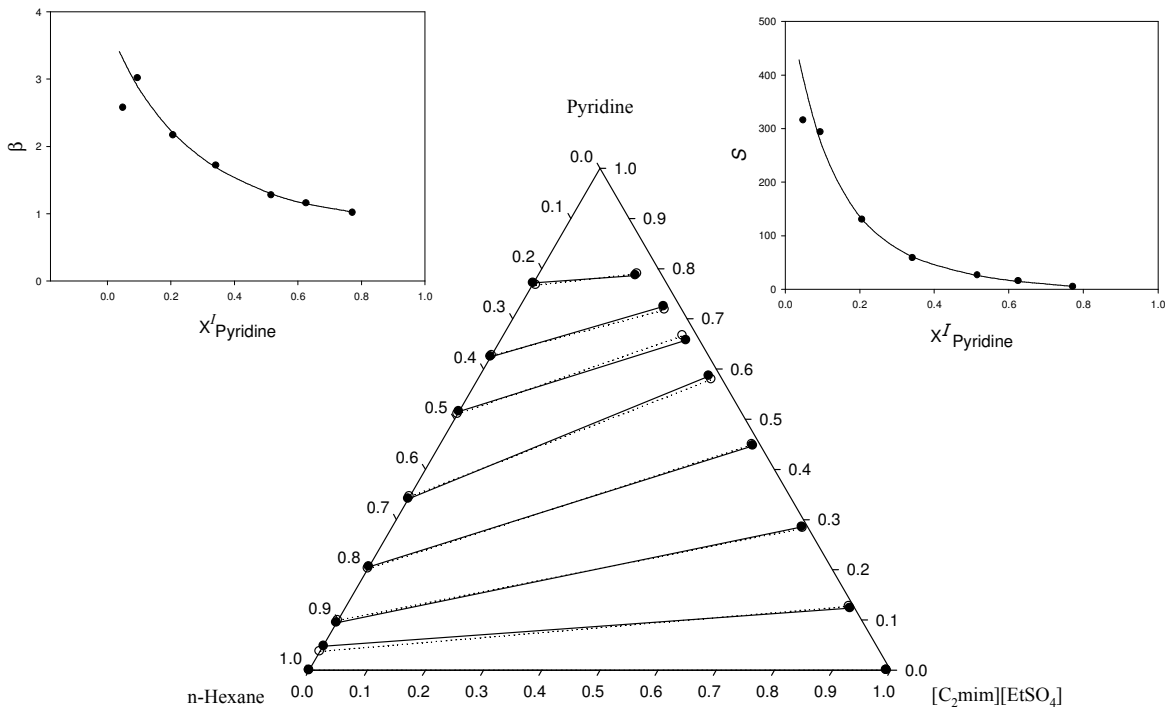

Figure 3.33. Experimental tie-lines (•, solid line), solute distribution ratio (β) and selectivites (S) for the LLE of the ternary system [C_2mim][$EtSO_4$] (1) + Pyridine (2) + *n*-Hexane (3) at 298.15 K and atmospheric pressure. The corresponding tie-lines (o, dotted line), β and S correlated by means of the NRTL equation, with $\alpha = 0.3$ are also plotted.

Table 3.24 Compositions of experimental tie-lines, solute distribution ratios (β) and selectivities (S) for {[C_6mmPy][NTf_2] (1) + Thiophene (2) + *n*-Hexane (3)} at 298.15 K and atmospheric pressure.

IL-rich phase			Hydrocarbon-rich phase			β	S
x^{II}_1	x^{II}_2	x^{II}_3	x^{I}_1	x^{I}_2	x^{I}_3		
0.795	0.000	0.205	0.000	0.000	1.000		
0.691	0.112	0.197	0.000	0.032	0.968	3.50	17.20
0.580	0.243	0.177	0.000	0.079	0.921	3.08	16.03
0.453	0.399	0.148	0.000	0.173	0.827	2.31	12.91
0.314	0.553	0.133	0.000	0.357	0.643	1.55	7.49
0.262	0.615	0.123	0.000	0.456	0.544	1.35	5.97
0.244	0.638	0.118	0.000	0.495	0.505	1.29	2.52
0.216	0.674	0.110	0.000	0.598	0.402	1.13	4.13
0.215	0.680	0.105	0.000	0.637	0.363	1.07	3.70
0.168	0.746	0.086	0.000	0.780	0.220	0.96	2.46
0.138	0.805	0.057	0.000	0.887	0.113	0.91	1.80
0.133	0.828	0.039	0.000	0.931	0.069	0.89	1.57
0.082	0.918	0.000	0.000	1.000	0.000	0.92	

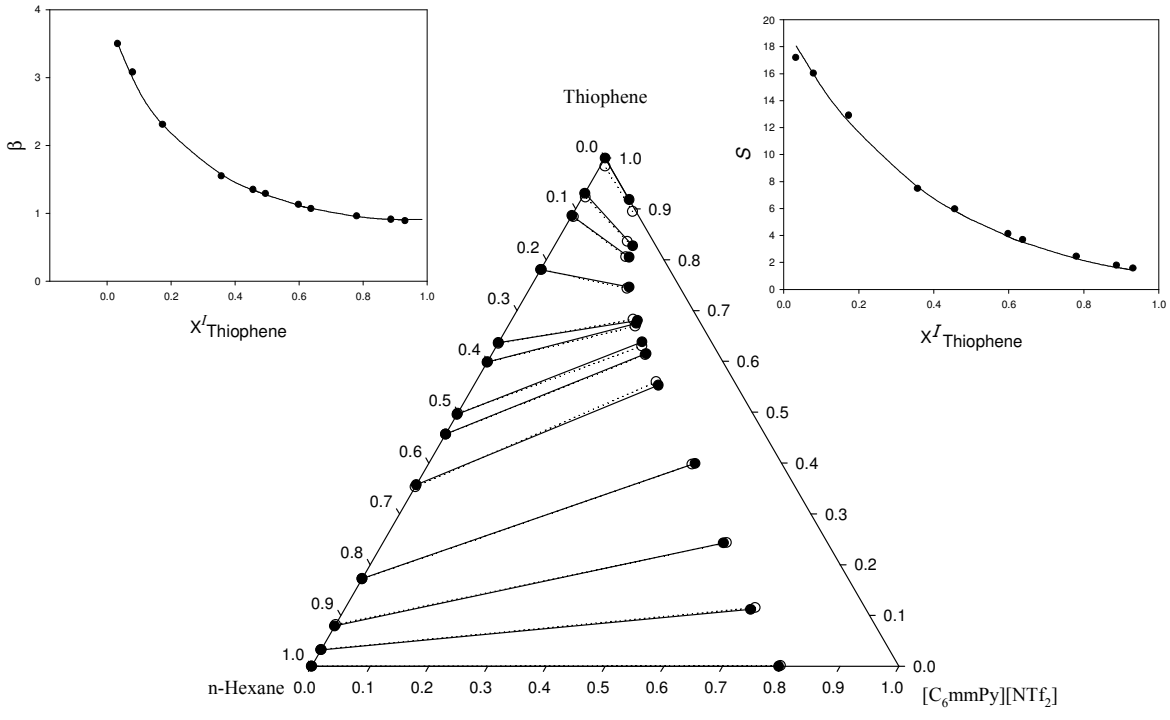

Figure 3.34. Experimental tie-lines (•, solid line), solute distribution ratio (β) and selectivites (S) for the LLE of the ternary system [C_6mmPy][NTf_2] (1) + Thiophene (2) + *n*-Hexane (3) at 298.15 K and atmospheric pressure. The corresponding tie-lines (o, dotted line), β and S correlated by means of the UNIQUAC equation, are also plotted.

Table 3.25 Compositions of experimental tie-lines, solute distribution ratios (β) and selectivities (S) for {[C_6mmPy][NTf_2] (1) + Thiophene (2) + *n*-Heptane (3)} at 298.15 K and atmospheric pressure.

IL-rich phase			Hydrocarbon-rich phase			β	S
x^{II}_1	x^{II}_2	x^{II}_3	x^{I}_1	x^{I}_2	x^{I}_3		
0.835	0.000	0.165	0.000	0.000	1.000		
0.690	0.157	0.153	0.000	0.061	0.939	2.57	15.77
0.581	0.273	0.146	0.000	0.134	0.866	2.04	12.10
0.484	0.381	0.135	0.000	0.220	0.780	1.73	10.00
0.424	0.436	0.140	0.002	0.287	0.711	1.52	7.72
0.371	0.496	0.133	0.000	0.371	0.629	1.34	6.34
0.323	0.554	0.123	0.000	0.443	0.557	1.25	5.66
0.255	0.630	0.115	0.000	0.595	0.405	1.06	3.73
0.198	0.695	0.107	0.000	0.739	0.261	0.94	2.29
0.134	0.794	0.072	0.000	0.843	0.157	0.94	2.05
0.082	0.918	0.000	0.000	1.000	0.000	0.92	

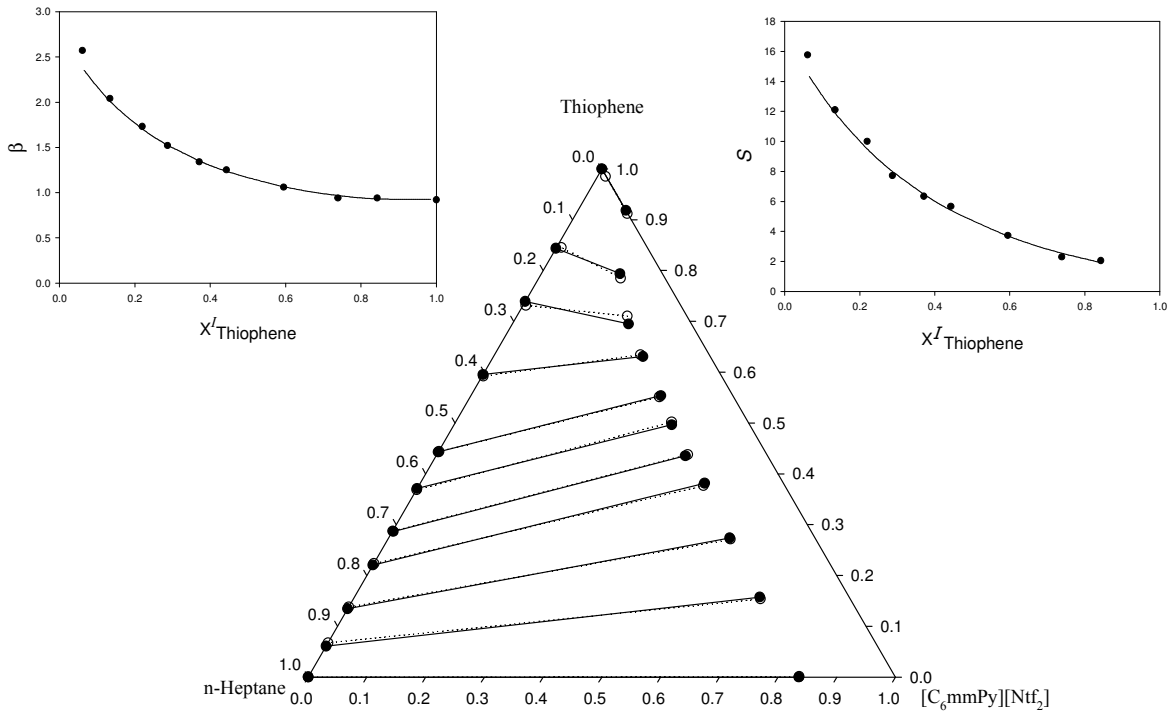

Figure 3.35. Experimental tie-lines (•, solid line), solute distribution ratio (β) and selectivites (S) for the LLE of the ternary system [C_6mmPy][NTf_2] (1) + Thiophene (2) + *n*-Heptane (3) at 298.15 K and atmospheric pressure. The corresponding tie-lines (o, dotted line), β and S correlated by means of the NRTL equation, with α = 0.3 equation, are also plotted.

Table 3.26 Compositions of experimental tie-lines, solute distribution ratios (β) and selectivities (S) for {[C_6mmPy][NTf_2] (1) + Thiophene (2) + *n*-Dodecane (3)} at 298.15 K and atmospheric pressure.

IL-rich phase			Hydrocarbon-rich phase			β	S
x^{II}_1	x^{II}_2	x^{II}_3	x^{I}_1	x^{I}_2	x^{I}_3		
0.947	0.000	0.053	0.000	0.000	1.000		
0.800	0.145	0.055	0.000	0.125	0.875	1.16	18.45
0.693	0.254	0.053	0.008	0.255	0.737	1.00	13.85
0.614	0.333	0.053	0.000	0.373	0.627	0.89	10.56
0.527	0.417	0.056	0.006	0.521	0.473	0.80	6.76
0.495	0.449	0.056	0.009	0.609	0.382	0.74	5.03
0.423	0.517	0.060	0.006	0.764	0.230	0.68	2.59
0.374	0.567	0.059	0.000	0.830	0.170	0.68	1.97
0.362	0.582	0.056	0.000	0.867	0.133	0.67	1.59
0.341	0.612	0.047	0.000	0.918	0.082	0.67	1.16
0.082	0.918	0.000	0.000	1.000	0.000	0.92	

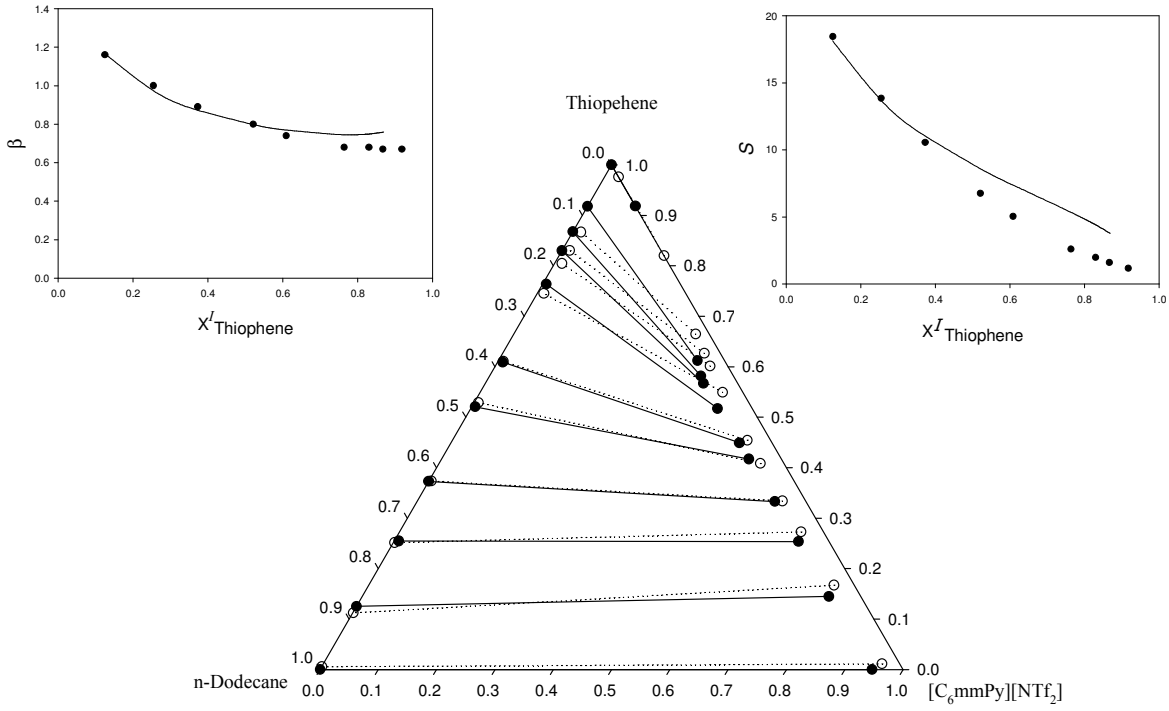

Figure 3.36. Experimental tie-lines (•, solid line), solute distribution ratio (β) and selectivites (S) for the LLE of the ternary system [C_6mmPy][NTf_2] (1) + Thiophene (2) + *n*-Dodecane (3) at 298.15 K and atmospheric pressure. The corresponding tie-lines (o, dotted line), β and S correlated by means of the NRTL equation, with $\alpha = 0.1$ are also plotted.

Table 3.27 Compositions of experimental tie-lines, solute distribution ratios (β) and selectivities (S) for {[C_6mmPy][NTf_2] (1) + Thiophene (2) + *n*-Hexadecane (3)} at 298.15 K and atmospheric pressure.

IL-rich phase			Hydrocarbon-rich phase				
x^{II}_1	x^{II}_2	x^{II}_3	x^{I}_1	x^{I}_2	x^{I}_3	β	S
0.968	0.000	0.032	0.000	0.000	1.000		
0.801	0.167	0.032	0.000	0.148	0.852	1.13	30.09
0.662	0.309	0.029	0.000	0.313	0.687	0.99	23.45
0.576	0.393	0.031	0.000	0.417	0.583	0.94	17.68
0.519	0.448	0.033	0.000	0.559	0.441	0.80	10.69
0.475	0.487	0.038	0.000	0.672	0.328	0.71	6.13
0.430	0.522	0.048	0.003	0.754	0.243	0.69	3.49
0.340	0.611	0.049	0.000	0.894	0.106	0.68	1.47
0.269	0.699	0.032	0.000	0.969	0.031	0.72	0.70
0.082	0.918	0.000	0.000	1.000	0.000	0.92	

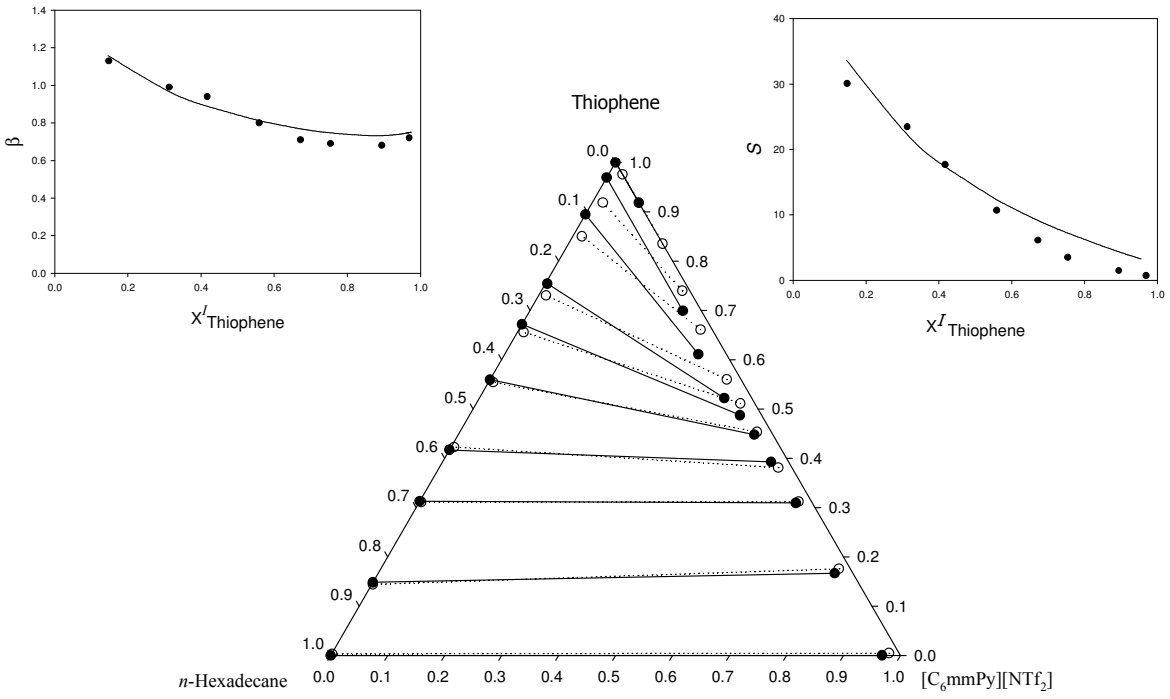

Figure 3.37. Experimental tie-lines (•, solid line), solute distribution ratio (β) and selectivites (S) for the LLE of the ternary system [C_6mmPy][NTf_2] (1) + Thiophene (2) + *n*-Hexadecane (3) at 298.15 K and atmospheric pressure. The corresponding tie-lines (o, dotted line), β and S correlated by means of the NRTL equation, with $\alpha = 0.2$ are also plotted.

Table 3.28 Compositions of experimental tie-lines, solute distribution ratios (β) and selectivities (S) for {[C_6mmPy][NTf_2] (1) + Thiophene (2) + i-octane (3)} at 298.15 K and atmospheric pressure.

IL-rich phase			Hydrocarbon-rich phase				
x^{II}_1	x^{II}_2	x^{II}_3	x^{I}_1	x^{I}_2	x^{I}_3	β	S
0.851	0.000	0.149	0.000	0.000	1.000		
0.548	0.310	0.142	0.000	0.118	0.882	2.63	16.32
0.365	0.515	0.120	0.000	0.283	0.717	1.82	10.87
0.318	0.575	0.107	0.000	0.404	0.596	1.42	7.93
0.298	0.596	0.106	0.000	0.545	0.455	1.09	4.70
0.243	0.667	0.090	0.000	0.697	0.303	0.96	3.22
0.194	0.728	0.078	0.000	0.818	0.182	0.89	2.08
0.097	0.873	0.030	0.000	0.952	0.048	0.92	1.47
0.082	0.918	0.000	0.000	1.000	0.000	0.92	

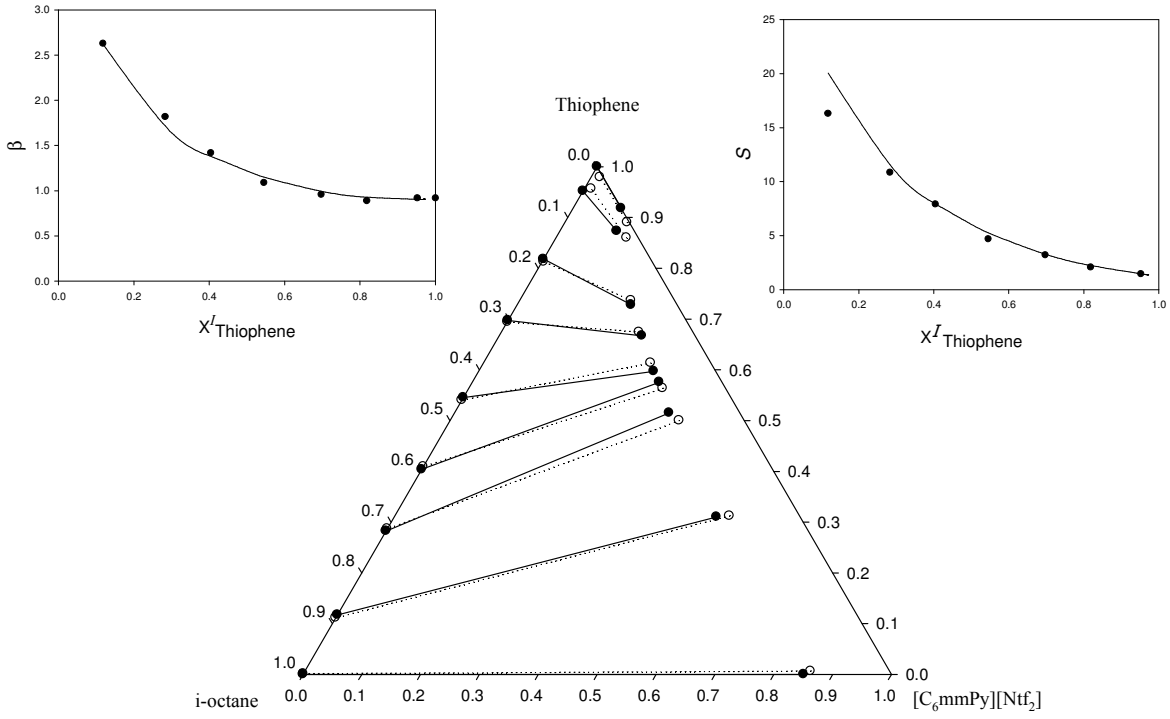

Figure 3.38. Experimental tie-lines (•, solid line), solute distribution ratio (β) and selectivites (S) for the LLE of the ternary system [C_6mmPy][NTf_2] (1) + Thiophene (2) + *i*-octane (3) at 298.15 K and atmospheric pressure. The corresponding tie-lines (o, dotted line), β and S correlated by means of the UNIQUAC equation, are also plotted.

Table 3.29 Compositions of experimental tie-lines, solute distribution ratios (β) and selectivities (S) for {[C_6mmPy][NTf_2] (1) + Thiophene (2) + Toluene (3)} at 298.15 K and atmospheric pressure.

IL-rich phase			Hydrocarbon-rich phase				
x^{II}_1	x^{II}_2	x^{II}_3	x^{I}_1	x^{I}_2	x^{I}_3	β	S
0.170	0.000	0.830	0.000	0.000	1.000		
0.169	0.078	0.753	0.000	0.097	0.903	0.80	0.96
0.159	0.184	0.657	0.000	0.223	0.777	0.82	0.97
0.154	0.258	0.588	0.004	0.308	0.688	0.84	0.98
0.152	0.352	0.496	0.000	0.426	0.574	0.83	0.96
0.154	0.448	0.398	0.000	0.538	0.462	0.83	0.96
0.143	0.517	0.340	0.000	0.616	0.384	0.84	0.95
0.139	0.574	0.287	0.000	0.678	0.322	0.85	0.95
0.124	0.644	0.232	0.000	0.748	0.252	0.86	0.93
0.074	0.808	0.118	0.000	0.882	0.118	0.92	0.92
0.082	0.918	0.000	0.000	1.000	0.000	0.92	

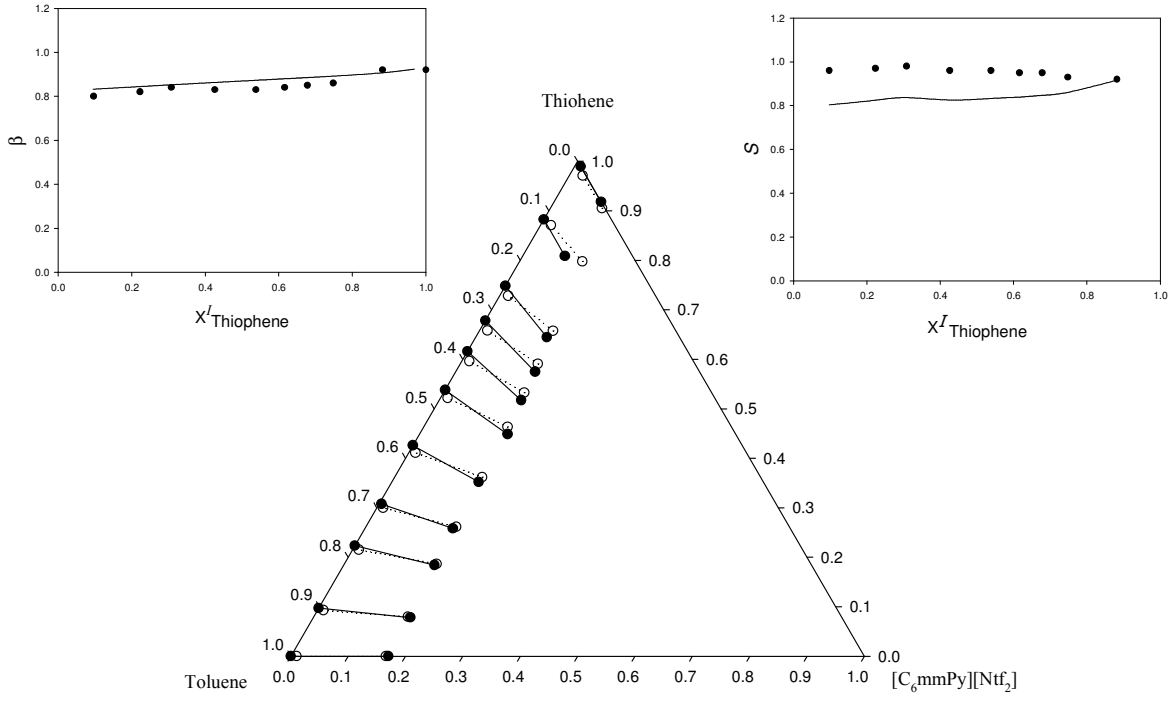

Figure 3.39. Experimental tie-lines (•, solid line), solute distribution ratio (β) and selectivites (S) for the LLE of the ternary system [C_6mmPy][NTf_2] (1) + Thiophene (2) + Toluene (3) at 298.15 K and atmospheric pressure. The corresponding tie-lines (o, dotted line), β and S correlated by means of the UNIQUAC equation, are also plotted.

Table 3.30 Compositions of experimental tie-lines, solute distribution ratios (β) and selectivities (S) for {[C_6mmPy][NTf_2] (1) + Pyridine (2) + *n*-Hexane (3)} at 298.15 K and atmospheric pressure.

IL-rich phase			Hydrocarbon-rich phase				
x^{II}_1	x^{II}_2	x^{II}_3	x^{I}_1	x^{I}_2	x^{I}_3	β	S
0.791	0.000	0.209	0.005	0.000	0.995		
0.641	0.171	0.188	0.000	0.009	0.991	19.00	100.15
0.544	0.276	0.180	0.005	0.030	0.965	9.20	96.50
0.412	0.424	0.164	0.004	0.070	0.926	6.06	34.22
0.271	0.575	0.154	0.000	0.100	0.900	5.75	33.60
0.166	0.653	0.181	0.000	0.216	0.784	3.02	13.08
0.101	0.678	0.221	0.000	0.326	0.674	2.08	6.34

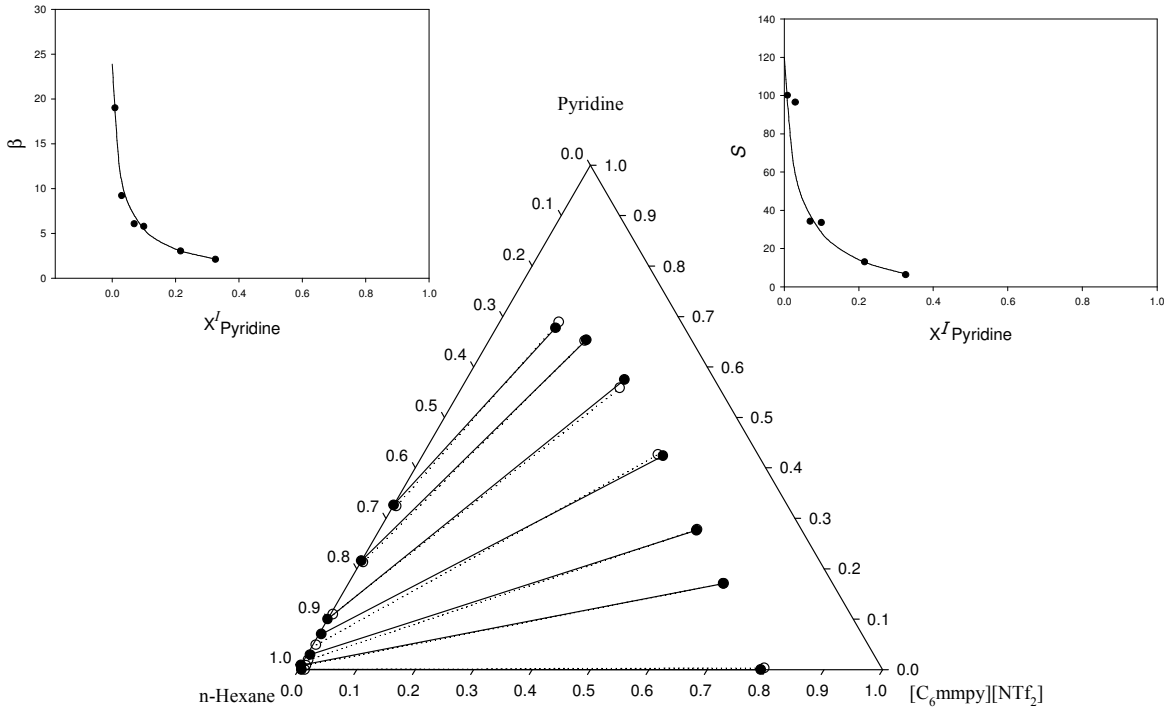

Figure 3.40. Experimental tie-lines (•, solid line), solute distribution ratio (β) and selectivites (S) for the LLE of the ternary system [C_6mmPy][NTf_2] (1) + Pyridine (2) + *n*-Hexane (3) at 298.15 K and atmospheric pressure. The corresponding tie-lines (o, dotted line), β and S correlated by means of the NRTL equation, with $\alpha = 0.2$ equation, are also plotted.

3.2.5. Data Correlation

In order to facilitate their use in simulation and design processes, experimental data are correlated using the NRTL [220] and UNIQUAC [221] equations. The value of the non-randomness parameter α in the NRTL equation was pre-fixed at 0.1, 0.2 and 0.3.

The binary interaction parameters were obtained using a computer program described by Sϕrensen and Arlt [222], which uses two objective functions to fit the experimental phase which uses two objective functions. First, F_a, does not require any previous guess for parameters, and after convergence these parameters are used in the second function, F_b, to fit the experimental concentrations:

$$F_a = \sum_k \sum_i \left[\left(a_{ik}^I - a_{ik}^{II} \right) / \left(a_{ik}^I + a_{ik}^{II} \right) \right]^2 + Q \sum_n P_n^2 \qquad [3.90]$$

$$F_b = \sum_k \min \sum_i \sum_j (x_{ijk} - \hat{x}_{ijk})^2 + Q \sum P_n^2 + \left[\ln \left(\frac{\gamma_{S\infty}^I}{\gamma_{S\infty}^{II}} \beta_\infty \right) \right]^2 \qquad [3.91]$$

where a is the activity, x is the experimental composition in mole fraction, and $\hat{x}$ the corresponding calculated composition. Subscripts and superscripts are: i for components of the mixture, j for phases (I, II) and k for tie-lines. Both functions include a penalty term (the second term) to reduce the risks of multiple solutions associated with parameters of high value, in which $Q = 10^{-6}$ for eq. [3.90] and $Q = 10^{-10}$ for eq. [3.91], and P_n are the adjustable parameters. F_b also includes a third term to correctly fit experimental results when working with low solute concentrations, in which $\gamma_{S\infty}^I$ and $\gamma_{S\infty}^{II}$ represent the solute activity coefficients calculated at infinite dilution in both phases and β_∞ is the solute molar distribution ratio at infinite dilution.

The quality of correlation is measured by the residual function F and the mean error of the solute distribution ratio, $\Delta\beta$:

$$F = 100 \times \left[\sum_k \min \sum_i \sum_j \frac{(x_{ijk} - \hat{x}_{ijk})^2}{6M} \right]^{0.5} \qquad [3.92]$$

$$\Delta\beta = 100 \times \left[\sum_{k} \frac{((\beta_k - \hat{\beta}_k)/\beta_k)^2}{M} \right]^{0.5} \quad [3.93]$$

where M refers to the number of experimental tie-lines.

In this work, experimental data were correlated in two ways: without defining an *a priori* value of β_∞, causing the last term of Eq. [3.89] to become zero, and specifying an optimal value of this parameter. An appropriate given value of β_∞ can improve the fit at low solute concentrations. Here, the value of β_∞ minimizing the goodness-of-fit index $\Delta\beta$ was found by trial and error.

Following, in next step, β∞ is fixed as some given optimised value driving the correlation to lower residual values of the mean error of the solute distribution ratio, $\Delta\beta$, Sometimes, lower values of $\Delta\beta$ fixing this parameter do not necessarily imply lower values of F which may be increased, but anyway, minimization of residual Δβ was taken as optimisation criterium.

The structural parameters for the application of the UNIQUAC equation were taken from the literature [223- 226] and are shown in Table 3.31.

Table 3.31. UNIQUAC structural parameters

Component	r	q	Ref.
n-Hexane	4.4998	3.856	[223]
n-Heptane	5.1742	4.396	[223]
n-Dodecane	8.5462	7.096	[223]
n-Hexadecane	11.2438	9.256	[223]
Toluene	3.9228	2.968	[223]
i-octane	5.8463	5.008	[223]
Thiophene	2.8569	2.140	[223]
Pyridine	2.9993	2.113	[223]
$[C_6mmPy][NTf_2]$	11.8526	10.0659	[224]*
$[C_2mim][EtSO_4]$	7.94	7.21	[225]
$[C_8mim][NTf_2]$	9.31	13.8	[226]
$[C_8mim][BF_4]$	13.187	8.357	[224]*

* Calculated from parameters presented in reference [224]

Tables 3.32 to 3.59 show the binary interaction parameters and residuals for the NRTL and UNIQUAC correlations of the ternary data, without fixing an optimal value for the solute distribution ratio at infinite dilution. For the NRTL model, the value of the non-randomness parameter was fixed at recommended values α = 0.1, 0.2 and 0.3.

The results of the correlations when an optimal value for the solute distribution ratio at infinite dilution was fixed at a value found by trial and error which minimizes $\Delta\beta$. For the NRTL model, the same optimal values of the non-randomness parameter were found for each system as in the previous correlation. When the solute distribution ratio at infinite dilution, β_∞, is defined, the residual $\Delta\beta$ decreases extensively and the residual F in some cases slightly increases.

Figures 3.13 to 3.40 show the experimental and correlated tie-lines.

Table 3.32 Binary interaction parameters (Δg_{ij}, Δg_{ji} *for NRTL model ;* Δu_{ij}, Δu_{ji} for *UNIQUAC model*) and root mean square deviations (F, $\Delta\beta$) for the correlation of {[C_8mim][NTf_2] (1) + thiophene (2) + *n*-hexane (3)} at 298.15 K and atmospheric pressure.

NRTL				
Residuals		Components	Parameters	
		i–j	Δg_{ij} / $J{\cdot}mol^{-1}$	Δg_{ji} / $J{\cdot}mol^{-1}$
		α=0.3 Not optimised		
		1-2	-6668.7	16849
F	0.588	1-3	1627.2	11812
$\Delta\beta$	3.60	2-3	-381.15	-192.10
		α=0.3	Optimised β_∞=2.90	
		1-2	-4882.5	13631
F	2.0646	1-3	1119.5	9901.7
$\Delta\beta$	3.4	2-3	2073.4	-188.97
UNIQUAC				
Residuals		Components	Parameters	
		i–j	Δu_{ij} / $J{\cdot}mol^{-1}$	Δu_{ji} / $J{\cdot}mol^{-1}$
			Not optimised	
		1-2	221.76	-306.99
F	7.4063	1-3	269.46	-252.24
$\Delta\beta$	15.7	2-3	141.45	137.40
			Optimised β_∞=2.70	
		1-2	168.53	-337.80
F	2.2139	1-3	230.85	-242.75
$\Delta\beta$	2.0	2-3	70.874	42.945

Table 3.33 Binary interaction parameters (Δg_{ij}, Δg_{ji} *for NRTL model;* Δu_{ij}, Δu_{ji} for *UNIQUAC model*) and root mean square deviations (F, $\Delta\beta$) for the correlation of {[C_8mim][NTf_2] (1) + Thiophene (2) + *n*-Heptane (3)} at 298.15 K and atmospheric pressure.

NRTL				
Residuals		Components	Parameters	
		i–j	Δg_{ij} / $J{\cdot}mol^{-1}$	Δg_{ji} / $J{\cdot}mol^{-1}$
		α=0.3 Not optimised		
		1-2	-6036.6	15755
F	1.0623	1-3	2134.8	12088
$\Delta\beta$	6.4	2-3	495.79	238.22
		α=0.3	Optimised β_∞=4.85	
		1-2	-6157.0	16039
F	1.0493	1-3	2071.6	11629
$\Delta\beta$	5.3	2-3	463.62	-59.145
UNIQUAC				
Residuals		Components	Parameters	
		i–j	Δu_{ij} / $J{\cdot}mol^{-1}$	Δu_{ji} / $J{\cdot}mol^{-1}$
			Not optimised	
		1-2	1791.3	-3077.6
F	1.9398	1-3	1559.6	-1916.8
$\Delta\beta$	5.8	2-3	-564.17	1605.8
			Optimised β_∞=3.75	
		1-2	1691.7	-3007.2
F	1.9796	1-3	1582.9	-1928.4
$\Delta\beta$	4.6	2-3	-372.26	1390.6

Table 3.34 Binary interaction parameters (Δg_{ij}, Δg_{ji} *for NRTL model;* Δu_{ij}, Δu_{ji} for *UNIQUAC model*) and root mean square deviations (F, $\Delta\beta$) for the correlation of {[C_8mim][NTf_2] (1) + Thiophene (2) + *n*-Dodecane (3)} at 298.15 K and atmospheric pressure.

NRTL				
Residuals		Components	Parameters	
		i–j	Δg_{ij} / $J{\cdot}mol^{-1}$	Δg_{ji} / $J{\cdot}mol^{-1}$
		α=0.3 Not optimised		
		1-2	-5466.8	14703
F	1.5090	1-3	4564.1	9848.5
$\Delta\beta$	6.6	2-3	711.47	-2393.4
		α=0.3	Optimised $\beta_\infty=1.62$	
		1-2	-5735.3	15116
F	1.4999	1-3	4646.6	10327
$\Delta\beta$	4.6	2-3	229.29	-2711.9
UNIQUAC				
Residuals		Components	Parameters	
		i–j	Δu_{ij} / $J{\cdot}mol^{-1}$	Δu_{ji} / $J{\cdot}mol^{-1}$
			Not optimised	
		1-2	1034.2	-2527.1
F	2.2923	1-3	1891.3	-2253.5
$\Delta\beta$	5.2	2-3	-221.31	1048.9
			Optimised $\beta_\infty=1.35$	
		1-2	913.18	-2425.8
F	1.9796	1-3	1897.6	-2258.8
$\Delta\beta$	4.6	2-3	-102.71	928.31

Table 3.35 Binary interaction parameters (Δg_{ij}, Δg_{ji} *for NRTL model;* Δu_{ij}, Δu_{ji} for *UNIQUAC model*) and root mean square deviations (F, $\Delta\beta$) for the correlation of {[C_8mim][NTf_2] (1) + Thiophene (2) + *n*-Hexadecane (3)} at 298.15 K and atmospheric pressure.

NRTL				
Residuals		Components	Parameters	
		i–j	Δg_{ij} / $J{\cdot}mol^{-1}$	Δg_{ji} / $J{\cdot}mol^{-1}$
		α=0.3 Not optimised		
		1-2	-3630.4	11832
F	2.7860	1-3	5746.5	11077
$\Delta\beta$	9.9	2-3	887.08	-2605.2
		α=0.3	Optimised $\beta_\infty=0.71$	
		1-2	-3773.0	13135
F	3.1316	1-3	5156.2	11018
$\Delta\beta$	8.7	2-3	1287.4	-3422.9
UNIQUAC				
Residuals		Components	Parameters	
		i–j	Δu_{ij} / $J{\cdot}mol^{-1}$	Δu_{ji} / $J{\cdot}mol^{-1}$
			Not optimised	
		1-2	979.44	-2391.2
F	3.6425	1-3	2190.9	-2424.2
$\Delta\beta$	11.7	2-3	462.62	92.083
			Optimised $\beta_\infty=0.69$	
		1-2	926.15	-2322.6
F	3.3764	1-3	1968.7	-2436.8
$\Delta\beta$	9.5	2-3	444.81	-19.453

Table 3.36 Binary interaction parameters (Δg_{ij}, Δg_{ji} *for NRTL model;* Δu_{ij}, Δu_{ji} for *UNIQUAC model*) and root mean square deviations (F, $\Delta\beta$) for the correlation of {[C_8mim][NTf_2] (1) + Thiophene (2) + *i*-octane (3)} at 298.15 K and atmospheric pressure.

NRTL				
Residuals		Components	Parameters	
		i–j	Δg_{ij} / $J{\cdot}mol^{-1}$	Δg_{ji} / $J{\cdot}mol^{-1}$
		α=0.3 Not optimised		
		1-2	-7659	19173
F	0.7290	1-3	2253	11051
$\Delta\beta$	10.2	2-3	741.6	-1594
		α=0.3	Optimised β_∞=4.75	
		1-2	-8091.6	19622
F	1.0323	1-3	2277.1	11017
$\Delta\beta$	4.3	2-3	341.4	-2502.0
UNIQUAC				
Residuals		Components	Parameters	
		i–j	Δu_{ij} / $J{\cdot}mol^{-1}$	Δu_{ji} / $J{\cdot}mol^{-1}$
		Not optimised		
		1-2	-1489.0	3248.0
F	0.5620	1-3	-1297.0	3759.0
$\Delta\beta$	4.40	2-3	-340.40	1367.0
		Optimised β_∞=3.03		
		1-2	-1489.0	3248.0
F	0.5620	1-3	-1297.0	3759.0
$\Delta\beta$	4.40	2-3	-340.40	1367.0

Table 3.37 Binary interaction parameters (Δg_{ij}, Δg_{ji} *for NRTL model;* Δu_{ij}, Δu_{ji} for *UNIQUAC model*) and root mean square deviations (F, $\Delta\beta$) for the correlation of {[C_8mim][NTf_2] (1) + Thiophene (2) + Toluene (3)} at 298.15 K and atmospheric pressure.

NRTL				
Residuals		Components	Parameters	
		i–j	Δg_{ij} / $J{\cdot}mol^{-1}$	Δg_{ji} / $J{\cdot}mol^{-1}$
		α=0.3 Not optimised		
		1-2	-1653.0	13183
F	14.4682	1-3	-2106.0	12832
$\Delta\beta$	29.90	2-3	300.90	242.00
		α=0.3	Optimised β_∞=*1.21*	
		1-2	-2861.9	12698
F	8.1977	1-3	-2687.9	12157
$\Delta\beta$	10.9	2-3	1237.4	1384.3
UNIQUAC				
Residuals		Components	Parameters	
		i–j	Δu_{ij} / $J{\cdot}mol^{-1}$	Δu_{ji} / $J{\cdot}mol^{-1}$
			Not optimised	
		1-2	-499.60	1826.0
F	1.6702	1-3	-1163.0	2545.0
$\Delta\beta$	3.70	2-3	-117.80	76.800
			Optimised β_∞=*0.92*	
		1-2	-134.50	1442.0
F	2.5057	1-3	-803.70	1999.0
$\Delta\beta$	3.3	2-3	-53.800	22.310

Table 3.38 Binary interaction parameters (Δg_{ij}, Δg_{ji} *for NRTL model;* Δu_{ij}, Δu_{ji} for *UNIQUAC model*) and root mean square deviations (F, $\Delta\beta$) for the correlation of {[C_8mim][NTf_2] (1) + Pyridine (2) + *n*-Hexane (3)} at 298.15 K and atmospheric pressure.

NRTL				
Residuals		Components	Parameters	
		i–j	Δg_{ij} / $J{\cdot}mol^{-1}$	Δg_{ji} / $J{\cdot}mol^{-1}$
		α=0.3 Not optimised		
		1-2	-6343.1	4109.6
F	0.5272	1-3	1608.8	11758
$\Delta\beta$	8.4	2-3	3203.3	1187.6
		α=0.3	Optimised β_∞=*10.53*	
		1-2	-5326.9	3740.2
F	0.5789	1-3	1735.7	12808
$\Delta\beta$	5.5	2-3	3492.6	1484.8
UNIQUAC				
Residuals		Components	Parameters	
		i–j	Δu_{ij} / $J{\cdot}mol^{-1}$	Δu_{ji} / $J{\cdot}mol^{-1}$
			Not optimised	
		1-2	1212.5	-1709.6
F	0.4733	1-3	367.76	737.90
$\Delta\beta$	6.9	2-3	-589.21	1982.0
			Optimised β_∞=*13.21*	
		1-2	1088.6	-1536.9
F	0.4878	1-3	347.60	769.45
$\Delta\beta$	4.4	2-3	-563.68	2007.4

Table 3.39 Binary interaction parameters (Δg_{ij}, Δg_{ji} *for NRTL model;* Δu_{ij}, Δu_{ji} for *UNIQUAC model*) and root mean square deviations (F, $\Delta\beta$) for the correlation of {[C_8mim][BF_4] (1) + Thiophene (2) + *n*-Hexane (3)} at 298.15 K and atmospheric pressure.

NRTL				
Residuals		Components	Parameters	
		i–j	Δg_{ij} / $J{\cdot}mol^{-1}$	Δg_{ji} / $J{\cdot}mol^{-1}$
		α=0.3 Not optimised		
		1-2	-6029.8	16296
F	0.7364	1-3	3303.9	9842.7
$\Delta\beta$	3.3	2-3	1038.1	-1209.8
		α=0.3	Optimised β_∞=*4.01*	
		1-2	-6029.8	16296
F	0.7364	1-3	3303.9	9842.7
$\Delta\beta$	3.3	2-3	1038.1	-1209.8
UNIQUAC				
Residuals		Components	Parameters	
		i–j	Δu_{ij} / $J{\cdot}mol^{-1}$	Δu_{ji} / $J{\cdot}mol^{-1}$
			Not optimised	
		1-2	-1405.0	3250.5
F	0.5613	1-3	-1213.1	3168.2
$\Delta\beta$	7.1	2-3	-924.40	2017.8
			Optimised β_∞=*2.7*	
		1-2	-1542.9	3528.0
F	0.5170	1-3	-1308.9	3585.9
$\Delta\beta$	5.9	2-3	-1191.4	2455.3

Table 3.40 Binary interaction parameters (Δg_{ij}, Δg_{ji} *for NRTL model;* Δu_{ij}, Δu_{ji} for *UNIQUAC model*) and root mean square deviations (F, $\Delta\beta$) for the correlation of {[C_8mim][BF_4] (1) + Thiophene (2) + *n*-Heptane (3)} at 298.15 K and atmospheric pressure.

NRTL				
Residuals		Components	Parameters	
		i–j	Δg_{ij} / $J{\cdot}mol^{-1}$	Δg_{ji} / $J{\cdot}mol^{-1}$
		α=0.3 Not optimised		
		1-2	-4182.0	13277
F	1.7087	1-3	3773.7	12470
$\Delta\beta$	4.6	2-3	415.80	-1.1951
		α=0.3	Optimised β_∞=*2.37*	
		1-2	-4202.3	13069
F	1.6742	1-3	3794.6	12686
$\Delta\beta$	4.6	2-3	494.64	-109.91
UNIQUAC				
Residuals		Components	Parameters	
		i–j	Δu_{ij} / $J{\cdot}mol^{-1}$	Δu_{ji} / $J{\cdot}mol^{-1}$
			Not optimised	
		1-2	-580.73	1805.2
F	1.5516	1-3	-546.82	2159.3
$\Delta\beta$	5.7	2-3	-412.91	1424.5
			Optimised β_∞=*1.8*	
		1-2	-547.27	1790.3
F	1.6437	1-3	-596.61	2298.3
$\Delta\beta$	3.9	2-3	-606.82	1810.1

.

Table 3.41 Binary interaction parameters (Δg_{ij}, Δg_{ji} *for NRTL model;* Δu_{ij}, Δu_{ji} for *UNIQUAC model*) and root mean square deviations (F, $\Delta\beta$) for the correlation of {[C_8mim][BF_4] (1) + Thiophene (2) + *n*-Dodecane (3)} at 298.15 K and atmospheric pressure.

NRTL				
Residuals		Components	Parameters	
		i–j	Δg_{ij} / $J{\cdot}mol^{-1}$	Δg_{ji} / $J{\cdot}mol^{-1}$
		α=0.3 Not optimised		
		1-2	-3449.9	12343
F	2.3103	1-3	5768.8	8955.6
$\Delta\beta$	4.7	2-3	1568.0	-1939.9
		α=0.3	Optimised β_∞=*1.12*	
		1-2	-3440.9	12083
F	2.1455	1-3	6697.3	13430
$\Delta\beta$	4.6	2-3	990.84	-1568.4
UNIQUAC				
Residuals		Components	Parameters	
		i–j	Δu_{ij} / $J{\cdot}mol^{-1}$	Δu_{ji} / $J{\cdot}mol^{-1}$
			Not optimised	
		1-2	-413.53	1840.7
F	1.9547	1-3	-863.21	2376.6
$\Delta\beta$	6.3	2-3	-1680.9	3301.9
			Optimised β_∞=*1.25*	
		1-2	-397.23	1813.4
F	1.8934	1-3	-881.17	2389.5
$\Delta\beta$	5.7	2-3	-1477.8	2879.1

Table 3.42 Binary interaction parameters (Δg_{ij}, Δg_{ji} *for NRTL model;* Δu_{ij}, Δu_{ji} for *UNIQUAC model*) and root mean square deviations (F, $\Delta\beta$) for the correlation of {[C_8mim][BF_4] (1) + Thiophene (2) + *n*-Hexadecane (3)} at 298.15 K and atmospheric pressure.

NRTL				
Residuals		Components	Parameters	
		i–j	Δg_{ij} / $J{\cdot}mol^{-1}$	Δg_{ji} / $J{\cdot}mol^{-1}$
		α=0.3 Not optimised		
		1-2	-3263.0	12088
F	2.7699	1-3	7429.0	7479.7
$\Delta\beta$	12.3	2-3	2579.1	-4217.6
		α=0.3	Optimised β_∞=*1.12*	
		1-2	-3459.7	13370
F	3.2649	1-3	6956.8	6579.5
$\Delta\beta$	10.7	2-3	2969.2	-4482.0
UNIQUAC				
Residuals		Components	Parameters	
		i–j	Δu_{ij} / $J{\cdot}mol^{-1}$	Δu_{ji} / $J{\cdot}mol^{-1}$
			Not optimised	
		1-2	410.99	1056.6
F	3.1092	1-3	-631.52	-1629.1
$\Delta\beta$	8.8	2-3	-755.93	-3639.9
			Optimised β_∞=*0.64*	
		1-2	310.57	1140.2
F	2.8464	1-3	-747.04	-1439.0
$\Delta\beta$	7.7	2-3	-451.80	-3739.4

Table 3.43 Binary interaction parameters (Δg_{ij}, Δg_{ji} *for NRTL model;* Δu_{ij}, Δu_{ji} for *UNIQUAC model*) and root mean square deviations (F, $\Delta\beta$) for the correlation of {[C_8mim][BF_4] (1) + Thiophene (2) + *i*-octane (3)} at 298.15 K and atmospheric pressure.

NRTL				
Residuals		Components	Parameters	
		i–j	Δg_{ij} / $J{\cdot}mol^{-1}$	Δg_{ji} / $J{\cdot}mol^{-1}$
			α=0.2 Not optimised	
		1-2	-11935	29552
F	0.7053	1-3	2739.0	11620
$\Delta\beta$	9.4	2-3	-739.00	-4675.0
		α=0.2	Optimised β_∞=*3.1*	
		1-2	-7603.2	18197
F	1.5332	1-3	1626.1	12016
$\Delta\beta$	3.8	2-3	12205	-4666.6
UNIQUAC				
Residuals		Components	Parameters	
		i–j	Δu_{ij} / $J{\cdot}mol^{-1}$	Δu_{ji} / $J{\cdot}mol^{-1}$
			Not optimised	
		1-2	-2501.2	6527.4
F	0.4876	1-3	-1254.5	5222.0
$\Delta\beta$	1.9	2-3	-1369.2	2135.1
			Optimised β_∞=*2.59*	
		1-2	-2512.6	6585.9
F	0.4870	1-3	-1272.7	5379.6
$\Delta\beta$	1.9	2-3	-1408.4	2203.8

Table 3.44 Binary interaction parameters (Δg_{ij}, Δg_{ji} *for NRTL model;* Δu_{ij}, Δu_{ji} for *UNIQUAC model*) and root mean square deviations (F, $\Delta\beta$) for the correlation of {[C_8mim][BF_4] (1) + Thiophene (2) + Toluene (3)} at 298.15 K and atmospheric pressure.

NRTL				
Residuals		Components	Parameters	
		i–j	Δg_{ij} / $J{\cdot}mol^{-1}$	Δg_{ji} / $J{\cdot}mol^{-1}$
		α=0.3 Not optimised		
		1-2	-4431.0	13358
F	1.5664	1-3	-2305.0	11464
$\Delta\beta$	4.9	2-3	408.50	390.10
		α=0.2	Optimised $\beta_\infty=1.2$	
		1-2	-4766.8	13345
F	1.5419	1-3	-2309.1	11456
$\Delta\beta$	4.8	2-3	359.76	298.50
UNIQUAC				
Residuals		Components	Parameters	
		i–j	Δu_{ij} / $J{\cdot}mol^{-1}$	Δu_{ji} / $J{\cdot}mol^{-1}$
			Not optimised	
		1-2	-1211.8	2909.8
F	0.4842	1-3	1581.2	4077.4
$\Delta\beta$	4.4	2-3	-207.27	396.21
			Optimised $\beta_\infty=1.1$	
		1-2	-1245.8	2967.1
F	0.5807	1-3	-1733.1	4696.3
$\Delta\beta$	3.5	2-3	-803.86	1242.4

Table 3.45 Binary interaction parameters (Δg_{ij}, Δg_{ji} *for NRTL model;* Δu_{ij}, Δu_{ji} for *UNIQUAC model*) and root mean square deviations (F, $\Delta\beta$) for the correlation of {[C_8mim][BF_4] (1) + Pyridine (2) + *n*-Hexane (3)} at 298.15 K and atmospheric pressure.

NRTL

Residuals		Components	Parameters	
		i–j	Δg_{ij} / $J{\cdot}mol^{-1}$	Δg_{ji} / $J{\cdot}mol^{-1}$
		α=0.2 Not optimised		
		1-2	-7894.0	7358.7
F	0.4736	1-3	1031.3	13641
$\Delta\beta$	6.70	2-3	4491.9	-659.82
		α=0.2	Optimised β_∞=8.6	
		1-2	-6829.3	6065.8
F	0.5383	1-3	1183.0	16888
$\Delta\beta$	2.60	2-3	4841.3	-618.28

UNIQUAC

Residuals		Components	Parameters	
		i–j	Δu_{ij} / $J{\cdot}mol^{-1}$	Δu_{ji} / $J{\cdot}mol^{-1}$
			Not optimised	
		1-2	387.1	-1283.2
F	0.6625	1-3	929.4	355.0
$\Delta\beta$	6.6	2-3	175.4	551.8
			Optimised β_∞=10.7	
		1-2	380.3	-1275.8
F	0.6625	1-3	925.2	359.9
$\Delta\beta$	6.5	2-3	174.4	553.5

Table 3.46 Binary interaction parameters (Δg_{ij}, Δg_{ji} *for NRTL model;* Δu_{ij}, Δu_{ji} for *UNIQUAC model*) and root mean square deviations (F, $\Delta\beta$) for the correlation of {[C_2mim][$EtSO_4$] (1) + Thiophene (2) + *n*-Hexane (3)} at 298.15 K and atmospheric pressure.

NRTL				
Residuals		Components	Parameters	
		i–j	Δg_{ij} / $J{\cdot}mol^{-1}$	Δg_{ji} / $J{\cdot}mol^{-1}$
		α=0.1 Not optimised		
		1-2	-10917	23990
F	1.0422	1-3	14266	16721
$\Delta\beta$	4.3	2-3	2097.8	-1527.9
		α=0.2	Optimised β_∞=*2.43*	
		1-2	-10917	23990
F	1.0422	1-3	14266	16721
$\Delta\beta$	4.3	2-3	2097.8	-1527.9
UNIQUAC				
Residuals		Components	Parameters	
		i–j	Δu_{ij} / $J{\cdot}mol^{-1}$	Δu_{ji} / $J{\cdot}mol^{-1}$
			Not optimised	
		1-2	-1112.6	3198.0
F	1.7633	1-3	3157.1	134.1
$\Delta\beta$	14.8	2-3	1765.8	-715.2
			Optimised β_∞=*2.09*	
		1-2	-897.55	2582.1
F	0.8138	1-3	2666.9	2191.3
$\Delta\beta$	3.7	2-3	-1078.3	2692.7

Table 3.47 Binary interaction parameters (Δg_{ij}, Δg_{ji} *for NRTL model;* Δu_{ij}, Δu_{ji} for *UNIQUAC model*) and root mean square deviations (F, $\Delta\beta$) for the correlation of {[C_2mim][$EtSO_4$] (1) + Thiophene (2) + *n*-Heptane (3)} at 298.15 K and atmospheric pressure.

NRTL				
Residuals		Components	Parameters	
		i–j	Δg_{ij} / $J{\cdot}mol^{-1}$	Δg_{ji} / $J{\cdot}mol^{-1}$
		α=0.1 Not optimised		
		1-2	-10639	23983
F	1.0168	1-3	16990	18471
$\Delta\beta$	3.6	2-3	9066.1	-5775.3
		α=0.1	Optimised β_∞=*2.28*	
		1-2	-10639	23983
F	1.0168	1-3	16990	18471
$\Delta\beta$	3.6	2-3	9066.1	-5775.3
UNIQUAC				
Residuals		Components	Parameters	
		i–j	Δu_{ij} / $J{\cdot}mol^{-1}$	Δu_{ji} / $J{\cdot}mol^{-1}$
			Not optimised	
		1-2	-261.37	1616.1
F	1.3953	1-3	2633.5	702.11
$\Delta\beta$	14.3	2-3	1489.0	-263.72
			Optimised β_∞=*1.97*	
		1-2	-757.89	2410.7
F	0.9511	1-3	3396.6	2282.3
$\Delta\beta$	4.3	2-3	-680.43	2219.7

Table 3.48 Binary interaction parameters (Δg_{ij}, Δg_{ji} *for NRTL model;* Δu_{ij}, Δu_{ji} for *UNIQUAC model*) and root mean square deviations (F, $\Delta\beta$) for the correlation of {[C_2mim][$EtSO_4$] (1) + Thiophene (2) + *n*-Dodecane (3)} at 298.15 K and atmospheric pressure.

NRTL				
Residuals		Components	Parameters	
		i–j	Δg_{ij} / $J{\cdot}mol^{-1}$	Δg_{ji} / $J{\cdot}mol^{-1}$
		α=0.3 Not optimised		
		1-2	-646.79	10229
F	3.5418	1-3	9509.3	11073
$\Delta\beta$	13.0	2-3	3799.7	-2352.8
		α=0.3	Optimised β_∞=0.52	
		1-2	-543.21	10150
F	3.5765	1-3	10126	10946
$\Delta\beta$	9.3	2-3	3984.8	-1754.9
UNIQUAC				
Residuals		Components	Parameters	
		i–j	Δu_{ij} / $J{\cdot}mol^{-1}$	Δu_{ji} / $J{\cdot}mol^{-1}$
			Not optimised	
		1-2	156.40	1350.9
F	3.4586	1-3	1282.2	1551.3
$\Delta\beta$	14.7	2-3	-172.95	580.25
			Optimised β_∞=0.52	
		1-2	629.23	876.43
F	3.4418	1-3	1662.6	1698.1
$\Delta\beta$	8.1	2-3	-712.98	1672.5

Table 3.49 Binary interaction parameters (Δg_{ij}, Δg_{ji} *for NRTL model;* Δu_{ij}, Δu_{ji} for *UNIQUAC model*) and root mean square deviations (F, $\Delta\beta$) for the correlation of {[C_2mim][$EtSO_4$] (1) + Thiophene (2) + *n*-Hexadecane (3)} at 298.15 K and atmospheric pressure.

NRTL

Residuals		Components i–j	Parameters Δg_{ij} / $J{\cdot}mol^{-1}$	Δg_{ji} / $J{\cdot}mol^{-1}$
		α=0.3 Not optimised		
		1-2	-999.40	9403.7
F	3.1191	1-3	7524.8	9618.2
$\Delta\beta$	30.1	2-3	2705.3	-4819.3
		α=0.3	Optimised β_∞=*0.32*	
		1-2	-662.30	9866.0
F	3.8338	1-3	9141.8	8898.2
$\Delta\beta$	21.8	2-3	3574.7	-2918.2

UNIQUAC

Residuals		Components i–j	Parameters Δu_{ij} / $J{\cdot}mol^{-1}$	Δu_{ji} / $J{\cdot}mol^{-1}$
		Not optimised		
		1-2	235.70	1237.6
F	3.3072	1-3	966.73	1322.9
$\Delta\beta$	22.2	2-3	-298.42	610.63
		Optimised β_∞=*0.86*		
		1-2	230.15	1334.8
F	3.4327	1-3	1366.8	1476.8
$\Delta\beta$	9.8	2-3	-2052.3	4761.4

Table 3.50 Binary interaction parameters (Δg_{ij}, Δg_{ji} *for NRTL model;* Δu_{ij}, Δu_{ji} for *UNIQUAC model*) and root mean square deviations (F, $\Delta\beta$) for the correlation of {[C_2mim][$EtSO_4$] (1) + Thiophene (2) + *i*-octane (3)} at 298.15 K and atmospheric pressure.

.**NRTL**				
Residuals		Components	Parameters	
		i–j	Δg_{ij} / $J{\cdot}mol^{-1}$	Δg_{ji} / $J{\cdot}mol^{-1}$
		α=0.2 Not optimised		
		1-2	-3020.3	11535
F	2.6644	1-3	7640.3	11476
$\Delta\beta$	9.1	2-3	2993.1	-505.56
		α=0.2	optimised β_∞=*1.16*	
		1-2	-3020.3	11535
F	2.6644	1-3	7640.3	11476
$\Delta\beta$	9.1	2-3	2993.1	-505.56
UNIQUAC				
Residuals		Components	Parameters	
		i–j	Δu_{ij} / $J{\cdot}mol^{-1}$	Δu_{ji} / $J{\cdot}mol^{-1}$
			Not optimised	
		1-2	-91.094	1488.0
F	2.4137	1-3	1392.4	1701.0
$\Delta\beta$	12.2	2-3	8.9356	719.81
			Optimised β_∞=*0.82*	
		1-2	46.170	1275.4
F	1.9265	1-3	2108.9	2113.6
$\Delta\beta$	10.0	2-3	-845.59	2297.9

Table 3.51 Binary interaction parameters (Δg_{ij}, Δg_{ji} *for NRTL model;* Δu_{ij}, Δu_{ji} for *UNIQUAC model*) and root mean square deviations (F, $\Delta\beta$) for the correlation of {[C_2mim][$EtSO_4$] (1) + Thiophene (2) + Toluene (3)} at 298.15 K and atmospheric pressure.

NRTL				
Residuals		Components	Parameters	
		i–j	Δg_{ij} / $J{\cdot}mol^{-1}$	Δg_{ji} / $J{\cdot}mol^{-1}$
			α=0.3 Not optimised	
		1–2	-2471.5	11655
F	0.6911	1–3	2861.0	16593
$\Delta\beta$	2.3	2–3	-829.09	-249.60
		α=0.2	optimised β_∞=0.71	
		1-2	-2576.9	12331
F	0.4664	1-3	2566.7	15548
$\Delta\beta$	2.9	2-3	-1210.8	-190.19
UNIQUAC				
Residuals		Components	Parameters	
		i–j	Δu_{ij} / $J{\cdot}mol^{-1}$	Δu_{ji} / $J{\cdot}mol^{-1}$
			Not optimised	
		1-2	-816.29	2457.0
F	0.3720	1-3	-799.48	3964.1
$\Delta\beta$	2.8	2-3	-726.76	1117.0
			Optimised β_∞=0.75	
		1-2	-706.11	2260.0
F	0.3830	1-3	-1025.6	5111.6
$\Delta\beta$	2.0	2-3	516.28	-235.61

Table 3.52 Binary interaction parameters (Δg_{ij}, Δg_{ji} for NRTL model; Δu_{ij}, Δu_{ji} for UNIQUAC model) and root mean square deviations (F, $\Delta\beta$) for the correlation of {[C_2mim][$EtSO_4$] (1) + Pyridine (2) + *n*-Hexane (3)} at 298.15 K. and atmospheric pressure.

NRTL				
Residuals		Components	Parameters	
		i–j	Δg_{ij} / $J{\cdot}mol^{-1}$	Δg_{ji} / $J{\cdot}mol^{-1}$
		α=0.3 Not optimised		
		1–2	-20213	4537.4
F	1.0814	1–3	9596.6	14532
$\Delta\beta$	5.9	2–3	8247.3	-18003
		α=0.3	Optimised $\beta_\infty=2.75$	
		1-2	-21005	4748.2
F	1.0744	1-3	9561.7	14850
$\Delta\beta$	5.8	2-3	8186.2	-18848
UNIQUAC				
Residuals		Components	Parameters	
		i–j	Δu_{ij} / $J{\cdot}mol^{-1}$	Δu_{ji} / $J{\cdot}mol^{-1}$
			Not optimised	
		1-2	62.700	188.40
F	0.447	1-3	2680.6	699.60
$\Delta\beta$	10.1	2-3	663.10	732.90
			Optimised $\beta_\infty=1.08$	
		1-2	-685.03	-21.190
F	1.1890	1-3	156.81	286.01
$\Delta\beta$	8.3	2-3	756.20	-825.21

Table 3.53 Binary interaction parameters (Δg_{ij}, Δg_{ji} *for NRTL model;* Δu_{ij}, Δu_{ji} for *UNIQUAC model*) and root mean square deviations (F, $\Delta\beta$) for the correlation of {[C_6mmPy][NTf_2] (1) + Thiophene (2) + *n*-Hexane (3)} at 298.15 K and atmospheric pressure.

NRTL				
Residuals		Components	Parameters	
		i–j	Δg_{ij} / $J{\cdot}mol^{-1}$	Δg_{ji} / $J{\cdot}mol^{-1}$
		α=0.2 Not optimised		
		1–2	-26396	3843.4
F	2.6202	1–3	252.72	17920
$\Delta\beta$	8.8	2–3	30937	-22950
		α=0.2	Optimised β_∞=*3.95*	
		1-2	-26101	3268.5
F	2.6240	1-3	243.20	18402
$\Delta\beta$	6.9	2-3	30187	-22567
UNIQUAC				
Residuals		Components	Parameters	
		i–j	Δu_{ij} / $J{\cdot}mol^{-1}$	Δu_{ji} / $J{\cdot}mol^{-1}$
			Not optimised	
		1-2	-1312.0	2872.4
F	0.7193	1-3	-632.89	3783.2
$\Delta\beta$	6.7	2-3	12.175	1138.44
			Optimised β_∞=*3.99*	
		1-2	-1287.7	2798.2
F	0.5568	1-3	-974.71	5971.9
$\Delta\beta$	1.1	2-3	-443.78	1895.4

Table 3.54 Binary interaction parameters (Δg_{ij}, Δg_{ji} *for NRTL model;* Δu_{ij}, $\Delta u_{j\ i}$for *UNIQUAC model*) and root mean square deviations (F, $\Delta\beta$) for the correlation of {[C_6mmPy][NTf_2] (1) + Thiophene (2) + *n*-Heptane (3)} at 298.15 K and atmospheric pressure.

NRTL				
Residuals		Components	Parameters	
		i–j	Δg_{ij} / $J{\cdot}mol^{-1}$	Δg_{ji} / $J{\cdot}mol^{-1}$
		α=0.3 Not optimised		
		1–2	-5733.7	15447
F	0.6755	1–3	3404.9	13183
$\Delta\beta$	3.4	2–3	1154.1	-748.32
		α=0.3	Optimised β_∞=*4.00*	
		1-2	-5899.9	15670
F	0.6299	1-3	3298.0	12813
$\Delta\beta$	2.4	2-3	1119.9	-1033.9
UNIQUAC				
Residuals		Components	Parameters	
		i–j	Δu_{ij} / $J{\cdot}mol^{-1}$	Δu_{ji} / $J{\cdot}mol^{-1}$
			Not optimised	
		1-2	-1123.5	2477.8
F	0.4557	1-3	-544.87	384.88
$\Delta\beta$	3.6	2-3	-738.09	3200.1
			Optimised β_∞=*2.81*	
		1-2	-1263.1	2707.8
F	0.4055	1-3	-686.80	3699.5
$\Delta\beta$	2.6	2-3	-960.40	2183.9

Table 3.55 Binary interaction parameters (Δg_{ij}, Δg_{ji} *for NRTL model;* Δu_{ij}, Δu_{ji} for *UNIQUAC model*) and root mean square deviations (F, $\Delta\beta$) for the correlation of {[C_6mmPy][NTf_2] (1) + Thiophene (2) + *n*-Dodecane (3)} at 298.15 K and atmospheric pressure.

NRTL				
Residuals		Components	Parameters	
		i–j	Δg_{ij} / $J{\cdot}mol^{-1}$	Δg_{ji} / $J{\cdot}mol^{-1}$
		α=0.1 Not optimised		
		1-2	-646.79	10229
F	3.5418	1-3	9509.3	11073
$\Delta\beta$	13.0	2-3	3799.7	-2352.8
		α=0.1	Optimised β_∞=*1.67*	
		1-2	5138.4	-4193.5
F	2.8070	1-3	37.207	-1140.7
$\Delta\beta$	6.6	2-3	20.669	-10.016
UNIQUAC				
Residuals		Components	Parameters	
		i–j	Δu_{ij} / $J{\cdot}mol^{-1}$	Δu_{ji} / $J{\cdot}mol^{-1}$
			Not optimised	
		1-2	-44.204	1155.1
F	2.6595	1-3	-222.30	1862.9
$\Delta\beta$	12.2	2-3	-1625.4	3166.4
			Optimised β_∞=*1.45*	
		1-2	-46.219	1230.8
F	2.8213	1-3	-164.97	2001.3
$\Delta\beta$	9.5	2-3	-1567.6	3257.7

Table 3.56 Binary interaction parameters (Δg_{ij}, Δg_{ji} *for NRTL model;* Δu_{ij}, Δu_{ji} for *UNIQUAC model*) and root mean square deviations (F, $\Delta\beta$) for the correlation of {[C_6mmPy][NTf_2] (1) + Thiophene (2) + *n*-Hexadecane (3)} at 298.15 K and atmospheric pressure.

NRTL				
Residuals		Components	Parameters	
		i–j	Δg_{ij} / $J{\cdot}mol^{-1}$	Δg_{ji} / $J{\cdot}mol^{-1}$
		α=0.2 Not optimised		
		1-2	-999.40	9403.7
F	3.1191	1-3	7524.8	9618.2
$\Delta\beta$	30.1	2-3	2705.3	-4819.3
		α=0.2	Optimised β_∞=1.51	
		1-2	-5016.0	15.024
F	3.6611	1-3	4761.7	10.893
$\Delta\beta$	4.9	2-3	4353.5	-2629.5
UNIQUAC				
Residuals		Components	Parameters	
		i–j	Δu_{ij} / $J{\cdot}mol^{-1}$	Δu_{ji} / $J{\cdot}mol^{-1}$
			Not optimised	
		1-2	245.64	868.86
F	2.7083	1-3	-321.91	1859.1
$\Delta\beta$	12.7	2-3	-824.26	1851.3
			Optimised β_∞=1.52	
		1-2	41.725	1086.9
F	2.3808	1-3	-235.64	1918.9
$\Delta\beta$	9.5	2-3	-1446.6	3332.3

Table 3.57 Binary interaction parameters (Δg_{ij}, Δg_{ji} *for NRTL model;* Δu_{ij}, Δu_{ji} for *UNIQUAC model*) and root mean square deviations (F, $\Delta\beta$) for the correlation of {[C_6mmPy][NTf_2] (1) + Thiophene (2) + *i*-octane (3)} at 298.15 K.

NRTL				
Residuals		Components	Parameters	
		i–j	Δg_{ij} / $J{\cdot}mol^{-1}$	Δg_{ji} / $J{\cdot}mol^{-1}$
		α=0.3 Not optimised		
		1-2	14555	2395.7
F	6.4142	1-3	9940.8	10702
$\Delta\beta$	11.8	2-3	11927	-12564
		α=0.3	Optimised β_∞=*5.10*	
		1-2	-5005.5	14370
F	1.4393	1-3	3337.8	11640
$\Delta\beta$	3.7	2-3	2749.4	-103.82
UNIQUAC				
Residuals		Components	Parameters	
		i–j	Δu_{ij} / $J{\cdot}mol^{-1}$	Δu_{ji} / $J{\cdot}mol^{-1}$
			Not optimised	
		1-2	-871.27	2126.5
F	1.0130	1-3	-1167.9	6354.8
$\Delta\beta$	2.6	2-3	-1084.9	3128.2
			Optimised β_∞=*4.10*	
		1-2	-848.82	2085.1
F	0.9638	1-3	-1299.6	8147.4
$\Delta\beta$	2.4	2-3	-1009.7	2945.9

Table 3.58 Binary interaction parameters (Δg_{ij}, Δg_{ji} *for NRTL model;* Δu_{ij}, Δu_{ji} for *UNIQUAC model*) and root mean square deviations (F, $\Delta\beta$) for the correlation of {[C_6mmPy][NTf_2] (1) + Thiophene (2) + Toluene (3)} at 298.15 K and atmospheric pressure.

NRTL				
Residuals		Components	Parameters	
		i–j	Δg_{ij} / $J{\cdot}mol^{-1}$	Δg_{ji} / $J{\cdot}mol^{-1}$
		α=0.3 Not optimised		
		1-2	-2118.0	11928
F	9.7227	1-3	9940.8	11538
$\Delta\beta$	40.5	2-3	-37.250	254.90
		α=0.3	Optimised $\beta_\infty=1.20$	
		1-2	-3409.2	12303
F	3.6536	1-3	-2741.4	11134
$\Delta\beta$	76.9	2-3	929.9	1191.9
UNIQUAC				
Residuals		Components	Parameters	
		i–j	Δu_{ij} / $J{\cdot}mol^{-1}$	Δu_{ji} / $J{\cdot}mol^{-1}$
			Not optimised	
		1-2	-763.26	1946.3
F	1.2314	1-3	-1213.6	2596.8
$\Delta\beta$	5.9	2-3	-105.09	-1.1822
			Optimised $\beta_\infty=0.80$	
		1-2	-584.77	1714.6
F	1.3521	1-3	-1260.7	2659.2
$\Delta\beta$	3.5	2-3	-236.37	43.687

Table 3.59 Binary interaction parameters (Δg_{ij}, Δg_{ji} *for NRTL model;* Δu_{ij}, Δu_{ji} for *UNIQUAC model*) and root mean square deviations (F, $\Delta\beta$) for the correlation of {[C_6mmpy][NTf_2] (1) + Pyridine (2) + *n*-Hexane (3)} at 298.15 K.

NRTL				
Residuals		Components	Parameters	
		i–j	Δg_{ij} / $J{\cdot}mol^{-1}$	Δg_{ji} / $J{\cdot}mol^{-1}$
			α=0.2 Not optimised	
		1-2	1098.7	3306.5
F	0.6556	1-3	12831	28.768
$\Delta\beta$	19.2	2-3	3035.4	-7089.6
		α=0.2	Optimised $\beta_\infty=25$	
		1-2	874.68	3632.6
F	0.6723	1-3	12463	67.081
$\Delta\beta$	18.5	2-3	1516.3	-6709.5
UNIQUAC				
Residuals		Components	Parameters	
		i–j	Δu_{ij} / $J{\cdot}mol^{-1}$	Δu_{ji} / $J{\cdot}mol^{-1}$
			Not optimised	
		1-2	3602.9	-1354.0
F	0.7995	1-3	5556.0	-1689.1
$\Delta\beta$	20.8	2-3	-922.07	-2162.7
			Optimised $\beta_\infty=25$	
		1-2	3557.8	-1358.7
F	0.8094	1-3	5745.1	-1711.8
$\Delta\beta$	19.3	2-3	-447.56	-2430.2

3.2.6. Discusion

As can be seen, all of the studied ternary systems with Thiophene show Type 2 behaviour, with two of their constituent pairs exhibiting partial immiscibility and with only one immiscibility region, but the ones which contain pyridine correspond to Type I with only one immiscible region and only one pair presenting partial immiscibility.

As practical application of the desulfurization process corresponds to low concentrations of nitrogen- and sulfur-containing compounds, the lower part of the diagrams must be analysed. All of the {IL+thiophene+linear hydrocarbon} systems display a solutropic behaviour with positive slopes which turn negative for hydrocarbons with small molecular weights. This is also reflected in the solute distribution ratio (β) values, changing from greater to less than one. By increasing the hydrocarbon chain (in the case of *n*-Dodecane with $[C_8mim][BF_4]$ and $[C_2mim][EtSO_4]$ and in the case of *n*-Hexadecane with $[C_8mim][BF_4]$, $[C_8mim]$ $[NTf_2]$ and $[C_2mim][EtSO_4]$) the tie lines turn negative in the whole diagram. For linear hydrocarbons, the larger the hydrocarbon chain is, the lower the solute distribution ratio values were found. From more to less favourable values of solute distribution ratio, the studied ionic liquids rank their β values as $[C_6mmPy]$ $[NTf_2]$ > $[C_8mim]$ $[NTf_2]$ >$[C_8mim]$ $[BF_4]$ > $[C_2mim]$ $[EtSO_4]$. From the practical point of view, the lower the β values, the higher the amount of solvent is required for the extraction. Ranking the studied ionic liquids in terms of selectivity values, *S* tendency was found as $[C_2mim]$ $[EtSO_4]$ >> $[C_8mim][BF_4]$ ~ $[C_6mmPy]$ $[NTf_2]$ > $[C_8mim]$ $[NTf_2]$. The more significant difference was found for $[C_2mim][EtSO_4]$ ionic liquid because of the almost total immiscibility of the hydrocarbons in the ionic liquid. High selectivities imply a lesser number of required equilibrium stages in the extraction process.

For non-linear hydrocarbons, represented by *i*-octane, all of the studied ternary systems present solutropic behaviour. For the four ionic liquids, β values rank as $[C_8mim][NTf_2]$ > $[C_6mmPy][NTf_2]$ ~ $[C_8mim]$ $[BF_4]$ > $[C_2mim]$ $[EtSO_4]$. Selectivity, *S*, for all these systems is greater than one, once again underlining the high values found with $[C_2mim]$ $[EtSO_4]$.

As in the rest of hydrocarbons relative low solubilities in all of the ionic liquids were found, nonetheless in the case of toluene-containing ternary systems it can be observed that solubilities of this aromatic compound in ionic liquids are in any case high. Solute distribution ratio values for these systems showed, for all of the studied ionic liquids, values lower than one. Due to toluene solubility in the ionic liquids, selectivity values showed values close to or slightly higher that unit, except in the case of $[C_2mim]$ $[EtSO_4]$ which always presents the higher values of this parameter.

In the case of pyridine-containing ternary systems, the immiscible region is greatly reduced. For all cases and studied ionic liquids, both β and S values are clearly higher than one.

All of studied ternary systems were correlated by means of NRTL and UNIQUAC equations. As was explained in section 3.1.5, first, the experimental data were fitted without defining a value to the solute distribution ratio at infinite dilution, β_∞, and then the optimal β_∞ was found by trial and error with $\Delta\beta$ as optimality criterion. Often when β_∞ is defined, the residual $\Delta\beta$ decreases extensively, and the residual F slightly increases. As the residual $\Delta\beta$ shows the fitness of the LLE data at low solute concentrations, and due to the importance of this region, the correlation defining β_∞ is usually preferred.

Correlation of systems containing linear hydrocarbons achieve good results at low concentrations of thiophene but deviations increase at the higher part of the ternary diagrams. These deviations from experimental values in tie-lines extremes also increase as the hydrocarbon length chain is increased. More successful correlation results were found in the case of *i*-octane and toluene-containing systems. Pyridine-containing systems were successfully correlated in all cases with both models. In general, no conclusions can be established about what is the best model to correlate LLE data in these systems involving ionic liquids. Only in the case of Toluene-containing compounds it can be concluded that better correlation results were found employing UNIQUAC equations.

3.3. Model Oil Desulfurization

3.3.1 Solvent extraction as chosen separation process

Liquid-liquid extraction is a reasonably mature separation operation, although not as mature or as widely applied as distillation, absorption and stripping. Liquid-liquid extraction, often loosely referred to as *solvent extraction* or *liquid extraction*, was carried out as early as Roman times when silver and gold were extracted from molten copper using lead as solvent. This was followed by the discovery that sulfur could selectively dissolve silver from an alloy with gold. However, it was not until the early 1930s that the first large-scale liquid-liquid extraction process began operation. The first significant industrial application of solvent extraction was in the petrochemical industry. Following, new applications came up as the recovery of vegetable oils and the purification of penicillin, and since 1945 in the nuclear industry in the refining of uranium, plutonium, and other radioisotopes. Since 1960, solvent extraction has been applied on a large scale in the refining of other nonferrous metals, particularly copper. Most recently, it has gained increasing importance as a separation technique in biotechnology [231]. Liquid-liquid extraction has grown in importance in recent years because of the growing demand for temperature-sensitive products, higher-purity requirements, more efficient equipment and availability of solvents with higher selectivity [233].

Solvent extraction is the separation of constituents of a liquid solution by contact with another insoluble liquid. If the substances constituting the original solution distribute themselves differently between the two liquid phases, a certain degree of separation will result, and this can be enhanced by use of multiple contacts or their equivalent in the manner of gas absorption and distillation [203].

In liquid liquid extraction, a liquid feed of two or more components to be separated is contacted with a second liquid phase, called the *solvent*, which is immiscible or only partly miscible with one or more of the other components of the liquid feed. In all such operations, the solution which is to be extracted is called the *feed*, and the liquid with which the feed is contacted is the *solvent*. The solvent-rich product of the operation is called the *extract*, and the residual liquid from which solute has been removed is the *raffinate.* Liquid-liquid extraction can purify a solute component with respect to dissolved ones which are not soluble in the solvent, and often, the extract solution contains a higher concentration in the solute component that the initial solution. In the process of fractional extraction, two or more cosolute components can be extracted and also separated if these have different distribution ratios between the two solvents.

The key to an effective extraction process is the discovery of a suitable solvent. In addition to be stable, nontoxic, inexpensive and easily recoverable, a good solvent should be relatively immiscible with feed components to other than the solute and have different density from the feed to facilitate phase separation. Also, it must have a very high affinity for the solute from which it should be easily separated by distillation, crystallization or other methods. Ideally the solvent distribution ratio between the two liquid phases and selectivity should be greater than 1. Otherwise a large solvent-to-feed ratio and a higher number of equilibrium stages in the extraction column is required.

3.3.1.1. Fields of usefulness

Applications of liquid extraction can be classified into two categories: those where extraction is in direct competition with other separation techniques and those in where it seems uniquely qualified [203]:

In competition with other mass transfer operations:

Distillation and evaporation are direct separation methods, the products of which are composed of essentially pure substances. However, in general, extraction is preferred to distillation for the following applications [233]:

- In the case of dissolved or complexed inorganic substances in organic or aqueous solutions
- The removal of a component present in small concentrations, such as color former in tallow or hormones in animal oil
- When a high-boiling component is present in relatively small quantities in aqueous waste stream. Extraction becomes competitive with distillation because of the expense of evaporating large quantities of water with its very high heat of evaporation.
- The recovery of heat-sensitive materials, where extraction may be less expensive than vacuum distillation
- The separation of a mixture according to chemical type rather than relative volatility
- The separation of close-melting or close-boiling liquids, where solubility differences can be exploited
- Mixtures that form azeotropes

As substitute for chemical methods

Chemical methods consume reagents and frequently lead to expensive disposal problems for chemical by-products. Liquid extraction can be a less-cost alternative, despite the fact that the cost of the solvent recovery must be included in the final reckoning.

Separations not possible by other methods

In distillation, where the vapor phase is created from the liquid by addition of heat, the vapor and liquid are necessarily composed of the same substances and therefore, chemically similar. The separation depends on the vapor pressures of the substances. By other hand, in liquid extraction the major constituent of the two phases are chemically different and this makes separations according to chemical type. For example, separation of aromatic and paraffinic hydrocarbons of nearly the same molecular weight. Many pharmaceutical products like penicillin are produced in mixtures so complex that only liquid extraction is a feasible separation device. Extraction processes are well suited to the petroleum industry because of the need to separate heat-sensitive liquids feeds according to chemical type rather than molecular weight or vapor pressure.

3.3.1.2. Current applications

Since the introduction of industrial liquid-liquid extraction processes, a large number of applications have been proposed and developed. Since 1930s, more than 1000 laboratory, pilot-plant and industrial extractors have been installed. Table 3.60 shows some representative, industrial extraction processes [233]:

Table 3.60 Representative Industrial Liquid-Liquid Extraction Processes

Solute	Carrier	Solvent
Acetic acid	Water	Ethyl acetate
Acetic acid	Water	Isopropyl acetate
Aconitic acid	Molasses	Methyl ethyl ketone
Ammonia	Butenes	Water
Aromatics	Paraffins	Diethylene glycol
Aromatics	Paraffins	Furfural
Aromatics	Kerosene	Sulfur dioxide
Aromatics	Paraffins	Sulfur dioxide
Asphaltenes	Hydrocarbon oil	Furfural
Benzoic acid	Water	Benzene
Butadiene	1-Butene	Aq. Cuprammonium acetate
Ethylene cyanohydrin	Methyl ethyl ketone	Brine liquor
Fatty acids	Oil	Propane
Formaldehyde	Water	Isopropyl ether
Formic acid	Water	Tetrahydrofuran
Glycerol	Water	High alcohols
Hydrogen peroxide	Anthrahydroquinone	Water
Methyl ethyl ketone	Water	Trichloroethane
Methyl borate	Methanol	Hydrocarbons
Naphthenes	Distillate oil	Nitrobenzene
Naphthenes/aromatics	Distillate oil	Phenol
Phenol	Water	Benzene
Phenol	Water	Chlorobenzene
Penicillin	Broth	Butyl acetate
Sodium chloride	Aq. Sodium hydroxide	Ammonia
Vanilla	Oxidized liquors	Toluene
Vitamin A	Fish-liver oil	Propane
Vitamin E	Vegetable oil	Propane
Water	Methyl ethyl ketone	Aq. Calcium chloride

The petroleum industry represent the largest-volume application for solvent extraction. By the 1960s, more than 100.000 m^3/day of liquid feed-stocks were being processed with physically selective solvents.

3.3.1.3. Equipment

A wide variety of industrial extraction equipment is available, making it necessary to consider many alternatives before making a final selection.[233, 203, 276 -279]

Despite the increasingly extensive application of liquid extraction, thanks to its great versatility, and the extensive amount of research that has been done, it is nevertheless a relatively immature unit operation. It is characteristic of such operations that equipment types change rapidly, new designs being proposed frequently and lasting through a few applications, only to be replaced by others. Design principles for such equipment are never fully developed and reliance must often be put on pilot-plant testing for new installations.

The extraction process always involves intimate contacting of the phases, so as to achieve a reasonable approach to phase equilibrium. The contacting/separation process is typically carried out continuously in three devices: mixer-settler systems, column contactors and centrifugal extractors.

Mixer-settler systems

These involve a mixing chamber for phase dispersion, followed by a settling chamber for phase separation. Several vertical and horizontal variations in the design are available. The horizontal arrangement saves headroom while the vertical one saves floor space. Dispersion in the mixing chamber can be achieved by pump recirculation, nonmechanical inline mixing, air agitation or, mechanical stirring.

Mixing-settler systems have a number of attractions including high stage efficiency, reliable scale up and operating flexibility. They can handle difficult to disperse systems, such as those having high interfacial tension and/or large phase density difference. They can also cope with highly viscous liquids and solid-liquid slurries.

However, considerable capital may be needed for pumps and piping, thus, mixer-settler applications are generally limited to those requiring few stages. Compact systems, with simple overflow-underflow arrangements, can be designed to minimize space and piping/pumping requirements

The mixer-settler concept suggests a general caution in any type of extractor design: Intense agitation to provide high rates of mass transfer, and close approaches to 100% stage efficiency, can lead to liquid-liquid dispersions that are difficult to settle into distinct phases. So, some balance between intensity of dispersion and time of settling must be reached.

The advantages and disadvantages of mixer-settler systems may be summarized as follows: Advantages: can handle solids; reliable scaleup; can handle difficult dispersion systems; high capacity; good flexibility. Disadvantages: high capital cost per stage; space requirements can be large; high inventory of material held up in vessels.

Proprietary column extractors

Many types of column contactor are in commercial use, most of them of a proprietary type. Examples are the Scheibel column (marketed as the York-Scheibel), the roteting-disc contactor (RDC), the reciprocating-plate column (marketed, for instance, as the Karr column), the Oldshue-Rushton contactor, and the Kühni column.

The *Scheibel column* is designed to simulate a series of mixer-settler extraction units, with self-contained mesh-type coalescers between each contact stage. The influence of speed and size of the agitators, geometry of the mixing compartments, and system physical properties on mass-transfer efficiency has been evaluated by Scheibel and Karr [280, 281]. Although moderately expensive, he Scheibel column offers a very high contacting efficiency.

The *rotating-disc contactor* was introduced in the 1950s by the Shell companies [282], and has been used extensively in the petroleum industry for extractions involving hydrocarbon systems. Rotors on a central shaft create a dispersion and movement of the phases, while stators provide the countercourrent staging. As with the Scheibel, the RDC's effectiveness can be controlled to some extent by varying the speed of rotation of the disc dispersers. This contactor has been used successfully for cases where the continuous phase is actually a liquid-solid slurry.

The *reciprocating-plate extractor* is a descendant of the pulsed-plate column popular in the mid-1950s. Whereas the pulse column had fixed plates with pulsed liquid, the modern version (typified by the Karr extractor [283] involves "pulsing" the plates in a steady-flow liquid medium. The Karr design relies on perforated plates having high open areas (for liquid flow) on one or more shafts. There are no upcomers or downcomers. The plate assembly is given a reciprocating movement by an overhead drive.

The *Oldshue-Rushton contactor* comprises several compartments separated by horizontal baffles [284]. Each compartment contains vertical baffles and an impeller mounted on central shaft. This design was developed in the 1950s, and columns of up to 9 ft-dia. have been reported in service. The extractor is said to have predictability in scaleup, but only a few dara are available. Oldshue has suggested some guidelines on scaleup and design [285].

The Kühni extractor [286] is similar to the Scheibel column, but without the coalescing sections. A baffled turbine impeller is used to promote radial discharge within a compartment, while horizontal baffles of variable hole arrangement are used to separate the compartments.

Nonproprietary column extractors

The important devices in this category are the spray, packed, sieve-tray, controlled-cycling-try and pulsed extractors.

The *spray extractor* comprises a vertical vessel with the only internal device being a distributor for the phase to be dispersed. The spray extractor is inexpensive but suffers low efficiency for two reasons: there is considerable back mixing in the continuous phase, thus lowering the available concentration driving force for diffusion; and the lack of reformation of drops penalizes the overall mass-transfer rate, since a significant portion of the total mass transfer occurs during drop formation. Measurements show that spray extractors do not normally produce more than one or two theoretical stages. Because of the simple construction, spray columns are still used for relatively uncomplicated operations such as washing, treating and neutralization.

The *packed extractor* is substantially more efficient than the spray column; the packing elements reduce back mixing in the continuous phase and promote mass transfer due to break up and distortion of the dispersed phase as it contacts the elements. They, of course, reduce the cross-sectional area for flow. Thus, the column diameter for a given rate will be greater than for a spray tower. This disadvantage, however, is offset by the increase mass-transfer efficiency. Packed extractors are designed on bases analogous to those for gas-liquid columns. Packing materials are the same (e. g., sadless, rings, or structured packing of the gauze or mesh type), and equivalent devices are used for phase distribution and collection. The maximum rates of phase flows are obtained from flood correlation, such as that of Nemunaitis et al.

The *sieve-tray extractor* resembles its distillation counterpart. Downcomers (or upcomers) are provided to move the continuous phase downward (or upward), depending on whether it is the heavy or the light phase. Tray perforations promote drop formation at each stage, aiding the mass-transfer process. However, because there is relatively little published information on the performance of large-scale units, engineering firms having experience with columns of such size essentially play a proprietary role.

In the *controlled-cycling-tray extractor* cycling increases both turbulence and interfacial area, and markedly improves mass-transfer efficiency in comparison with the steady-flow column. Back mixing is relatively minor, leading to improvement in efficiency. In controlled-

cycle operation, feed liquids are injected into the column under pressure in a time-controlled sequence. During injection, the intermittent countercurrent flow causes the liquids to be broken up by the tray perforations into extremely small droplets. This action creates an intimate mixing of liquids in the column, with resulting high rates of mass transfer. For example feed solution containing the solute is injected into the column for a set length of time and then, in the next sequence, the solvent is injected countercurrent to the feed solution for a specified time.

The *pulsed extractor* is based on a similar concept, that mass transfer efficiency of a packed or tray column can be appreciably increased by applying an oscillating pulse. Although pulsed extractors were popular in the 1950s, interest in them seems almost to have disappeared.

Centrifugal contactors

Unlike column contactors, which depend upon the force of gravity to allow phase separation, centrifugal units are based on centrifugal force to increase rates of countercurrent flow and separation of phases. The result is a more compact unit providing very short contact times. Another attraction of this contactor is that it can handle systems that tend to emulsify, as well as those with low density difference. They do not need too much space. Examples of these contactors are Podvielniak, Alfa-Laval, Quadronic, and Robatel.

Selection of an extraction device

Selection of a specific contactor is complicated by the large number of types available and the complexity of design variables. To help overcome the dilemma of selection table 3.61 is included in this section.

Table 3.61 Advantages and Disadvantages of Different Extraction Equipment [233]

Class of Equipment	Advantages	Disadvantages
Mixer-settlers	Good contacting Handles wide flow ratio Low headroom High efficiency Many stages available Reliable scale-up	Large holdup High power costs High investment Large floor space Interstage pumping may be required
Continuous, counter flow contactors (no mechanical drive)	Low initial cost Low operating cost Simplest construction	Limited throughput with small density difference Cannot handle high flow ratio High headroom Sometimes low efficiency Difficult scale-up
Continuous, counter flow contactors (mechanical agitation)	Good dispersion Reasonable cost Many stages possible Relative easy scale-up	Limited throughput with small density difference Cannot handle emulsifying systems Cannot handle high flow ratio
Centrifugal extractors	Handles low-density difference between phases Low holdup volume Short holdup time Low space requirements Small inventory of solvent	High initial costs High operating cost High maintenance cost Limited number of stages in single unit

3.3.1.4. Calculations

Procedures for determining the number of theoretical stages to achieve a desired solute recovery are well established. Material and energy balance equations can be written for any component in any stage for a multistage process.

Due to the fact that extraction process use to be isothermal, material balance equations and equilibrium equations (MES equations) must be combined to solve the problem.

However in thermodynamics of liquid-liquid extraction, no simple limiting theory exists. In many cases, experimental equilibrium data are preferred over predictions based on activity-coefficient correlations. However, such data can often be correlated well by semi-theoretical activity-coefficient equations such as the NRTL or UNIQUAC equations. Also, considerable laboratory effort may be required just to find an acceptable and efficient solvent.

Unfortunately, no generalized capacity and efficiency correlations are available for all equipment types.

3.3.2 Objective

In this section, the study of the extraction of sulfur and nitrogen containing compounds from synthetic fuels using ionic liquids as solvents is going to be carried out. For this purpose, synthetic mixtures simulating gasoline and diesel oil are going to be subjected to a three steps extraction process.

A model of gasoline fuel is formulated as a mixture of *n*-hexane, *n*-heptane, *iso*-octane, toluene, pyridine and thiophene, and a model of diesel fuel is formulated as a mixture of *n*-heptane, *n*-dodecane, *n*-hexadecane, toluene, pyridine, thiophene and dibenzothiophene. Afterwards, two steps are going to be performed:

- On the one hand, desulfurization and denitrogenation of these fuel models will be performed by multistage extraction using the four ILs, to comparative effects, in three successive stages.
- On the other hand, the simultaneous correlations of the ternary LLE involved in these desulfurizations will be carried out with the aim of obtaining the interaction parameters required in the design and simulation of extraction columns where the industrial processes would take place.

3.3.3 Experimental Procedure

Chemicals

n-Hexane (Fluka, puriss. p.a. ACS ≥99.0 wt%), *n*-Heptane (Fluka, >99.5 wt%), *n*-Dodecane and *n*-Hexadecane (Aldrich, purum, >99.0 wt%), Toluene (Sigma-Aldrich, purum, > 99.5 wt %), 2,2,4 Trimethylpentane (*i*-octane) (Fluka, purum, > 99.5 wt %), Thiophene (Aldrich, purum, >99.5 wt %), Dibenzotiophene (Aldrich, 98 wt%) and Pyridine (Riedel-de Häen, pruriss. ≥99.5 wt%, GC) were used as received from supplier without further purification. Gas chromatography (GC) analysis did not detect any appreciable peak of impurities. The ionic liquids used in this work were synthesized in our laboratory as previously explained in section 3.1.3 of this work.

Procedure

Synthetic fuel models composed by 26 wt% *n*-Hexane, 26wt% *n*-Heptane, 26 wt% i-octane, 10 wt% Toluene, 6 wt% Thiophene and 6 wt% Pyridine, simulating a commercial gasoline, and some other model oils composed by 26% *n*-Heptane, 26% *n*-Dodecane, 26% n-Hexadecane 10% Toluene, 3% Thiophene, 6% Pyridine and 3% Dibenzothiophene, simulating a commercial diesel, were prepared by weigh. They were introduced into 30 ml glass jacketed vessels with ionic liquid following a similar procedure as related for the determination of liquid-liquid equilibrium data.

Samples of raffinate phase were withdrawn after 24h of stirring and overnight to settle down for composition determination by GC and the remainder mixture was decanted and model-oil phase was used as feed in the next extraction step.

The employed equipment for analysis was the same one used to determine equilibrium data for ternary systems, and the GC operating conditions are given in Table 3.62. The uncertainty in the determination of mole fraction compositions for gasoline model oil is ±0.001 and ±0.003 for diesel.

Table 3.62 Chromatographic conditions for compositions analysis

Column	SPB^{TM}-1 SULFUR (30m x 0.32mm x 4μm)	
Detector type	FID	
Detector temperature	250 ºC	
Carrier gas	Helium	Split ratio 50:1
Injector temperature	275 ºC	Injection 1μL
▪ **Gasoline-model fuel**		
Flow rate	1.5 mL·min^{-1}	
Column oven	70 ºC, 40 min isothermal.	
▪ **Diesel-model fuel**		
Flow rate	1.9 mL·min^{-1} (10 min)—› 2.5 mL·min^{-1} (1 mL/min), 5 min	
Column oven	100 ºC (4 min) —› 250 ºC (20 ºC/min), 10 min	

3.3.4 Results

Figures 3.41 to 3.44 present the composition (wt %) of each component in the simulated gasoline, and raffinate product after one, two and three extraction stages when the four ionic liquids are used as solvents.Figures 3.45 to 3.48 are the correspondent representations for the case of diesel model oil.

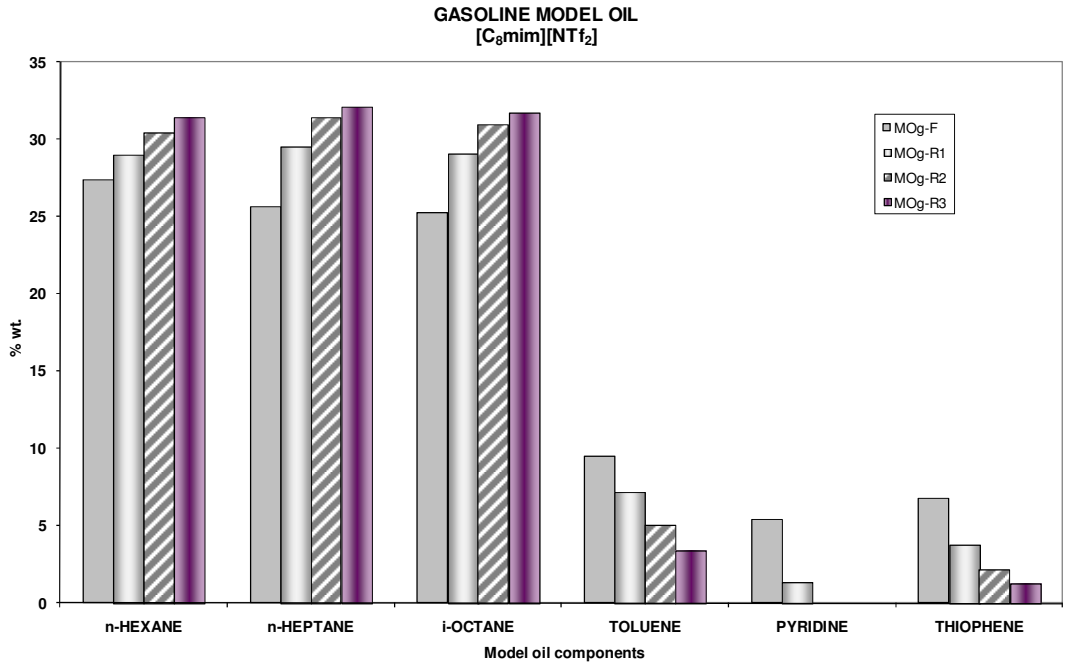

Figure 3.41 Evolution of simulated gasoline components in a three step extraction process using $[C_8mim][NTf_2]$ as solvent. MOg represents gasoline model oil, F, fresh mixture, and R1, R2, and R3, raffinate composition after each extraction step.

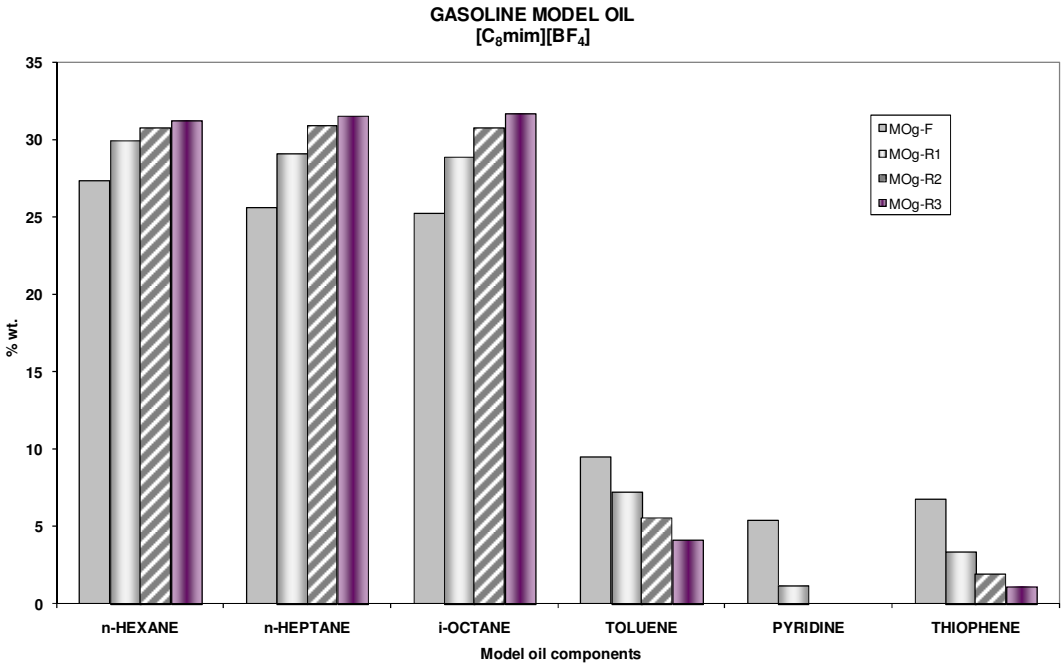

Figure 3.42 Evolution of simulated gasoline components in a three step extraction process using $[C_8mim][BF_4]$ as solvent. MOg represents gasoline model oil, F, fresh mixture, and R1, R2, and R3, raffinate composition after each extraction step.

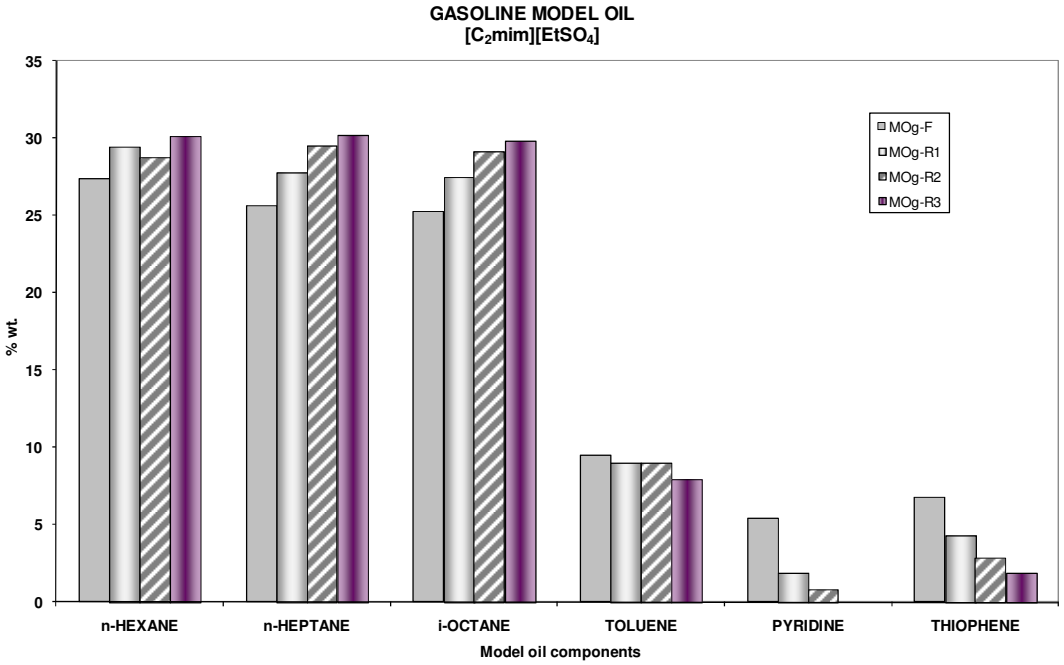

Figure 3.43 Evolution of simulated gasoline components in a three step extraction process using $[C_2mim][EtSO_4]$ as solvent. MOg represents gasoline model oil, F, fresh mixture, and R1, R2, and R3, raffinate composition after each extraction step.

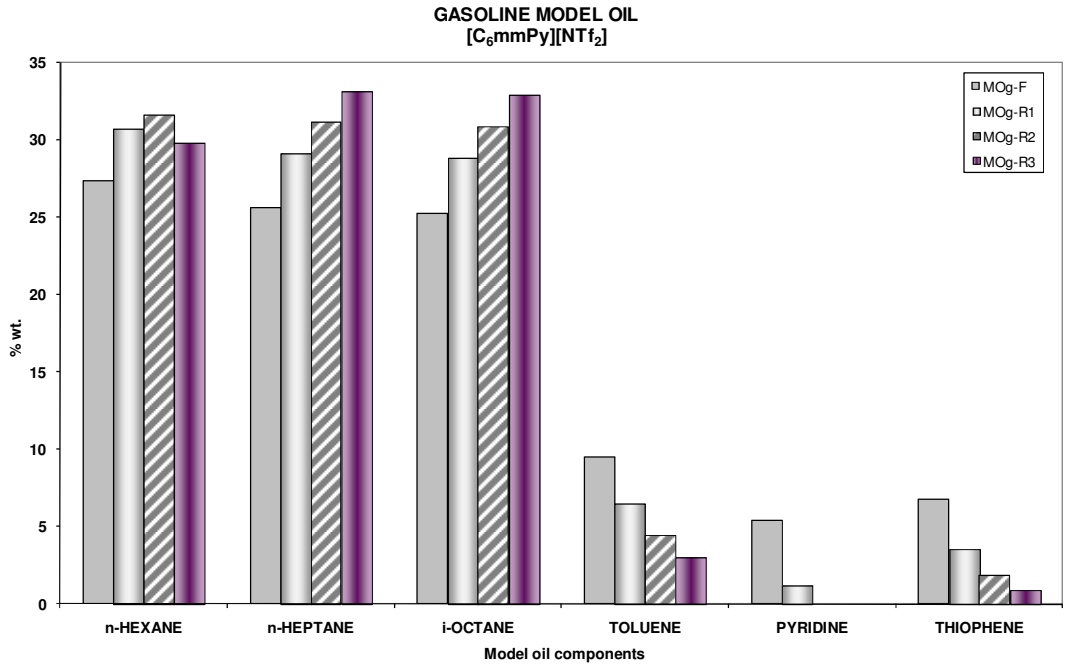

Figure 3.44 Evolution of simulated gasoline components in a three step extraction process using $[C_6mmPy][NTf_2]$ as solvent. MOg represents gasoline model oil, F, fresh mixture, and R1, R2, and R3, raffinate composition after each extraction step.

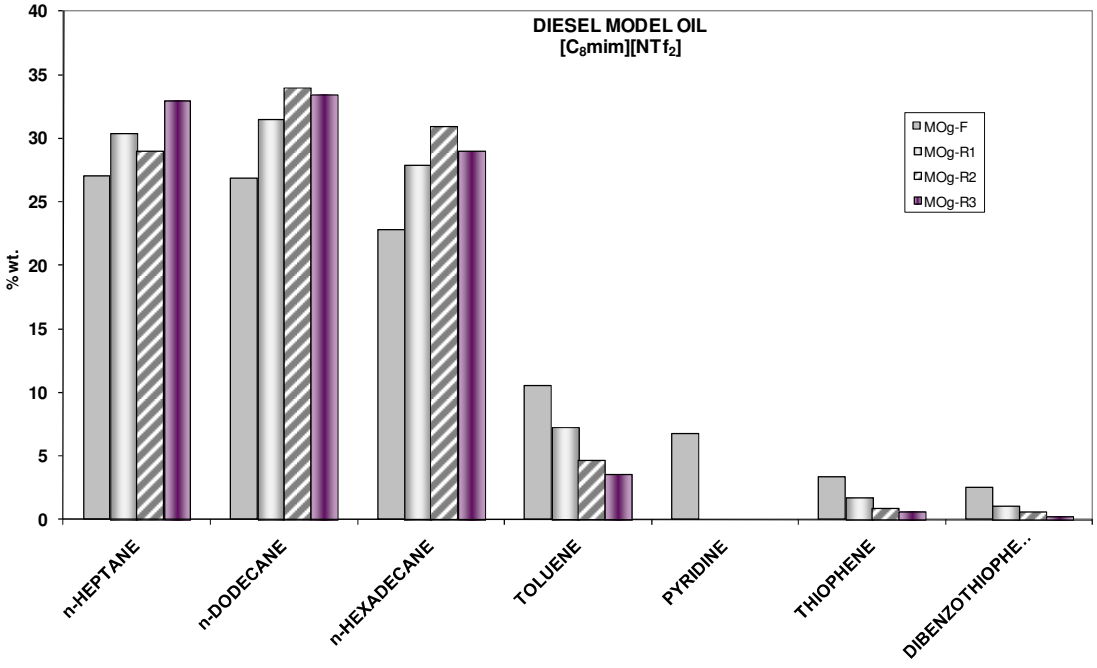

Figure 3.45 Evolution of simulated diesel components in a three step extraction process using $[C_8mim][NTf_2]$ as solvent. MOg represents diesel model oil, F, fresh mixture, and R1, R2, and R3, raffinate composition after each extraction step.

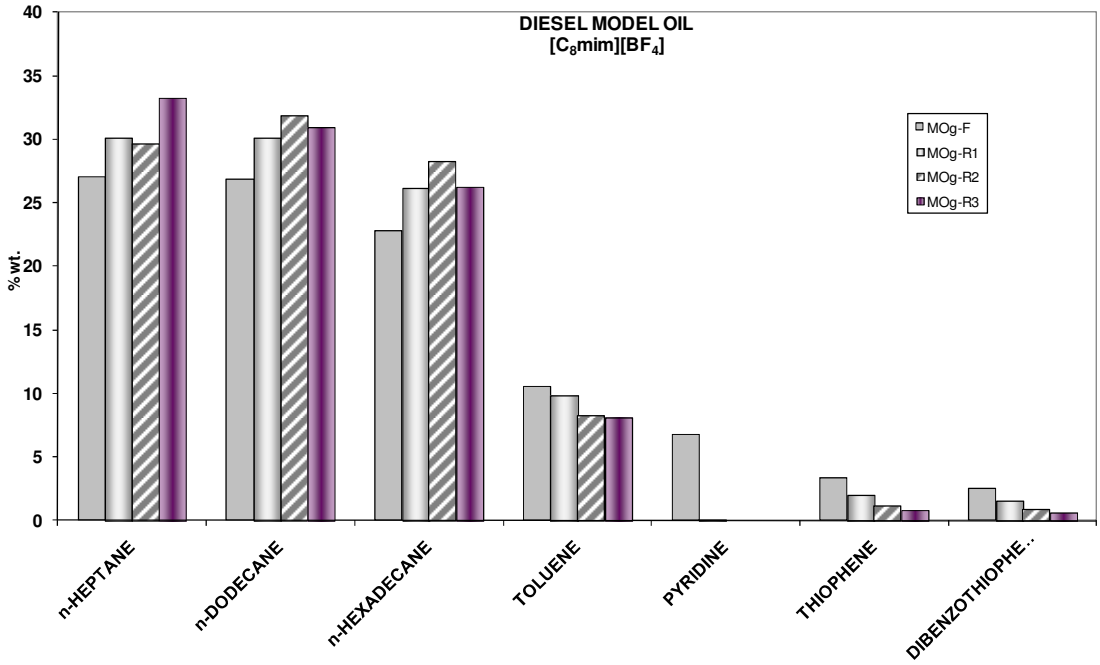

Figure 3.46 Evolution of simulated diesel components in a three step extraction process using $[C_8mim][BF_4]$ as solvent. MOg represents diesel model oil, F, fresh mixture, and R1, R2, and R3, raffinate composition after each extraction step.

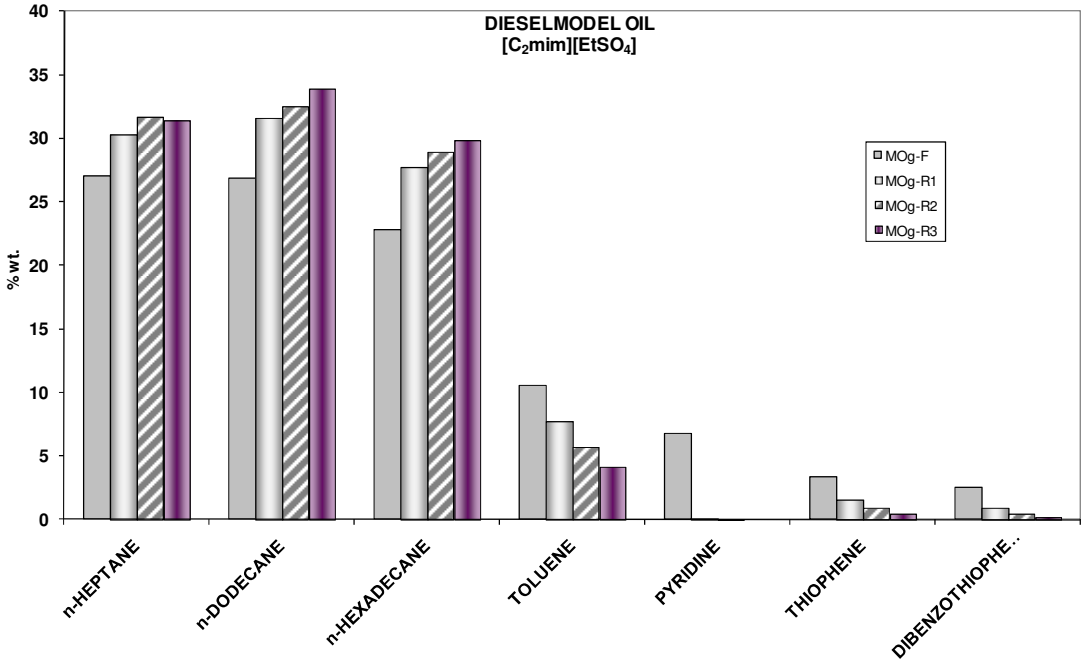

Figure 3.47 Evolution of simulated gasoline components in a three step extraction process using $[C_2mim][EtSO_4]$ as solvent. MOg represents diesel model oil, F, fresh mixture, and R1, R2, and R3, raffinate composition after each extraction step.

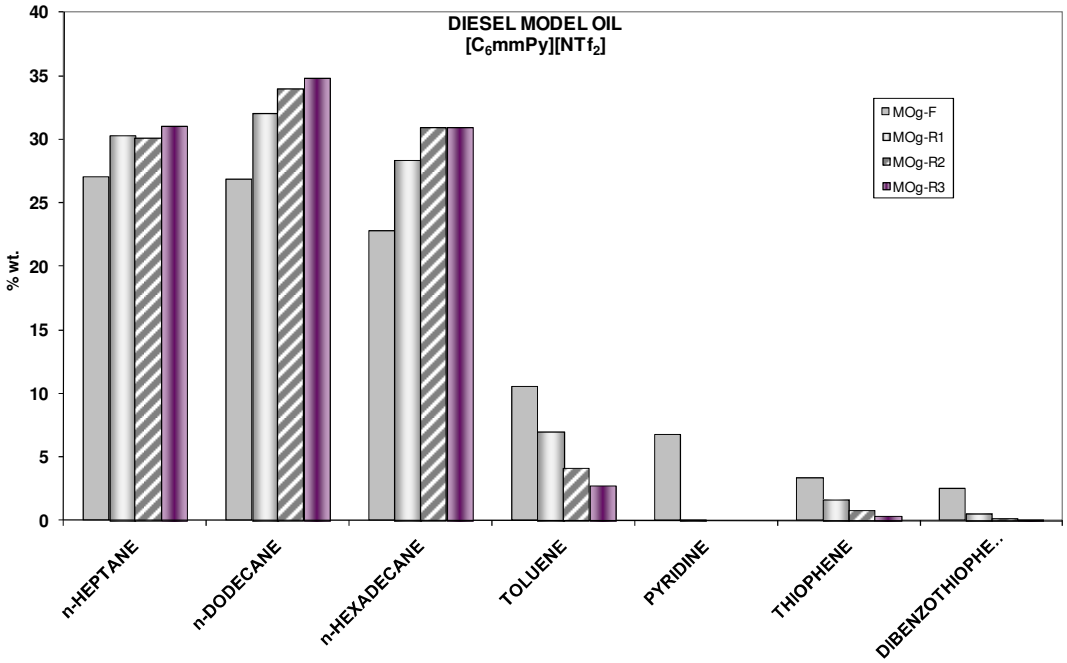

Figure 3.48 Evolution of simulated diesel components in a three step extraction process using $[C_6mmPy][NTf_2]$ as solvent. MOg represents diesel model oil, F, fresh mixture, and R1, R2, and R3, raffinate composition after each extraction step.

In both cases, for gasoline and diesel, Thiophene is extracted by all of the ILs and its composition in the raffinate products decreases rapidly, as it is reflected in Figures 3.49 and 3.51 represented just for comparative purposes.

Comparing the behavior of these ILs, as it is reflected in Figures 3.49 to 3.51 the $[C_6mmpy][NTf_2]$ has showed the largest capacity extraction, being the thiophene composition reduced around the 86 wt% in the case of gasoline and 88 wt% in the case of diesel, after three extraction stages. The desulfurization yield for the four studied ionic liquids ranks in this case as $[C_6mmpy][NTf_2] > [C_8mim][BF_4] \geq [C_8mim][NTf_2] > [C_2mim][EtSO_4]$.In the case of diesel model oil, best results for extraction of Thiophene and Dibenzothiophene were found for the same ionic liquid $[C_6mmpy][NTf_2]$ being reduced around 98 wt% after three extraction stages.The ranking in this case corresponds to $[C_6mmpy][NTf_2] > [C_2mim][EtSO_4] > [C_8mim][NTf_2] > [C_8mim][BF_4]$.

In the gasoline model, as it was expected by the LLE determined in this work, denitrogenation with all of the ionic liquids is total. The pyridine concentration undetectable after the second stage for all the ionic liquids but in the case of $[C_2mim][EtSO_4]$ which needed three steps.Pyridine was undetectable after the first stage in the case of the diesel model for all of the studied ionic liquids.

Desulfurization and denitrogenation also are accompanied by dearomatization, reflected in a toluene composition reduction of 68 wt% in the case of gasoline model and 61% in the case of diesel for the ionic liquid which showed the higher extraction yield, $[C_6mmpy][NTf_2]$. All other hydrocarbons increase their compositions after each extraction stage.

In all cases (fuel models for gasoline and diesel), the ionic liquid composition in raffinates was undetectable.

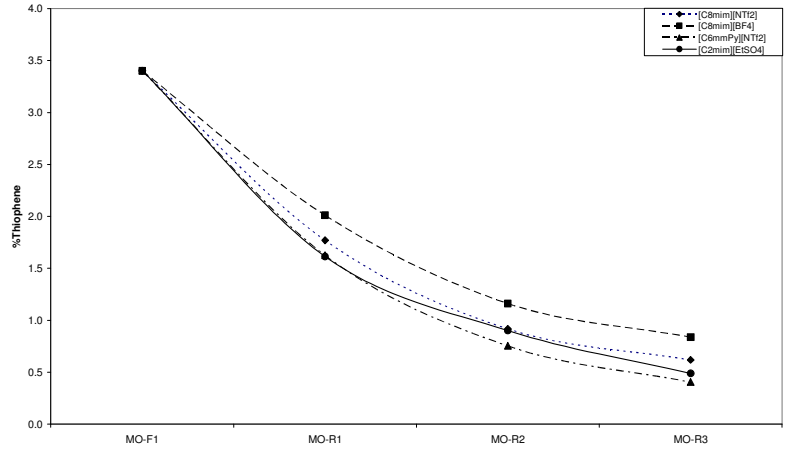

Figure 3.49 Evolution of thiophene composition in simulated diesel three step extraction process using ionic liquids as solvents. MO represents diesel model oil, F, fresh mixture, and R1, R2, and R3, raffinate composition after each extraction step.

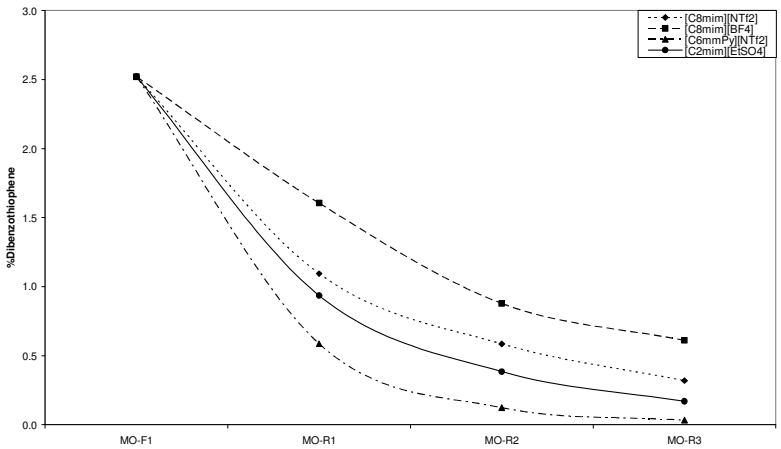

Figure 3.50 Evolution of dibenzothiophene composition in simulated diesel three step extraction process using ionic liquids as solvents. MO represents diesel model oil, F, fresh mixture, and R1, R2, and R3, raffinate composition after each extraction step.

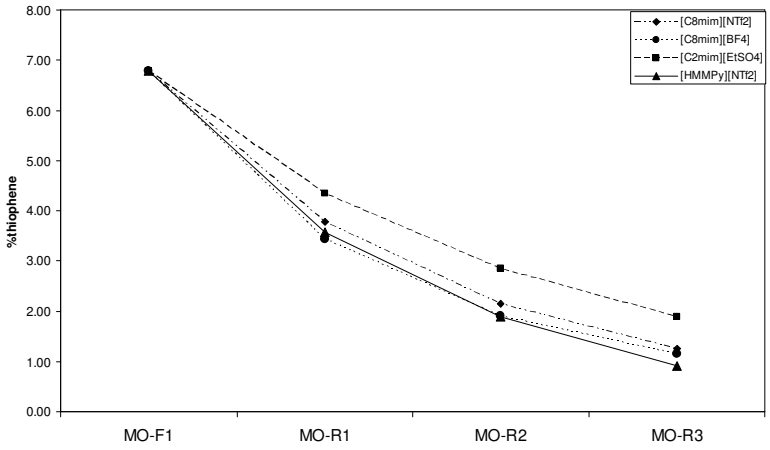

Figure 3.51 Evolution of thiophene composition in simulated gasoline three step extraction process using ionic liquids as solvents. MO represents diesel model oil, F, fresh mixture, and R1, R2, and R3, raffinate composition after each extraction step.

3.3.5 Data Treatment

By using the same correlation program previously cited [222], the simultaneous correlation of the studied ternary systems involved in the gasoline desulfurization was carried out with the NRTL[220] and UNIQUAC [221] equations without defining an a priori value of β_{∞}. Tables 3.63 to 3.70 show the binary interaction parameters and residuals for each ternary system when $[C_8mim][BF_4]$, $[C_8mim][NTf_2]$, $[C_2mim][EtSO_4]$ and $[C_6mmpy][NTf_2]$ are, respectively, the ILs involved in desulfurization. α=0.3 fixed as the optimal value which drove to better results in most of the cases.

The simultaneous correlation of the ternary systems involved in the diesel desulfurization was also carried out. Tables 3.71 to 3.78 show the binary interaction parameters and residuals for each ternary system when $[C_8mim][BF_4]$, $[C_8mim][NTf_2]$, $[C_2mim][EtSO_4]$ and $[C_6mmPy][NTf_2]$ are, respectively, the ILs involved in desulfurization.

Table 3.63 Binary Interaction Parameters and Residuals for the Simultaneous Correlation of all ternary Systems Involved on Gasoline-synthetic Desulfurization Using the NRTL (α=0.3) Equation at 298.15 K and atmospheric pressure with $[C_8mim][NTf_2]$.

	NRTL (α=0.3)	
Ternary System	***F***	***Δβ***
$[C_8mim][NTf_2]$ + thiophene + *n*-hexane	4.7790	21.2
$[C_8mim][NTf_2]$ + thiophene + *n*-heptane	3.4244	22.6
$[C_8mim][NTf_2]$ + thiophene + *i*-octane	3.7548	39.5
$[C_8mim][NTf_2]$ + thiophene + toluene	10.0927	15.1
$[C_8mim][NTf_2]$ + pyridine + *n*-hexane	2.7869	10.8

Components		**Parameters**	
i	**j**	Δg_{ij}/J·mol^{-1}	Δg_{ji}/J·mol^{-1}
$[C_8mim][NTf_2]$	thiophene	-5103.2	17153
$[C_8mim][NTf_2]$	*n*-hexane	2876.2	12878
thiophene	*n*-hexane	2025.4	809.50
$[C_8mim][NTf_2]$	*n*-heptane	2947.8	10051
thiophene	*n*-heptane	2037.5	1365.0
$[C_8mim][NTf_2]$	isooctane	2790.6	11995
thiophene	isooctane	2583.4	1755.9
$[C_8mim][NTf_2]$	toluene	-2084.0	12986
thiophene	toluene	-71.427	-56.631
$[C_8mim][NTf_2]$	pyridine	-4281.2	1047.3
pyridine	*n*-hexane	3073.5	1603.3

Table 3.64 Binary Interaction Parameters and Residuals for the Simultaneous Correlation of all ternary Systems Involved on Gasoline-synthetic Desulfurization Using the UNIQUAC Equation at 298.15 K and atmospheric pressure with [C_8mim][NTf_2]

	UNIQUAC	
Ternary System	***F***	***Δβ***
[C_8mim][NTf_2] + thiophene + *n*-hexane	1.1436	4.7
[C_8mim][NTf_2] + thiophene + *n*-heptane	1.3553	7.0
[C_8mim][NTf_2] + thiophene + *i*-octane	0.7939	7.8
[C_8mim][NTf_2] + thiophene + toluene	1.394	6.1
[C_8mim][NTf_2] + pyridine + *n*-hexane	1.0589	8.1

Components		**Parameters**	
i	**j**	Δu_{ij}/J·mol^{-1}	Δu_{ji}/J·mol^{-1}
[C_8mim][NTf_2]	thiophene	-1549.2	3467.2
[C_8mim][NTf_2]	*n*-hexane	-521.93	2108.2
thiophene	*n*-hexane	670.82	-30.467
[C_8mim][NTf_2]	*n*-heptane	-618.46	2125.3
thiophene	*n*-heptane	536.82	141.20
[C_8mim][NTf_2]	isooctane	-1006.4	2765.1
thiophene	isooctane	406.46	502.89
[C_8mim][NTf_2]	toluene	-1226.4	2654.1
thiophene	toluene	-57.602	124.23
[C_8mim][NTf_2]	pyridine	-188.20	-1098.5
pyridine	*n*-hexane	181.40	601.73

Table 3.65 Binary Interaction Parameters and Residuals for the Simultaneous Correlation of all ternary Systems Involved on Gasoline-synthetic Desulfurization Using the NRTL (α=0.3) Equation at 298.15 K and atmospheric pressure with [C_8mim][BF_4]

	NRTL (α=0.3)	
Ternary System	***F***	***Δβ***
[C_8mim][BF_4] + thiophene + *n*-hexane	1.2924	5.5
[C_8mim][BF_4] + thiophene + *n*-heptane	1.7466	6.2
[C_8mim][BF_4] + thiophene + *i*-octane	1.7256	13
[C_8mim][BF_4] + thiophene + toluene	1.3784	5.1
[C_8mim][BF_4] + pyridine + *n*-hexane	1.1411	7.5

Components		**Parameters**	
i	**j**	**Δg_{ij}/J·mol^{-1}**	**Δg_{ji}/J·mol^{-1}**
[C_8mim][BF_4]	thiophene	-4951.5	14207
[C_8mim][BF_4]	*n*-hexane	3652.2	11918
thiophene	*n*-hexane	1127.9	505.94
[C_8mim][BF_4]	*n*-heptane	3739.3	12732
thiophene	*n*-heptane	406.88	-1129.9
[C_8mim][BF_4]	isooctane	4408.0	7398.0
thiophene	isooctane	5379.9	-1384.1
[C_8mim][BF_4]	toluene	-2302.2	11306
thiophene	toluene	-420.47	124.48
[C_8mim][BF_4]	pyridine	-3529.0	2744.5
pyridine	*n*-hexane	5147.3	755.33

.

Table 3.66 Binary Interaction Parameters and Residuals for the Simultaneous Correlation of all ternary Systems Involved on Gasoline-synthetic Desulfurization Using the UNIQUAC Equation at 298.15 K and atmospheric pressure with $[C_8mim][BF_4]$.

		UNIQUAC	
Ternary System		***F***	***Δβ***
$[C_8mim][BF_4]$ + thiophene + *n*-hexane		0.9751	8.6
$[C_8mim][BF_4]$ + thiophene + *n*-heptane		2.3133	11.3
$[C_8mim][BF_4]$ + thiophene + *i*-octane		0.8251	4.6
$[C_8mim][BF_4]$ + thiophene + toluene		0.6603	4.6
$[C_8mim][BF_4]$ + pyridine + *n*-hexane		0.9124	2.9
Components		**Parameters**	
i	**j**	Δu_{ij}/J·mol^{-1}	Δu_{ji}/J·mol^{-1}
$[C_8mim][BF_4]$	thiophene	-1536.8	3596.8
$[C_8mim][BF_4]$	*n*-hexane	130.30	1333.6
thiophene	*n*-hexane	508.06	135.15
$[C_8mim][BF_4]$	*n*-heptane	-917.25	2898.9
thiophene	*n*-heptane	547.55	-392.59
$[C_8mim][BF_4]$	isooctane	-1126.9	3954.5
thiophene	isooctane	1299.8	-278.64
$[C_8mim][BF_4]$	toluene	-1060.1	2707.1
thiophene	toluene	714.82	-555.51
$[C_8mim][BF_4]$	pyridine	-424.33	-558.62
pyridine	*n*-hexane	293.29	397.51

Table 3.67 Binary Interaction Parameters and Residuals for the Simultaneous Correlation of all ternary Systems Involved on Gasoline-synthetic Desulfurization Using the NRTL (α=0.3) Equation at 298.15 K and atmospheric pressure with [C_2mim][$EtSO_4$].

	NRTL (α=0.3)	
Ternary System	***F***	***Δβ***
[C_2mim][$EtSO_4$] + thiophene + n-hexane	1.6217	9.2
[C_2mim][$EtSO_4$] + thiophene + n-heptane	1.3301	10.1
[C_2mim][$EtSO_4$] + thiophene + i-octane	3.0131	20.3
[C_2mim][$EtSO_4$] + thiophene + toluene	1.1043	6.3
[C_2mim][$EtSO_4$] + pyridine + n-hexane	1.2170	7.8

Components		**Parameters**	
i	**j**	**Δg_{ij}/J·mol^{-1}**	**Δg_{ji}/J·mol^{-1}**
[C_2mim][$EtSO_4$]	thiophene	-1930.3	10737
[C_2mim][$EtSO_4$]	n-hexane	10973	12940
thiophene	n-hexane	4055.8	-666.15
[C_2mim][$EtSO_4$]	n-heptane	12357	12925
thiophene	n-heptane	4992.5	-1035.3
[C_2mim][$EtSO_4$]	isooctane	11978	12682
thiophene	isooctane	4677.6	-2761.7
[C_2mim][$EtSO_4$]	toluene	2220.1	13981
thiophene	toluene	-207.51	573.84
[C_2mim][$EtSO_4$]	pyridine	-15305	4458.8
pyridine	n-hexane	7972.4	-12738

Table 3.68 Binary Interaction Parameters and Residuals for the Simultaneous Correlation of all ternary Systems Involved on Gasoline-synthetic Desulfurization Using the UNIQUAC Equation at 298.15 K and atmospheric pressure with [C_2mim][$EtSO_4$].

	UNIQUAC	
Ternary System	***F***	***Δβ***
[C_2mim][$EtSO_4$] + thiophene + n-hexane	1.3372	6.8
[C_2mim][$EtSO_4$] + thiophene + n-heptane	1.0582	8.1
[C_2mim][$EtSO_4$] + thiophene + i-octane	1.9889	13.8
[C_2mim][$EtSO_4$] + thiophene + toluene	0.6467	2.1
[C_2mim][$EtSO_4$] + pyridine + n-hexane	0.5008	8.7
Components		**Parameters**
i	**j**	Δu_{ij}/J·mol^{-1}	Δu_{ji}/J·mol^{-1}
[C_2mim][$EtSO_4$]	thiophene	-289.99	1648.3
[C_2mim][$EtSO_4$]	n-hexane	1162.2	4321.0
thiophene	n-hexane	-16.123	1240.0
[C_2mim][$EtSO_4$]	n-heptane	2101.7	2493.1
thiophene	n-heptane	103.57	1101.9
[C_2mim][$EtSO_4$]	isooctane	4993.8	3361.5
thiophene	isooctane	-1447.6	3359.0
[C_2mim][$EtSO_4$]	toluene	-583.95	3211.3
thiophene	toluene	697.97	-257.79
[C_2mim][$EtSO_4$]	pyridine	-942.03	1512.5
pyridine	n-hexane	-627.27	2272.0

Table 3.69 Binary Interaction Parameters and Residuals for the Simultaneous Correlation of all ternary Systems Involved on Gasoline-synthetic Desulfurization Using the NRTL (α=0.3) Equation at 298.15 K and atmospheric pressure with [C_6mmpy][NTf_2]

	NRTL (α=0.3)	
Ternary System	***F***	***Δβ***
[C_6mmpy][NTf_2]+ thiophene + *n*-hexane	8.5116	55.0
[C_6mmpy][NTf_2]+ thiophene + *n*-heptane	4.8924	23.9
[C_6mmpy][NTf_2]+ thiophene + *i*-octane	10.8476	66.6
[C_6mmpy][NTf_2]+ thiophene + toluene	6.2713	22.5
[C_6mmpy][NTf_2]+ pyridine + *n*-hexane	4.9808	17.8

Components		**Parameters**	
i	**j**	**Δg_{ij}/J·mol^{-1}**	**Δg_{ji}/J·mol^{-1}**
[C_6mmpy][NTf_2]	thiophene	-1142.2	15876
[C_6mmpy][NTf_2]	*n*-hexane	9343.0	3445.5
thiophene	*n*-hexane	-1005.6	110.15
[C_6mmpy][NTf_2]	*n*-heptane	3779.2	13519
thiophene	*n*-heptane	2993.0	1901.3
[C_6mmpy][NTf_2]	isooctane	1991.6	5524.0
thiophene	isooctane	601.98	436.42
[C_6mmpy][NTf_2]	toluene	964.15	10578
thiophene	toluene	127.25	41.640
[C_6mmpy][NTf_2]	pyridine	2440.2	2790.3
pyridine	*n*-hexane	-905.70	-2476.6

Table 3.70 Binary Interaction Parameters and Residuals for the Simultaneous Correlation of all ternary Systems Involved on Gasoline-synthetic Desulfurization Using the UNIQUAC Equation at 298.15 K and atmospheric pressure with $[C_6mmpy][NTf_2]$

	UNIQUAC	
Ternary System	***F***	***Δβ***
$[C_6mmpy][NTf_2]$+ thiophene + *n*-hexane	3.6380	14.9
$[C_6mmpy][NTf_2]$+ thiophene + *n*-heptane	1.2557	9.0
$[C_6mmpy][NTf_2]$+ thiophene + *i*-octane	7.5918	33.2
$[C_6mmpy][NTf_2]$+ thiophene + toluene	1.7893	10.1
$[C_6mmpy][NTf_2]$+ pyridine + *n*-hexane	3.4154	52.9

Components		**Parameters**	
i	**j**	Δu_{ij}/J·mol^{-1}	Δu_{ji}/J·mol^{-1}
$[C_6mmpy][NTf_2]$	thiophene	-996.66	2250.1
$[C_6mmpy][NTf_2]$	*n*-hexane	5793.9	-1674.5
thiophene	*n*-hexane	-169.71	-2077.0
$[C_6mmpy][NTf_2]$	*n*-heptane	-27.134	1807.2
thiophene	*n*-heptane	652.74	265.24
$[C_6mmpy][NTf_2]$	isooctane	354.05	2243.1
thiophene	isooctane	-460.75	-381.84
$[C_6mmpy][NTf_2]$	toluene	-712.13	1791.4
thiophene	toluene	1805.6	-1649.2
$[C_6mmpy][NTf_2]$	pyridine	1362.9	255.99
pyridine	*n*-hexane	-2347.5	662.58

Table 3.71 Binary Interaction Parameters and Residuals for the Simultaneous Correlation of all ternary Systems Involved on Diesel-synthetic Desulfurization Using the NRTL (α=0.3) Equation at 298.15 K and atmospheric pressure with [C_8mim][NTf_2] .

	NRTL (α=0.3)	
Ternary System	***F***	***Δβ***
[C_8mim][NTf_2] + thiophene + n-heptane	5.0283	18.6
[C_8mim][NTf_2] + thiophene + n-dodecane	4.8224	52.3
[C_8mim][NTf_2] + thiophene + n-hexadecane	6.7629	62.6
[C_8mim][NTf_2] + thiophene + toluene	10.969	6.4
[C_8mim][NTf_2] + pyridine + n-hexane	3.8650	8.8

Components		**Parameters**	
i	**j**	**Δg_{ij}/J·mol^{-1}**	**Δg_{ji}/J·mol^{-1}**
C_8mim][NTf_2]	thiophene	-4073.4	15288
[C_8mim][NTf_2]	n-heptane	2867.8	10547
thiophene	n-heptane	2325.4	1898.2
[C_8mim][NTf_2]	n-dodecane	4195.1	10982
thiophene	n-dodecane	2391.9	766.08
[C_8mim][NTf_2]	n-hexadecane	4824.1	8639.6
thiophene	n-hexadecane	1599.5	-142.22
[C_8mim][NTf_2]	toluene	-2034.6	13363
thiophene	toluene	134.10	127.60
[C_8mim][NTf_2]	n-hexane	3257.6	9580.0
[C_8mim][NTf_2]	pyridine	-5613.4	1359.7
n-hexane	pyridine	399.87	3094.0

Table 3.72 Binary Interaction Parameters and Residuals for the Simultaneous Correlation of all ternary Systems Involved on Diesel-synthetic Desulfurization Using the UNIQUAC Equation at 298.15 K and atmospheric pressure with $[C_8mim][NTf_2]$.

	UNIQUAC	
Ternary System	***F***	***Δβ***
$[C_8mim][NTf_2]$ + thiophene + n-heptane	3.1733	4.3
$[C_8mim][NTf_2]$ + thiophene + n-dodecane	3.3762	13.5
$[C_8mim][NTf_2]$ + thiophene + n-hexadecane	4.6965	24.2
$[C_8mim][NTf_2]$ + thiophene + toluene	3.8161	5.8
$[C_8mim][NTf_2]$ + pyridine + n-hexane	2.4330	8.4
Components		**Parameters**
i	**j**	Δu_{ij}/J·mol^{-1}	Δu_{ji}/J·mol^{-1}
$C_8mim][NTf_2]$	thiophene	-139.06	1602.0
$[C_8mim][NTf_2]$	n-heptane	-205.59	1555.8
thiophene	n-heptane	198.37	1428.8
$[C_8mim][NTf_2]$	n-dodecane	-1019.0	2703.8
thiophene	n-dodecane	-81.440	1386.3
$[C_8mim][NTf_2]$	n-hexadecane	-878.67	2310.5
thiophene	n-hexadecane	376.50	488.29
$[C_8mim][NTf_2]$	toluene	-592.54	1779.3
thiophene	toluene	205.80	262.43
$[C_8mim][NTf_2]$	n-hexane	208.13	867.20
$[C_8mim][NTf_2]$	pyridine	-1413.6	-536.67
n-hexane	pyridine	-510.72	726.63

Table 3.73 Binary Interaction Parameters and Residuals for the Simultaneous Correlation of all ternary Systems Involved on Diesel-synthetic Desulfurization Using the NRTL (α=0.3) Equation at 298.15 K and atmospheric pressure with [C_8mim][BF_4].

		NRTL (α=0.3)	
Ternary System		***F***	***Δβ***
[C_8mim][BF_4] + thiophene + n-heptane		1.8974	5.5
[C_8mim][BF_4] + thiophene + n-dodecane		2.0049	7.0
[C_8mim][BF_4] + thiophene + n-hexadecane		2.7342	17.3
[C_8mim][BF_4] + thiophene + toluene		2.0802	4.2
[C_8mim][BF_4] + pyridine + n-hexane		1.1070	5.6
Components		**Parameters**	
i	**j**	**Δg_{ij}/J·mol^{-1}**	**Δg_{ji}/J·mol^{-1}**
[C_8mim][BF_4]	thiophene	-3921.5	12762
[C_8mim][BF_4]	n-heptane	3680.3	12445
thiophene	n-heptane	813.77	264.63
[C_8mim][BF_4]	n-dodecane	5761.9	10601
thiophene	n-dodecane	1175.2	-2553.0
[C_8mim][BF_4]	n-hexadecane	7517.1	7182.1
thiophene	n-hexadecane	2547.5	-5437.9
[C_8mim][BF_4]	toluene	-2233.9	11325
thiophene	toluene	528.25	912.93
[C_8mim][BF_4]	n-hexane	3680.8	11200
[C_8mim][BF_4]	pyridine	-3680.6	2568.4
n-hexane	pyridine	693.21	5123.2

Table 3.74 Binary Interaction Parameters and Residuals for the Simultaneous Correlation of all ternary Systems Involved on Diesel-synthetic Desulfurization Using the UNIQUAC Equation at 298.15 K and atmospheric pressure with $[C_8mim][BF_4]$.

	UNIQUAC	
Ternary System	***F***	***Δβ***
$[C_8mim][BF_4]$ + thiophene + n-heptane	1.4604	3.8
$[C_8mim][BF_4]$ + thiophene + n-dodecane	2.0870	6.7
$[C_8mim][BF_4]$ + thiophene + n-hexadecane	2.4372	16.4
$[C_8mim][BF_4]$ + thiophene + toluene	1.5964	6.0
$[C_8mim][BF_4]$ + pyridine + n-hexane	0.7028	3.2

Components		**Parameters**	
i	**j**	Δu_{ij}/J·mol^{-1}	Δu_{ji}/J·mol^{-1}
$[C_8mim][BF_4]$	thiophene	-507.06	1948.8
$[C_8mim][BF_4]$	n-heptane	-633.33	2393.9
thiophene	n-heptane	-973.46	2198.1
$[C_8mim][BF_4]$	n-dodecane	-1099.0	2881.5
thiophene	n-dodecane	-951.01	1642.9
$[C_8mim][BF_4]$	n-hexadecane	-700.09	1753.8
thiophene	n-hexadecane	-86.055	-124.24
$[C_8mim][BF_4]$	toluene	-846.16	2330.2
thiophene	toluene	651.90	-414.88
$[C_8mim][BF_4]$	n-hexane	377.96	1073.6
$[C_8mim][BF_4]$	pyridine	-435.93	-566.90
n-hexane	pyridine	647.99	15.429

Table 3.75 Binary Interaction Parameters and Residuals for the Simultaneous Correlation of all ternary Systems Involved on Diesel-synthetic Desulfurization Using the NRTL (α=0.3) Equation at 298.15 K and atmospheric pressure with [C_2mim][$EtSO_4$].

	NRTL (α=0.3)	
Ternary System	***F***	***Δβ***
[C_2mim][$EtSO_4$] + thiophene + n-heptane	1.8078	467.7
[C_2mim][$EtSO_4$] + thiophene + n-dodecane	3.7819	39.5
[C_2mim][$EtSO_4$] + thiophene + n-hexadecane	2.9146	33.3
[C_2mim][$EtSO_4$] + thiophene + toluene	1.5845	4.1
[C_2mim][$EtSO_4$] + pyridine + n-hexane	1.4023	9.0

Components		**Parameters**	
i	**j**	**Δg_{ij}/J·mol^{-1}**	**Δg_{ji}/J·mol^{-1}**
[C_2mim][$EtSO_4$]	thiophene	-1426.2	9787.8
[C_2mim][$EtSO_4$]	n-heptane	10619	11182
thiophene	n-heptane	5414.2	-556.52
[C_2mim][$EtSO_4$]	n-dodecane	9701.4	12683
thiophene	n-dodecane	4912.7	-4539.1
[C_2mim][$EtSO_4$]	n-hexadecane	7350.9	12108
thiophene	n-hexadecane	5406.2	-6535.1
[C_2mim][$EtSO_4$]	toluene	1619.5	11856
thiophene	toluene	5195.2	-1756.0
[C_2mim][$EtSO_4$]	n-hexane	9631.5	11997
[C_2mim][$EtSO_4$]	pyridine	-11496	3465.5
n-hexane	pyridine	-9018.7	8507.4

Table 3.76 Binary Interaction Parameters and Residuals for the Simultaneous Correlation of all ternary Systems Involved on Diesel-synthetic Desulfurization Using the UNIQUAC Equation at 298.15 K and atmospheric pressure with [C_2mim][$EtSO_4$]

	UNIQUAC	
Ternary System	***F***	***Δβ***
[C_2mim][$EtSO_4$] + thiophene + n-heptane	1.3495	9.1
[C_2mim][$EtSO_4$] + thiophene + n-dodecane	3.6563	32.1
[C_2mim][$EtSO_4$] + thiophene + n-hexadecane	2.4549	31.5
[C_2mim][$EtSO_4$] + thiophene + toluene	0.9723	2.2
[C_2mim][$EtSO_4$] + pyridine + n-hexane	0.5405	10.0

Components		**Parameters**	
i	**j**	Δu_{ij}/J·mol^{-1}	Δu_{ji}/J·mol^{-1}
[C_2mim][$EtSO_4$]	thiophene	-162.16	1513.7
[C_2mim][$EtSO_4$]	n-heptane	2248.0	896.05
thiophene	n-heptane	330.47	882.58
[C_2mim][$EtSO_4$]	n-dodecane	916.50	1760.4
thiophene	n-dodecane	1342.0	-1407.6
[C_2mim][$EtSO_4$]	n-hexadecane	662.66	1818.0
thiophene	n-hexadecane	1562.0	-1656.2
[C_2mim][$EtSO_4$]	toluene	-419.12	2757.8
thiophene	toluene	1155.1	-565.92
[C_2mim][$EtSO_4$]	n-hexane	2196.4	3223.2
[C_2mim][$EtSO_4$]	pyridine	-429.53	738.67
n-hexane	pyridine	2482.9	-731.40

Table 3.77 Binary Interaction Parameters and Residuals for the Simultaneous Correlation of all ternary Systems Involved on Diesel-synthetic Desulfurization Using the NRTL (α=0.3) Equation at 298.15 K and atmospheric pressure with [C_6mmpy][NTf_2]

	NRTL (α=0.3)	
Ternary System	***F***	***Δβ***
[C_6mmpy][NTf_2]+ thiophene + n-heptane	1.9499	16.5
[C_6mmpy][NTf_2]+ thiophene + n-dodecane	5.8886	59.5
[C_6mmpy][NTf_2]+ thiophene + n-hexadecane	8.1248	50.4
[C_6mmpy][NTf_2]+ thiophene + toluene	2.8827	18.3
[C_6mmpy][NTf_2]+ pyridine + n-hexane	1.9018	19.5

Components		**Parameters**	
i	**j**	**Δg_{ij}/J·mol^{-1}**	**Δg_{ji}/J·mol^{-1}**
[C_6mmpy][NTf_2]	thiophene	-4738.6	14106
[C_6mmpy][NTf_2]	n-heptane	3467.6	13688
thiophene	n-heptane	1995.0	885.49
[C_6mmpy][NTf_2]	n-dodecane	7794.6	3528.3
thiophene	n-dodecane	9291.4	-1523.3
[C_6mmpy][NTf_2]	n-hexadecane	5396.3	6498.8
thiophene	n-hexadecane	3755.1	-718.50
[C_6mmpy][NTf_2]	toluene	-2706.0	10835
thiophene	toluene	149.54	443.94
[C_6mmpy][NTf_2]	n-hexane	9216.6	3071.6
[C_6mmpy][NTf_2]	pyridine	2507.3	3725.1
n-hexane	pyridine	-2661.7	-903.20

Table 3.78 Binary Interaction Parameters and Residuals for the Simultaneous Correlation of all ternary Systems Involved on Diesel-synthetic Desulfurization Using the UNIQUAC Equation at 298.15 K and atmospheric pressure with $[C_6mmpy][NTf_2]$

	UNIQUAC	
Ternary System	***F***	***Δβ***
$[C_6mmpy][NTf_2]$+ thiophene + n-heptane	2.2307	6.5
$[C_6mmpy][NTf_2]$+ thiophene + n-dodecane	4.4803	33.5
$[C_6mmpy][NTf_2]$+ thiophene + n-hexadecane	3.2056	22.1
$[C_6mmpy][NTf_2]$+ thiophene + toluene	3.0712	12.5
$[C_6mmpy][NTf_2]$+ pyridine + n-hexane	3.3648	45.8

Components		**Parameters**	
i	**j**	Δg_{ij}/J·mol^{-1}	Δg_{ji}/J·mol^{-1}
$[C_6mmpy][NTf_2]$	thiophene	-806.15	2325.3
$[C_6mmpy][NTf_2]$	n-heptane	-2.8163	1755.8
thiophene	n-heptane	694.17	573.98
$[C_6mmpy][NTf_2]$	n-dodecane	2911.2	-1047.7
thiophene	n-dodecane	2885.8	-482.11
$[C_6mmpy][NTf_2]$	n-hexadecane	2383.8	-812.72
thiophene	n-hexadecane	2415.1	-364.27
$[C_6mmpy][NTf_2]$	toluene	-616.70	1701.1
thiophene	toluene	1994.3	-1225.6
$[C_6mmpy][NTf_2]$	n-hexane	8566.1	-1769.0
$[C_6mmpy][NTf_2]$	pyridine	1374.1	327.09
n-hexane	pyridine	-162.66	-2152.9

3.3.6 Simulation

The simulation of an extraction column was done in order to analyze the possibility of getting the required 10 ppm of sulfur content. Simulation of the process was done using Aspen Plus (v2004.1) software from Aspen Technology, Inc (Cambridge, MA). An isothermal operation at 298.15 K and at 101.32 kPa was selected.

For simulation, gasoline feed had the same composition than model oil (26 wt% n-Hexane, 26wt% *n*-Heptane, 26 wt% isooctane, 10 wt% Toluene, 6 wt% Thiophene and 6 wt% Pyridine) and a 100 $kg \cdot h^{-1}$ mass flow. In the case of diesel, feed composition also coincides with model oil (26% *n*-Heptane, 26% *n*-Dodecane, 26% *n*-Hexadecane 10% Toluene, 3% Thiophene, 6% Pyridine and 3% Dibenzothiophene) and had a 100 $kg \cdot h^{-1}$ mass flow. Solvent mass flow, in order to get a solvent-to-feed ratio *S/F*, and equilibrium stages *N* were varied in simulations.

Figure 3.52 shows the tiophene concentration (ppm) in rafinatte plotted against the number of equilibrium stages, *N*, and the solvent-to-feed ratio, *S/F* for the case of gasoline desulfurization. Ten stages and *S/F* ratios close to or larger than 2 allowed to reach less than 10 ppm of sulfur and traces of pyridine. Figure 3.53 shows the thiophene and benzothiophene concentrations after diesel desulfurization. In this case, a more difficult operation was found with the need of around 25 stages and ratios *S/F* close to or bigger than 2 to get the desired desulfurization and traces of pyridine.

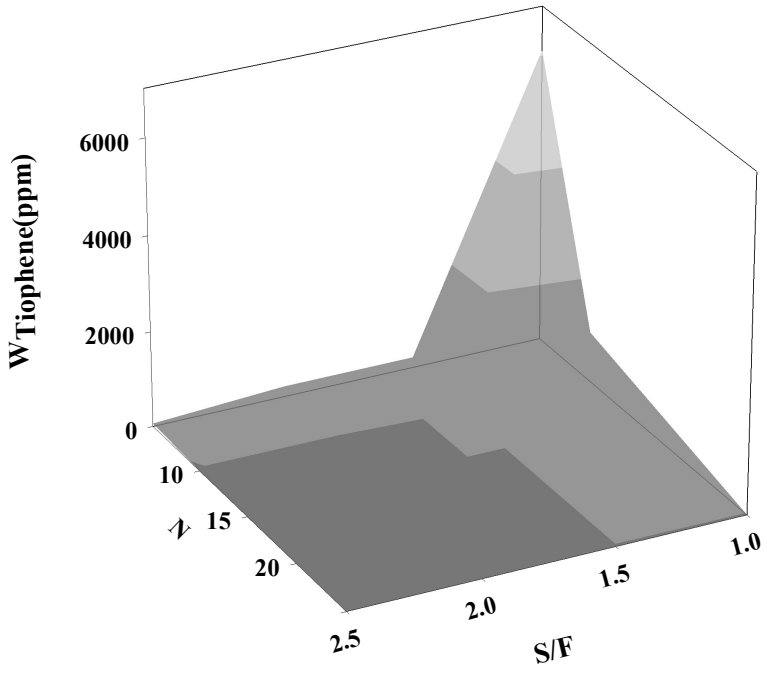

Figure 3.52 Thiophene mass fraction (ppm) in raffinatte as a function of the solvent-to-feed ratio, *S/F*, and number of equilibrium stages, *N*, when $[C_6mmpy][NTf_2]$ is used as solvent in desulfurization of a gasoline.

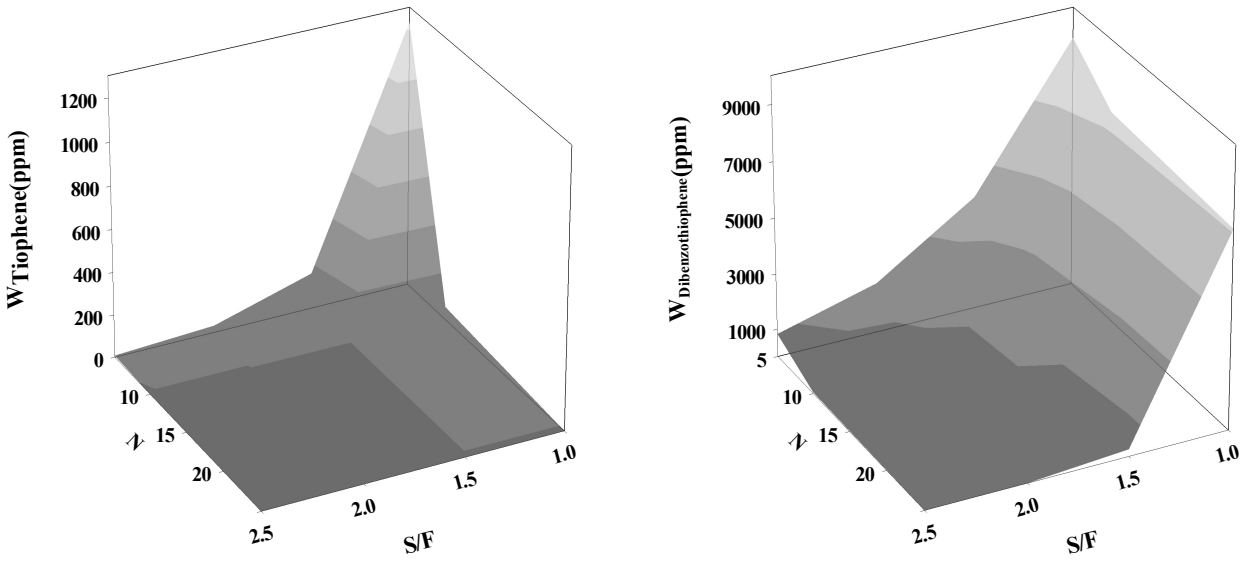

Figure 3.53 Thiophene and dibenzothiophene mass fractions (ppm) in raffinatte as a function of the solvent-to-feed ratio, *S/F*, and number of equilibrium stages, *N*, when $[C_6mmpy][NTf_2]$is used as solvent in desulfurization of a diesel.

3.3.7 Discusion

In the case of gasoline, the desulfurization yield for the four studied ionic liquids ranks as $[C_6mmpy][NTf_2]$ > $[C_8mim][BF_4]$ ≥ $[C_8mim][NTf_2]$ >$[C_2mim][EtSO_4]$. The $[C_6mmpy][NTf_2]$ ionic liquid showed the largest extraction capacity, being the Thiophene composition reduced around the 86 wt% after three extraction stages. The ranking in the case of diesel model oil desulfurization corresponds to $[C_6mmpy][NTf_2]$ > $[C_2mim][EtSO_4]$ > $[C_8mim][NTf_2]$ > $[C_8mim][BF_4]$. As in the case of gasoline, $[C_6mmpy][NTf_2]$ showed the best results for extraction of Thiophene and Dibenzothiophene, being Thiophene content reduced around 88wt% and Dibenzothiophene around 98 wt% after three extraction stages.

In the gasoline model, denitrogenation with all of the ionic liquids is total. The pyridine concentration was undetectable after the second stage for all the ionic liquids, except in the case of $[C_2mim][EtSO_4]$ which needed three steps. In the case of the diesel model, Pyridine was undetectable after the first stage for all of the studied ionic liquids.

Desulfurization and denitrogenation are also accompanied by dearomatization, reflected in a toluene composition reduction of 68 wt% in the case of gasoline model and 61% in the case of diesel for the ionic liquid which showed the higher desulfurization yield, $[C_6mmpy][NTf_2]$. All other hydrocarbons present in model oils increase their compositions after each extraction stage.

In all cases (fuel models for gasoline and diesel), the ionic liquid composition in raffinates was undetectable.

The simultaneous correlation of the studied ternary systems involved in the gasoline and diesel desulfurization was carried out with the NRTL and UNIQUAC equations. Although in every case relative high deviations on F and $\Delta\beta$ were found, in this simultaneous correlation UNIQUAC seems to give slightly better results than NRTL model.

With the obtained interaction parameters, simulation of an extraction column has confirmed the capability of $[C_6mmpy][NTf_2]$ to lead to desulfurization levels in accordance with legislation requirements. Nonetheless, due to the order of deviations found with the correlation equations, this only can be understood as a qualitative exercise simulation.

3.4. Real Samples Desulfurization

3.4.1 Contextualization

Fuel quality has a significant effect on the emissions produced by cars. In this regard, it is especially important to reduce the sulfur content of fuels. For this reason, Repsol YPF has hydrodesulfuration (HDS) units for diesel, paraffin and petrol at its production centres.

The design of the Repsol Technology Centre has taken into consideration the diversity of the activities developed by the company (exploration and production, refinery, gas, chemistry...), as well as the various potential stages of R&D&I projects, technological support (laboratory scales, microplant, pilot plant...) and, in view of the high turnover of technology, the need to adapt the facilities in response to the continuous changes likely to occur during its useful life (40-50 years).

On account of Repsol YPF's unswerving commitment to the environment and the customer, at its Technology Centre, Repsol YPF has a modern warehouse of pilot plants for studying and optimising hydrodesulfuration processes and catalysts.

In hydrodesulfurization processes, the hydrocarbon is made to react with hydrogen, in the presence of a catalytic layer and at moderate pressure (between 20 and 70 bars) and temperature (between 270ºC and 400ºC). The sulfur atoms present in the hydrocarbon molecules combine with the H_2 (hydrogen), giving rise to a sulfurous gas, SH_2. This gas is subsequently treated in sulfur recovery units which transform it into pure sulfur. Figures 3.54 and 3.55 show the Hydrotreatment Pilot Plant of Repsol YPF.

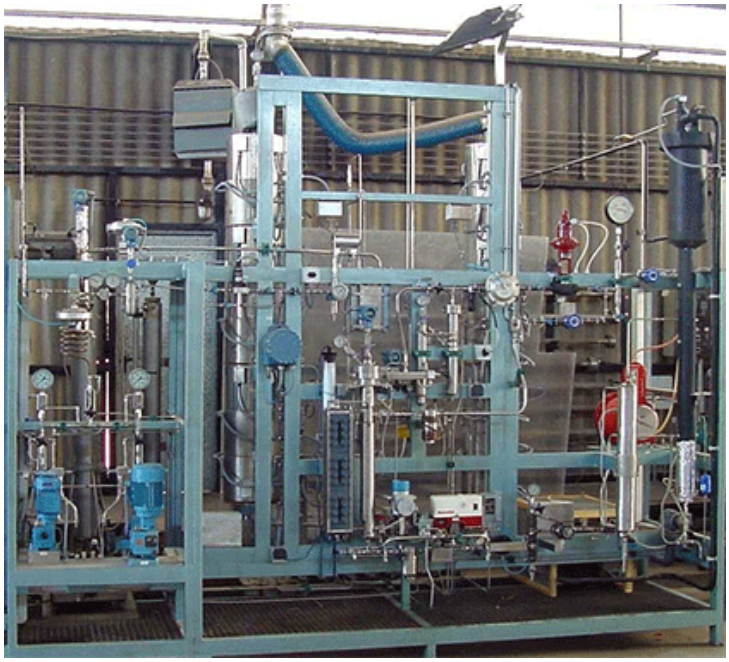

Figure 3.54 Hydrotreatment Pilot Plant in Repsol YPF.

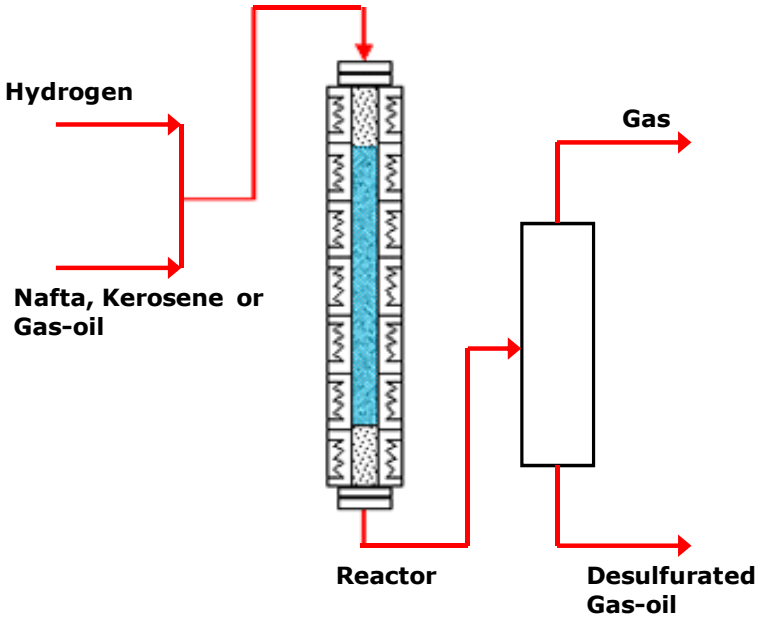

Figure 3.55 Hydrotreatment Pilot Plant Scheme, Repsol YPF.

3.4.2 Objective

In this section, the study of the desulfurization yield of the ionic liquids is going to be tested by using real samples of diesel and light naphta previous to desulfurization process in the refinery. Three steps extraction process is going to be carried out with the aim of following sulfur content evolution in raffinate along the different stages. A comparation between the desulfurization ability of the four ionic liquids is going to be analyzed to verify the consistency of the real fuel results with the obtained results in previous sections.

3.4.3. Experimental Procedure

Chemicals

Real light naphtha and diesel samples, previous refinery desulfurization, were provided by Repsol IPF.

Procedure

Desulfurization was carried out in three extraction stages, exactly with the same experimental procedure that in the case of synthetic model oils.

Samples of both streams were introduced into 30 ml glass jacketed vessels (Figure 3.56) with the four ionic liquids following a similar procedure as related for the determination of liquid-liquid equilibrium data. Samples of raffinate phase were withdrawn after 24h of stirring and overnight to settle down for total sulfur content analysis.

Figure 3.56. Glass jacketed vessel employed in real simples extraction process.

In this case, the sulfur content was determined with an uncertainty of ± 1 ppm by using a Total Sulfur Analyser TS 3000 (Figure 3.57) for low sulfur content mixtures and with an uncertainty of ± 20 ppm by using a Oxford Lab-X 3000S sulfur analyser (Figure 3.58) for high sulfur content mixtures (sulfur content >0.1% mass).

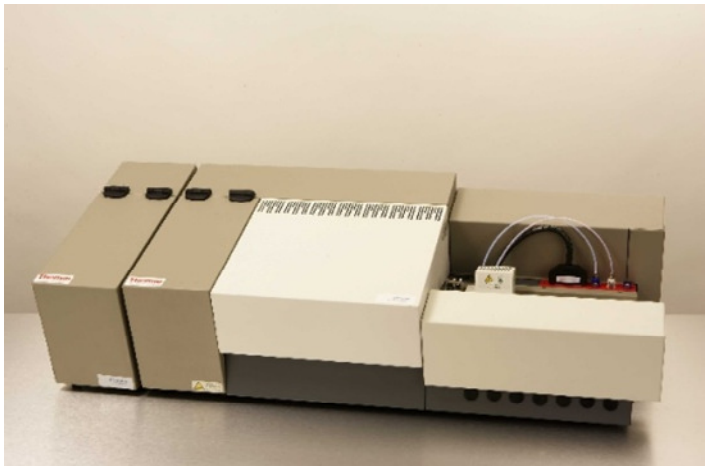

Figure 3.57 Total Sulfur Analyser TS 3000.

Figure 3.58 Oxford Lab-X 3500S sulfur analyser.

3.4.4 Results

Figure 3.59 shows how total sulfur concentration diminishes when a real gasoline is submitted to the same multistage extraction performed for synthetic model oils. Ionic liquids behaviour are coincident with above section and [C_6mmPy][NTf_2] gives better results than those found for previously studied ILs.

Figure 3.60 shows how total sulfur concentration diminishes when a real diesel is submitted to the multistage extraction process. Conclusions are coincident with above section and [C_6mmPy][NTf_2] gives the best results.

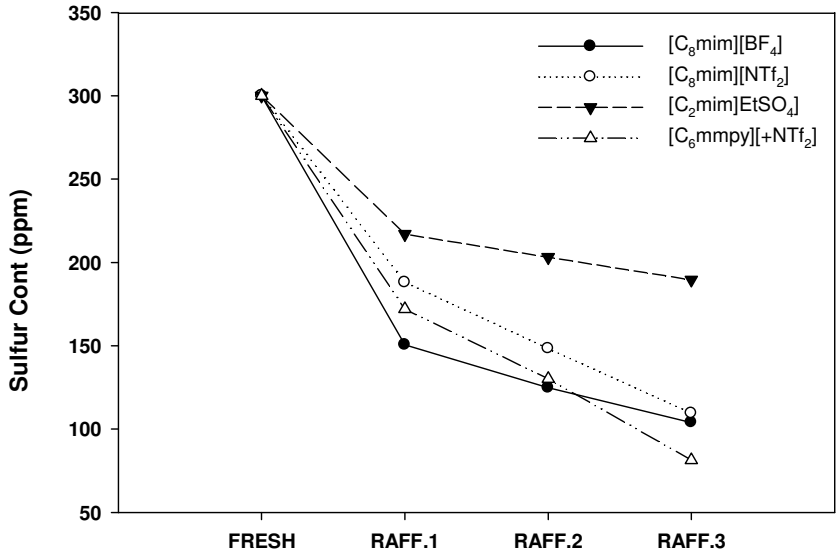

Figure 3.59 Sulfur content evolution of a light naphtha in a three step extraction process.

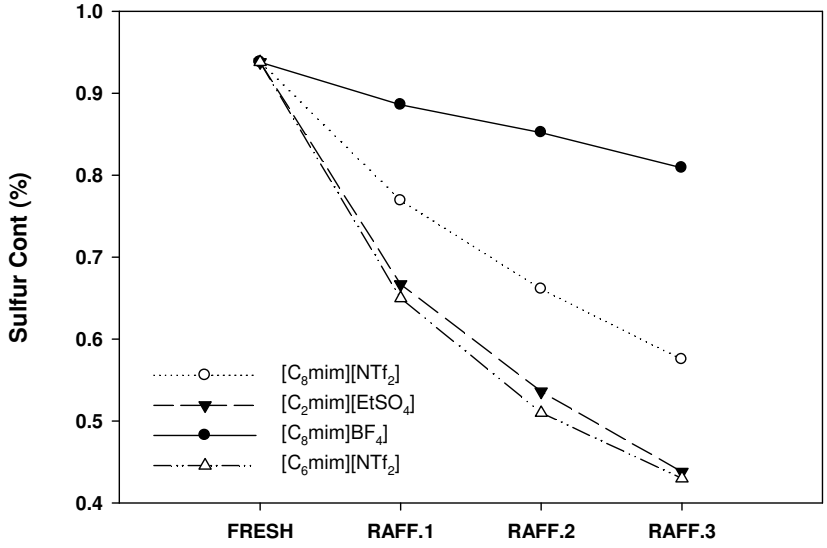

Figure 3.60 Sulfur content evolution of a diesel in a three step extraction process.

3.4.5 Discusion

The ability of ionic liquids $[C_8mim][BF_4]$, $[C_8mim][NTf_2]$, $[C_2mim][EtSO_4]$ and $[C_6mmPy][NTf_2]$ has been tested performing the extraction experiments with real samples of light naphta and diesel fuel obtained previous to desulfurization process in the refinery streams. Sulfur content along the three extraction steps has been reduced for the four ionic liquids ranking their desulfurization yield as following: $[C_6mmPy][NTf_2] > [C_8mim][BF_4] \geq [C_8mim][NTf_2] > [C_2mim][EtSO_4]$ in the case of light naphtha and $[C_6mmPy][NTf_2] > [C_2mim][EtSO_4] \geq [C_8mim][NTf_2] > [C_8mim][BF_4]$ in the case of diesel samples. Obtained results are consistent with model oil experiments and ensure that no ionic liquid is solubilized by hydrocarbon phase, because if that would have happened inherent sulfur content of $[C_6mmPy][NTf_2]$ and $[C_2mim][EtSO_4]$ would have increased the total sulfur content of samples.

4. CONCLUSIONS

4. CONCLUSIONS

In this work, feasibility of the $[C_8mim][BF_4]$, $[C_8mim][NTf_2]$, $[C_2mim][EtSO_4]$, and $[C_6mmPy][NTf_2]$ ionic liquids as solvents for extraction of sulfur- and nitrogen-containing compounds from fuels has been studied. Extraction power of these four ionic liquids has been tested by studying liquid-liquid equilibrium data and a three-step extraction process of both synthetic model oils and real fuels previous to HDS process in refinery.

From the obtained liquid-liquid equilibrium data it can be concluded that these four ionic liquids are able to extract sulfur-containing compounds from fuels. Best results in terms of solute distribution ratios (β) were found for $[C_6mmPy]$ $[NTf_2]$ but $[C_2mim]$ $[EtSO_4]$ showed the highest values for selectivity (S). Solubility of aromatic compounds represented by toluene was found high for all the studied ionic liquids. This means that a certain degree of aromatic compounds extraction can be predicted simultaneously to desulfurization process. These results indicate that in the case of a practical application a compromise between desulfurization and dearomatization must be achieved in order to comply with transportation fuel specifications and keep the octane number of gasoline. All of the four Pyridine-containing ternary systems showed high values for selectivity and solute distribution ratio, for this reason it can be concluded that denitrogenation could be easily reached with any of these ionic liquids.

Liquid-liquid equilibrium data of the ternary systems studied were correlated by means of NRTL and UNIQUAC equations. Overall, satisfactory results have been found and no conclusions could be established about what is the best model to correlate LLE data of these ionic liquid-containing systems. When the simultaneous correlation of the ternary systems studied involved in gasoline and diesel desulfurization was carried out with these models, relative large deviations were found, and UNIQUAC seems to give slightly better results than NRTL model.

Results found in model oil extraction are in agreement with what could be expected from liquid-liquid equilibrium data. In the case of gasoline, the desulfurization yield for the four ionic liquids studied ranks as $[C_6mmpy][NTf_2] > [C_8mim][BF_4] \geq [C_8mim][NTf_2] > [C_2mim][EtSO_4]$ and in the case of the diesel model oil as $[C_6mmpy][NTf_2] > [C_2mim][EtSO_4] > [C_8mim][NTf_2] > [C_8mim][BF_4]$. The $[C_6mmpy][NTf_2]$ ionic liquid showed the largest desulfurization capacity. Aside desulfurization, denitrogenation with all of the ionic liquids is total in the first stage of extraction for diesel models and in the second stage for the case of gasoline except with $[C_2mim][EtSO_4]$ which needed a third extraction step. Desulfurization and denitrogenation are also accompanied by dearomatization. In all the extractions performed with these model oils, the ionic liquid composition in raffinates was undetectable.

Exactly the same results obtained for model oils were found for real oil samples, light naphta and diesel obtained previous to desulfurization process in refinery streams, when analysing sulfur reduction in the three-step extraction. This ensures that in the case of $[C_6mmPy][NTf_2]$ and $[C_2mim][EtSO_4]$, no ionic liquid is solubilized by hydrocarbon phase, because if that would have happened inherent sulfur content of these salts would have increased the total sulfur content of samples.

From all the ionic liquids studied, $[C_6mmPy][NTf_2]$ seems to be the most adequate candidate to carry out fuel-oil desulfurization. Simulation of the extraction process using available process-software confirms the capacity of this ionic liquid to lead to desulfurization levels in accordance with legislation requirements. Nonetheless, due to the order of deviations found with the correlation equations, this can only be understood as a qualitative simulation exercise. Pilot plant testing, economical studies, life cycle assessment…are necessary steps to continue this study.

LIST OF SYMBOLS

LIST OF SYMBOLS

A	Holtz energy
a	activity
C	molar heat capacity
c	number of components
c	specific heat capacity F residual function
F	fresh model oil mixture
F_a	objective function (activities)
F_b	objective function (compositions)
FRESH	fresh feed in real samples extraction process
f	fugacity
f	number of degrees of freedom
G	Gibbs energy
g	binary energy interaction parameter in the NRTL model
H	enthalpy
i	generic species
j	generic species
k	generic species
l	parameter in the UNIQUAC model
M	generic property
M	molecular weight
M	number of tie-lines
m	degree of a polynomial expansion
m	number of components
m	number of phases
MO	model oil

N number of theoretical equilibrium stages

n degree of a polynomial expansion

n number of carbon atoms in an alkyl substituent chain of the imidazolium cation of an ionic liquid

n number of moles

n refractive index

P pressure

P_f Poynting factor

P_n binary interaction parameter

Q empirical constant, in the expression of F_a

Q generic property

Q heat

q area molecular-structure constant in the UNIQUAC model

R universal constant of gases

R1, R2, R3 raffinate composition after each extraction step

r volume molecular-structure constant in the UNIQUAC model

S entropy

S selectivity

S/F solvent-to-feed ratio

T temperature

U internal energy

u_{ij} binary energy interaction parameter in the UNIQUAC model

V (molar) volume

W mass fraction in raffinate

ω water content

w mass fraction

X mass fraction

x mole fraction

z lattice coordination number

Subscripts

a	in function of activity
b	in function of compositions
C	combinatorial part in the UNIQUAC equation
D	sodium line
calc	calculated value
exp	experimental value
i	component
i	inert
i	counter
j	component
j	counter
k	component
k	counter
n	constant number of moles
n	counter
HC	Hidrocarbon-rich phase
IL	Ionic Liquid-rich phase
p	constant pressure
P	constant pressure
R	residual part in the UNIQUAC equation
s	solute
S	constant entropy
T	constant temperature
v	constant volume
w	mass-based parameter
∞	infinite dilution
1, 2	state 1 and 2
G	gasoline

Superscripts

E	excess property
I	raffinate phase
II	extract phase
id	ideal solution property
k	generic phase
0	standard state
s	saturated

Greek letters

α	non-randomness parameter in the NRTL model
α	volume expansivity; coefficient of thermal expansion
β	solute distribution ratio; partition coefficient
γ	activity coefficient
Δ	variation of property
$\Delta\beta$	mean error of the solute distribution ratio
θ	area fraction in the UNIQUAC model
μ	chemical potential
ρ	density
τ_{ij}	parameter in the NRTL or UNIQUAC models
ϕ	number of phases
ϕ	segment fraction in the UNIQUAC model
ϕ	fugacity coefficient
λ_{ij}	parameter of potential energy

Symbols on top

^	calculated value
--	partial molar property

REFERENCES

REFERENCES

[1] http://science.larc.nasa.gov/biomass_burn/glossary.html

[2] Likens, G. E., F. H. Bormann and N. M. Johnson. 1972. Acid rain. Environment 14 (2)33

[3] http://www.epa.gov/acidrain/

[4] http://www.unece.org/env/lrtap/

[5] European Directive for emissions of light duty vehicles (70/220/CE amended by 99/69/EC as Euro3 and 2002/80/EC as Euro4), European Directive for emissions of heavy duty vehicles (88/77/CE amended by 1999/96/CE as Euro4 and Euro5).

[6] Directive of the European Parliament and of the Council, Brussels COM (11.05.2001) 241 final (BS EN 590-2004/DIN EN 590-2004) Automotive fuels, Diesel, Requirements and test methods; and 2003/17/EC OJ L 76, 22.3.2003, p. 10.

[7] EPA-Diesel RIA, United States Environmental Protection Agency, Air and Radiation,EPA 420-R-00-026, December 2000; and Clean Air Act Tier 2; 1999.

[8] J. G. Speight, The Chemistry and Technology of Petroleum, 4th Ed.(2007), CRC Press (USA)

[9] I. Mochida, K. H. Choi, J. Jpn Petrol Inst., 47 (2004) 145

[10] H. Topsøe, B. S. Clausen, F. E. Massoth, Catalysis: science and technology, vol. 11(1996) 310

[11] A. Rothlishberger, R. Prins, J.Catal. 235 (2005) 229

[12] Z. Jiang, Y. Liu, X. Sun, F. Tian, F. Sun, C. Linang, W. You, C. Han and C. Li, Langmuir 19 (2003) 731

[13] X. Ma, K. Sakanishi and I. Mochida, Ind.Eng.Chem.Res. 33 (1994) 218

[14] R. Shafi, G. J. Hutcnings, Catal. Today, 59 (2000) 423-442

[15] C. Song, X. Ma, Appl. Catal. B 41 (2003) 207

[16] S. K. Beg, S. K. Maty, U. T. Turaga, Energy Fuels 18 (2004) 1227

[17] J. G. Michael, C. C. Bruce, Ind. Eng. Chem. Res., 30 (1991) 2021

[18] K. Heeyeon, J. Jung, S. Lee, M. Heup, Appl. Catal. B- Environ. 44 (2003) 287

[19] I. V. Babich, J. A. Moulijn, Fuel 52 (2003) 607-631

[20]U.S. Energy Information Administration. The Transition to Ultra-Low-Sulfur Diesel Fuel: Effects on Prices and Supply, SR/OIAF/2001-01 (2001) 13-22

[21] H. Rang, J. Kann, V. Oja, Oil Shale 23 (2006) 164

[22] S. Brunet, D. Mey, G. Pérot, C. Bouchy, F. Diehl, Appl. Catal. A 278 (2005) 143

[23] E. Ito, J. A. Rob van Veen, Catal. Today 116 (2006) 446

[24] Y. Shiraishi, T. Hirai, I. Komasawa, Ind. Eng. Chem. Res. 40 (2001) 293

[25] T. Viveros-García, J.A. Ochoa-Tapia, R. Lobo-Oehmichen, J.A. de los Reyes-Heredia, E. S. Pérez-Cisneros, Chem. Eng. J., 106 (2005) 119

[26] G.A. Huff, O.S. Owen, B.D. Alexander, D.N. Rundel, W.J. Reagen, J.S. Yoo, WO 9909117, 1999.

[27] J. Wiltshire BP Technol Mag. (2000) 32:10

[28] BP tests alkylation/fractionation process for sulfur removal. Octane Week 9.10.2000

[29] V. Bellière, C. Geantet, M. Vrinat, Y. Ben-Taarit, Y. Yoshimura, Energy Fuels 18 (2004) 1806

[30] Z. Zhang, X. Niu, S. Liu, X. Zhu, H. Yu, L. Xu, Catal. Commun. 9 (2008) 60

[31] R. M Acheson, D. R. Harrison, J. Chem. Soc. D, (1969)724

[32]R. M Acheson, D. R. Harrison, J. Chem. Soc. C, (1970)1764

[33] Y. Shiraishi, Y. Taki, T. Hirai, I. Komasawa, Ind. Eng. Chem. Res.40 (2001) 1213

[34] Y. Shiraishi, K. Tachibana, Y. Taki, T. Hirai, I. Komasawa, Ind. Eng. Chem. Res.40 (2001) 1225

[35] Y. Shiraishi, K. Tachibana, T. Hirai, I. Komasawa, Ind. Eng. Chem. Res.40 (2001) 3390

[36] Y. Shiraishi, T. Hirai, I. Komasawa, Ind. Eng. Chem. Res.40 (2001) 3398

[37] V .Meille, E. Shulz, M . Vrinat, M. Lemaire, Chem. Commun. (1998) 305.

[38] A . Milenkovic, E . Shulz, V. Meille, D. Lofferda, M. Forissier, M. Vrinat, P. Sautet, M. Lemaire , Energy Fuels 13(1999)881.

[39] T. Aida, D. Yamamoto, M. Iwata, K. Sakata, Rev Heteroatom Chem 22 (2000) 241

[40] Ford JF, Rayne TA, Adlington DG. US Patent 3,341,448

[41] H. Gilman, D. L. Esmay, J. Am. Chem. Soc. 74 (1952) 2021

[42] J. H. Ramsden, R. S. Drago, R. Riley, J. Am. Chem. Soc. 111 (1989) 3958

[43] F. M. Collins, A. R. Lucy, J. Mol. Catal. A: Chem 117 (1997) 397

[44] O. Bortolini, F. D. Furia, G. Modena, R. Seraglia, J. Org. Chem. 50 (1985) 2688

[45] A. Srivastav, V. C. Srivastava, J. Hazard. Mater., 170 (2009) 1133

[46] V. Selvavathi, V. Chidambaram, A. Meenakshisundaram, B. Sairam, B. Sivasankar, Catal. Today, 141 (2009) 99.

[47] M. V. Landau, M. Herskowitz, T. Hoffman, D. Fucks, E. Liverts, D. Vingurt, N. Froumin, Ind. Eng. Chem. Res.48 (2009) 5239

[48] Z. Y. Zhang, T. B. Shi, C. Z. Jia, W. J. Ji, Y. Chen, M. Y. He, Appl. Catal., B: 82 (2008) 1

[49] J. H. Kim, X. Ma, A. Zhou, C. Song, Catal. Today 111 (2006) 74

[50] X. Ma, L. Sun, C. Song, Catal. Today 77 (2002) 107

[51] D. J. Monticello, Chemtech 28 (1998) 38

[52] B. L. McFarland, D. J. Boron, W. Deever, J. A. Meyer, A. R. Johnson, R. M. Atlas, Crit. Rev. Microbiol. 24 (1998) 99

[53] M. Ayala, R. Tinoco, V. Hernández, P. Bremauntz, R. Vazquez-Duhalt, Fuel Process. Technol. 57 (1998) 101

[54] K. A. Gray, O. S. Pogrebinsky, G. T. Mranchko, L. Xi, D. J. Monticello, C. H. Squires, Nat. Biotechnol. 14 (1996) 1705

[55] J. R. Gallagher, E. S. Olson, D. C. Stanley, FEMS Microbiol. Lett. 107 (1993) 31

[56] L. Setti, P. Faarinelli, S. Di Martino, S. Frassinetti, G. Lanzarini, P. G. Pifferi, Appl. Microbiol. Biotechnol. 52 (1999) 111

[57] B. L. McFarland, Curr. Opin.. Microbiol., 2 (1999) 257

[58] K. A. Gray, G. T. Mrachko, C. H. Squires, Curr. Opin. .Biotechnol., 6 (2003) 229

[59] L. Setti, G. Lanzarini, P. G. Pifferi, Fuel Process. Technol. 52 (1997) 145

[60] A. A. Maliyantz, Azerbaidzhanskoe Neftyanoe Khoz., 6 (1935) 89-93 (cited in Ref. 55).

[61] K. A. Malik, Process Biochem., 13 (1978) 10-12, 35

[62] J. L. Shennan. J. Chem. Tech. Biotechnol. (1996), 67, 109

[63] M. E. Gallardo, A. Ferrandez, V. de Lorenzo, J. L. García, E. Díaz, J. Bacteriol. 179 (1997) 7156

[64] D. J. Monticello, Curr. Opin. Biotechnol. 11 (2000)540

[65] T. Ohshiro, Y. Izumi, Biosci. Biotechnol. Biochem. 63 (1)(1999)1

[66] S. Abbad-Andaloussi, M. Warzywoda, M. Monot, Oil & Gas Science and Technology, Rev. IFP, 58(2003)505

[67] J. D. Van Hamme, A. Singh, O. Pl Ward, Microbiol. Mol. Biol. Rev.67(2003) 503

[68] J. J. Kibane II, Current Opin. Biotechnol. 17 (2006) 305

[69] M. Soleimani, A. Bassi, A. Margaritis, Biotechnology Advances, 25(2007) 570

[70] Funakoshi I, Aida T. US Patent 5,753,102.

[71] Forte P. US Patent 5,582,714.

[72] L. H. Thompsom, L. K. Doraiswamy, Ind. Eng. Chem. Res. 38 (1999)1215

[73] H. Mei, B. W. Mei, T. F. Yen, Fuel 82 (2003)405

[74] A. Deshpande, A. Bassi, A. Prakash, Energy Fuels, 19 (2005) 28

[75] Y. Shiraishi, T. Hirai, I. Komasawa, Ind. Eng. Chem. Res.37 (1998)203

[76] Y. Shiraishi,Y. Taki, T. Hirai, I. Komasawa, Ind. Eng. Chem. Res.38 (1999)3310

[77] Y. Shiraishi, T. Hirai, I. Komasawa, Ind. Eng. Chem. Res.40 (2001)293

[78] S. Otsuki, T. Nonaka, N. Takashima, W. Qian, A. Ishihara, T. Imai, T. Kabe, Energy Fuels, 14(2000) 1232

[79] T. Aida, D. Yamamoto, M. Iwata, K. Sakata, Rev. Heteroatom. Chem. 22 (2000)241

[80] J. F. Brennecke, E. J. Maggin, AIChE J. 47 (2001) 2384

[81] J. S. Wilkes, Green Chem. 4 (2002)73

[82] R. D. Rogers, K. R. Seddon, Science 302 (2003) 792

[83] J. S. Wilkes, Ionic Liquids in Synthesis, eds. Peter Wasserchеid and Tom Welton. 2003 Wiley-VCH, Weinheim,1

[84] F. H. Hurley, US Pat. 4,446,331 (1948), T. P. Wier Jr, US Pat. 4,446,350 (1948)

[85] F. H. Hurley, T. P. Wier, J. Electrochem. Soc, 98 (1951)207

[86] J. S. Wilkes, J. A. Levisky, R. A. Wilson, C. L. Hussey, Inorg. Chem. 21 (1982)1263

[87] T. Welton, Chem. Rev., 99 (1999)2071

[88] H. L. Chum, V. R. Koch, L. L. Miller and R. A. Osteryoung, J. Am. Chem. Soc. 97 (1975)3264

[89] R. J. Gale, V. Gilbert and R. A. Osteryoung, Inorg. Chem. 17(1978) 2728

[90] J. L. Atwood, D. J. Atwood, Advances in Chemistry Series, 150,American Chemical Society, Washington D. C., (1976) 112

[91] J. C. Nardi, C. L. Hussey, L. A. King, U.S. Pat., 4,122,245 (1978)

[92] J. S. Wilkes, M. J. Zawototko, J. Chem. Soc., Chem Commun,13 (1992) 965

[93]K. R. Seddon, J. Chem. Technol. Biotechnol.,68 (1997) 351

[94] K. R. Seddon, Kinet. Catal. (1997)

[95] J. D. Holbrey, K. R. Seddon , Clean Prod. Proc., 1(1999) 223

[96] M. Freemantle, Chem. Eng. News 76 (1998) 30th March,32

[97] A. Heintz, J. Chem. Thermodyn., 37 (2005) 525

[98] L. A. Blanchard and J. F. Brennecke, Ind. Eng. Chem. Res., 40 (2001) 287

[99] J. D. Holbrey, R. D. Rogers, Ionic Liquids in Synthesis, eds. Peter Wasserchеid and Tom Welton. 2003 Wiley-VCH, Weinheim,41

[100] J. Fuller, R. T. Carlin, H. C. De Long, D. Haworth, J. Chem. Soc., Chem. Com., (1994) 299

[101] H. Weingärtner, Angew. Chem. Int. Ed. 47 (2008) 654

[102] J. D. Holbrey, R. D. Rogers, Ionic Liquids in Synthesis, eds. Peter Wassercheid and Tom Welton. 2003 Wiley-VCH, Weinheim,68

[103] J. G. Huddleston, H. D. Willaurer, R. P. Swatlosi, A. E. Visser, R. D. Rogers, Chem. Com. (1998) 1765

[104] P. Wassserchеid, M. Sesing, W. Korth, Green Chem., 4 (2002) 134

[105] Y. Yang, Y. Kou, Chem. Commun. (2004) 226

[106] G. P. Smith, A. S. Dworkin, R. M. Pagni, S. P. Zingg, J. Am. Chem. Soc.111(1989)525

[107] G. P. Smith, A. S. Dworkin, R. M. Pagni, S. P. Zingg, J. Am. Chem. Soc.111(1989)5075-

[108] J. F. Huang, H. Luo, C. Liang, I. W. Sun, G. A. Baker, S. Day, J. Am. Chem. Soc.127 (2005) 12784

[109] K. N. Marsh, J. A. Boxall, R. Lichtenthaler, Fluid Phase Equilib. 219 (2004) 93

[110] M. J. Earle, K. R. Seddon, Pure Appl. Chem. 72 (7) (2000) 1391

[111] M. J. Earle, J. M. S. S. Esperanca, M. A. Gilea, J. N. Canoniga Lopes, L. P. N. Rebelo, J. W. Magee, K. R. Seddon, J. A: Widegreen, Nature 439 (2006) 831

[112] Y. U. Paulechka, D. H. Zaitsau, G. J. Kabo, A. A. Strechan, Thermochim. Acta 439 (2005) 158

[113] D. H. Zaitsau, G. J. Kabo, A. A: Strechan, Y. U. Paulechka, A. T.schersich, S. P. Verevkin, A. Heinz, J. Phys. Chem A, 110 (2006) 7303

[114] N. V. Plechkova, K. R. Seddon, Chem. Soc. Rev., 37 (2008)123

[115] W. M. Nelson, Industrial Applications for Green Chemistry, ACS Symposium Series 818, Eds R. D. Rogers and K. R. Seddon, ACS, Washington, (2002) 30

[116] J. S. Wilkes, Industrial Applications for Green Chemistry, ACS Symposium Series 818, Eds R. D. Rogers and K. R. Seddon, ACS, Washington, (2002) 214

[117] Y. Chauvin, H. Oliver-Bourbigou, Chemtech, 26 (2005)

[118] U. Kragl, M. Eckstein, N. Kaftzik, Ionic Liquids in Synthesis, eds. Peter Wassercheid and Tom Welton. 2003 Wiley-VCH, Weinheim,336

[119] E. Rodil, L. Aldous, C. Harddacre, M .C. Lagunas, Nanotechnology 19 (2008) 105603

[120] M. S: Selvan, M. D. McKinley, R. H. Dubois, J. L. Atwook, J. Chem. Eng. Data 45 (2000)841

[121] A. Arce, H. Rodríguez, A. Soto, Green Chem 9 (2007)247

[122] A. B. Pereiro, E. Tojo, A. Rodríguez, J. Canosa, J. Tojo, Green Chem. 8 (2006) 307

[123] J.Q. Zhu, J. Chen, C. Y. Li, W. Y. Fei, Fluid Phase Equilib. 247 (2006)102

[124] A. Arce, M. J. Earle, H. Rodríguez, K. R. Seddon, Green Chem. 9 (2007) 70

[125] J. L. Anthony, Z. Gu, L. A.Blanchard, E. J. Maginn, J. F. Brennecke, ACS Meeting 2001

[126] D. J. Tempel, P. B. Henderson, J. R. Brzozowski, R. M. Pearlstein, J. J. Hart, D. Tavianini, 1st International Congress on Ionic Liquids (COIL) Book of Abstracts, DECHEMA e. V., Salzburg (2005)p.35

[127] N. J. Bridges, K. E. Gutowski, R. D. Rogers, Green Chem. 9 (2007) 177

[128] H. Rodríguez, M. Francisco, M. Tahman, N. Sun, R. D. Rogers, Phys. Chem. Chem. Phys., 11(2009) 10916

[129] J. L. Anderson, J. Ding, T. Welton, D. W. Amstrong, J. Am. Chem. Soc., 124 (2002) 14247

[130] A. Berthod, M. J. Ruiz-Angel, S. Carda-Broch, J. Chromatogr.A 1184 (2008) 6

[131] H. Zhao, S. Xia, P. Ma, J.Chem. Technol. Biotechnol. 80 (2005) 1089-

[132]M. Freemantle, "Ionic liquids show promise for clean separation technology", Chem. Eng. News, 76 (34) (1998)

[133] A. Arce, M. J. Earle, H. Rodríguez, K. R. Seddon, A. Soto, Green Chem. 11 (2009) 365

[134] A. Arce, M. J. Earle, H. Rodriguez, K. R. Seddon, A. Soto, Green Chem. 10 (2008) 1294-

[135] A. Arce, M. J. Earle, S. P. Katdare, H. Rodríguez, K. Seddon, Phys. Chem. Chem. Phys., 10 (2008) 2538

[136] A. Arce, M. J. Earle, H. Rodríguez, K. R. Seddon, J. Phys. Chem. B, 111(2007)4732

[137] A. Arce, A. Pobudkowska, O. Rodríguez, A. Soto, Chem. Eng. J. 133 (2007) 213

[138] A. Arce, O. Rodríguez, A. Soto, Chem. Eng. Sci., 61 (2006) 6929

[139] A. Arce, H. Rodríguez, A. Soto, Fluid Phase Equilib. 242 (2006) 164

[140] A. Arce, A. Marchiaro, O. Rodríguez, A. Soto, AIChE J. 52 (2006) 2089

[141] A. Arce, M. J. Earle, S. P. Katdare, H. Rodríguez, K. R. Seddon, Chem. Commun. (2006)2548

[142] A. Arce, H. Rodríguez, A. Soto, Chem.l. Eng. J., 115 (2006) 219

[143]A. Arce, A. Marchiaro, J. M. Martinez-Ageitos, A. Soto, Can. J. Chem. Eng. 83 (2005) 366

[144] A. Soto, A. Arce, M. K. Khoshkbarchi, Sep. Purif. Technol., 44 (2005) 242.

[145] A. Arce, O. Rodriguez, A. Soto, J. Chem. Eng. Data 49 (2004), 514.

[146] A. Arce, O. Rodriguez, A.Soto, Fluid Phase Equilib., 224 (2004) 185.

[147] Pereiro, A. B, Rodríguez, A., Ind. Eng. Chem. Res., 48 (2009) 1579

[148] E. J. González, N. Calvar, E. Gómez, A. Domínguez, J. Chem Thermodyn., 42 (2010) 104.

[149] U. Domańska, A. Rekawek, J. Solution Chem., 38 (2009) 739

[150] L. A. Blanchard, D. Hancu, E. J. Beckman, J. F. Brennecke, Nature 399 (1999)28

[151] A. M. Scurto, S. N. V. Aki, J. F. Brennecke, J. Am. Chem. Soc. 124 (2002) 10276

[152] L. A. Blanchard, J. F. Brennecke, Ind. Eng. Chem. Res. 40 (2001) 287

[153] L. A. Blanchard, Z. Gu, J. F. Brennecke, J. Phys. Chem. B. 105 (2001) 2437

[154] J. L. Anthony, E. J. Maggin, J. F. Brennecke, J. Phys. Chem. B. 106 (2002) 7315

[155] S. N. V. K. Aki, A. M Scurto, J. F. Brennecke, Ind. Eng. Chem. Res. 45 (2006) 5574

[156] K. E. Gutowski, G. A. Broker, H. D. Willauer, J. G. Huddleston, R. P. Swatloski, J. D. Holbrey, R. D. Rogers, J. Am. Chem. Soc. 125 (2003)6632

[157] S. Han, H. T. Wong, A. G. Livingston, Chem. Eng. Res. Des.83 (2005) 309

[158] A. Bösmann, L. Datsevich, A. Jess, A. Lauter, C. Schimthz, P. Wassercheid, Chem. Commun. (2001) 2494

[159] Phillips, Energy Fuels, 22 (2008) 1774

[160] L. Shyu, Z. Zhang, Q. Zhang, International PCT Publication, WO 01/40150 A1,2001

[161] S. Zhang, Q. Zhang, Green Chem., 4 (2002) 376

[162] S. Zhang, Q. Zhang, Z. C. Zhang, Ind. Eng. Chem. Res. 43 (2004) 614

[163] C. Xuemei, H. Yufeng, L. Jiguang, L. Qianqing, L. Yansheng, Z. Xianming, P. Xiaoming, Y. Wenjia, Chin. J. Chem. Eng., 16 (2008) 881

[164] L. Alonso, A. Arce, M. Francisco, O. Rodríguez, A. Soto, J. Chem. Eng. Data, 52 (2007) 1729

[165] L. Alonso, A. Arce, M. Francisco, A. Soto, J. Chem. Thermodyn. 40 (2008) 966

[166] L. Alonso, A. Arce, M. Francisco, O. Rodríguez, A. Soto, AIChE J. 53 (2007) 3108

[167] J. Zhou, J. Mao, S. Zhang, Fuel Process. Technol. 89 (2008) 1456

[168] R. P. Swatloski, J. D. Holbrey, R. D. Rogers, Green Chem. 5 (2003) 361

[169] J. Eβer, P. Wasserscheid, A. Jess, Green Chem. 6 (2004) 316

[170] Y. Mochizuki, K. Sugawara, Energy Fuels 22 (2008) 3303

[171] L. Alonso, A. Arce, M. Francisco, A. Soto, Fluid Phase Equilib. 270 (2008) 97

[172] L. Alonso, A. Arce, M. Francisco, A. Soto, J. Solution Chem 37 (2008) 1355

[173] L. Alonso, A. Arce, M. Francisco, A. Soto, J. Chem. Eng. Data 52 (2007) 2409

[174] L. Alonso, A. Arce, M. Francisco, A. Soto, J. Chem. Eng. Data 53 (2008) 1750

[175] L. Alonso, A. Arce, M. Francisco, A. Soto, Fluid Phase Equilib. 263 (2008) 176

[176] C. C. Cassol, A. P. Umpierre, G. Ebeling, B. Ferrera, S. S. X. Chiaro, J. Dupont, Int. J. Mol. Sci. 8 (2007)593

[177] C. Huang, B. Chen, J. Zhang, Z. Liu, Y. Li, Energy Fuels 18 (2004) 1862

[178] J. Feng, C. X. Li, H. Meng, Z. H. Wang , Petrochem. Technol. 35 (2006) 272

[179] Y. Nie, C. Li, A. Sun, H. Meng, Z. Wang, Energy Fuesl 20 (2006) 2083

[180] Y. Nie, C. Li, Z. H. Wang, Ind. Chem. Res. 46 (2007) 5108

[181] X. Jiang, Y. Nie, C. Li, Z. Wang, Fuel 87 (2008) 79

[182] Y. Nie, H. Meng, Z. Wang, Fuel Process. Technol. 89 (2008) 978

[183] J. D. Holbrey, I. López-Martin, G. Rothenberg, K. R. Seddon, G. Silveiro, X. Zheng, Green Chem. 10 (2008)87

[184] H. Gao, M. Luo, J. Xing, Y. Wu, Y. Li, W. Li, Q. Liu, H. Liu, Ind. Eng. Chem. Res. 47(2008) 8384

[185] H. Gao, Y. Li, Y. Wu, M. Luo, Q. Li, J. Xing, H. Liu, Energy Fuels 23 (2009) 2690

[186] U. Domanska, M. Krolikowski, K. Slesinska, J. Chem. Thermodynamics 41 (2009) 1303

[187] A. A. P. Kumar, T. Banerjee, Fluid Phase Equilib. 278 (2009) 1

[188] Y. Shiraishi, K. Tachibana, T. Hirai, I. Komasawa, Ind. Eng. Chem. Res. 41 (2002) 4362

[189] L. Lu, S. Cheng, J. Gao, G. Gao, M. He, Energy Fuesl 21 (2007) 383

[190] W-H. Lo, H-Y. Yang, G-T. Wei, Green Chem., 5 (2003) 639

[191] H. Li, L. He, J. Lu, W. Zhu, X. Jiang, Y. Wang, Y. Yan, Energy Fuels, 23 (2009) 1354

[192] H. Li, X. Jiang, W. Zhu, J. Lu, H. Shu, Y. Yan, Ind. Eng. Chem. Res. 48 (2009) 9034

[193] D. Xu, W. Zhu, H. Li, J. Zhang, F. Zou, H. Shi, Y. Yan, Energy Fuels, (2009) DOI 10.1021/ef900686q

[194] D. Zhao, Z. Sun, F. Li, R. Liu, H. Shan, Energy Fuel, 22 (2008) 3065

[195] W. Zhu, H. Li, X. Jianf, Y. Yan, J. Lu, J. Xia, Energy Fuels, 21 (2007) 2514

[196] E. Lissner, W. F. De Sousa, B. Ferrera, J. Dupont, Chem. Sus. Chem., 2 (2009) 962

[197] J. Wang, D. Zhao, K. Li, Energy Fuels, 23 (2009)3831

[198] D. Zhao, J. Wang, E. Zhou, Green Chem. 9 (2007) 1219

[199] R. Smith, Energy Fuels, 22 (2008) 1774

[200] D. Zhao, Z. Sun, F. Li, H. Shan, Journal of Fuel Chemistry and Technology 37 (2009) 194

[201] H. Li, W. Zhu, Y. Wang, J. Zhang, J. Lu, Y. Yan, Green Chem. 11 (2009) 810

[202a] C. Huang, B. Chen, J. Zhang, Z. Liu, Y. Li, Energy Fuels, 18 (2004) 1862

[202b] F. Li, R. Liu, J. Wen, D. Zhao, Z. Sun, Y. Liu, Green Chem. 11 (2009) 883

[203] R. E. Treybal, Liquid extraction, 3th edition, McGraw Hill, New York, 1980

[204] J. M. Smith, H. C. Van Ness, and M. M.Abbott, Introduction to Chemical Engineering Thermodynamics 3th edition, McGraw Hill, New York, 2005.

[205] J. M. Prausnitz, R. N. Lichtenthaler, E. Gomes de Azevedo, Molecular Thermodynamics of Fluid Phase Equilibria, 3th edition, Prentice Hall, Upper Saddle River, 1999.

[206]A. E. Bradley, C. Hardacre, J. D. Holbrey, S. Johnston, S. E. J. McMath, M. Nieuwenhuyzen, Chem. Mater. 14 (2002) 629

[207] P. Bonhôte, A.-P. Dias, N. Papageorgiou, K. Kalyanasundaram, M. Grätzel, Inorg. Chem. 35 (1996) 1168.

[208] P. Bonhôte, A.-P. Dias, M. Armand, N. Papageorgiou, K. Kalyanasundaram, M. Grätzel, Inorg. Chem. 37 (1998) 166

[209] A. Stark, M. J. Torres, K. R. Seddon, Pure Appl. Chem. 72 (2000) 2275

[210] Arce, A.; Rodil, E.; Soto, A. Solution Chem. 2006, 35, 63

[211]A. Arce, E. Rodil, A. Soto, J. Chem. Eng. Data 51 (2006) 1453

[212] J. Crosthwaite, J. Chem. Thermodyn.. 37 (2005) 559.

[213] J. A. Riddick, W. B. Bunger, T. K. Sakano, Organic Solvents. Physical properties and Methods of Purification. 4th ed., John Wiley & Sons 1986.

[214] M. Fermeglia, G. Toriano, J. Chem. Eng. Data, 44 (199) 965

[215] C. Cadena, Q. Zhao, R. Q. Snurr, E. J. Maginn, J. Phys. Chem. B, 110 (2006) 2821

[216] Y.A. Sanmamed, D. Gonzalez-Salgado, J. Troncoso, C.A. Cerdeirina, L. Romani, Fluid Phase Equilib. 252 (2007) 92.

[217] K. Przybysz, E. Drzewinska, A. Stanislawska, A. Wysocka-Robak, A. Cieniecka-Roslonkiewicz, J. Foksowicz-Flaczyk, J. Pernak, Ind. Eng. Chem. Res. 44 (2005) 4599.

[218] N. Papaiconomou, N. Yakelis, J. Salminen, R. Bergman, J.M. Prausnitz J. Chem. Eng. Data 51 (2006) 1389.

[219] E. Gómez, B. González, N. Calvar, E. Tojo, A. Domínguez, J. Chem. Eng. Data 51 (2006) 2096.

[220] H. Renon, J.M. Prausnitz, AIChE J. 14 (1968) 135.

[221] D.S. Abrams, J.M. Prausnitz, AIChE J. 21 (1975) 116.

[222] J.M. Sorensen, W. Arlt, Liquid-Liquid Equilibrium Data Collection, DECHEMA, Frankfurt 1980.

[223] J.M. Prausnitz, T.F. Anderson, E.A. Grens, C.A. Eckert, R. Hsieh, J.P. O´Connel, Prentice Hall, Englewood Cliffs, New York, 1980,.

[224] Z. Lei, J. Zang, Q. Li, B. Chen, Ind. Eng. Chem. Res. 48 (2009) 2697

[225] R. Kato, M. Krummen, J. Gmehling, Fluid Phase Equilib. 224 (2004) 47

[226] L. D. Simoni, Y. Lin, J. F. Brennecke, M.A. Stadther, Ind. Eng. Chem. Res., 47, 256

[227] S. M. Walas, Phase Equilibria in Chemical Engineering. Butleworth Publishers, Boston 1985

[228] R. E. Treybal, Mass Transfer Operations, 3th Edition, McGraw Hill Book Company, Singapore, 1981

[229] D. M. T. Newsham, Liquid-liquid Equilibria, Ed. J. D. Thorton, Science and Practice of Liquid-Liquid Extraction, Clarendon Press, 1992, 1

[230] J. M. Sϕrensen, Doctoral Thesis, Correlation of liquid-liquid equilibrium data, Danmarks Tekniske Hϕjskole, Lingby (Denmark), 1980

[231] Kirk-Othmer, Encyclopedia of Separation Technology, -Wiley Interscience Publications, USA

[232] R. H. Perry, D. W. Green,Maloey JO Editors, Manual del Ingeniero Químico, 4th ed. McGraw-Hill/Interamericana de España, S.A. U., 2001

[233] J. D. Seader, E. J. Henley, Liquid-Liquid Extraction with Ternary Systems, Thomas Kulesa, ed. Separation Process Principles, 2nd ed. John Wiley &Sons, Inc. 2006, 295

[234] G. Kolasinska, Fluid Phase Equilib., 27 (1956) 289

[235] G. H. Georgeton, R. L. Smith, A. S. Teja, Application of cubic equations of state to polar fluids and fluid mixtures. Eds. K. C. Chao and J. Robinson. Equations of State.: Theories and Applications, 1986, p.434

[236] J. Huang, Fluid Phase Equilib., 101 (1994) 27

[237] F. C. Verotti, Fluid Phase Equilib., 116 (1996) 503

[238] J. Simonetty, D. Yee, D. Tassios, Industrial & Engineering Chemistry Process Design and Development, 21 (1982) 174

[239] F. García-Sánchez, Fluid Phase Equilib., 121 (1996) 207

[240] J. A. Mollerup, Fluid Phase Equilib. 7 (1981) 121

[241] G. Wilson, J. Am. Chem. Soc., 86 (1964)127

[242] R. Scott, The Journal of Chemical Physics, 25 (1956)193

[243] H. Renon, J. M. Prausnitz, Industrial & Engineering Chemistry Process Design and Development, 8 (1969) 413

[244] H. Renon, AIChE J., 15 (1969) 785

[245] J. M. Marina, D. P. Tassios, Industrial & Engineering Chemistry Process Design and Development, 12 (1973) 271

[246] R. Heidemann, Chem. Eng. Sci., 28 (1973)1213

[247] F. Van Zandijcke, Journal of applied chemistry biotechnology, 24 (1974)709

[248] R. de Fre, Journal of applied chemistry biotechnology, 27 (1977) 667

[249] H. Sugi, J. Chem. Eng. Jpn., 11 (1978) 167

[250] J. L. Cruz, H. Renon, AIChE J., 24 (1978)817

[251] H. Renon, Fluid Phase Equilib., 30 (1986) 181

[252] C. C. Chen, L. B. Evans, AIChE J., 32 (1986) 444

[253] P. Gierycz, Thermochim. Acta 116 (1987), 267.

[254] M. Connemann, Fluid Phase Equilib., 60 (1990) 99

[255] Y. Demirel,. Fluid Phase Equilib. 86 (1993) 1.

[256] I. Nagata, J. Nakajima, Fluid Phase Equilib. 70 (1991) 275

[257] Y-T. Wu, Z-Q.Zhu,, D-Q. Lin, L-H. Mei, Fluid Phase Equilib., 121 (1996) 125.

[258] E. A. Guggenheim, Mixtures. The theory of the Equilibrium Properties of Some Simple Classes of Mixtures, Solutions and Alloys, Clarendon Press, Oxford, 1952.

[259] A. Bondi, J. Phys. Chem. 68 (1964)441

[260] A. Bondi, Physical Properties of Molecular Crystals, Liquids, and Glasses, John Wiley & Sons, New York, 1968

[261] M. S. Selvan, M. D. McKinley, R. H. Dubois, J. L. Atwood, J. Chem. Eng. Data, 45 (2000) 841

[262] T. M. Letcher, N. Deenadayalu, J. Chem.Thermodyn. 35(2003) 67

[263] A. Arce, O. Rodríguez, A. Soto, J. Chem. Eng. Data, 49 (2004)514

[264] A. Arce, O. Rodríguez, A. Soto, Ind. Eng. Chem. Res.43 (8323)

[265] T. M. Letcher, P. Reddy, Fluid Phase Equilib. 219 (2004) 107

[266] T. M. Letcher, P. Reddy, J. Chem. Thermodyn, 37 (2005) 415

[267] A. Arce, A. Marchiaro, O. Rodríguez, A. Soto, AIChE J., 52 (2006) 2089

[268] G. W. Meindersma, A. Podt, A. B. de Haan, J. Chem. Eng. Data, 51 (20 6) 1814

[269] A. B. Pereiro, E. Tojo, A. Rodríguez, J. Canosa, J. Tojo, Green Chem., 8 (2006)307

[270] T. Barerjee, M. K. Singh, R. K. Sahoo, A. Khanna, Fluid Phase Equilib., 234 (2005) 64

[271] R. Kato, M. Krummen, J. Gmehling, Fluid Phase Equilib. 224 (2004) 47

[272] R. Kato, J. Gmehling, Fluid Phase Equilib., 231 (2005) 38

[273] U. Domanska, Pure Appl. Chem. 77 (2005) 543

[274] R. S. Santiago, G. R. Santos, M. Aznar, Fluid Phase Equilib., 278 (2009) 54

[275] A. B. Pereiro, A. Rodríguez, J. Chem. Thermodyn., 40 (2008) 1282.

[276] P. J. Bayles, C. Hanson, M. A. Hughes, Chem. Eng., 83 (1976) 86

[277] T. C. Lo, M. H. I. Baird, C. Hanson, , Eds., Handbook of Solvent Extraction, Willey-Interscience, New York, (1983)

[278] M. R. Fenske, C. S. Carlson, D. Quiggle, Ind. Eng. Chem., 39 (1947) 1932

[279] E. G. Scheibel, AIChE J., 2 (1956) 74

[280] E. G. Scheibel, A. E. Karr, Ind. Eng. Chem., 42 (1950) 1048

[281] A. E. Karr, E. G. Scheibel, Chem. Eng. Prog. Symp. Ser. 50 (1954) 73

[282] C. P. Strand, R. B. Olney, G. H. Ackerman, AIChE J., 8 (1962) 252

[283] A. E. Karr, AIChE J., 5 (1959) 446

[284] J. Y. Oldshue, J. H. Rushton, Chem. Eng. Progr. 48 (1952) 297

[285] J. Y. Oldshue, F. Hodgkinson, J. C. Pharamond, Proc. Int. Solv. Extr. Conf., 2 (1974) 1651

[286] A. Fischer, Verfahrenstechnik, 5 (1971) 360

APENDIX A: ^{1}H NMR and ^{13}C NMR of ILs

APENDIX A: ^{1}HNMR and ^{13}C NMR Spectra of the ionic liquids

1-Methyl-3-octylimidazolium bis{(trifluoromethyl)sulfonyl}amide: ([C_8mim][NTf_2])

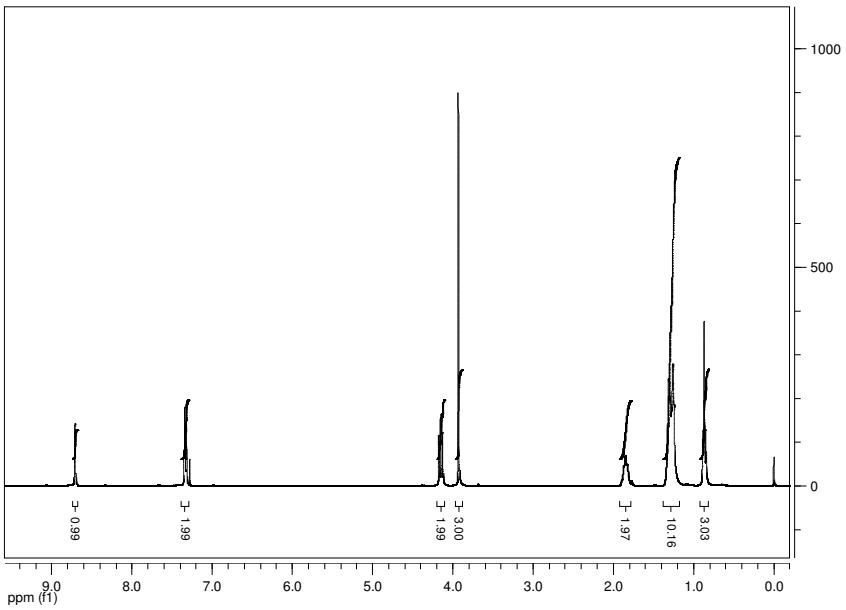

^{1}H NMR, δ_H ($CDCl_3$, 300 MHz): 0.87 (t, J = 6.7 Hz, 3H, CH_2CH_3), 1.18-1.39 (m, unresolved, 10H, $NCH_2CH_2(CH_2)_5CH_3$), 1.79-1.93 (m, unresolved, 2H, NCH_2CH_2), 3.93 (s, 3H, NCH_3), 4.15 (t, J = 7.5 Hz, 2H, NCH_2), 7.29-7.37 (m, unresolved, 2H, C(4)H and C(5)H), 8.71 (s, 1H, C(2)H).

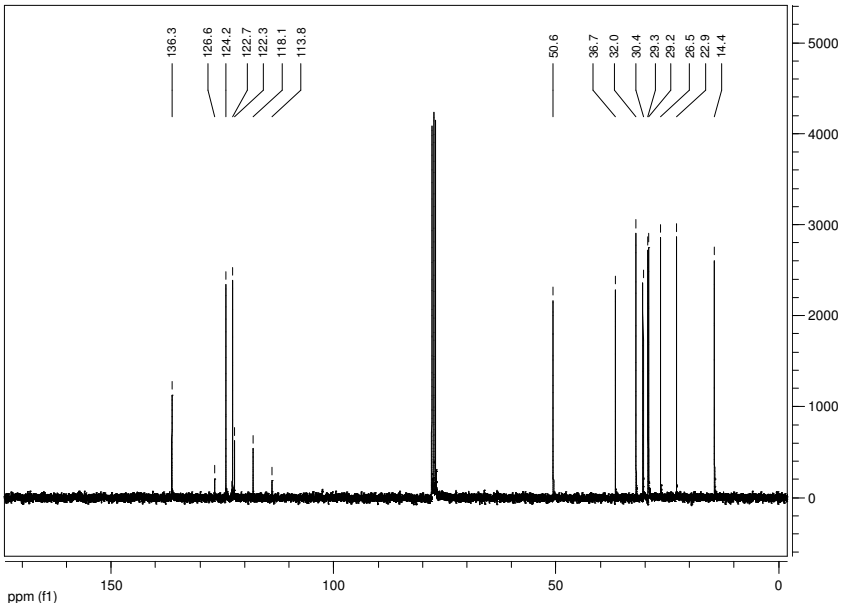

^{13}C NMR, δ_C ($CDCl_3$, 75.4 MHz): 14.4 ($N(CH_2)_7CH_3$), 22.9 ($N(CH_2)_6CH_2$), 26.5 ($N(CH_2)_5CH_2$), 29.2 ($N(CH_2)_4CH_2$), 29.3 ($N(CH_2)_3CH_2$), 30.4 ($N(CH_2)_2CH_2$), 32.0 (NCH_2CH_2), 36.7 (NCH_3), 50.6 (NCH_2), 120.2 (q, $J_{C\text{-}F}$ = 321 Hz, 2 × CF_3), 122.7 (C(5)H), 124.2 (C(4)H), 136.3 (C(2)H).

1-Methyl-3-octylimidazolium tetrafluoborate: ([C_8mim][BF_4])

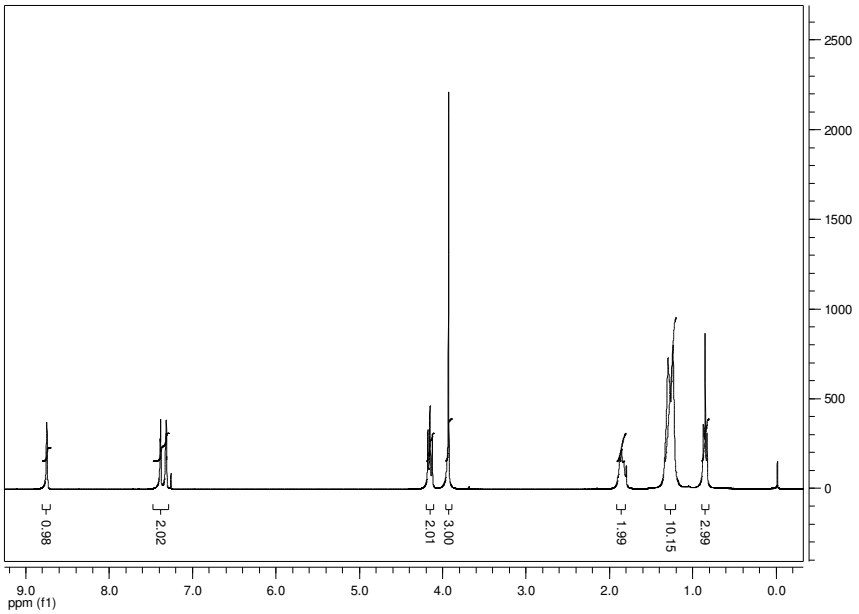

^{1}H NMR, δ_H ($CDCl_3$, 300 MHz): 0.87 (t, J = 6.7 Hz, 3H, $CH_2C\underline{H_3}$), 1.18-1.39 (m, unresolved, 10H, $NCH_2CH_2(C\underline{H_2})_5CH_3$), 1.79-1.93 (m, unresolved, 2H, $NCH_2C\underline{H_2}$), 3.93 (s, 3H, NCH_3), 4.15 (t, J = 7.5 Hz, 2H, NCH_2), 7.29-7.37 (m, unresolved, 2H, C(4)H and C(5)H), 8.71 (s, 1H, C(2)H).

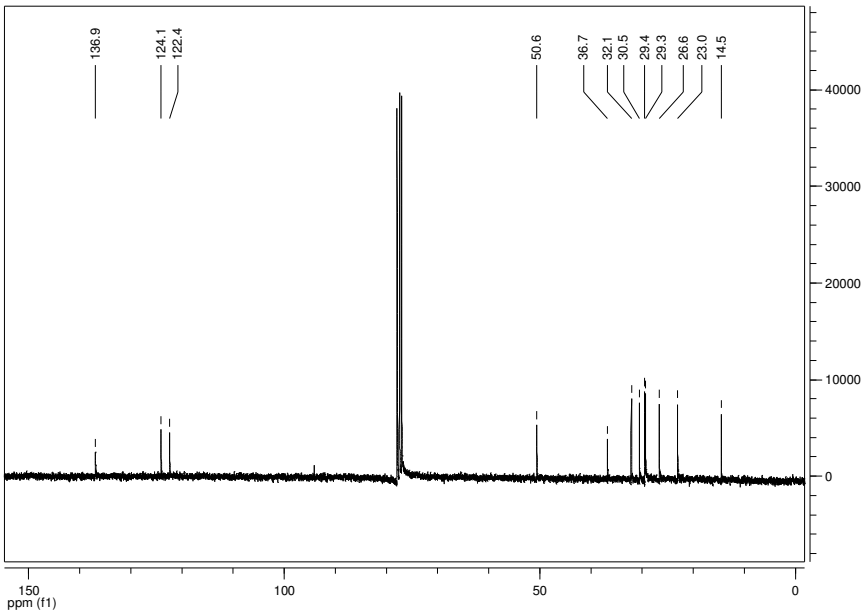

^{13}C NMR, δ_C ($CDCl_3$, 75.4 MHz): 14.5 ($N(CH_2)_7\underline{C}H_3$), 23.0 ($N(CH_2)_6\underline{C}H_2$), 26.6 ($N(CH_2)_5\underline{C}H_2$), 29.3 ($N(CH_2)_4\underline{C}H_2$), 29.4 ($N(CH_2)_3\underline{C}H_2$), 30.5 ($N(CH_2)_2\underline{C}H_2$), 32.1 ($NCH_2\underline{C}H_2$), 36.7 ($NCH_3$), 50.6 ($NCH_2$), 122.4 (C(5)H), 124.1 (C(4)H), 136.9 (C(2)H).

1-Ethyl-3-methylimidazolium ethylsulfate ([C_2mim][$EtSO_4$])

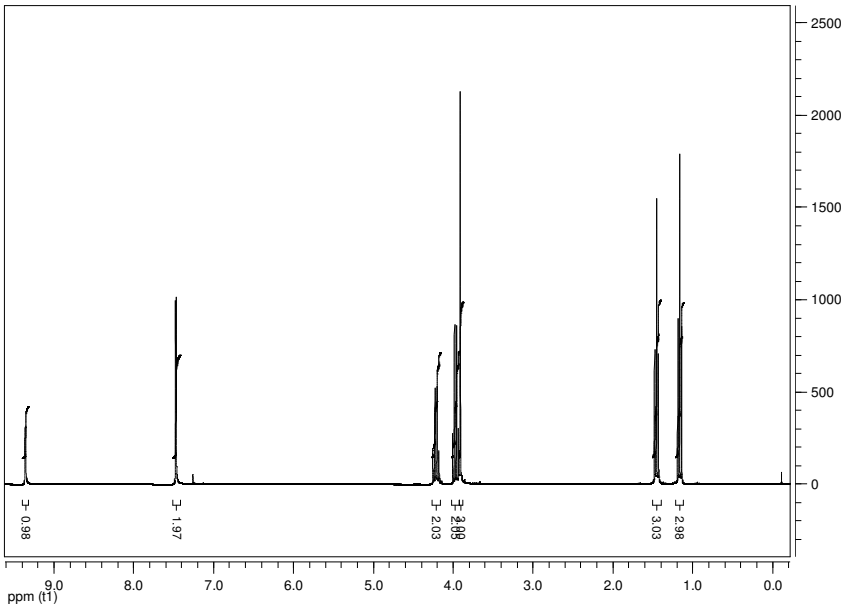

^{1}H NMR, δ_H ($CDCl_3$, 300 MHz): 1.16 (t, J = 7.1 Hz, 3H, $OCH_2C\underline{H_3}$), 1.45 (t, J = 7.4 Hz, 3H, $NCH_2C\underline{H_3}$), 3.91 (s, 3H, NCH_3), 3.97 (q, J = 7.1 Hz, 2H, OCH_2), 4.22 (q, J = 7.3 Hz, 2H, NCH_2), 7.47 (dd, J = 1.6 Hz, 2H, C(5)H and C(4)H), 9.36 (1H, s, C(2)H).

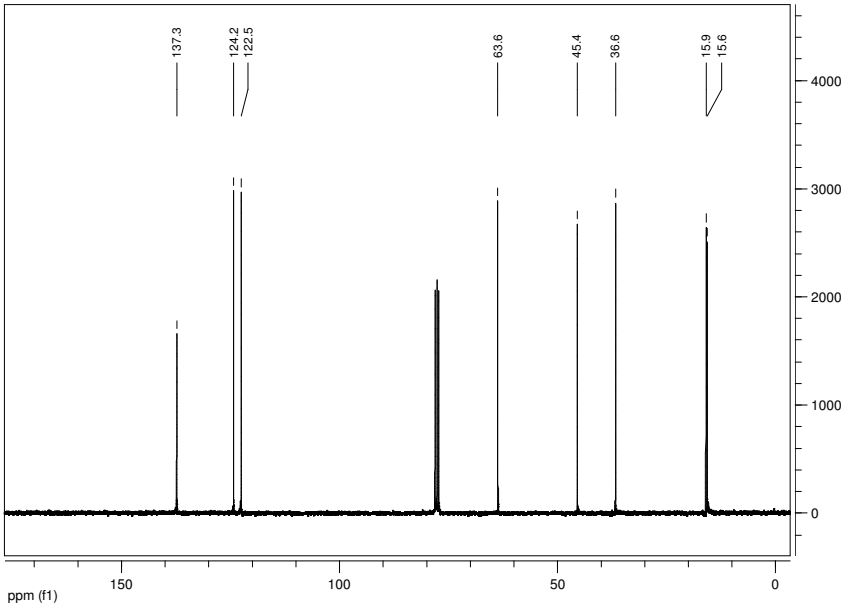

^{13}C NMR, δ_C ($CDCl_3$, 75.4 MHz): 15.6, 15.9 ($OCH_2\underline{C}H_3$, $NCH_2\underline{C}H_3$), 36.6 (OCH_2), 45.4 (NCH_3), 63.6 (NCH_2), 122.5 (C(4)H), 124.2 (C(5)H), 137.3 (C(2)H).

1-Hexyl-3,5-dimethylpyridinium bis{(trifluoromethyl)sulfonyl}amide: ([C_6mmPy][NTf_2])

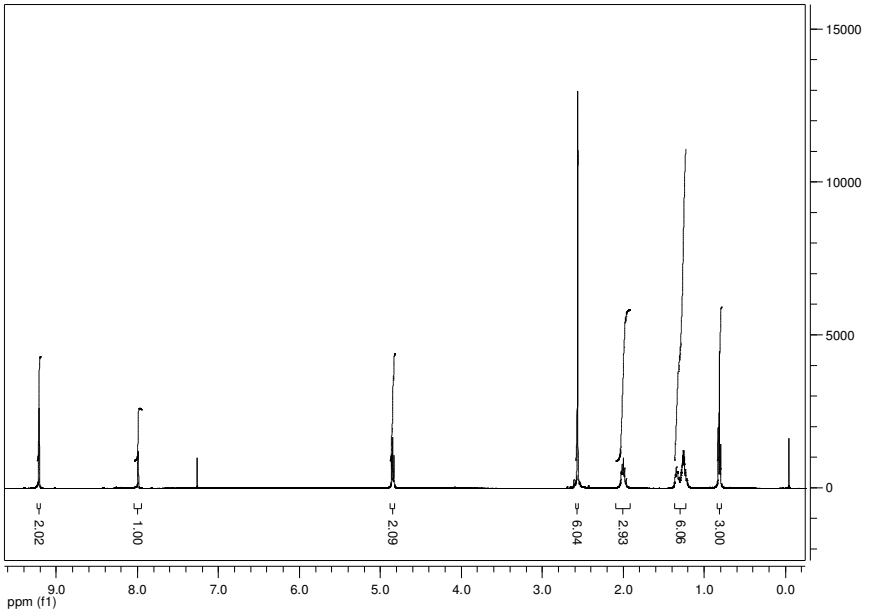

^{1}H NMR, δ_H ($CDCl_3$, 300 MHz): 0.81 (t, J = 7.1 Hz, 3H, $CH_2C\underline{H_3}$), 1.25-1.27 (m, unresolved, 6H, $NCH_2CH_2(C\underline{H_2})_3CH_3$), 2.01 (m, unresolved, 2H, $NCH_2C\underline{H_2}$), 2.56 (s, 6H, 2x$NC\underline{H_3}$), 4.85 (t, J = 7.5 Hz, 2H, $NC\underline{H_2}$), 7.99 (s, 2H, $NC\underline{H_2}$), 9.21 (s, 2H, 2x$NC\underline{H}$).

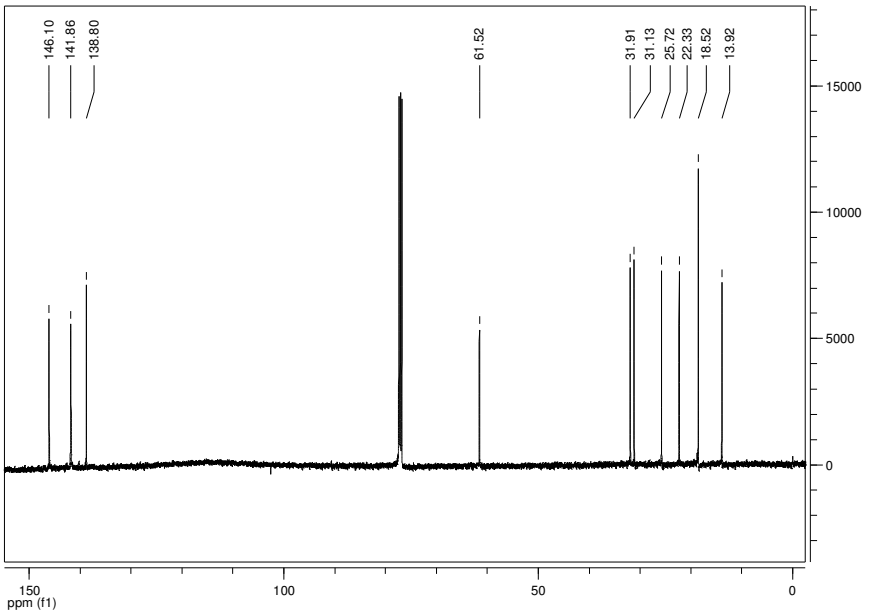

^{13}C NMR, δ_C ($CDCl_3$, 75.4 MHz): 13.9 ($N(CH_2)_5\underline{C}H_3$), 18.5 ($N(CH_2)_3\underline{C}H_2$), 22.3 ($N(CH_2)_2\underline{C}H_2CH_3$), 25.7 ($N(CH_2)\ \underline{C}H_2\ CH_2CH_3$), 31.1 ($CH\underline{C}H_3$), 31.9 ($CH\underline{C}H_3$), 61.5 ($NCH_3$), 36.7 ($NCH_2\ \underline{C}H_2$), 61.5 ($N\underline{C}H_3$), 138.8 (C(5)H), 141.9 (C(4)H), 146.1 (C(2)H).

APENDIX B: RESUMEN(SUMMARY)

RESUMEN (Summary, in Spanish)

La presente tesis estudia la viabilidad de llevar a cabo la desulfuración y desnitrogenación de combustibles (gasolina y gasoil) mediante extracción empleando líquidos iónicos como disolventes.

Contexto

Este estudio surge de la necesidad de buscar nuevas tecnologías alternativas a la Hidrodesulfuración (HDS) en las refinerías, que permitan alcanzar los bajos niveles de azufre en combustibles exigidos por las nuevas especificaciones ambientales establecidas por la Unión Europea. Se pretende evitar los elevadísimos costes y drásticas condiciones de operación que supondría el proceso de hidrotratamiento para alcanzar ese mínimo contenido en compuestos azufrados.

Una posible alternativa a estudiar consiste en la extracción desulfurativa (EDS), que no es más que una extracción líquido-líquido, una operación de transferencia de materia en la cual una disolución líquida (alimentación) se pone en contacto con un segundo líquido inmiscible o parcialmente miscible (disolvente) que permita extraer de forma selectiva uno o varios componentes de la mezcla (solutos). El reto principal que plantea esta operación básica radica en encontrar el disolvente adecuado para llevarla a cabo, siendo imprescindible que provoque la formación de dos fases líquidas inmiscibles de densidades lo más diferentes posibles para que facilite su posterior separación. En su elección deben tenerse en cuenta factores como la solubilidad y la selectividad (debe disolver preferentemente el componente a extraer), debe ser fácilmente recuperable, no corrosivo, no tóxico, no contaminante, económico…

Líquidos Iónicos

El uso de los líquidos iónicos como potenciales agentes separadores se plantea debido a sus prometedoras cualidades como disolventes, entre las que se destaca el hecho de que son sales líquidas a temperatura ambiente (y en un amplio rango de temperaturas), su estabilidad química y térmica y su baja presión de vapor (despreciable volatilidad) que a su vez implica una fácil recuperación del disolvente y que sean compuestos respetuosos con el Medioambiente. Por todo ello y por sus atractivas y peculiares características, como la posibilidad de que sus propiedades se

puedan "diseñar" prácticamente a medida mediante una correcta selección del anión y el catión para una determinada aplicación, estos compuestos se han ido convirtiendo en poderosas alternativas a gran cantidad de disolventes orgánicos tradicionales siendo cada vez más ampliamente utilizados en múltiples procesos industriales.

Selección de los líquidos iónicos

El primer objetivo planteado en este trabajo consiste en la selección de los líquidos iónicos a considerar como posibles agentes desulfuradores. Para ello, y como primera aproximación, se llevan a cabo una serie de ensayos de solubilidades por punto de niebla con el fin de evaluar cuáles son los líquidos iónicos en principio más prometedores para este cometido. Se procura una alta solubilidad del componente azufrado (tiofeno) en el mismo, con alta insolubilidad del resto de los compuestos constituyentes del fuel. La dificultad de este cometido radica precisamente en que estos líquidos iónicos actúan en la mayoría de los casos como buenos disolventes tanto de sustancias orgánicas como inorgánicas, polares o apolares.

Los líquidos iónicos finalmente seleccionados son tres con catión comun imidazolio: 1-octyl-3-methyl imidazolium tetrafluoborate ($[C_8mim][BF_4]$), 1-octyl-3-methyl imidazolium bis{(trifluoromethyl sulfonyl)imide} ($[C_8mim][NTf_2]$) y 1-ethyl-3-methyl imidazolium ethylsulfate ($[C_2mim][EtSO_4]$). Posteriormente, un cuarto líquido iónico con catión piridinio, 1-hexyl-3,5-dimethyl pyridinium bis(trifluoromethyl sulfonyl)imide ($[C_6mmPy][NTf_2]$) se selecciona en base a las publicaciones más recientes y a las estimaciones con COSMO-RS.

Equilibrio Líquido-líquido

Para una correcta evaluación de un disolvente como agente extractor es necesario recurrir al estudio de los equilibrios implicados en el proceso. Para ello se han determinado experimentalmente las rectas de reparto para los sitemas ternarios constituidos por cada uno de los componentes del combustible, el compuesto azufrado o nitrogenado y el líquido iónico empleado como disolvente.

Se han elegido como componentes representativos típicos de la gasolina el hexano, heptano, isooctano, tolueno, piridina y tiofeno. Como componentes del diesel, el hexadecano, dodecano, heptano, tolueno, tiofeno, piridina y dibenzotiofeno.

El hecho de incluir la piridina entre los compuestos que forman parte del combustible permite determinar el efecto del agente extractor sobre los derivados de nitrógeno. El interés de este estudio radica en que el proceso de hidrotratamiento que se lleva a cabo en la actualidad conlleva además de la desulfuración la eliminación de los componentes orgánicos nitrogenados, considerados agentes potencialmente contaminantes en las emisiones atmosféricas, que juntamente con los derivados de azufre contribuyen a la problemática ambiental de la acidificación. Se analiza además el comportamiento de los compuestos aromáticos, representados por el tolueno. No es inconveniente cierto grado de desaromatización pero deben tenerse en cuenta las especificaciones exigidas para los combustibles a este respecto ya que obligarán necesariamente a adoptar una solución de compromiso que permita satisfacer el nivel mínimo de aromáticos que éstos deben contener. En todo caso la desaromatización no representaría un problema ya que un adecuado blending posterior podría incorporar estos componentes de forma más precisa.

La determinación de los equilibrios entre los componentes seleccionados implica el desarrollo de un método experimental que permita la determinación de las composiciones de equilibrio. Para la obtención de estos datos se introducen las mezclas de los tres constituyentes del sistema ternario en celdas de vidrio encamisadas y termostatizadas para garantizar una temperatura constante de 298.5 K y correctamente aisladas para impedir la captación de humedad del ambiente. Se requiere una agitación vigorosa para una completa mezcla entre los componentes y un tiempo de agitación determinado experimentalmente para cada sistema ternario concreto con el fin de garantizar que se alcance el estado de equilibrio. Una vez que se garantiza una composición estable, se deja decantar el sistema para una correcta separación de las fases y se lleva a cabo la toma de muestra de cada fase para proceder a la determinación de la composición de cada una de ellas. Dada la despreciable presión de vapor que presentan estos compuestos es posible recuperarlos con la pureza requerida mediante evaporación de los demás componentes presentes en la mezcla.

El análisis cuantitativo se lleva a cabo mediante cromatografía de gases empleando el método del patrón interno, siendo la composición del líquido iónico (no volátil) calculada por diferencia. En base a los datos de equilibrio se puede determinar la distribución del soluto (compuesto que se desea extraer) entre las dos fases, la rica en disolvente (extracto) y la rica en inerte (refinado). Así, mediante la determinación de dos parámetros: relación de distribución de

soluto en ambas fases (β) y selectividad (S) se analiza la viabilidad del empleo del disolvente elegido como agente extractor.

Los diagramas de fases para los sistemas ternarios que contienen tiofeno muestran una gran región de inmiscibilidad. Se encuadran dentro de los diagramas triangulares de tipo II con una única región inmiscible y dos pares parcialmente solubles para los dos líquidos iónicos. Destaca la despreciable solubilidad del líquido iónico en los hidrocarburos, que evita posibles efectos de contaminación del refinado por parte del disolvente en el proceso de extracción. La elevada solubilidad del tiofeno en el disolvente implica la viabilidad de la extracción del compuesto azufrado de la mezcla hidrocarbonada mediante extracción si se emplea la cantidad suficiente de líquido iónico en el proceso. Para todos los sistemas ternarios que contienen tiofeno, se puede observar cómo para los hidrocarburos de bajo peso molecular, se puede apreciar un fenómeno de solutropía reflejado en valores positivos de las pendientes de reparto para bajas concentraciones de soluto, que se van haciendo más negativos a medida que ésta se incrementa. Este comportamiento se puede observar también en los valores de coeficiente de distribución, β, que pasan de ser mayores o iguales a la unidad a ser inferiores a 1. Para hidrocarburos de mayor peso molecular (caso del *n*-dodecano con los líquidos iónicos $[C_8mim][BF_4]$ y $[C_2mim][EtSO_4]$ y en el caso del *n*-hexadecano con $[C_8mim][BF_4]$, $[C_8mim]$ $[NTf_2]$ y $[C_2mim][EtSO_4]$) las pendientes se hacen negativas en la totalidad del diagrama ternario. Se observa, pues, para los hidrocarburos lineales que a mayor longitud de cadena hidrocarbonada, son menores los valores obtenidos para β. De más a menos favorables valores de β los líquidos iónicos estudiados seguirían la tendencia: $[C_6mmPy]$ $[NTf_2]$ > $[C_8mim]$ $[NTf_2]$ >$[C_8mim]$ $[BF_4]$ > $[C_2mim]$ $[EtSO_4]$. Desde el punto de vista práctico, valores más bajos de β implican una mayor cantidad de disolvente requerida para el proceso de extracción. En cuanto a la selectividad, la tendencia de S se muestra como: $[C_2mim]$ $[EtSO_4]$ >> $[C_8mim][BF_4]$ ~ $[C_6mmPy]$ $[NTf_2]$ > $[C_8mim]$ $[NTf_2]$. La diferencia más significativa ha sido encontrada para el líquido iónico $[C_2mim][EtSO_4]$ debido a la *quasi*-total inmiscibilidad de los hidrocarburos en este líquido iónico. Cuanto mayor sea la selectividad, menor número de etapas de equilibrio se requiere para un proceso de extracción dado.

Para hidrocarburos no lineales, representados por el *i*-octano todos los sistemas ternarios estudiados presentan comportamiento solutrópico. Para los cuatro líquidos ióncios, los valores del coeficiente de distriución β siguen la tendencia $[C_8mim][NTf_2]$ > $[C_6mmPy][NTf_2]$ ~ $[C_8mim]$ $[BF_4]$ > $[C_2mim]$ $[EtSO_4]$. En cuanto a la selectividad, S, presenta valores mucho mayors que la unidad para todos los líquidos iónicos, destacando nuevamente los altos valores encontrados para el $[C_2mim]$ $[EtSO_4]$.

Así como para el resto de los hidrocarburos se han encontrado valores relativamente bajos de solubilidad en todos los líquidos iónicos, no sucede así en el caso de los sistemas con tolueno, encontrándose valores relativamente altos de solubilidad de este compuesto en los líquidos iónicos. Los valores de los coeficientes de distribución para todos los líquidos iónicos se muestran bajos. Debido a la alta solubilidad del tolueno en los líquidos iónicos estudiados, la selectividad muestra valores próximos a la unidad, excepto para el caso del $[C_2mim]$ $[EtSO_4]$ que presenta siempre valores muy elevados para este parámetro. Esto implica que un cierto grado de extracción de los compuestos aromáticos tendrá lugar de forma simultánea a la desulfuración. Estos resultados implican que desde un punto de vista práctico deba ser adoptada una solución de compromiso entre el grado de desulfuración y el de desaromatización con el fin de cumplir la legislación vigente en términos de índice de octano para combustibles.

En el caso de los sistemas ternarios que contienen piridina, la región de inmiscibilidad se ve altamente reducida. Para todos los líquidos iónicos estudiados, los valores de β y S son claramente superiores a la unidad, lo que implica una predecible facilidad de extracción de los compuestos nitrogenados por parte de estos líquidos iónicos.

Una vez obtenidos los datos experimentales se procede además al tratamiento termodinámico de los mismos. Se lleva a cabo la correlación en base a los modelos NRTL y UNIQUAC obteniendo los parámetros binarios de interacción correspondientes con el fin de modelizar el comportamiento de las mezclas a considerar, lo que permitiría el diseño de una unidad de separación multicomponente.

En primer lugar, los datos experimentales son correlacionados sin definir un valor *a priori* para los coeficientes de reparto a dilución infinita, β_∞. Posteriormente, se fija un valor óptimo para β_∞ mediante ensayos de prueba y error con $\Delta\beta$ como criterio de optimización. Normalmente, cuando se define β_∞ el valor del residual $\Delta\beta$ disminuye considerablemente, y el residual F se ve ligeramente aumentado. La correlación optimizando el valor para β_∞ es preferible dado que el mayor interés en el ajuste de los datos de ELL se plantea para bajas concentraciones de soluto.

Se obtienen muy buenos resultados para la correlación de los sistemas que contienen hidrocarburos lineales a bajas concentraciones de soluto, pero los desvíos se hacen mayores en la parte superior del diagrama. Estos valores se ven incrementados a medida que se ve incrementado el peso molecular de hidrocarburo.

Los resultados más satisfactorios se encuentran para la correlación de los sistemas con i-octano y tolueno. Los sistemas con piridina se correlacionan adecuadamente mediante ambos modelos. En general, no se pueden establecer conclusiones sobre el mejor modelo de correlación para los datos de equilibrio líquido - líquido con sistemas que contengan líquidos iónicos. Solo en el caso de los sistemas con tolueno podemos decir que se obtienen menores desvíos mediante el modelo UNIQUAC. En general ambos modelos se consideran satisfactorios para la correlación de los datos de equilibrio líquido-líquido en sistemas con líquidos iónicos.

Desulfuración de combustibles sintéticos

En una etapa posterior se preparan dos mezclas modelo simulando gasolina y diesel con una composición en peso de 26 % hexano, 26% heptano, 26 % isooctano, 10 % tolueno, 6 % tiofeno and 6 % piridina, para una gasoline comercial, y otra mezcla multicomponente constituída en porcentajes en peso por 26% heptano, 26% dodecano, 26% hexadecano 10% tolueno, 3% thiopheno, 6% piridina and 3% dibenzotiofeno, simulando un diesel comercial. Se sigue un procedimiento experimental al que se lleva a cabo para la determinación de los datos de equilibrio líquido-líquido siendo la cromatografía de gases la técnica instrumental elegida para la medida cuantitativa de las composiciones.

Se extrae muestra de la fase refinado tras 24h de agitaión y el tiempo requerido de reposo para la separación de las fases y se procede a la determinación de composiciones mediante GC. La mezcla restante se separa mediante decantación de la fase rica en líqido iónico y es tomanda como alimentación para la siguiente etapa de etracción.

Los resultados encontrados en los experimentos de extracción llevados a cabo sobre combustibles sintéticos confirman el comportamento esperado para estos líquidos iónicos y estudiado mediante los datos de equilibrio líquido-líquido obtenidos previamente.

En el caso de la gasolina, el porcentaje de desulfuración para los cuatro líquidos iónicos estudiados sigue la tendencia: $[C_6mmpy][NTf_2]$ > $[C_8mim][BF_4]$ ≥ $[C_8mim][NTf_2]$ >$[C_2mim][EtSO_4]$. El liquid iónico $[C_6mmpy][NTf_2]$ muestra la mayor capacidad de extacción, siendo la composición de tiofeno reducida alrededor de un 86 % en peso tras tres etapas de extracción. El ranking en el caso del modelo de diesel en cuanto a rendimiento de desulfuración sigue la serie: $[C_6mmpy][NTf_2]$ > $[C_2mim][EtSO_4]$ > $[C_8mim][NTf_2]$ > $[C_8mim][BF_4]$. Al igual que en el caso de la gasolina, el $[C_6mmpy][NTf_2]$ muestra los mejores resultados de extracción para tiofeno y dibenzotiofeno, siendo el contenido en tiofeno reducido alrededor de un 88 % en peso y el de dibenzotiofeno sobre un 98 % en peso tras tres etapas de extracción.

En el caso de la gasolina sintética, la extracción de compuestos nitrogenados con los cuatro líquidos iónicos estudiados es total. La concentración de piridina se hace indetectable para todos los líquidos iónicos tras la segunda etapa de extracción, menos en el caso del $[C_2mim][EtSO_4]$ que requiere tres etapas. Para la mezcla sintética que simula el diesel, la concentración de piridina se vuelve indetectable después de una sola etapa de extracción para todos los líquidos iónicos objeto de estudio.

La desulfuración y la desnitrogenación van en cualquier caso acompañadas de un cierto grado de desaromatización, reflejado en una disminución del 68 % en peso en la concentración de tolueno en el caso de la gasolina modelo y un 61% en peso para el caso del diesel con los cuatro líquidos iónicos .El mayor grado de desulfuración se encontró asimismo para el $[C_6mmpy][NTf_2]$. El resto de los hidrocarburos constituyentes de los combustibles sintéticos incrementa su concentración tras cada etapa de extracción.

En ningún caso (para gasolina y gasoil sintéticos), la concentración de líquido iónico en el refinado es detectable.

Cabe mencionar que, como es de sobra conocido, una operación de extracción en una columna en contracorriente incrementaría notablemente la capacidad de separación obtenida en el proceso de extracción discontinuo de tres etapas.

La correlación simultánea de los sistemas ternarios implicados en la desulfuración de gasolina y diesel se lleva a cabo mediante las ecuaciones de los modelos NRTL y UNIQUAC. Aunque en cualquiera de los casos se encuentran valores relativamente altos para los residuales F y $\Delta\beta$, para la correlación conjunta, UNIQUAC parece proporcionar valores ligeramente inferiores para estos desvíos a los obtenidos mediante el modelo NRTL.

Con los parámetros de interacción obtenidos, se ha llevado a cabo la simulación de una columna de extracción real con el fin de confirmar la capacidad del líquido iónico 1-hexyl-3,5-dimethyl pyridinium bis(trifluoromethyl sulfonyl)imide ($[C_6mmpy][NTf_2]$) para alcanzar los niveles de desulfuración requeridos por la legislación vigente. Sin embargo, debido al orden de magnitud encontrado en los desvíos obtenidos para la correlación conjunta mediante los modelos estudiados, esta etapa del trabajo sólo puede ser evaluada desde un punto de vista meramente cualitativo.

Desulfuración de muestras reales

La capacidad de los líquidos iónicos [C_8mim][BF_4], [C_8mim][NTf_2], [C_2mim][$EtSO_4$] y [C_6mmPy][NTf_2] como disolventes de extracción ha sido verificada experimentalmente mediante la extracción de muestras reales de diesel y nafta ligera procedentes de corrientes de refinería previas al proceso de desulfurization.

El contenido en azufre a lo largo de las tres etapas de extracción se ha visto reducido para el caso de los cuatro líquidos iónicos, siguiendo la evolución del grado de desulfurization de la siguiente manera: [C_6mmPy][NTf_2] > [C_8mim][BF_4] ≥ [C_8mim][NTf_2] > [C_2mim][$EtSO_4$] en el caso de la nafta ligera y [C_6mmPy][NTf_2] >[C_2mim][$EtSO_4$] ≥ [C_8mim][NTf_2] > [C_8mim][BF_4] en el caso de las muestras de diesel.

Exactamente los mismos relusltados obtenidos empleando gasolinas y gasóleos sinténticos fueron encontrados al llevar a cabo los experimentos con muestras de combustibles reales, procedentes de las corrientes de refinería correspondientes a nafta ligera y diesel previas al proceso de hidrodesulfuración. Se demuestra además que en el caso de los líquidos iónicos [C_6mmPy][NTf_2] y [C_2mim][$EtSO_4$] el líquido iónico es inmiscible en la fase rica en hidrocarburos, dado que en el caso de estas sales, ambas contienen átomos de azufre en su propio anión, lo que incrementaría el contenido en azufre en las muestras.

Conclusiones Generales

Como una más de sus aplicaciones de interés práctico, en esta tesis se ha estudiado la viabilidad de llevar a cabo un proceso de desulfuración mediante extracción empleando líquidos iónicos como disolventes. Se ha confirmado tanto su capacidad desulfuradora como la de extracción de compuestos nitrogenados, tanto desde el punto de vista teórico, mediante el estudio de los datos termodinámicos de equilibrio líquido-líquido y su posterior tratamiento, como desde un punto de vista más práctico llevando a cabo experimentos con combustibles reales procedentes de corrientes de refinería previos a la hidrodesulfuración.

Además a lo largo del desarrollo experimental se ha comprobado la capacidad de regeneración de éstos disolventes mediante destilación a vacío. Los líquidos ióncos sintetizados en el propio laboratorio fueron reutilizados como disolventes una vez comprobada su pureza mediante técnicas de RMN y medida de propiedades físicas y contenido en agua.

De los líquidos iónicos estudiados, el $[C_6mmPy][NTf_2]$ se presenta como el mejor candidato como disolvente para llevar a cabo la desulfuración de combustibles. La simulalción de un proceso de extracción empleando un software de simulación de procesos confirma la capacidad de este líquido iónico para alcanzar los niveles de desulfuración requeridos por la legislación vigente. La simulaciób n se ha llevado a cabo variando tanto el poder separador de la columna (número de etapas teóricas) como la relación disolvente/alimentación. Los satisfactorios resultados obtenidos en la misma se muestran en la presente memoria. Sin embargo, debido los desvíos encontrados para la correlación simultánea, si bien éstos son relativamente bajos, no son del orden de magnitud requerido para llevar a cabo una valoración cuantitativa de los resultados obtenidos. Sería necesario llevar a cabo experimentos en planta piloto, estudios de viabilidad económica, análisis de ciclo de vida…como pasos necesarios para continuar este estudio.

PUBLICATIONS:

1. Luisa Alonso, Alberto Arce, María Francisco, Oscar Rodríguez and Ana Soto.
"Liquid-Liquid Equilibria for systems composed by 1-methyl-3-octylimidazolium tetrafluoroborate ionic liquid, thiophene and n-hexane or cyclohexane"
J. Chem. Eng. Data , 52 (2007) 1729-1732

2. Luisa Alonso, Alberto Arce, María Francisco, Oscar Rodríguez and Ana Soto.
" Gasoline Desulfurization using Extraction with $[C_8min][BF_4]$ Ionic Liquid."
AIChe J., 53(2007) 3108-3115

3. Luisa Alonso, Alberto Arce, María Francisco and Ana Soto.
" Measurement and Correlation of liquid liquid equilibria of two Imidazolium Ionic Liquid with Thiophene and Methylcyclohexane."
J. Chem. Eng. Data , 52 (2007) 2409-2412

4. Luisa Alonso, Alberto Arce, María Francisco, and Ana Soto
" Phase behaviour of 1-methyl-3-octylimidazolium bis[trifluoromethylsulfonyl]imide with thiophene and aliphatic hydrocarbons: The influence of n-alkane chain length."
Fluid Phase Equilibr., 263 (2008) 176-181

5. Luisa Alonso, Alberto Arce, María Francisco, and Ana Soto
" (Liquid-Liquid) Equilibria of $[C_8mim][NTf_2]$ ionic liquid with a sulfur-component and hydrocarbons"
J. Chem. Thermodyn, 40 (2008) 265-270

6. Luisa Alonso, Alberto Arce, María Francisco, and Ana Soto
"Solvent extraction of thiophene from n-alkanes (C7, C12 and C16) using the ionic liquid $[C_8mim][BF_4]$"
J. Chem. Thermodyn, 40 (2008) 966-972

7. Luisa Alonso, Alberto Arce, María Francisco, and Ana Soto
" Liquid-liquid Equilibria for the $[C_8mim][NTf_2]$ + Thiophene + 2,2,4-Trimethylpentane or Toluene"
J. Chem. Eng. Data, 53 (2008) 1750-1755

8. Luisa Alonso, Alberto Arce, María Francisco, and Ana Soto
" Liquid-liquid equilibria of ($[C_2mim][EtSO_4]$ + thiophene + 2,2,4 trimethylpentane) and ($[C_2mim][EtSO_4]$ + thiophene + toluene): experimental data and correlation"
J. Solution Chem., 37 (2008) 1355-1363

9. Alonso, Luisa; Arce, Alberto; Francisco, Maria
" Thiophene separation from aliphatic hydrocarbons using the 1-ethyl-3-methylimidazolium ethylsulfate ionic liquid."
Fluid Phase Equilibr., 270 (2008) 97-102

10. Héctor Rodríguez, María Francisco, Mustafizur Rahman, Ning Sun and Robin D. Rogers
"Biphasic liquid mixtures of ionic liquids and polyethylene glycols"
Phys. Chem. Chem. Phys., 11 (2009) 10916-10922

11. María Francisco, Alberto Arce, Ana Soto
"Ionic Liquids on desulfurization of fuel oils"
Fluid Phase Equilibr., *in press* (2010)

12. Alberto Arce, María Francisco and Ana Soto
"Evaluation of the polysubstituted pyridinium ionic liquid [hmmpy][Ntf_2]as suitable solvent for desulfurization: phase equilibria"
J. Chem. Thermodyn., *in press* (2010)

13. L. Alonso, A. Arce, M. Francisco and A. Soto
"A comparative study on fuel-oil desulfurization and denitrogenation by using ionic liquids"
J. Chem. Eng. Data, Sent Paper (2010)

14. M. Francisco, S. Lago, A. Soto and A. Arce
"Essential oil deterpenation by solvent extraction using ionic liquid 1-ethyl-3-methylimidazolium 2-(2-methoxiethoxi) ethylsufphate"
Fluid Phase Equilibr., Sent Paper (2010)